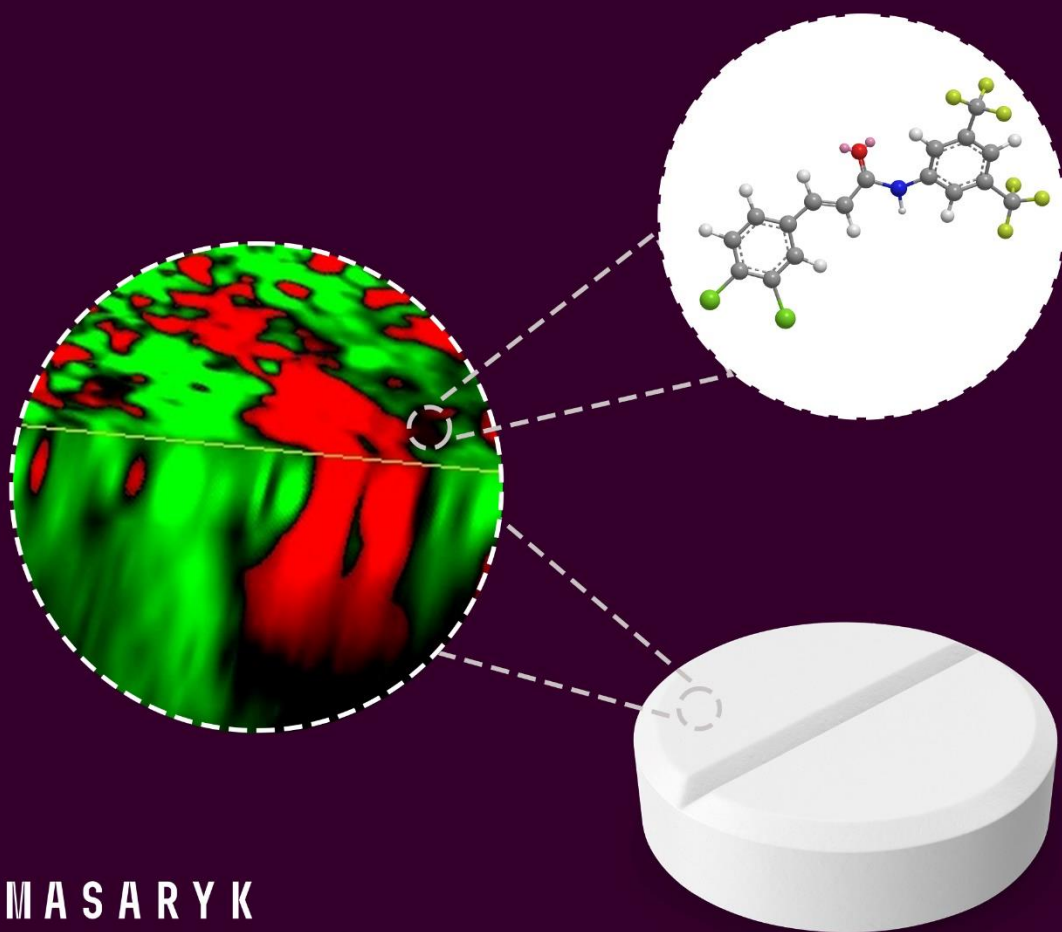


SELECTED ANALYTICAL TECHNIQUES OF SOLID STATE, STRUCTURE IDENTIFICATION, AND DISSOLUTION TESTING IN DRUG LIFE CYCLE

Martin Čulen, Jiří Dohnal, Josef Jampílek (eds.)



MASARYK
UNIVERSITY

**Selected Analytical Techniques of Solid State,
Structure Identification, and Dissolution Testing
in Drug Life Cycle**

**MUNI
PRESS**

**MUNI
PHARM**

**MUNI
MED**

Selected Analytical Techniques of Solid State, Structure Identification, and Dissolution Testing in Drug Life Cycle

Edited by:

Martin Čulen | Jiří Dohnal | Josef Jampílek

Masaryk University Press

Brno 2023

Reviewed by:

Witold Musial

Department of Physical Chemistry and Biophysics, Faculty of Pharmacy
Wroclaw Medical University, Wrocław, Poland

Kin Tam

Faculty of Health Sciences
University of Macau, Macau, China

The authors sincerely thank Ing. Kateřina Škrlová, Ph.D. (www.deart.cz) from VŠB-Technical University Ostrava (Czech Republic) for the design and realization of the book cover.



CC BY 4.0

© 2022 Masarykova univerzita, Josef Jampílek, Hana Brusová, Jaroslav Havlíček, Izabela Jendzejewska, Christelle Kadlec, Filip Kadlec, Bohumil Kratochvil, Lucie Krumbholcová, Tomáš Pekárek, Anna Řezáčová, Dita Spálovská

ISBN: 978-80-280-0193-3

<https://doi.org/10.5817/CZ.MUNI.O280-0193-2022>

Table of contents

PREFACE	1
1 INTRODUCTION	2
1.1 BRIEF HISTORY	2
1.2 CLASSIFICATION OF ANALYTICAL METHODS AND TECHNIQUES	4
1.3 PROCESS HARMONIZATION	6
2 INFRARED SPECTROSCOPY	9
2.1 INTRODUCTION	9
2.2 IR SPECTROSCOPY IN MID-REGION	11
2.2.1 <i>Theoretical principles of MIR spectrometry</i>	11
2.2.2 <i>Experimental setup for MIR spectrometry</i>	13
2.2.3 <i>Techniques for measuring MIR spectra</i>	17
2.2.4 <i>Application of MIR spectrometry in pharmaceutical industry</i>	19
2.3 IR SPECTROSCOPY IN NEAR REGION	24
2.3.1 <i>Theoretical basics of NIR spectroscopy</i>	24
2.3.2 <i>Experimental arrangement of NIR spectroscopy</i>	26
2.3.3 <i>NIR spectra measurement techniques</i>	29
2.3.4 <i>NIR analysis strategies</i>	35
2.3.5 <i>Application of NIR spectroscopy in pharmacy</i>	36
2.4 RESOURCES AND RECOMMENDED LITERATURE	50
3 RAMAN SPECTROSCOPY	54
3.1 INTRODUCTION	54
3.2 EXPERIMENTAL SETUP	59
3.3 APPLICATION OF RAMAN SPECTROSCOPY	62
3.3.1 <i>Identification of unknown samples</i>	62

3.3.2 <i>Identification of polymorphs, solvates and salts</i>	64
3.3.3 <i>Raman mapping and imaging</i>	66
3.4 RESOURCES AND RECOMMENDED LITERATURE	69
4 X-RAY DIFFRACTION	70
4.1 INTRODUCTION	70
4.2 CRYSTAL STRUCTURE, ITS GEOMETRY AND SYMMETRY	70
4.3 X-RAYS	74
4.3.1 <i>X-ray tube</i>	74
4.3.2 <i>Characterization of X-ray radiation</i>	77
4.4 ANALYTICAL X-RAY DIFFRACTION METHODS	78
4.4.1 <i>Interactions of X-rays with crystal</i>	82
4.4.2 <i>Powder methods</i>	95
4.5 APPLICATIONS OF X-RAY DIFFRACTION IN PHARMACY	102
4.5.1 <i>Characterization and identification of unknown samples</i>	102
4.5.2 <i>Crystalline phase control</i>	105
4.5.3 <i>Negative proof of crystalline phase – amorphous material</i>	107
4.5.4 <i>Observation of phase transformations</i>	108
4.5.5 <i>Study of substance behavior under defined conditions</i>	110
4.5.6 <i>Determination of structures of unknown impurities or molecule chirality</i>	112
4.5.7 <i>Calculation of powder diffraction patterns</i>	112
4.5.8 <i>Determination of a 3D crystal structure from X-ray powder data</i>	113
4.5.9 <i>Quantitative phase analysis</i>	115
4.6 SUMMARY	116
4.7 RESOURCES AND RECOMMENDED LITERATURE	117

5 NMR SPECTROSCOPY	119
5.1 BASIC PRINCIPLES	119
5.2 NMR SPECTROMETER	123
5.3 ¹ H NMR SPECTROSCOPY	126
5.3.1 <i>Signal position – chemical shift</i>	126
5.3.2 <i>Integral signal intensity</i>	129
5.3.3 <i>Signal multiplicity</i>	130
5.4 ¹³ C NMR SPECTROSCOPY	134
5.5 TWO-DIMENSIONAL NMR SPECTRA	138
5.6 APPLICATION OF LIQUID PHASE NMR SPECTROSCOPY IN PHARMACY	143
5.6.1 <i>Structural analysis of APIs</i>	143
5.6.2 <i>Structural analysis of impurities</i>	146
5.7 SOLID STATE NMR SPECTROSCOPY	148
5.7.1 <i>Theoretical introduction</i>	148
5.7.2 <i>Application of solid state NMR spectroscopy in pharmacy</i>	156
5.8 CONCLUSION	171
5.9 RESOURCES AND RECOMMENDED LITERATURE	172
6 TERAHERTZ TIME-DOMAIN SPECTROSCOPY	174
6.1 INTRODUCTION	174
6.2 OVERVIEW OF EXPERIMENTAL TECHNIQUES IN THZ SPECTROSCOPY	175
6.3 PRINCIPLES OF THZ TIME-DOMAIN SPECTROSCOPY	177
6.3.1 <i>Principle of THz pulse generation</i>	178
6.3.2 <i>Detection of THz pulses</i>	179

6.4 THZ SPECTRA MEASURING TECHNIQUES AND DATA PROCESSING	180
6.4.1 Transmittance measurements	180
6.4.2 Reflectance measurements	182
6.4.3 Attenuated total reflection	183
6.4.4 Time of flight measuring method	184
6.4.5 Imaging measurement	184
6.5 APPLICATIONS OF THZ SPECTROSCOPY IN PHARMACY	184
6.5.1 Identification of substances using THz spectra	184
6.5.2 Determination of hydration state of substances	186
6.5.3 Determination of tablet coating thickness	188
6.5.4 Determination of grain size	188
6.6 RESOURCES AND RECOMMENDED LITERATURE	189
7 MASS SPECTROMETRY	191
7.1 BASIC PRINCIPLES	191
7.2 IONIZATION TECHNIQUES	193
7.2.1 Electron ionization (EI)	195
7.2.2 Chemical ionization (CI)	196
7.2.3 Fast atom or ion bombardment ionization (FAB, FIB)	198
7.2.4 Matrix assisted laser desorption/ionization (MALDI)	198
7.2.5 Thermospray ionization (TSI)	199
7.2.6 Electrospray ionization (ESI)	200
7.2.7 Atmospheric pressure chemical ionization (APCI)	203
7.2.8 Atmospheric pressure photoionization (APPI)	204
7.2.9 New ionization techniques	205

7.3 MASS ANALYZERS	206
7.3.1 <i>Magnetic analyzer with simple magnetic focusing</i>	207
7.3.2 <i>Sector analyzer with double ion focusing</i>	208
7.3.3 <i>Quadrupole (Q)</i>	209
7.3.4 <i>Triple quadrupole analyzer (QqQ)</i>	209
7.3.5 <i>Ion trap (IT)</i>	210
7.3.6 <i>Linear ion trap (LIT)</i>	211
7.3.7 <i>Orbitrap</i>	212
7.3.8 <i>Time of flight analyzer (TOF)</i>	214
7.3.9 <i>Ion cyclotron resonance with Fourier transform (FT-ICR)</i>	215
7.4 ION DETECTION TECHNIQUES	216
7.5 IDENTIFICATION AND DETERMINATION OF COMPOUNDS	218
7.6 STRUCTURAL MS ANALYSIS IN PHARMACY	221
7.6.1 <i>Modern MS systems in pharmacy</i>	222
7.7 RESOURCES AND RECOMMENDED LITERATURE	225
8 THERMAL ANALYSIS	226
8.1 DEFINITION OF THERMAL ANALYSIS METHODS	226
8.2 GENERAL PRINCIPLE OF THERMAL ANALYSIS METHODS	227
8.3 THERMAL METHODS	229
8.3.1 <i>Basic measurement factors</i>	229
8.3.2 <i>Measuring procedure</i>	230
8.3.3 <i>Evaluation of thermoanalytical measurements</i>	231
8.3.4 <i>Differential scanning thermal analysis (DSC)</i>	234
8.3.5 <i>Hyper DSC</i>	239
8.3.6 <i>Micro DSC</i>	240

8.3.7 <i>Temperature modulated differential scanning calorimetry (TMDSC)</i>	249
8.3.8 <i>Thermogravimetry (TGA)</i>	254
8.3.9 <i>Thermally stimulated current (TSC)</i>	259
8.4 RESOURCES AND RECOMMENDED LITERATURE	262
9 DISSOLUTION TESTING IN PHARMACEUTICAL INDUSTRY	264
9.1 BIOPHARMACEUTICAL CLASSIFICATION SYSTEM	264
9.2 DISSOLUTION TESTING OF SUBSTANCES	266
9.2.1 <i>Intrinsic dissolution</i>	266
9.2.2 <i>Apparent dissolution</i>	271
9.3 DISSOLUTION TESTING OF SOLID DOSAGE FORMS	275
9.3.1 <i>Dissolution</i>	275
9.3.2 <i>Experimental dissolution methods</i>	277
9.3.3 <i>Dissolution apparatuses</i>	279
9.3.4 <i>Advanced dissolution systems</i>	289
9.4 RESOURCES AND RECOMMENDED LITERATURE	293
10 SUMMARY	295
11 ABBREVIATIONS	298
12 AUTHORS	303

Preface

According to the experience of the authors of this textbook, the activities of the pharmaceutical faculties focus primarily on preparing students for the work in community pharmacy. The field of pharmaceutical research, development and industrial applications, on the other hand, has been rather neglected. However, the modern pharmaceutical industry primarily needs well-prepared experts with solid knowledge across the entire pharmaceutical field. This book is intended to achieve this precise goal.

The foundation for the book “Selected Analytical Techniques of Solid State, Structure Identification, and Dissolution Testing in Drug Life Cycle” was a textbook created almost eleven years ago as a study material for a newly approved optional class “Analysis in pharmaceutical industry”, at the Faculty of Pharmacy, University of Veterinary and Pharmaceutical Sciences Brno.

The textbook covered a very wide area – methods used in analytical development and quality control (QC) of pharmaceutical products. Examples of the particular methods applied in solving of practical problems were implemented into most chapters.

The current version is focused mainly on solid state and structural analysis. The topics are not discussed in an exhaustive manner. Only the most important and prevalent methods and techniques are mentioned, and the text is simplified. On the other hand, the chapter on dissolution was extended by addition of special dissolution methods. The textbook thus covers three important areas: 1. structural analysis of drugs, 2. pharmaceutical analysis in solid state, 3. dissolution testing methods.

The structure and content of this textbook reflect the very experience of the authors who personally contributed or introduced the described approaches and methods into practice. The author team includes senior experts who were involved in the implementation of good practices in pharmacy and the according legislation, and also in providing the related technical and methodological requirements. At the same time, they were also at the very beginning of the harmonization process. The younger authors, on the other hand, brought innovative solutions to many problems.

Most of the authors work in academy and have thus extensive teaching experience.

It is up to the reader to assess whether we have accomplished to raise his the interest in the given areas and to provide necessary information.

1 Introduction

Jiří Dohnal

Motto:

“The laboratory is an extension of our senses, enabling us to obtain data on substances beyond what we can see with naked eye and in amounts that our hands could never grasp. These data are compiled into reports and are ultimately used for making decisions, decisions that cannot be confirmed with our unaided senses. The quality of any decision is absolutely dependent on the quality of the data; junk data lead to junk decisions.”

J. M. Miller

1.1 Brief history

The pharmaceutical quality system was developed in steps that can be characterized as follows:

Period up to the 60's of the past century, with a little alleviation, sometimes also called “the dark age”.

The dominant methods in pharmaceutical analysis were volumetric and gravimetric methods. Among the separation methods, thin layer chromatography showed more intensive use, but without the option to objectively quantify the results, in the beginnings.

Impurities in percentile quantities undetected by analysts were no exception! Little attention was paid to chirality and polymorphism, due to the lack of proper instruments for their differentiation. The analyses were in most cases carried out by dissolving the analysed compounds, hence making some of their original properties undetectable.

70's – cGMP

This period was marked by the progress in separation methods, particularly the gas chromatography (GC), and later also the high performance liquid chromatography (HPLC) which constituted a revolution in pharmaceutical analysis. The importance of this period also laid in the introduction of computational systems as operating units for analytical instruments and data processing.

The introduction of good laboratory practice (GMP) and other good practices in pharmaceutical development and production, together termed GxP, meant another step forward in means of safety and quality. Stricter limits for impurity contents were established and the separation methods became more common.

The GC analyses however had their disadvantages and often required a derivatization of the quantified compounds, which was time consuming and with a risk of artefact creation. The gas chromatography is of course still in use, but primarily for analysis of volatile substances and for analysis of residual solvents when used in headspace technique.

80's – validation

The 80's were marked by progress achieved in instrumental analysis, mainly the structural analysis methods, such as cryogenic nuclear magnetic resonance, new mass spectrometry methods and electrochemical methods, for example capillary isotachopheresis, and later also other electromigratory methods.

The term validation has a wider meaning, however due to the focus of this book, the validation of analytical methods will be only briefly communicated.

The first occurrence of the term validation is dated back to the turn of the 70's and 80's and is linked to common good manufacturing practice (cGMP) requirements in drug production.

Standard requirements on registration documentation appointed by the State Institute for Drug Control (SUKL), defined on the basis of USP XXII and European Community requirements on medicines, are valid since 1992 (former Republic of Czechoslovakia).

The validation policy was published in 1994 in the SUKL bulletin along with the list of analytical parameters inspected during method validation, including a brief procedure manual.

2000 – continual quality verification

Major part of quality control has been merged directly with production. Attributes which can play a key role in the changes of product quality are measured and analysed. The basis of Process Analytical Technology (PAT) is design, analysis and management of production by *in situ* measuring of the above-mentioned attributes. This was a revolutionary change in the approach to pharmaceutical analysis, as the main interest was formerly the outcome analysis of the final product. These new requirements lead to selection of suitable analytical methods which are often

mistaken with the PAT itself. The PAT depends mainly on the speed and the capability of these methods for monitoring of selected attributes.

Current approach – risk management-based approach

Quality risk management ICH Q9 and Technical and regulatory considerations for pharmaceutical life cycle management ICH Q12. Quality risk management is a systematic process for the assessment, control, communication and review of risks to the quality of the drug (medicinal) product across the product lifecycle.

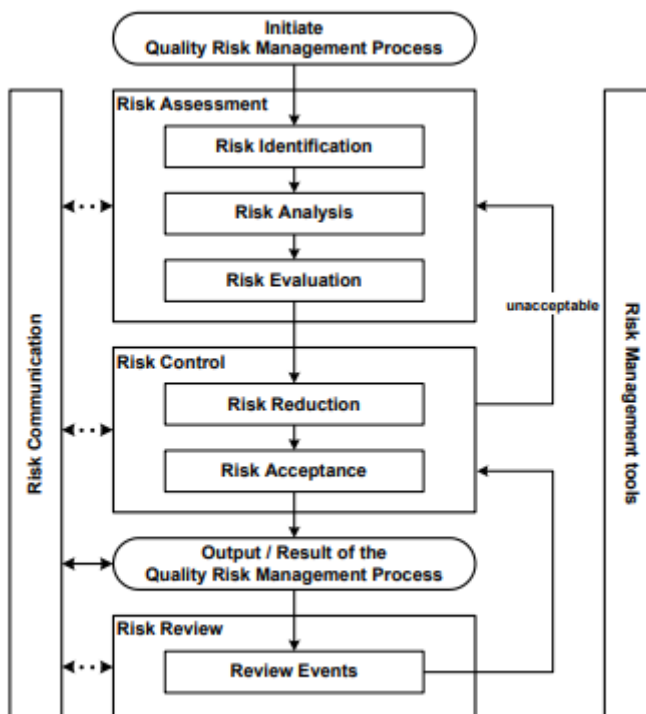


Figure 1.1. Overview of a typical quality risk management process (www.ich.org).

1.2 Classification of analytical methods and techniques

1. The selection of an appropriate analytical technique depends on the level of focus:
 - Molecular level: infrared spectrometry techniques – attenuated total reflectance (ATR) technique, diffuse reflectance infrared Fourier transform (DRIFT) technique, Raman spectrometry, X-ray structural

analysis of single crystal or powder material, solid state nuclear magnetic resonance (ssNMR) etc.

- Intermolecular level, particles: powder X-ray diffraction (PXRD), optical and electron microscopy – scanning electron microscopy (SEM) and its modification – electron tomography, transmission electron microscopy (TEM), terahertz spectroscopy (applies to intermolecular bond vibrations), and thermal methods – differential scanning calorimetry (DSC), micro DSC, hyper DSC, thermogravimetry analysis (TGA), thermally stimulated current (TSC).
 - Bulk: surface region – inverse gas chromatography (IGC), high energy regions, thickness, porousness, flow characteristics (of powders), dynamic vapour sorption (DVS); also small angle X-ray scattering (SAXS) for determination of particle size and shape etc.
2. Based on the physico-chemical principles and due to historical reasons, the analytical methods in pharmaceutical analysis are divided as follows:
- Classic: volumetry, gravimetry etc.
 - Electrochemical: potentiometry, amperometry, coulometry etc.
 - Optical methods: refractometry, polarimetry, turbidimetry, nephelometry etc.
 - Spectral: spectrometry in ultraviolet and visible region, spectrometry techniques based on rotational and vibrational transitions [infrared spectrometry in mid region (MIR) and near region (NIR), Raman spectrometry, terahertz spectrometry], circular dichroism, NMR, see Fig. 1.1.
 - Separation: thin layer chromatography (TLC), HPLC, GC, supercritical fluid chromatography (SFC), capillary electrophoresis (CE), extraction methods, e.g., supercritical fluid extraction (SFE) etc.
 - Techniques based on light scattering: PXRD, laser diffraction, dynamic diffraction, (Raman spectrometry) etc.
 - Thermal methods: DSC, TGA, TSC etc.

The first is the ICH Q2(R1) „*Analytical Validations – Validation of Analytical Procedures: Text and Methodology*“.

Formerly, the guideline was divided to Q2A (the primary guideline – October 1994), Q2B (supplement guideline regarding methodology – November 1996), Q2(R1) – November 2005.

The following items were subjects of validation:

- identity tests
- impurity quantification tests
- impurity control limit tests
- quantification tests for active pharmaceutical ingredient (API), dosage form (DF) or other selected product contents

The draft of the guideline ICH Q14 – “*Analytical Procedure Development*” was endorsed on 24 March 2022 and is currently under public consultation and a consensus guideline was published. The revised Q2(R1) will include validation principles that cover analytical use of spectroscopic or spectrometry data (e.g., NIR, Raman, NMR or MS), some of which often require multivariate statistical analyses. These types of validations are especially useful for methods described in the new edition of this book.

The quality related harmonization process also comprises the impurity issues. The Q series of the ICH guidelines belong to the most important ones and are divided as follows:

- Q3A(R2) “*Impurities in New Drug Substances*“ (October 2006),
- Q3B(R2) “*Impurities in New Drug Products*“ (June 2006),
- Q3C(R8) “*Impurities – Guideline for Residual Solvents*“ (1997, updates and appendices September 2002, October 2002 and November 2005).
- Q3D(R1) „*Guideline for Elemental Impurities*“ (March 2019)

Guidelines Q3A(R2) and Q3B(R2) deal with classification of impurities, reasons for impurity reporting and impurity control, which are divided into:

- organic impurities
- inorganic impurities
- solvents

They also describe analytical procedures, impurity contents in batches, specification list of impurities and classification of impurities. The guidelines include limits and decision trees.

The above mentioned guidelines do not concern polymorphism and optical purity. These issues are partly discussed in guideline Q6A “*Specifications: Test Procedures and Acceptance Criteria for New Drug Substances and New Drug Products*” (October 1999).

Guideline Q6B “*Specifications: Test Procedures and Acceptance Criteria for Biotechnological/Biological Products*” (March 1999), describes the testing procedures and acceptance criteria for new biotechnological/biological products.

The guideline Q6A can be divided into:

1. General tests:

- description
- specific identification tests
- content quantification, selective tests for stability monitoring
- impurities

2. Specific tests:

- physico-chemical characteristics (pH, T_m, refractive index etc.)
- particle size
- polymorphism (decision tree)
- set of tests for chiral API and DF
- water content
- inorganic impurities
- microbial limits

2 Infrared spectroscopy

Tomáš Pekárek, Josef Jampilek, Dita Spálovská

2.1 Introduction

Spectroscopy in infrared (IR) region is an analytical optical method based on the absorption of electromagnetic radiation from matter. Electron state of molecules is not altered, but changes occur in vibrational-rotational energy states of molecules, depending on changes in their dipole moment. The absorbed energy quanta increase the internal molecular energy, which is related to atomic bond vibrations and rotations of the individual parts of a molecule.

The IR spectroscopy methods in pharmaceutical industry have wide application in routine quality control as well as in development. The main advantages are the measurement speed (seconds to minutes), simple or no sample preparation, and relatively low instrument costs. For common measurements, an instrument may be operated by a person without any deep knowledge of the principles of the method, which lowers manpower costs. However, when dealing with more complex applications (such as measuring in complex dosage form matrices or quantification of components) where it is necessary to decide on the most appropriate experimental arrangement, and also when evaluating spectra of unknown substances or identifying structures, the knowledge of basic principles is necessary, as will be explained in the following sections. Since dealing with molecular (functional) analysis, the IR spectroscopy can provide valuable insight into the structural constitution of molecules, functional groups, qualitative and quantitative composition of mixtures of both solid and liquid samples (including suspensions and emulsions). IR spectroscopy is also used for determination of gases. However, the last application is not used in routine pharmaceutical practice, due to rarity of gaseous drugs. Besides, in case of aerosols, it is possible to analyze the condensed liquid or solid component.

IR techniques are recognized by state authorities as suitable methods for analysis of pharmaceuticals. Their brief description with instructions for calibration and validation of the instrument is listed in Pharmacopoeias (Ph. Eur.) and in guidelines.

It can be said that IR and also Raman spectroscopies (see below) are techniques of the first choice when a rapid, reliable, and validated analysis of drugs is required. Their general versatility and only small limitations make them applicable in almost each laboratory in both industry and development. Pharmaceutical development and industry are no exceptions in this regard.

2 Infrared spectroscopy

IR spectroscopy uses interaction between infrared radiation and matter. IR radiation is an electromagnetic radiation which can be considered both a wave and a stream of particles (photons). Radiation can be characterized by speed c , wavelength λ , frequency ν [Hz], wavenumber $\tilde{\nu}$ [cm^{-1}] and radiation energy E , to which the following relationships apply:

h – Planck constant

$$E = h\nu = \frac{hc}{\lambda} \quad \nu = \frac{c}{\lambda} \quad \tilde{\nu} = \frac{1}{\lambda}$$

Infrared radiation is an invisible thermal radiation which is generally emitted by all objects, especially at higher temperatures. IR radiation is surrounded by visible light on one side of the spectrum and by microwave radiation on the other side (Fig. 2.1). Its upper limit is determined by spectral sensitivity of the human eye, the lower limit by ability to create and detect IR radiation with the longest wavelengths. IR radiation partly overlaps with the area of microwave radiation (electronically produced electromagnetic radiation) on its bottom boundary and is defined by wavelengths λ in the range of 0.78–1000 μm . However, wavenumber is used as a unit much more frequently in infrared spectroscopy and is defined by the area of $\tilde{\nu} = 12800\text{--}5 \text{ cm}^{-1}$ (the boundaries are not sharp, different authors use different values).

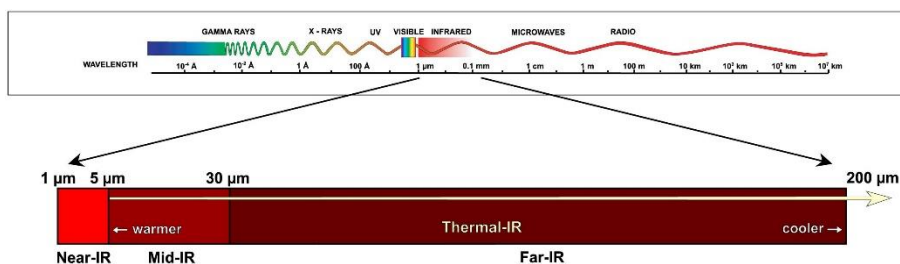


Figure 2.1. Wavelengths of individual areas of electromagnetic spectrum.

(Source: http://ipac.jpl.nasa.gov/media_images/screen_gif/background/spectrum_callout.gif, 10. 12. 2009.)

Given the very broad energy range of photons of the IR spectrum they may cause different energy transitions when they collide with molecules. Therefore, the infrared region is divided into three parts:

- Near-Infrared (NIR) 12800–4000 cm^{-1} (0.78–2.50 μm)
- Mid-Infrared (MIR) 4000–200 cm^{-1} (2.50–50 μm)
- Far-Infrared (FIR) 200–5 cm^{-1} (50–1 000 μm)

IR radiation in the FIR region has the lowest energy, which causes changes in rotational energy of molecules. FIR is therefore primarily the region of rotational

spectra and is of particular importance for theoretical chemistry and molecular physics. It has practically no use in pharmaceutical industry.

MIR region is the most important region in terms of pharmaceuticals analyses. It is a region where majority of the fundamental vibrations appear – the vibrational transitions from the ground to the first excited vibrational state, as described below. The focus of the analytical applications of these methods lies in the use in structural diagnosis, characterization and identification of organic and inorganic substances.

Photons in NIR region have the highest energy and can therefore vibrationally excite molecules into even higher excited vibrational states than the first level, i.e., the second, third, and others. These transitions are called overtones. Although the overtones are generally associated with lower absorption strength than the fundamental vibrations, the NIR spectroscopy has great analytical importance especially in many areas of practical and applied chemistry, particularly in qualitative and quantitative analyses.

2.2 IR spectroscopy in mid-region

2.2.1 Theoretical principles of MIR spectrometry

Mid-infrared region (MIR) uses radiation in the range of $4000\text{--}200\text{ cm}^{-1}$. No bond in molecules is rigid but still vibrates with a certain frequency. Non-linear molecule with N atoms has $3N$ degrees of freedom, three of which represent translational motion in mutually perpendicular directions (axes x , y , z) and three represent rotational movement along the axes x , y , z . The remaining $3N-6$ degrees of freedom represent the number of options how a non-linear molecule may vibrate – vibrational modes. A linear molecule is deprived of rotary motion around an axis intersecting the bonds because there is no regrouping of atoms, and the molecule then has one extra vibrational mode ($3N-5$).

As IR radiation passes through a sample, those parts of the radiation that match the frequency of bond vibrations in the molecule are absorbed. A vibration must meet a basic condition to be seen as a characteristic band in an IR spectrum and that is to have non-zero dipole moment change matching normal coordinate Q_i , that is:

$$\frac{\partial \mu}{\partial Q_i} \neq 0$$

Furthermore, anharmonicity (more information can be found in textbooks of physics and physical chemistry) partially suppresses selection rule, forbidding transitions between the vibrational levels by more than one level. Thus, the spectrum may

contain overtones, which is a case when a molecule transits to other than the next higher vibrational energy state and which may contain combination bands when combinations of various vibrational modes occur. When interpreting fundamental modes, overtone bands are usually not an obstacle as they have low intensity compared to the fundamental transitions.

A molecule can generally vibrate in several ways. The vibrations may be stretching when a change in bond length occurs or deformation when a change in a bond angle occurs. These basic types of vibrations have several subgroups. Stretching oscillations can be symmetrical or asymmetrical, deformation oscillations can be in-plane or out-of-plane. In-plane vibrations can be scissoring or rocking, out-of-plane can be wagging or twisting, as shown in Fig. 2.2. Stretching vibrations are denoted by ν , deformation vibrations by δ . Added footnote can be used to describe the type of the vibration, for example δ_{ω} will represent deformation wagging vibration. The symbol can be used alone to denote the vibration type, e.g., ω .

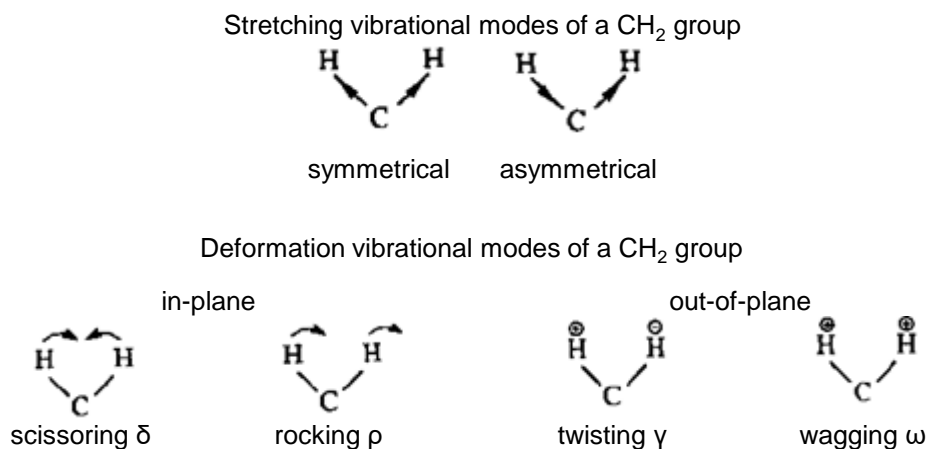


Figure 2.2. Vibrational modes.

(Edited according to: Socrates G. *Infrared and Raman Characteristic Group Frequencies*.
John Wiley & Sons, 2001.)

In the region between 4000 and 1500 cm^{-1} , vibrational transitions of atomic bonds of particular functional groups occur (oscillating with a particular frequency), while the rest of the molecule remains almost motionless, and positions of the particular absorption bands correspond to the particular functional groups with influence from the rest of the molecule. In other words, it is possible to deduce the presence of a certain functional group based on positions of bands in spectrum. Correlation tables are used for this purpose to simplify orientation in spectra. Examples of band assigning will be discussed in the applications section.

Skeletal vibrations are also found in the spectra, especially in region of 1500 to 200 cm^{-1} , and they result from vibrations of many atoms in a molecule. Such vibrations are not used to identify functional groups but can be used to distinguish structurally similar molecules.

To identify a molecule, it is not necessary to assign all the bands that appear in the spectrum, but it is necessary to find all bands belonging to vibrational modes of a particular functional group. Above mentioned means that there are no two compounds with identical IR spectra. Nowadays, when instruments are controlled by computers, it is possible to search for spectra in electronic spectral libraries, which significantly speeds up the whole process.

2.2.2 Experimental setup for MIR spectrometry

All optical parts of an instrument must be made from IR transparent material, mainly alkali metals and alkaline earth metals salts (KBr, NaCl, ZnSe). Fig. 2.3 shows general configuration scheme of spectrometers with Fourier transform, which are currently used almost exclusively.

All spectrometers are composed of three basic parts:

- source of radiation
- detector
- interferometer

MIR spectroscopy uses silicon carbide or NiCr resistance wire heated to a high temperature as a source of radiation. Infrared systems use two basic detection systems – thermal and quantum. In MIR spectroscopy, an example of a thermal detector is deuterated triglycine sulphate (DTGS) detector, and an example of a quantum detector is mercury cadmium telluride ($\text{Hg}_{1-x}\text{Cd}_x\text{Te}$, MCT) detector. The most important part of an instrument is an interferometer. Dispersion systems with a dispersion element (prism, grating) used for separation of beam were used in the past and are still being applied in some special applications. Common applications use almost exclusively interferometric systems with Fourier transform (FT). The principle of interferometry can be easily explained for a case where there is only one wave which is registered on the detector as a sine function. This simple function is used for monitoring and calibration of the position and movement of mirrors using an HeNe laser. High-intensity radiation proceeds to the interferometer. An interferometer consists of a beamsplitter that reflects half of the radiation onto a fixed mirror and another half passes further onto a moving mirror. The moving mirror reflects the radiation back, and the radiation thus travels a different optical

path than the radiation reflected from the fixed mirror. When these beams recombine back on the beamsplitter and the distance of the fixed and the moving mirror is such that the two waves are in phase, a constructive interference appears and there is a high detector response. If the distance between the two mirrors is such that the recombining waves are not in phase, there is a destructive interference at the beamsplitter. Therefore, the response of the detector will be lower. This difference in optical path is scanned and used for internal and absolute wavelength calibration.

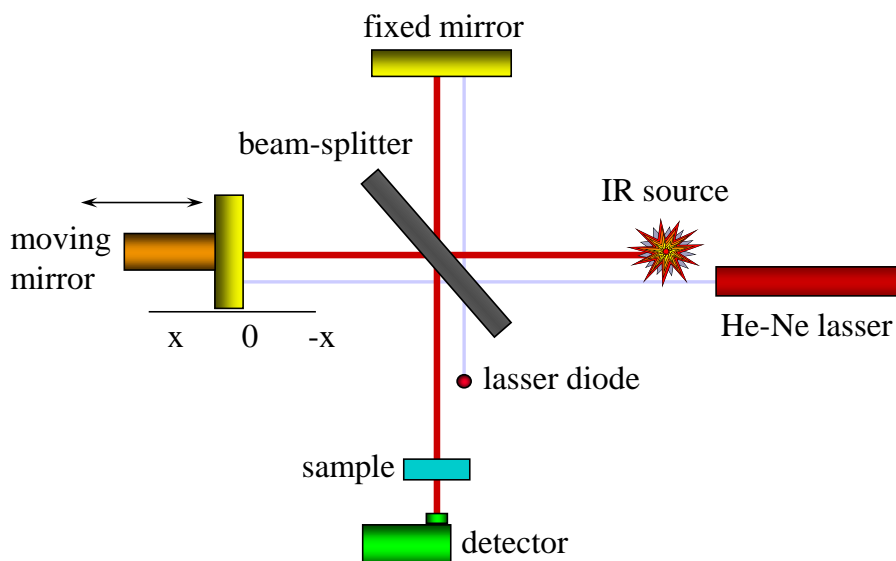


Figure 2.3. Basic construction scheme of a spectrometer with Fourier transform.

(Edited according to: Základy FT-NIR spektrometrie. Presentation. Nicolet CZ, 2008.)

The model becomes more complicated for two waves but remains valid even for many waves (a source with a wide range of wavelengths is used).

When measuring samples, recombination of beams occurs on the beamsplitter according to the above-mentioned rules, and the radiation is reflected further to the sample. The interferometer modulates the IR radiation and creates an interferogram containing the whole spectral information about the sample. The detector measures intensity of the modulated radiation.

Every moving part of the instrument is a subject to changes over time. To eliminate this device instability, a "Dynamic Alignment" function may be used, which is a continuous correction of the interferometer optics adjustment and is based on measurements of three laser signals in three different places. Slightest change in the movement leads to modulation of these signals, and the position of the fixed mirror is continuously finely adjusted by three electromagnetic transducers. This correction

is performed not only at the beginning of the measurement, but throughout its whole course.

To convert an interferogram into a spectrum, it is needed to change time domain represented by the interferogram to a frequency domain (spectrum). Fourier transform uses two parameters in IR spectrometry application. One is addition of zeros into the interferogram (zero filling), which is used to obtain interpolated spectrum values. And the second parameter is apodization. The interferogram is truncated by the apodization function.

Materials used in production of optical components of IR spectrometers are highly hygroscopic. For this reason, it is required to keep the spectrometer under voltage so the whole apparatus is permanently heated to prevent condensation of aqueous vapors on the optical elements. Furthermore, water strongly absorbs IR radiation and limits the use of IR spectroscopy for measurements of samples with high water content. This also results in the need to measure “background” to eliminate the effect of air molecules which create response on the IR detector (air humidity, carbon dioxide etc.). An example of the atmospheric spectral background is shown in Fig. 2.4. The spectrum contains four regions of evident absorptions (it is a transmittance measurement and the absorption region in the background measurement leads to decrease in the intensity of the signal incident on the detector). The regions 1 and 2 can be therefore assigned to vibrations of molecules of atmospheric humidity (stretching and deformation) and regions 3 and 4 belong to stretching and deformation vibrations of carbon dioxide.

In total, five types of interactions of radiation with solid sample can be distinguished (Fig. 2.5). When specific radiation passes through a homogenous environment, its initial intensity is attenuated by an extent which is absorbed by the environment. The intensity of radiation is thus reduced by absorption, but the wavelength or the wave number remains unchanged.

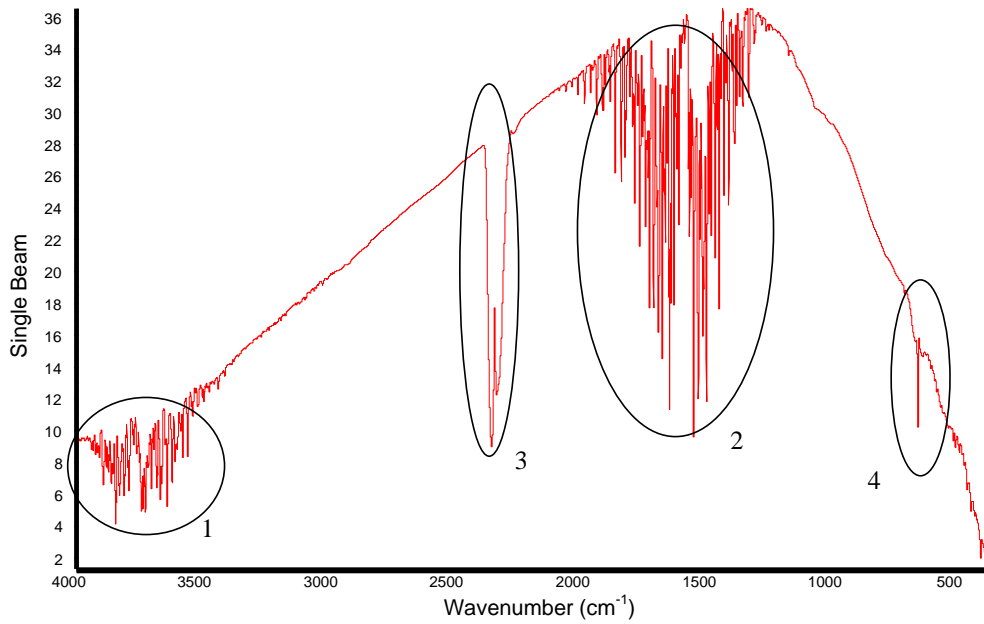


Figure 2.4. MIR spectrum of an atmospheric background.

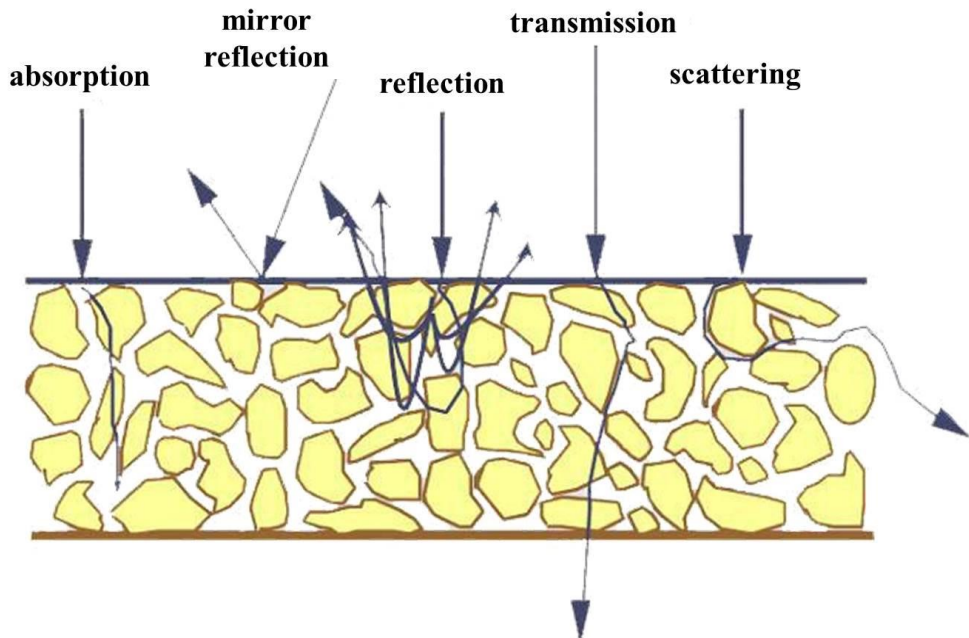


Figure 2.5. Interactions of radiation with solid matter.

(Edited according to: Giehl A. NIR reflectance spectroscopy in pharmaceutical drug product manufacture" Presentation. Bruker Optik GmbH Germany, 2006.)

When a light beam with intensity Φ_0 passes through a layer of absorbing environment with thickness l , a part of the beam is absorbed and a part with intensity Φ passes through. The following relationships apply:

$$T = \frac{\Phi}{\Phi_0} \quad T - \text{transmittance}$$

$$A = \log \frac{1}{T} \quad A - \text{absorbance}$$

$$100 T - \text{transmittance [\%]}$$

For reflectivity measurements, reflectance R [%] is often used and is defined as reflected radiation flow Φ_R divided by incident radiation flow Φ_0 .

$$R = \frac{\Phi_R}{\Phi_0}$$

The reflectance is then formally converted to absorbance A' using the relationship:

$$A' = \log \frac{1}{R}$$

Beer-Lambert law implies that absorbance is a linear function of concentration. By plotting dependence $A = f(c)$ at a constant wavelength λ (and wave number ν), a calibration line can be obtained. In presence of multiple components, the resulting absorbance is given by the sum of the absorbances of the individual components.

Beer-Lambert law:

$$A = \varepsilon c l$$

ε – molar absorption coefficient [l/(mol.cm)]

c – molar concentration [mol/l]

l – layer thickness [cm]

2.2.3 Techniques for measuring MIR spectra

IR spectra in mid region can be measured as attenuation of radiation flow after passing through a sample (transmission measurements) or after reflection of the radiation (reflection measurements).

Transmission measurements are used for analysis of gases, liquids, transparent films, and solids. Liquid samples must be measured in special cells which are made of, for example, KBr, NaCl, CaF₂, BaF₂, ZnSe, CsI, AgCl, AgBr, Ge, silicon, or mixed crystal of thallium iodide and bromide (KRS-5). Solvent selection must be well considered as the above-mentioned cell materials have different solubility in different solvents. A cuvette window must be made of a material sufficiently resistant to the applied solvent. The range of solvents is very wide and the most used are halogenated solvents, such as chloroform and carbon disulfide, since they provide a small number of characteristic bands in the spectrum. For measurements of samples in solid state, suspensions in paraffin oil or tablets created by compression of the sample with KBr are used.

Reflectance measurements which are currently the most widespread in practice usually use ATR (Attenuated Total Reflection) technique. Arrangement of this experiment involves a thin layer of a sample pressed on crystal mostly made of ZnSe, Ge, or Si, or diamond. Each material has different spectral and physico-chemical characteristics, and the crystal is chosen according to the requirements of the analysis. Infrared radiation impacts a thin (1 μm) layer of the sample, and the beam is reflected onto the crystal where it is refracted and continues through the optical system to the detector. Refraction on a crystal may be multiple or only single (Fig. 2.6). ATR technique enables measurement of solid samples, as well as liquids or various semi-solid materials. It should be emphasized, however, that while the transmission technique yields IR spectrum of an "averaged" sample, the ATR yields spectrum of an "actual" sample (sample surface facing the crystal). Unlike in transmission spectra, the ATR technique leads to highlighted intensity of bands in low wavenumber region, contrary to the bands with higher wavenumbers. Therefore, the spectra obtained by ATR technique are often mathematically corrected, to be closer to the transmission spectra.

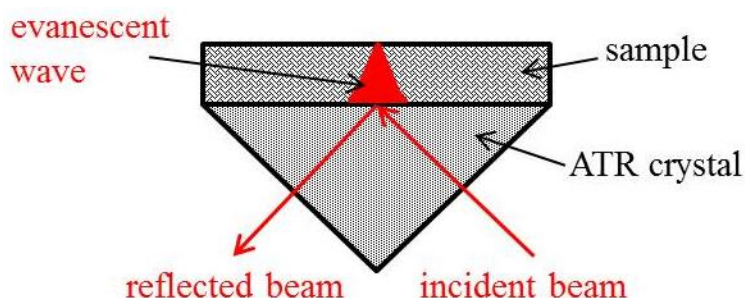


Figure 2.6. Scheme of IR beam reflection on an ATR crystal.

A very important and useful part of an IR spectrometer is a microscope connected to the spectrometer. The mapping function which measures spectra of spatially very close areas, point by point, and the imaging function which uses an area detector to

display an image of the studied sample, can be used to determine the size and distribution of individual components not only in powder mixtures but also directly in dosage forms, which is with comparable spectral and spatial resolution currently not possible by any other technique except Raman spectroscopy. This way, a spatial resolution in orders of microns can be achieved. Besides, it is possible to measure minimum sample amounts and detect foreign particles contained in mixtures and/or dosage forms.

Another advantage is the ability to lead the radiation outside of the spectrometer using optical fibers, which is applied when measuring with probes. Radiation is led from the spectrometer by optical fibers into a probe which measures in either the absorption or ATR arrangement. Signal attenuated by the absorbed part of the radiation is led by the fibers to the detector. The probe measurement approach does not change the principle of the method, only the layout of the experiment. The option to bring the spectrometer to the sample is mainly used for identification of substances in packages or in cases where sample collection is not possible or very difficult (reaction kinetics, samples packaged under controlled atmosphere, etc.).

Further details of experimental configuration, including appropriate sample preparation, then depend on the measurement type and will not be discussed further in this publication.

2.2.4 Application of MIR spectrometry in pharmaceutical industry

The first important application which shall be mentioned in this place is a verification of molecule structures or also identification of unknown substances. In production of substances or excipients, as well as when purchasing from a supplier, it is necessary to verify not only the identity of final products but also identity of intermediates and raw materials. The IR spectroscopy is a very suitable method for characterization of unknown samples or confirmation of structures. An example of assignment of characteristic bands of vibrational modes of functional groups is shown for acetylsalicylic acid in Fig. 2.7.

Besides structure confirmation and identification of unknown compounds, the IR spectroscopy is also used as a pharmacopeial method for identity confirmation using standards. Spectrum of an examined substance is compared either with a record of a standard, provided in a company norm with positions and relative intensities of bands, or it is compared using a software. In the latter case, computer compares the records according to the assigned parameters and provides the matching result. Both above mentioned applications are commonly used in research, development, and quality control laboratories.

2 Infrared spectroscopy

In research and development laboratories, the application of IR is even more extensive, because of the need of the most detailed information about the developed formulation. In case of generic companies, a thorough comparison of the developed formulation with original pharmaceutical is also required. Here, it is possible to apply the full potential of the IR spectroscopy. In analyses of active substances and certain excipients, an issue of polymorphism also emerges.

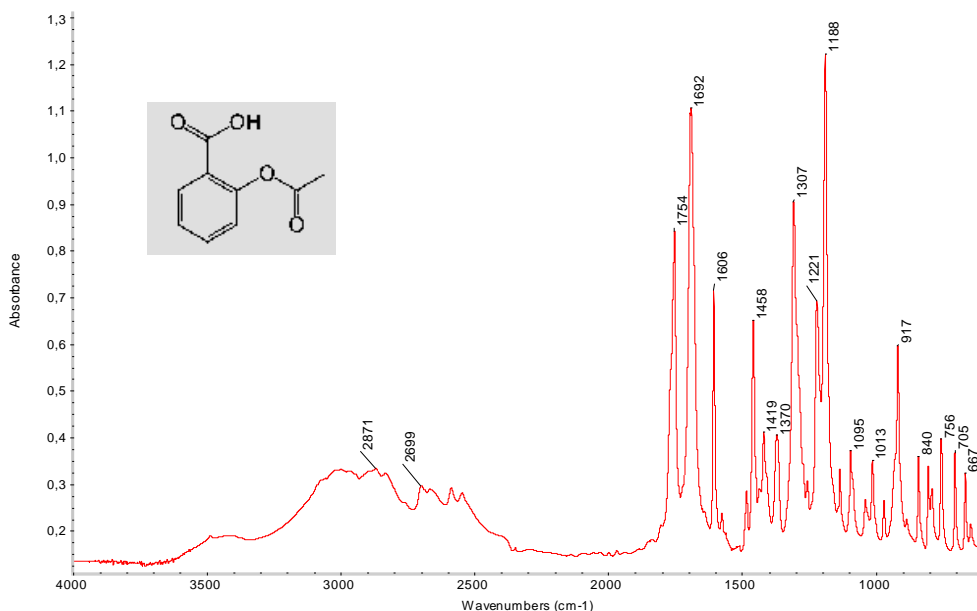


Figure 2.7. IR spectrum of acetylsalicylic acid.

Bands represent: 3000–2600 cm⁻¹ ν (O–H), 3100–3000 cm⁻¹ ν (C–H) aromatic ring, 3000–2800 cm⁻¹ ν (C–H) aliphatic chain, 1754 cm⁻¹ ν (C=O) ester, 1692 cm⁻¹ ν (C=O) acid, 1606 cm⁻¹ ν (C=C) aromatic ring, 1458 cm⁻¹ δ (CH₃), 1221 cm⁻¹ ν_{as} (C–O), 1188 cm⁻¹ ν_{sym} (C–O).

Crystalline substances can exist in different crystal modifications, as their atoms can be arranged in different crystal structures. This is called polymorphism. Depending on the type of the crystal modification, each polymorph of the same substance has different properties, such as melting point, dissolution rate, stability, etc. Besides other instrumental methods, such as X-ray powder diffraction and thermal analysis, IR spectroscopy can also be used to detect the type of a crystal modification or to distinguish between individual crystal modifications. It is however necessary to proceed with a parallel use of the powder X-ray diffraction which is the only technique able to identify polymorphic arrangement of molecules without a standard. Samples characterized this way can then be used as standards for IR identification of polymorphs. An example of comparison of infrared spectra of two polymorphic forms of one substance is shown in Fig. 2.8.

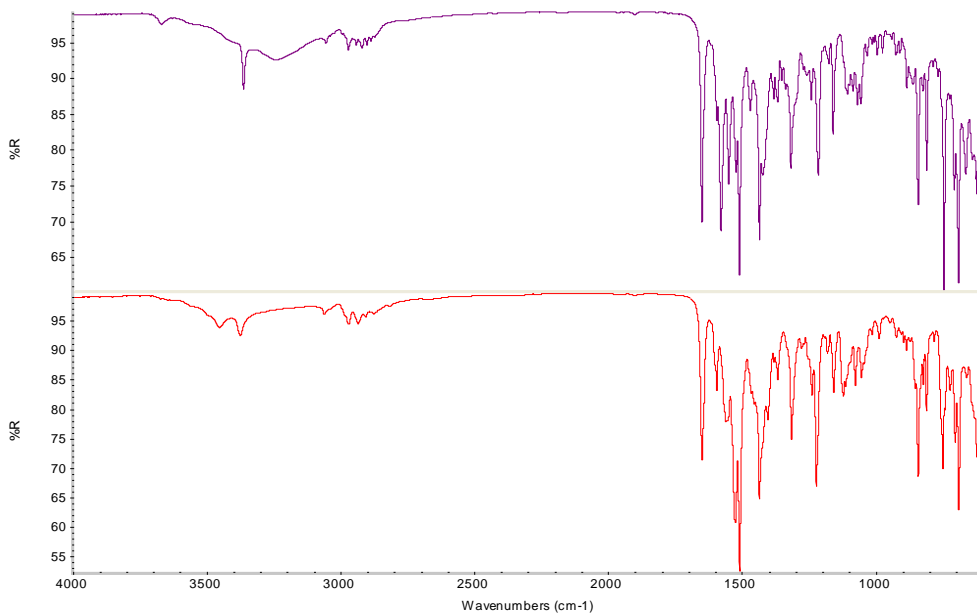


Figure 2.8. Example of comparison of two polymorphs of one compound.

When analyzing samples containing more than one substance (for example dosage forms), it is necessary to confirm the identity of the individual components and especially of the active substance. One of the tests (besides separation techniques) which can confirm the identity of an active substance, is IR spectroscopy. Ideally, the content of the active substance is high enough so that the bands of the active substance can be clearly identified in the spectra of the dosage form (Fig. 2.9). If the bands of the active substance are overlapped by signals of other components, the active substance must be extracted from the sample by an appropriate technique and subsequently identified or determined in the given extract. For such identification, it is necessary to be aware of the possibility of polymorph transformation during crystallization. Fig. 2.9 shows a spectrum in the range of $3600\text{--}600\text{ cm}^{-1}$, where a clear similarity between red spectrum (working standard) and magenta spectrum (dosage form) can be observed. These two spectra differ especially in the region around 1000 cm^{-1} where an obvious contribution of blue spectrum (placebo) occurs. In other words, the green curve is the sum of the red and the blue curve, in an appropriate ratio. This implies that IR spectrometry can be also used for semi-quantitative and quantitative analyses, assuming that the Beer-Lambert law is applicable. For such measurements, it is however necessary to provide a calibration curve or to use method of standard addition.

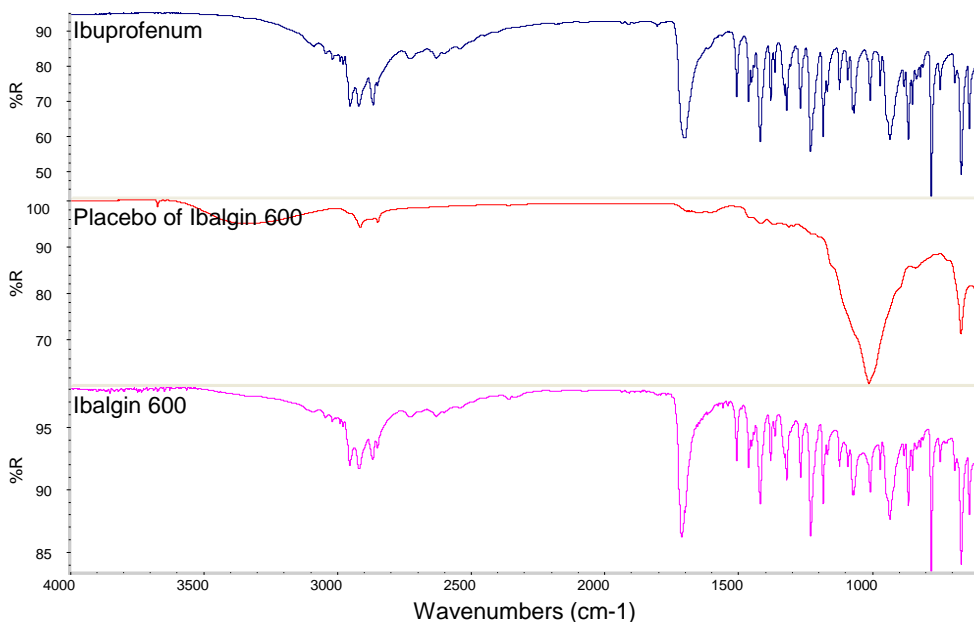


Figure 2.9. Example of confirmation and identification of active substance in Ibalgin® 600 dosage form. (Measurement in reflective setup – absorption regions oriented downwards). Working standard of the active substance (ibuprofen) – red, dosage form – green, placebo – blue.

IR spectroscopy can also distinguish different salts of one molecule. In production of dosage forms, the active substances are sometimes injected along with an equimolar amount of, for example, sodium hydroxide, which leads to preparation of a sodium salt. It is therefore necessary to monitor whether the salt conversion is fully completed and whether no unwanted ion exchange occurs. An example of the difference between IR spectra of different salts of one active substance is shown in Fig. 2.10

In addition to the several above-mentioned examples, IR spectroscopy can also be used for identification of excipients and packaging materials in pharmaceutical industry. Although arrangement and evaluation of the measurements then depend on the objectives and the information to be obtained, the principle is still the same – qualitative or quantitative determination as described above.

Mapping and imaging applications using connection of IR spectroscopy with IR microscope enable determination of very important information about particle size of active substances in tablets, their distribution (Fig. 2.11), and for example coating uniformity. The microscope also helps to easily identify even very small particles that stick to walls of ampoules, without the need for difficult separation or destructive analysis by other techniques.

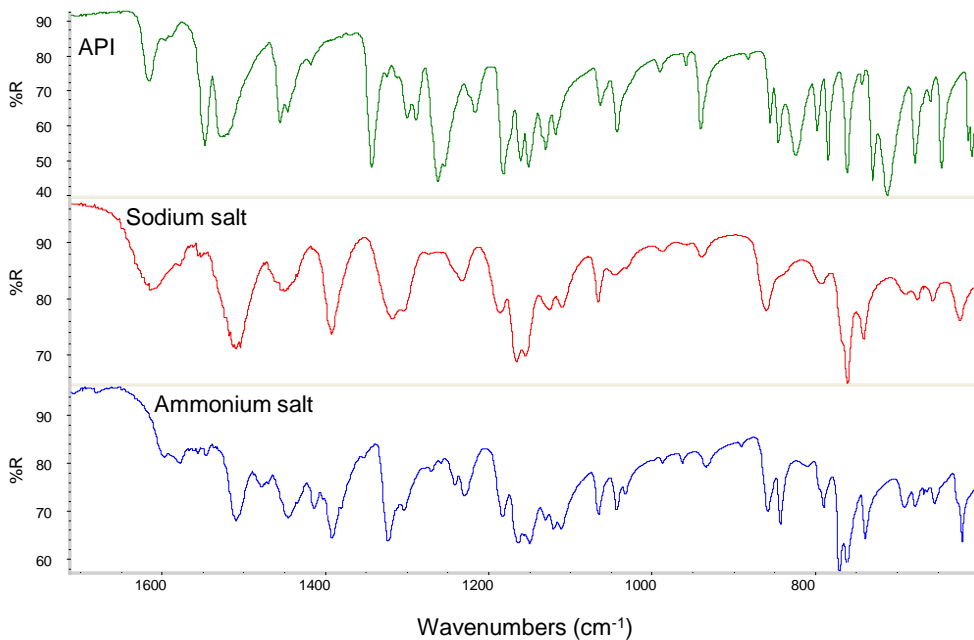


Figure 2.10. Comparison of different salts of one molecule; sodium salt, ammonium salt, acid.

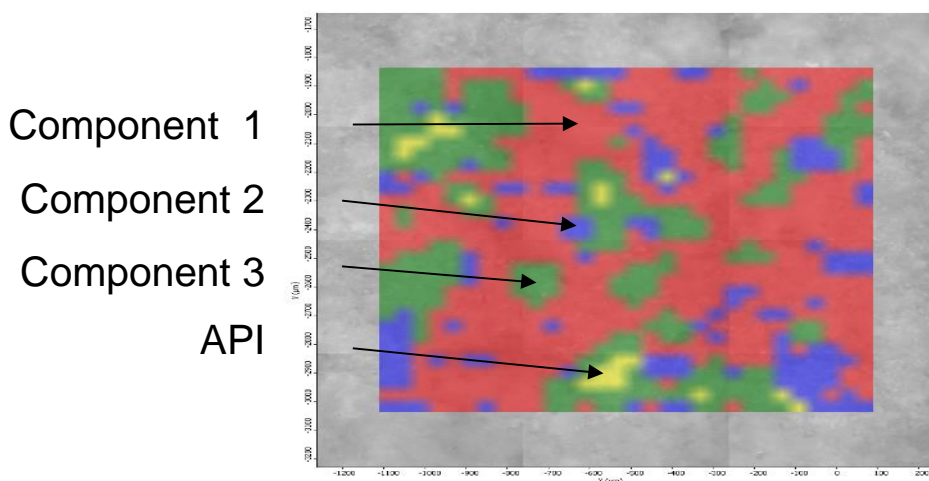


Figure 2.11. Example of component distribution (FTIR map), of a pharmaceutical tablet.

2.3 IR spectroscopy in near region

2.3.1 Theoretical basics of NIR spectroscopy

Spectroscopy in the near-infrared region (NIR) is a molecular spectroscopy method that uses radiation in the range between 12800 and 4000 cm^{-1} .

The physical principle for creation of NIR spectra is the same as for MIR spectroscopy. Absorption of photons with frequencies identical to bond vibrations leads to excitation of these bonds. Difference is in the higher energy of the NIR radiation. Absorption of radiation in the NIR region is usually based on higher energy transitions between vibrational levels of molecules, namely combination transitions and overtones, and not on fundamental transitions which are dominant in MIR region.

Combination transitions represent a simultaneous excitation of several vibrational modes. Transition energy equals the sum of the energies of fundamental transitions of the particular vibrational modes. Overtone then represents an excitation of a vibrational mode to a higher excited level. The first overtone corresponds approximately to twofold of the fundamental transition energy, second overtone to threefold, third overtone to fourfold etc. For a more accurate description, it is necessary to consider anharmonicity of vibrational modes as mentioned in section 2.2.1.1.

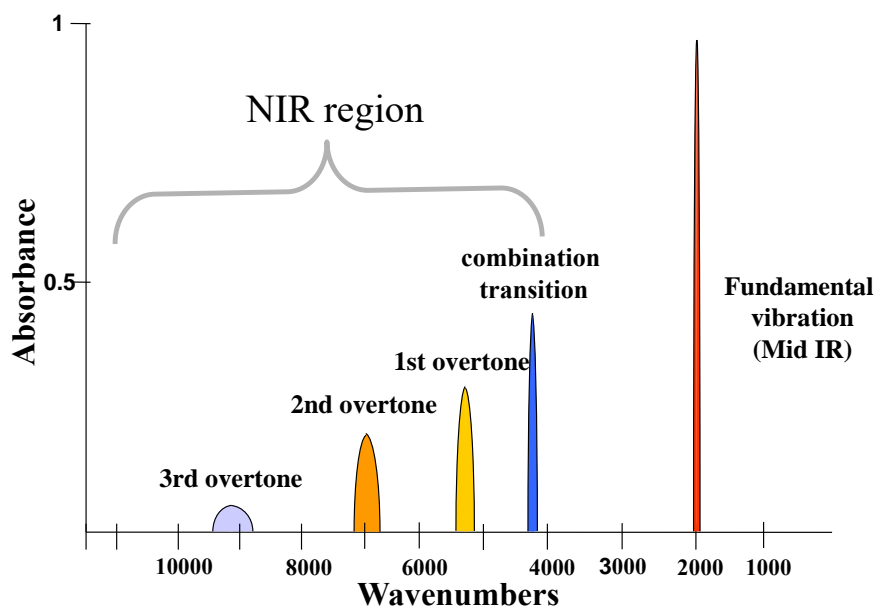


Figure 2.12. Intensity of absorption bands in NIR region compared to MIR region.

(Source: *Vzorkovací techniky v FT-NIR spektrometrii. Presentation. Nicolet CZ, 2008.*)

2 Infrared spectroscopy

Assignment of absorption bands to individual combinational transitions and overtones is difficult and often even impossible (Fig. 2.13), and the usual analysis is therefore not used to identify a particular functional group as with MIR spectra. It is possible to define regions where specific bands are dominant: combinational transitions (4000–5300 cm^{-1}), first overtones (4600–7300 cm^{-1}), second overtones (6000–10000 cm^{-1}) and third overtones (8800–12800 cm^{-1}), see Fig. 2.14.

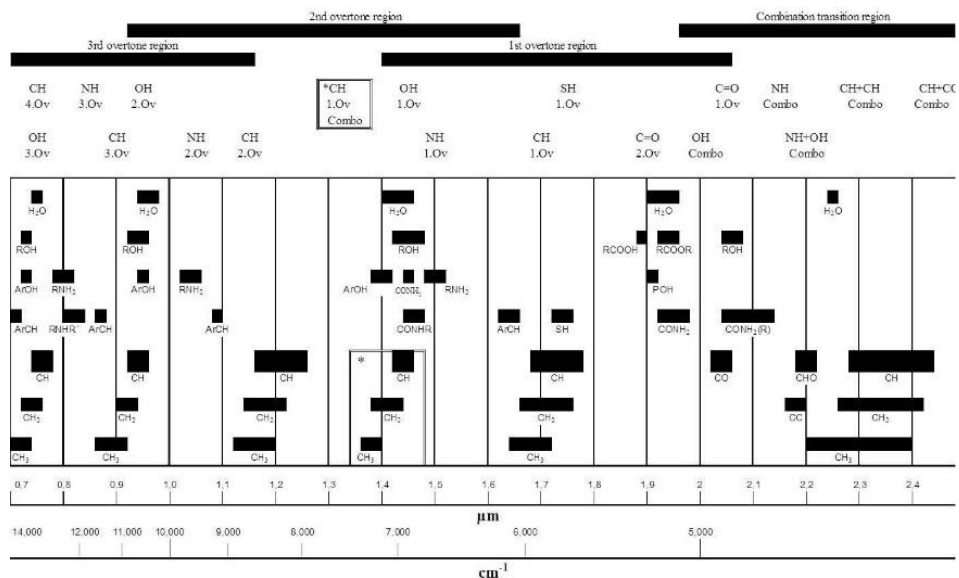


Figure 2.13. Absorption bands in NIR.

(Source: *Základy FT-NIR spektrometrie. Presentation. Nicolet CZ, 2008.*)

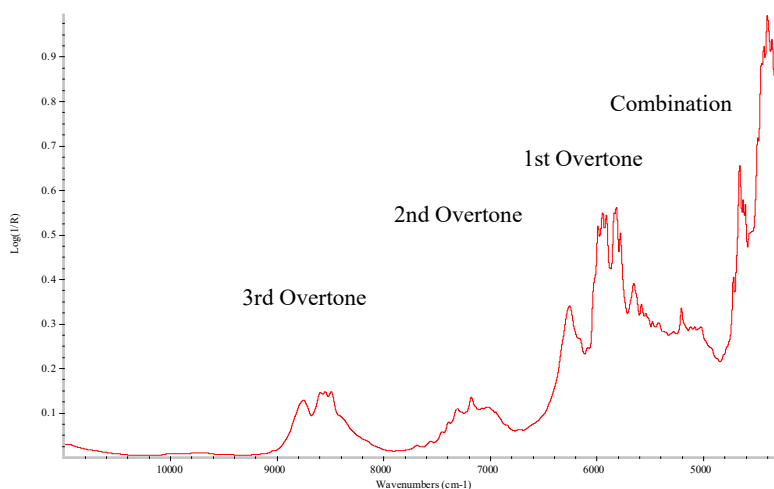


Figure 2.14. Example of a NIR spectrum.

(Source: *Základy FT-NIR spektrometrie. Presentation. Nicolet CZ, 2008.*)

2.3.2 Experimental arrangement of *NIR spectroscopy*

NIR spectrometers are less demanding on build materials than the instruments working in the MIR region, which is due to different radiation frequencies used in the NIR spectrometry. NIR radiation passes through quartz glass, and therefore any optics or cuvettes can be made of quartz that is commonly used in UV-VIS spectroscopy. Construction of NIR spectrometers with Fourier transform is the same as for MIR spectrometers, as shown in Fig. 2.3, described in section 2.2.1.2. All NIR spectrometers consist of three basic components:

- radiation source
- detector
- interferometer

Halogen bulbs are used as radiation sources. Various InGaAs, PbSe, PbS or Si detectors are applied, and beamsplitters are made of quartz or CaF₂. Similarly as in MIR, water molecules absorb NIR radiation, and it is therefore necessary to measure a reference spectrum (spectrum background) before the analysis to eliminate the environmental effects, especially atmospheric humidity. Example of atmospheric background is shown in Fig. 2.15.

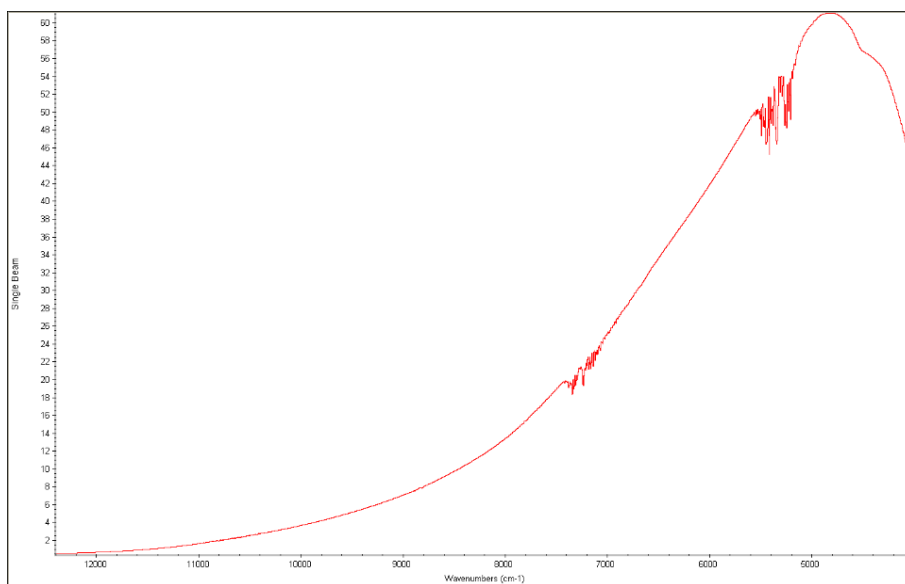


Figure 2.15. NIR spectrum of atmospheric background.

Due to the nature of the near IR radiation, the intensity of NIR spectra is inferior to MIR spectra. Fig. 2.16 shows MIR and NIR spectra of polystyrene. Fig. 2.17 then shows comparison of the same spectra in the same scale.

For qualitative purposes, it is necessary to compare the whole NIR spectrum or a characteristic region with spectra of pure substances, standards, or spectral libraries. Very often, the NIR spectra are sorted and classified using chemometric methods.

Same as for the mid IR region, a radiation passing through a homogenous environment is attenuated, and its initial intensity is lowered by an extent that is absorbed by this material. The absorption thus reduces the radiation intensity. Due to the nature of the NIR spectra – the bands are usually broad even for pure substances, and for mixtures, the shape of absorption bands can be affected by overlapping bands of different components or mutual effects of varying concentrations of individual components. It is therefore not possible to apply the simple Beer-Lambert law for this method.

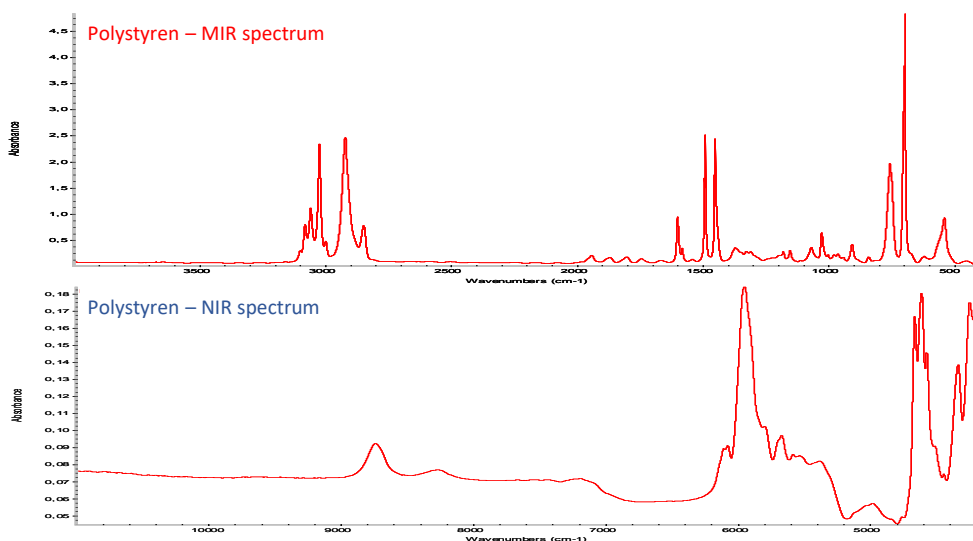


Figure 2.16. Spectrum of polystyrene in mid and near IR region.

(Source: *Základy FT-NIR spektrometrie. Presentation. Nicolet CZ, 2008.*)

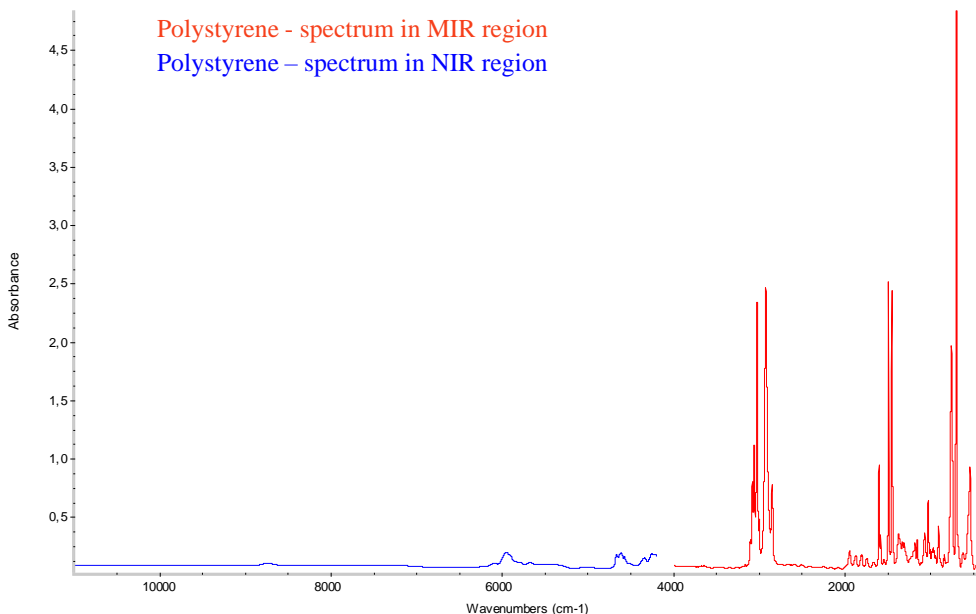


Figure 2.17. Comparison of a spectrum of polystyrene in near and mid IR regions.
(The same scale on the Y axis.)

(Source: *Základy FT-NIR spektrometrie. Presentation. Nicolet CZ, 2008.*)

Calibration for quantitative purposes in NIR spectrometry requires development of calibration models with the use of advanced chemometric algorithms which require an extensive set of standards (at least 30 calibration samples). The set must be sufficiently representative to cover the entire expected or predicted variability of the sample characteristics which are to be quantified. The most applied methods of chemometric algorithms are currently the methods of principal component regression (PCR), partial least squares (PLS), classical least squares (CLS), inverse least squares (ILS) and multiple linear regression (MLR). Calibration model using these regression methods uses an entire NIR spectrum or a spectrum section, whereas maximum absorbances of only selected bands are not sufficient. The aim is to find a relationship between the multidimensional spectral information (represented by a matrix of absorbance values in the selected spectral section of a calibration set) and the composition of samples (represented by a matrix of concentration values of an observed group of analytes from the set of the calibration samples).

The above discussed enables a wide use of quantitative NIR analysis in many industries, such as food processing, petrochemical and paper industry and pharmacy. It is also possible to quantify complex samples and to determine many components or variables together, because the spectrum is evaluated as a whole and practically forms a "fingerprint" for a given mixture. Acquisition of NIR spectra

requires several seconds and can be performed during manufacturing process. Therefore, the NIR spectroscopy is used for process analytical technology as it allows fast and continuous on-line analysis of the manufacturing process, monitoring of the whole production state, and immediate determination of any deviation and its following corrections. This enables simultaneous determination of fat, protein, lactose and urea contents in milk and dairy products (in various stages of their processing), or carbohydrate and ethanol content in alcoholic beverages (during ongoing fermentation), octane number in gasoline, etc.

2.3.3 NIR spectra measurement techniques

Main advantage of the NIR spectroscopy is the ability to measure samples through glass and other transparent packaging materials. The measurement is fast, non-destructive, and requires no special sample preparation. This minimizes the consumption of chemicals and disposable analytical material. Much more laborious and time-consuming than the actual spectra measurement is the subsequent processing and evaluation of measured data.

Radiation can interact with solid matter in several ways, as illustrated in Fig. 2.5. The appropriate NIR measurement mode will be dictated by the optical properties of the samples. Transparent materials are usually measured in transmittance mode (A). Turbid liquids or semi-solids, and solids may be measured in diffuse transmittance (B), diffuse reflectance (C) or transreflectance (D/E) modes, depending on their absorption and scattering characteristics. NIR radiation is specifically modulated by interaction of a diffuse reflectance with particles of different size (Fig. 2.18).

In general, NIR spectra can be measured as attenuation of radiation flow after passage through a sample (transmittance measurements) or after reflection on the sample (reflectance technique). The principle is illustrated in Fig. 2.19. Identically as in the mid region, the spectra measured in transmittance or reflectance modes are afterwards converted into absorbance.

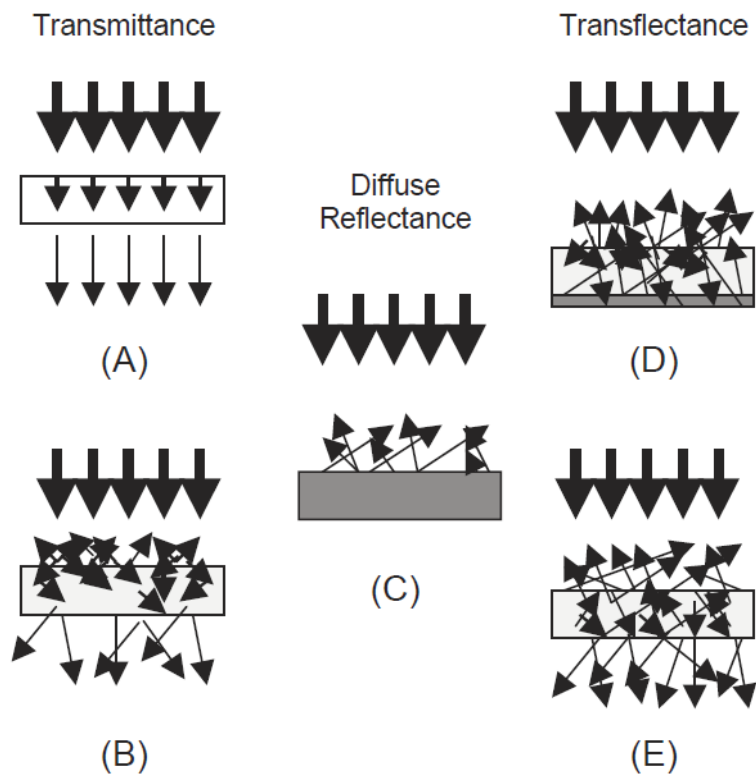


Figure 2.18. NIR measuring modes: transmittance (A/B), diffuse reflectance (C) and transflectance (D/E).

(Edited according to: Reich G. *Near-infrared spectroscopy and imaging: Basic principles and pharmaceutical applications*. *Adv. Drug Deliv. Rev.* 2005, 57, 1109–1143.)

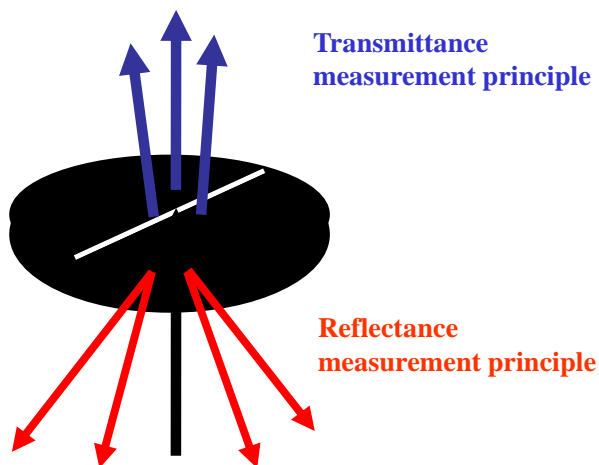


Figure 2.19. Principle of transmittance and reflectance measurements.

(Edited according to *Vzorkovací techniky v FT-NIR spektrometrii*. Presentation. Nicolet CZ, 2008.)

The most applied principle in reflectance techniques is the diffuse reflectance infrared Fourier transform (DRIFT) where the incident radiation is reflected from the surface of individual small powder particles (Fig. 2.20). This approach is most often applied in pharmaceutical industry analysis.

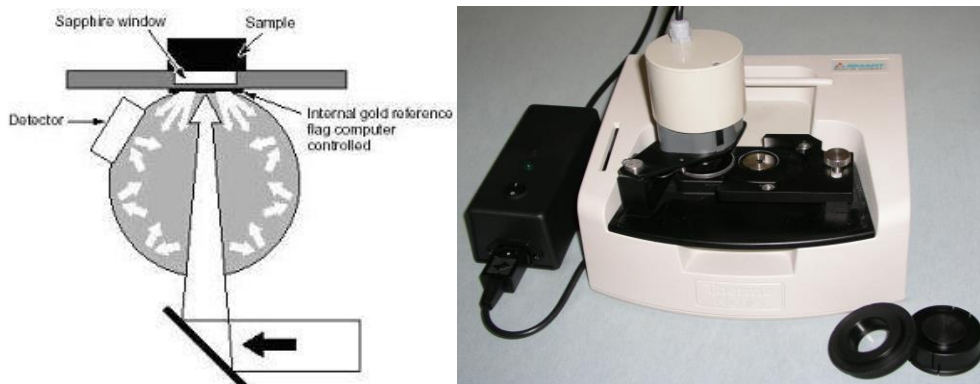


Figure 2.20. Diffuse reflectance (DRIFT) principle and UpDrift adapter with modification for sample rotation.

(Source: *Vzorkovací techniky v FT-NIR spektrometrii. Presentation. Nicolet CZ, 2008.*)

Transmittance measurements are used for measurement of liquids, mash samples, and polymeric films. Liquid samples must be measured in cells. Optical layer thickness of cuvettes ranges from 1 to 10 mm, and their selection is optimized depending on the actual concentration of the analyte in solution and depending on the optical properties of the solvent.

Combination of the two above mentioned approaches is a technique called “transflectance”. It can be used for measurements of thin suspensions, liquids, or solutions. The technique uses special cells with bottom covered with by a totally reflective (mirror) thin layer which reflects the radiation passed through the sample, providing repeated passage through the sample and continuation to the detector (Fig. 2.21).

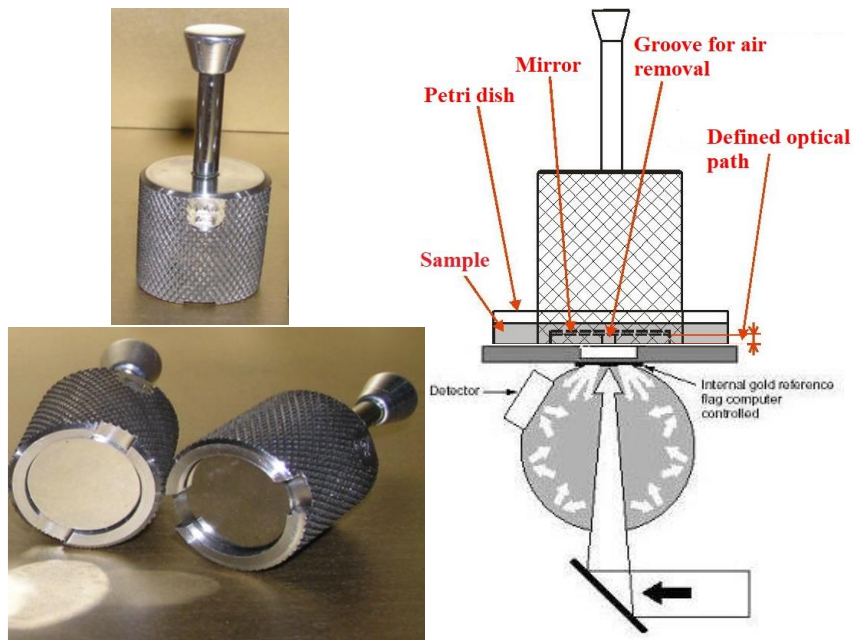


Figure 2.21. Cuvettes for transfection NIR measurements and the measurement principle.

(Source: *Vzorkovací techniky v FT-NIR spektrometrii. Presentation. Nicolet CZ, 2008.*)

Besides the above-mentioned procedures where the sample is placed in a holder, variously modified instruments (Fig. 2.22) for reflectance measurements often use fiber optics with different probes (Fig. 2.23) that can be placed directly in a production apparatus or in the measured sample (Fig. 2.24).

NIR techniques maintain a special position in PAT (process analytical technology). Whole NIR spectrometers can be attached to other devices so that an entire production process can be directly observed, and its course monitored on-line/in-line. In pharmacy, an entire powder production process can be monitored this way. This arrangement used in PAT thus represents a completely non-contact analysis and offers a possibility for monitoring of standard deviations for individual components and the final mixture. This enables an on-line control of powder mixture uniformity or real-time analytical control of tablet blending and eliminates losses caused by imperfect production control. The device is shown in Fig. 2.25.



Figure 2.22. Various instruments for reflectance measurements.
(Source: *Vzorkovací techniky v FT-NIR spektrometrii*. Presentation, Nicolet CZ, 2008.)



Figure 2.23. NIR-Multiplexer system with different types of probes.
(Source: *Vzorkovací techniky v FT-NIR spektrometrii*. Presentation, Nicolet CZ, 2008.)



Figure 2.24. NIR analyzers for remote process monitoring with simultaneous fiber multiplexing technology and integrated communication for real-time feedback or direct control of the production process in real time by deployment to production equipment.

(Source: Vzorkovací techniky v FT-NIR spektrometrii. Presentation. Nicolet CZ, 2008.)



Figure 2.25. NIR analyzers connected to a homogenization apparatus. Integration of in-line NIR analysis in a fluid bed dryer.

(Source: Vzorkovací techniky v FT-NIR spektrometrii. Presentation. Nicolet CZ, 2008. Metrohm AG and AZO Materials, 2022)

2.3.4 NIR analysis strategies

NIR instrumentation can be installed in a laboratory or directly implemented in a manufacturing process or reactor. Overall, the most appropriate NIR measurement mode and location of the NIR analyzer is dictated by the optical properties of the sample, required analyte selectivity and sensitivity, duration of the process run, and the monitoring and control requirements. Analysis strategies can thus be distinguished according to the general application:

- laboratory
- at-line
- on-line
- in-line

Laboratory analysis is represented by a single NIR instrument that can support multiple manufacturing operations from raw material inspection or in-process analysis to finished product release. This configuration provides the greatest flexibility as both the reflectance and transmittance measurements can be performed on processed samples, feedstock, ingredients, raw materials, effluents, and final products. Laboratory strategies require manual sampling, and the turnaround time can thus take up to 1 hour even though the NIR analysis requires less than a minute. This strategy is most useful for supporting pilot plant/scale up facilities, or measurement for long duration runs where the process information is required infrequently.

For at-line analysis strategy, a NIR analyzer is located close to a process stream. This analyzer configuration is dedicated to performing a particular analysis on a specific sample type, e.g., transmittance measurements of solid dosage forms. The at-line analysis strategies require manual sampling, and the analyzer must meet appropriate classification. This strategy is well fit for process monitoring and control strategies, and for manufacturing operations.

When a NIR analyzer is incorporated into a process using a sample-loop and performs a particular analysis on a particular sample type, the strategy can be designated as on-line. Here, the NIR measurements are performed on a continuous flow of a sample as it passes through a flow-cell. Side-streams provide a convenient means for sample conditioning such as heating, filtering, or degassing or for maintenance, calibration, sample collection – all while the process is running. On-line strategies provide automatic and near real-time (results in < 10 s) analyses of specific media and are always optimized for one application. This strategy is well

suited for closed-loop monitoring and control strategies for scale-up and manufacturing operations.

With the in-line analysis strategy, a process NIR analyzer is implemented directly into the process using a fiber optics and a stainless steel (or other material) probe that is inserted directly into a port installed into the process stream or vessel. This analyzer configuration is dedicated to performing a particular analysis on a specific sample type, e.g., reflectance analysis in a dryer. A direct interface requires minimal additional hardware, but its maintenance cannot be performed unless the process is shut down. In addition, for transmittance analysis, the narrow optical path lengths and fluid dynamics of the process streams can sometimes make this analysis strategy difficult to implement. An in-line analyses provides automatic, near real-time (results in < 10 s) measurement of specific media and is optimized for one particular application. This strategy is well suited for closed-loop monitoring and control strategies for scale-up and manufacturing operations.

2.3.5 Application of NIR spectroscopy in pharmacy

The application of NIR spectroscopy is expanding since the 90's of the 20th century, along with the development of new IR spectrometers with Fourier transformation for near region. FT-NIR spectroscopy is a fast non-destructive, non-invasive analytical method which currently offers a wide application range and allows to replace more laborious and demanding methods in analytical chemistry. It can be used for testing of final products, product uniformity monitoring, and verification of raw materials. It allows on-line/in-line monitoring of production processes and is widely used in PAT.

The measured spectra can be used for both qualitative and quantitative analysis. Data processing depends on its application. The spectra obtained for qualitative evaluation need to be compared with the spectra of a standard, and this approach is suitable for small sample numbers. Large sets of spectra are better evaluated using chemometric statistical data processing. Statistical evaluation of qualitative and quantitative data is possible by several evaluation methods. The most general categorization of statistical methods is the division into one-dimensional and multidimensional data analysis, and analysis of variance.

In pharmacy, the NIR spectroscopy is used for both qualitative and quantitative application. It must be pointed out that for both qualitative and quantitative analyses, it is required to measure a standard or series of standards. The data processing in most of the applications requires multivariate calibration models which are often automated.

The most common NIR applications are:

- identification of all raw materials
- identification of polymorphism of active substances and excipients
- API content monitoring
- content uniformity testing for batch units
- stability testing
- compatibility testing
- water content, residual solvents monitoring
- particle size determination
- hardness determination
- prediction of dissolution
- homogeneity determination, NIR-imaging (with microscope)
- on-line/in-line analyses, PAT

NIR spectroscopy can be used to distinguish structurally related molecules. Fig. 2.26 shows examples of different alcoholic sugars, and Fig. 2.27 shows common hexoses.

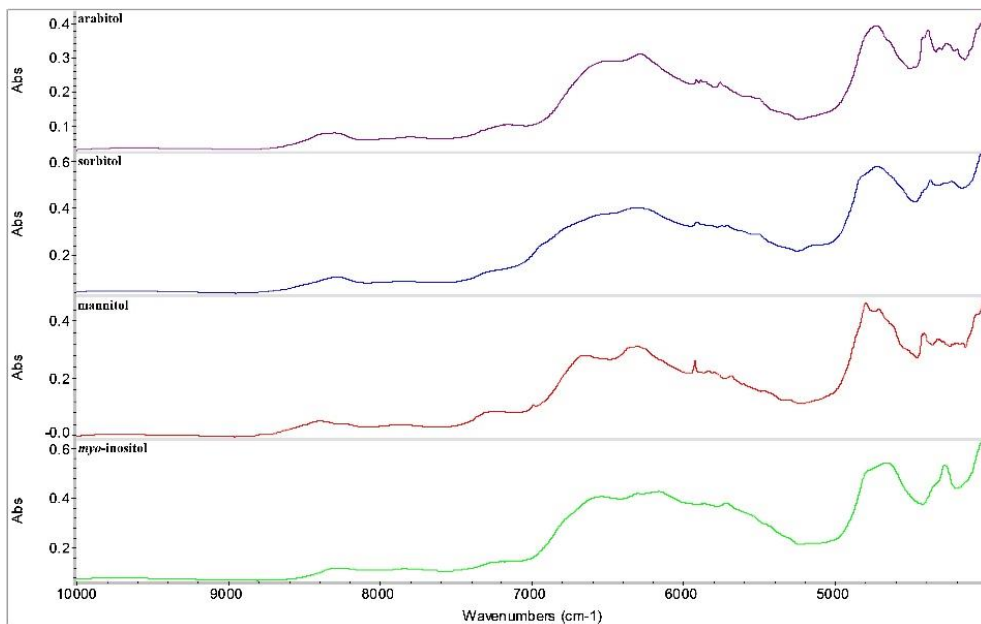


Figure 2.26. NIR spectra of alcoholic sugars.

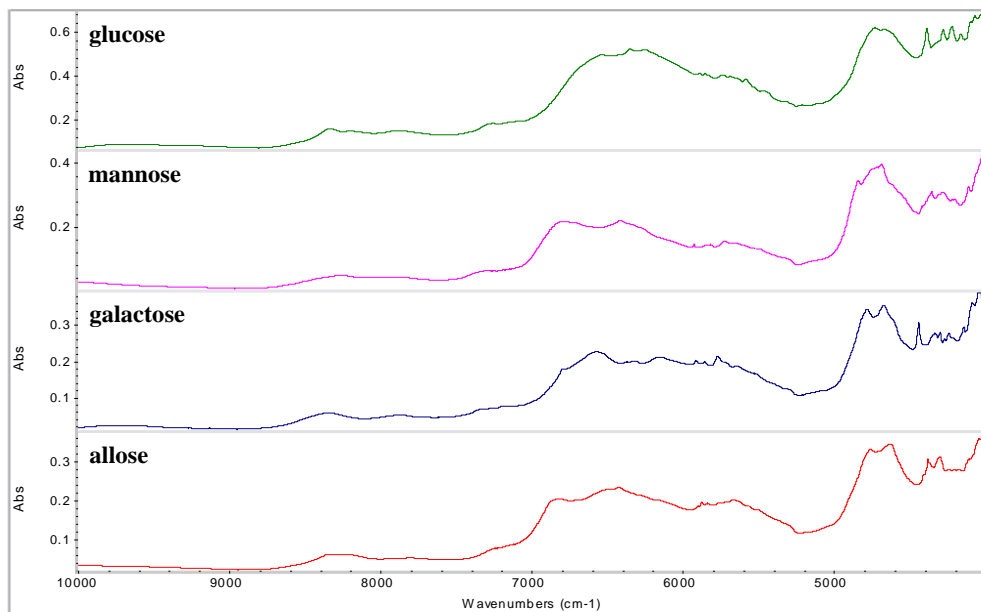


Figure 2.27. NIR spectra of hexoses (pyranoses).

Discrimination between salts and free acids or bases, as well as identification of a particular salt type (sodium, potassium or also monosodium, disodium) is very important. Fig. 2.28 illustrates examples of tartaric acid and its various salts.

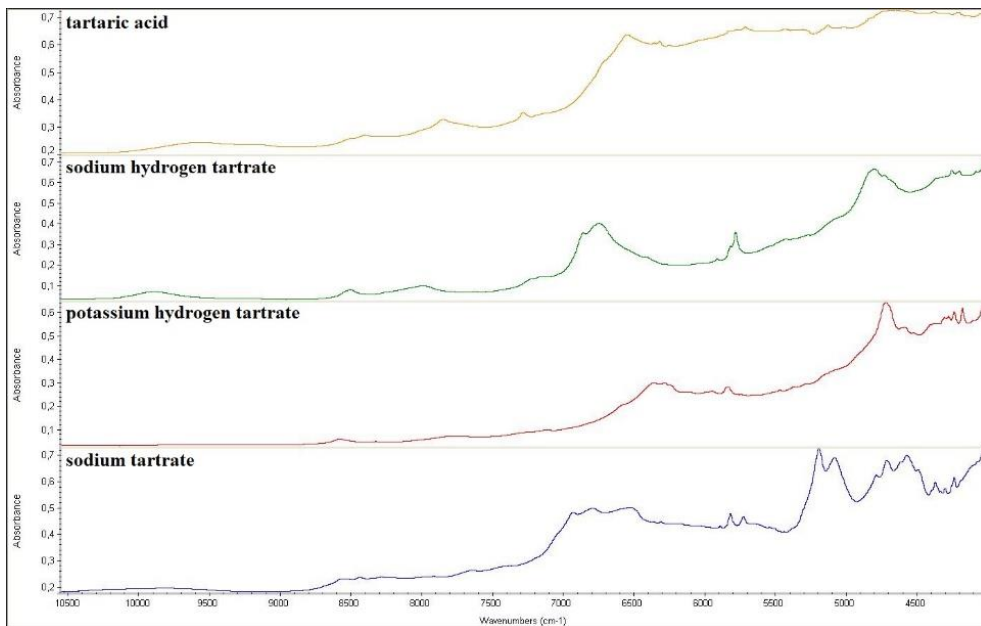


Figure 2.28. NIR spectra of tartaric acid and its various salts.

A very important application is the recognition of individual API polymorphs. Fig. 2.29 contains examples of NIR spectra of different polymorphs of one API.

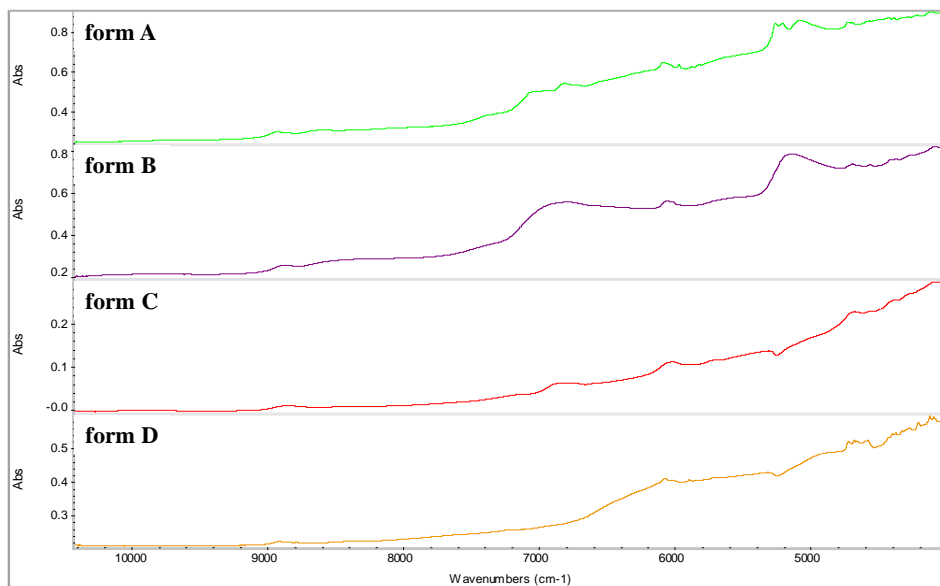


Figure 2.29. NIR spectra of different polymorphs of one API.

Fig. 2.30 shows examples of spectra of a desired API polymorph and polymorphically impure API. All measured spectra were subsequently evaluated by discriminant analysis and the record is shown in Fig. 2.31.

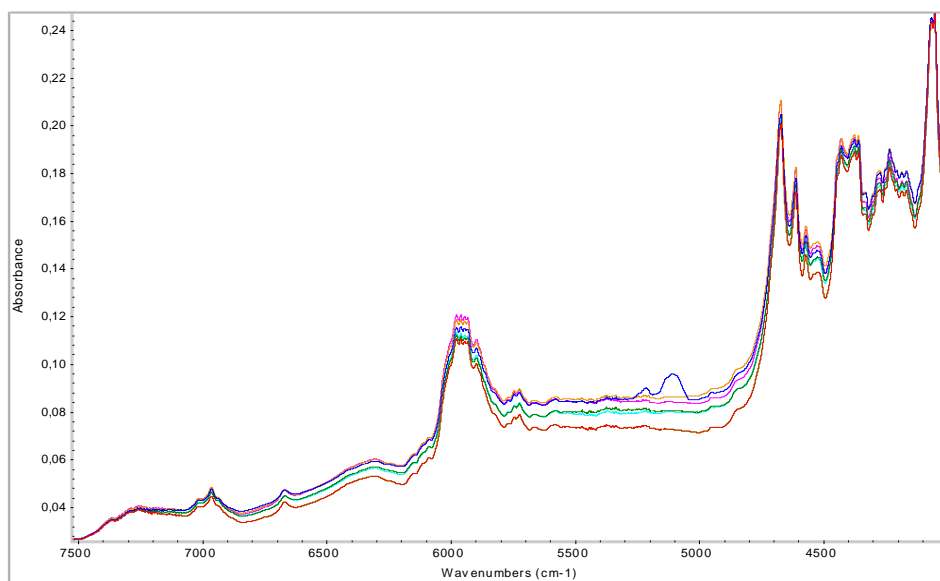


Figure 2.30. A clearly visible change in $5000\text{--}5300\text{ cm}^{-1}$ range for an API of the undesired polymorph in comparison with spectra of other samples.

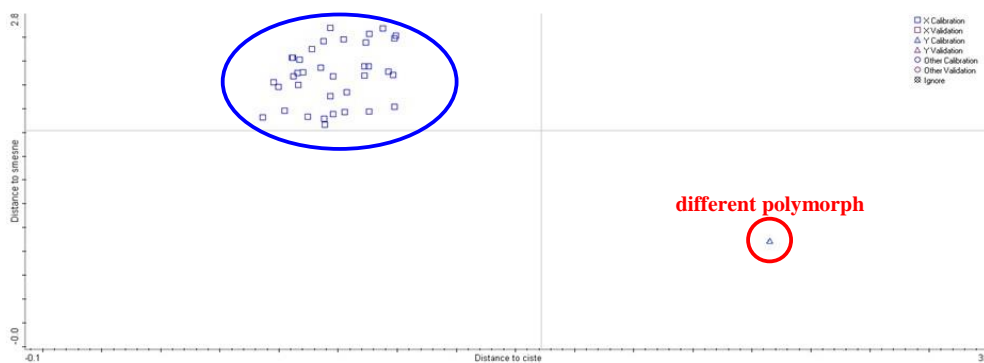


Figure 2.31. Resolution of polymorphically different API samples, 2D view.

At this point, it should be noted that the NIR spectra are similar to fingerprints. Beer-Lambert law cannot be used for NIR spectrometry. Instead, a set of standards is needed for accurate quantification, and the above-mentioned chemometrics must be used. Both the solid phase form and the particle size, moisture (residual solvent

content), compression, production method, impurities, etc., are projected into the spectra. Figure 2.32 shows spectra processed by discriminant analysis for APIs that meet the specification criteria/limits but were produced by two different manufacturers.

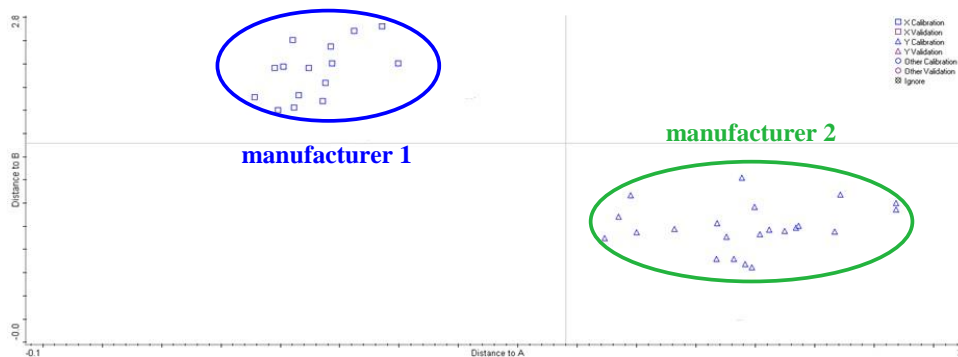


Figure 2.32. Resolution of the same API of two different manufacturers, 2D view.

As mentioned, particle size has great influence on NIR spectra shape. Fig. 2.33 shows spectra of sucrose compressed into tablets under high pressure, crystalline sucrose, and a finely ground sucrose. Differences are apparent especially in height of the particular bands.

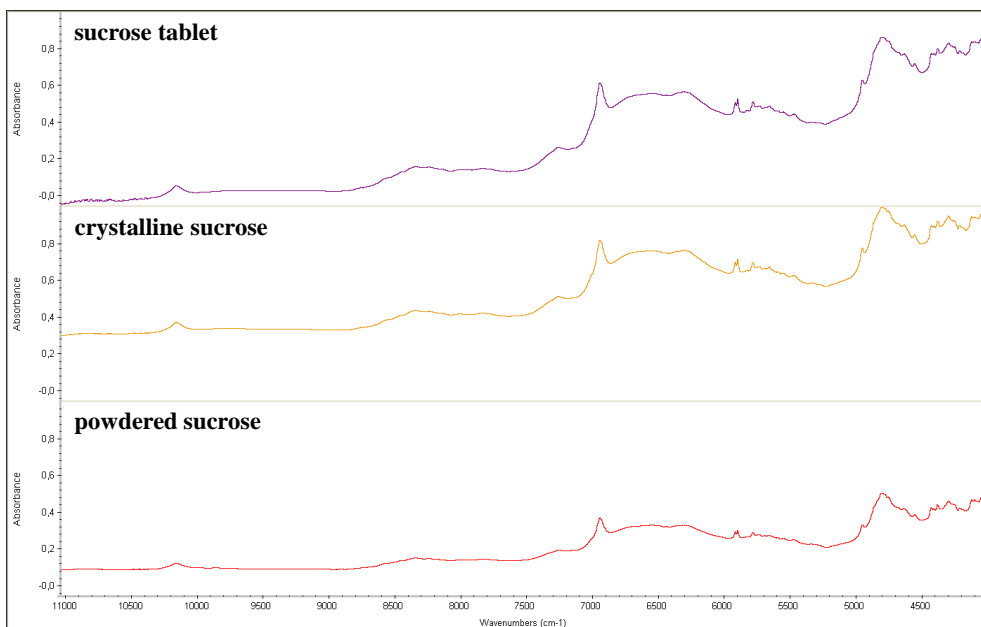


Figure 2.33. NIR spectra of sucrose, differing in particle size.

Fig. 2.34 shows the NIR spectra of different API batches with different particle size. The differences are evident in the height of the individual bands. All measured spectra were subsequently processed by chemometrics with the partial least square method. The sample evaluation was based on the differences in the height of the individual bands with a correlation for the particle size values measured by the laser diffraction method. The result is shown in Fig. 3.35.

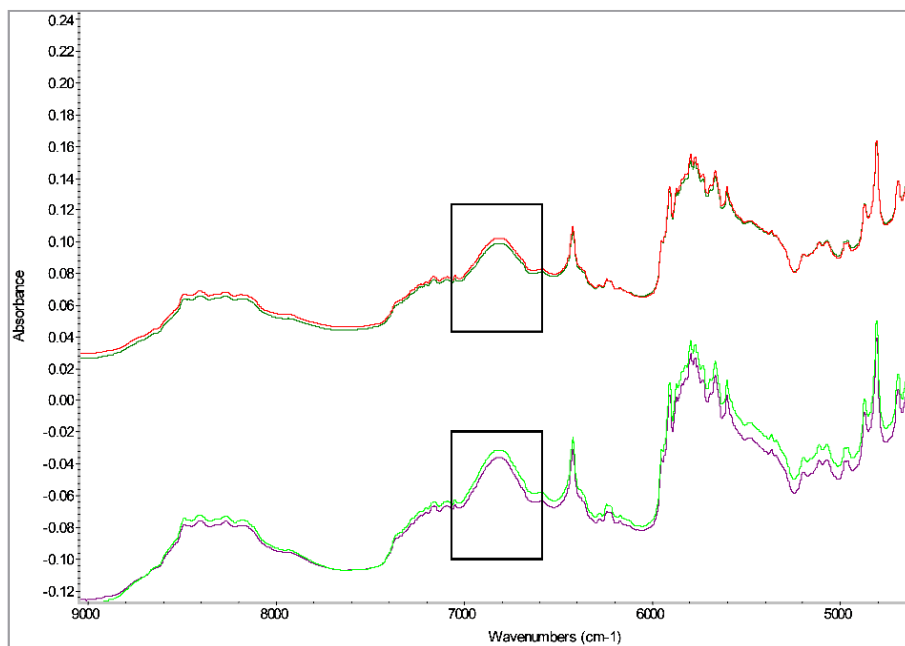


Figure 2.34. NIR spectra of different batches of an API with different particle size, projected to the height of individual bands.

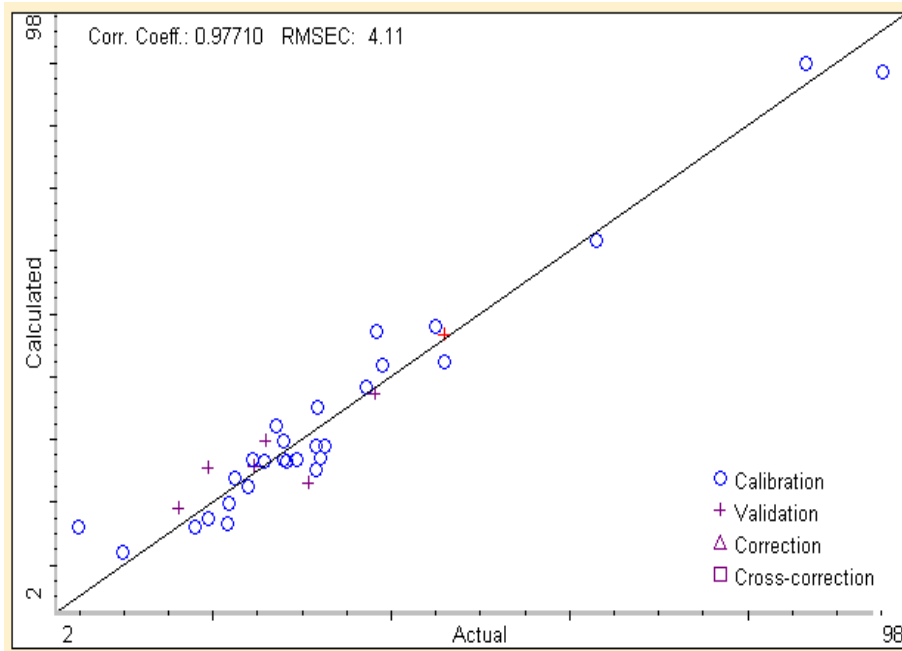


Figure 2.35. Sample evaluation based on differences in the height of individual bands vs. values from laser diffraction. Processed by partial least squares.

Tablets of different hardness (i.e., tableted at different pressures) were measured by NIR spectrometry. Calibration was performed based on the height of the selected band in the NIR spectra compared to the measured hardness. Fig. 2.36 shows 3 groups of tablets with different hardness, as evaluated by principal component analysis method.

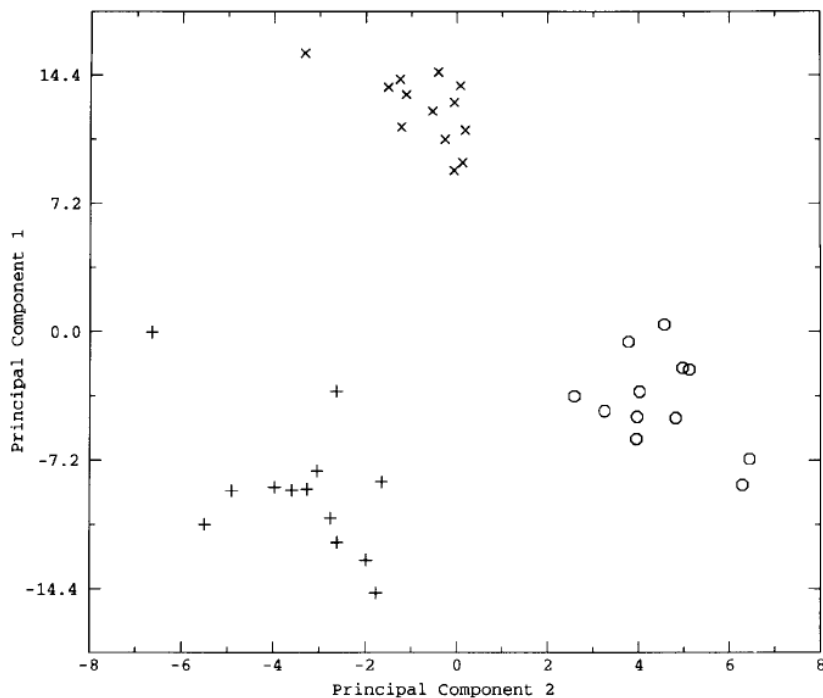


Figure 2.36. Result of the evaluation of samples of tablets of different hardness processed by principal component analysis method.

It is also possible to determine the content of residual solvents in APIs. Fig. 2.37 shows spectra of an API with various residual ethanol content. The exact ethanol content was determined using gas chromatography. Subsequently, a calibration for following NIR-based API testing was created through assigning NIR spectra to specific ethanol content values (Fig. 2.38).

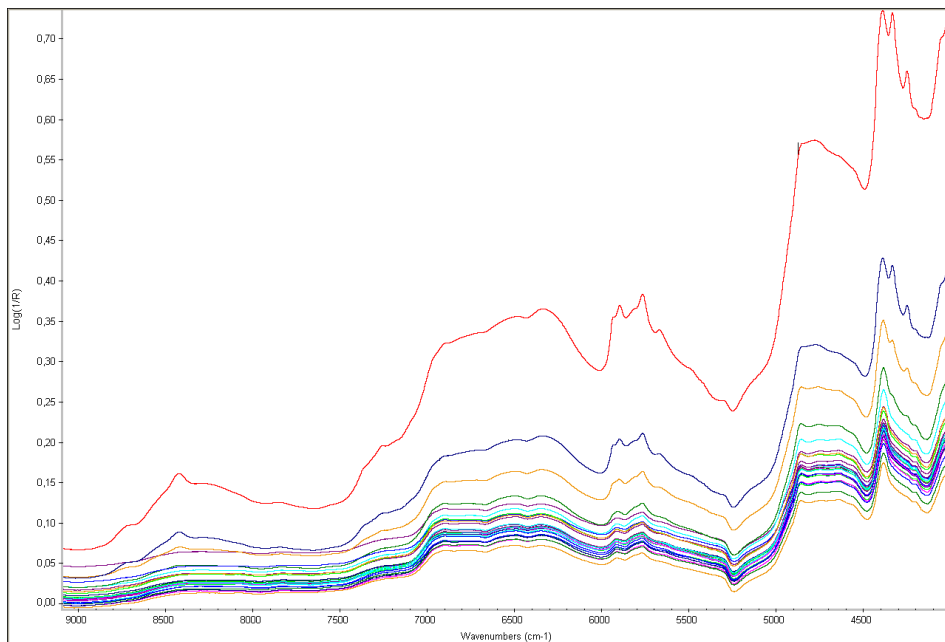


Figure 2.37. NIR spectra of an API with different residual ethanol content.

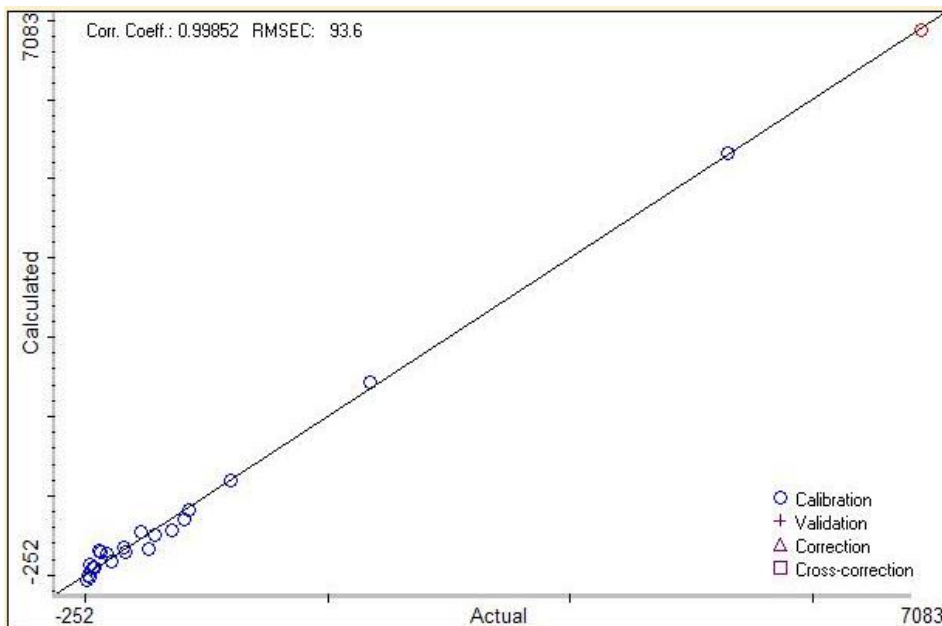


Figure 2.38. Evaluation of residual ethanol content in an API. The calibration and evaluation of samples is based on comparing the differences in individual spectra vs. gas chromatography. Processed by discriminant analysis.

The evaluation of API content in tablets is widespread; an example is shown in Fig. 2.39. For this purpose, various autosamplers and adapters for reflectance measurements are preferably used (as shown, for example, in Fig. 2.22). This is an excellent quantification method because it can be fully automated. On the other hand, the implementation of such methodology is more demanding as many standards must be prepared so the methodology is suitable for frequent routine analyzes of large product volumes within the output quality control. A crucial condition for the application of the method is a sufficient API amount in the tablet (at least 2%) and non-interfering excipients.

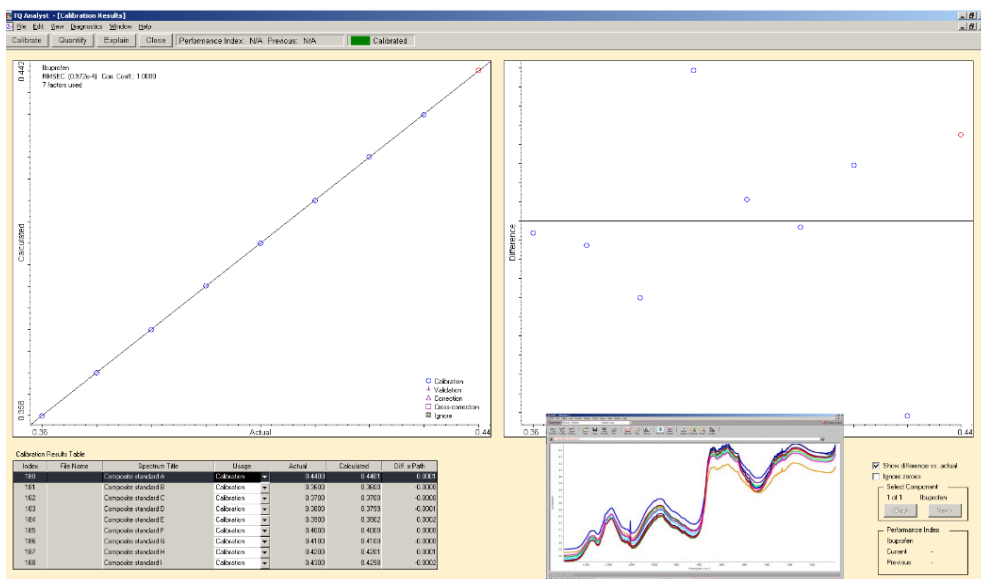


Figure 2.39. Determination of API content in tablets.

(Source: *Základy NIR spektrometrie a její praktické využití. Presentation. Nicolet CZ, 2009.*)

Currently, dissolution represents one of the key methods for evaluation of solid oral dosage forms and their release, consistency, similarity, and therapeutic efficacy. Dissolution testing however involves a series of time-consuming analytical tasks which require labor-intensive protocols, such as instrument calibration, media preparation, sample collection, data collection, and drug assays. Some approaches interconnecting dissolution testing and NIR spectroscopy were therefore developed:

- monitoring of the effect of humidity stress on dissolution quality
- monitoring of the effect of core coating layer on dissolution quality
- monitoring of the effect of particle size on dissolution quality

All these methods correlate the NIR spectra and changes in monitored dissolution parameter (% of released API).

For dissolution quality and humidity stress monitoring, the NIR spectra are measured first along with the dissolution of an unstressed sample. Then, the samples are treated in stability chamber at a defined humidity, and the NIR spectra and dissolution of the stressed samples is measured in parallel at predefined time intervals. Correlation of the changes in a selected dissolution parameter and the NIR spectra is performed after dependence determination. Afterwards, the NIR spectroscopy can be used for further analyses.

Monitoring of the effect of tablet core coating layer on dissolution requires a preparation of a series of coated tablets with a defined coating layer thickness. Afterwards, the NIR spectra are measured along with dissolution of the coated cores, and the correlation between dissolution performance and the NIR spectra is performed after dependence determination. Afterwards, the NIR spectroscopy can be used for further analyses.

For monitoring of particle size effect on the dissolution of a final drug formulation manufactured with a standard process and a constant composition, the calibration and sample evaluation is based on differences in height of individual bands.

Chemical mapping is a technique combining spatial and chemical information. It provides advantages for both powder mixture and drug formulation analyses, such as determination of component size and distribution, polymorphic distribution, hydration degree, detection of heterogeneous particles or determination of coating type and thickness. Spatial resolution is in the order of micrometers. The acquired data can be used for both understanding and optimization of the applied technology and processes.

NIR enables to monitor homogeneity of both API and the whole sample for example during granule production or tableting. NIR spectra measured using traditional UpDrift (reflectance) are illustrated in Fig. 2.40. Several positions on a tablet are measured and the variance in individual spectra from one and several tablets is evaluated.

Tablet homogeneity can also be determined by NIR imaging. The surface of the sample is measured using a microscope coupled to a NIR spectrometer and then the spectra are processed by chemometrics. Examples of this measurement type are shown in Fig. 2.41.

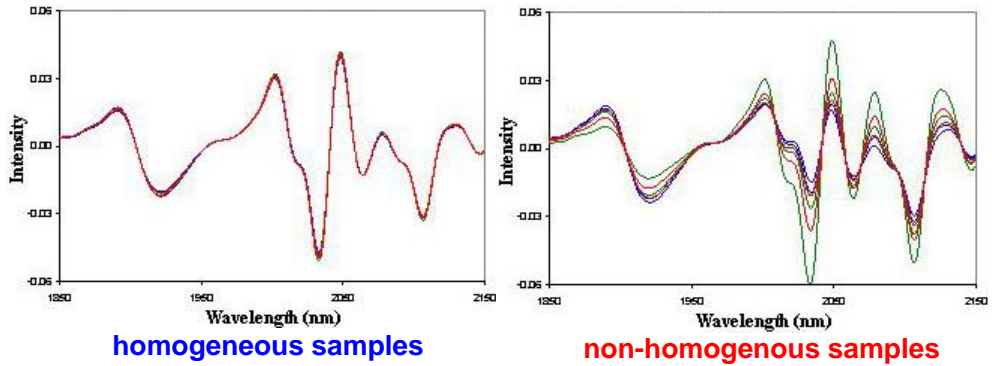


Figure 2.40. Difference in spectra of homogeneous and non-homogeneous tablets.

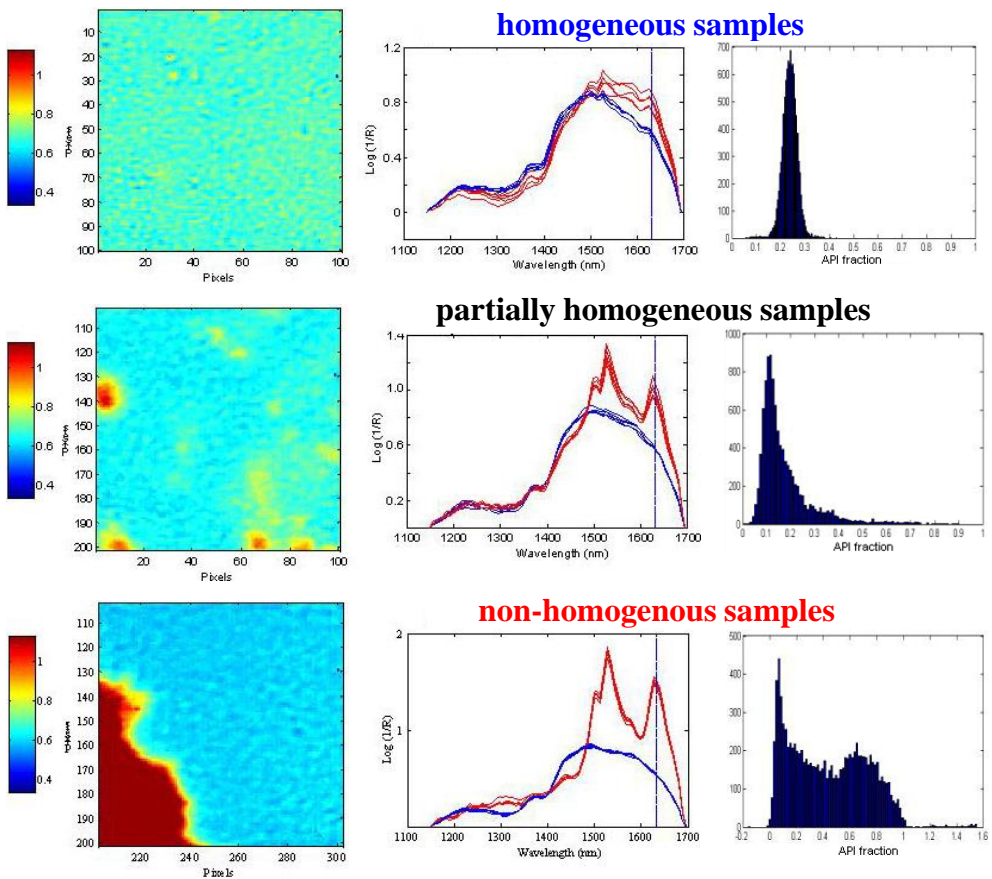


Figure 2.41. NIR imaging applied in tablet homogeneity evaluation.

As indicated above, NIR is advantageously used in PAT. The non-contact analysis is used primarily for manufacturing process control, e.g., during granulation or direct compaction, homogeneity monitoring (deviations in single components, as well as of whole mixtures), see Fig. 2.42. The monitoring of these processes plays an important role in quality maintenance for various “high-risk formulations”. A disadvantage is the limit of detection, where the monitored component is required to be present in at least 2%.

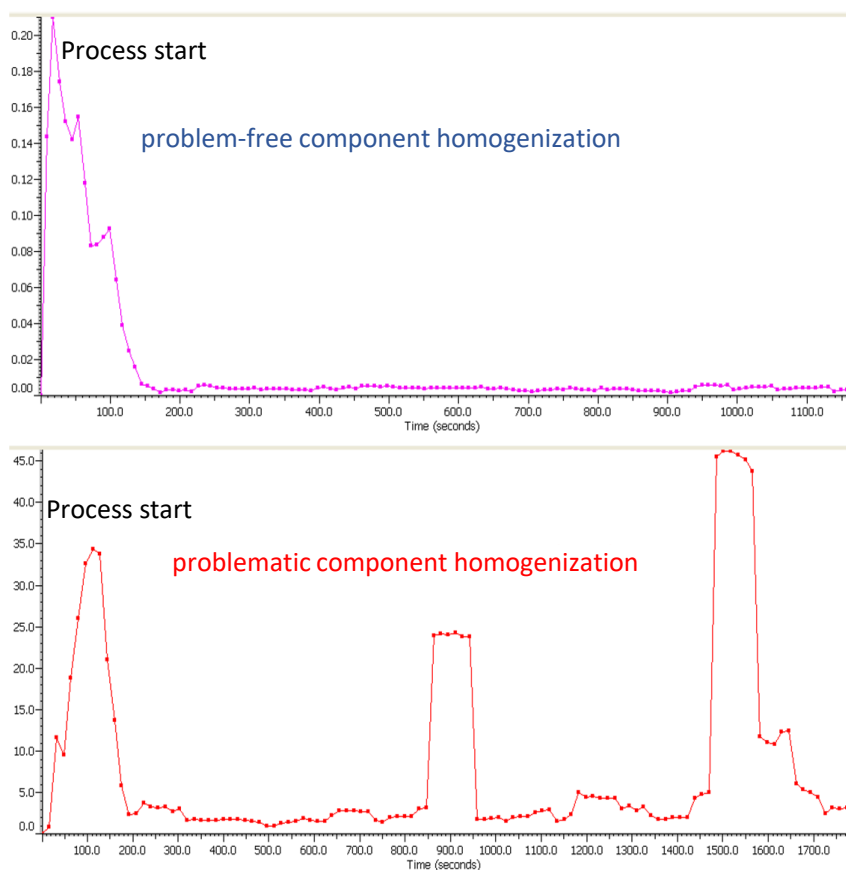


Figure 2.42. The course of NIR analysis recording during homogenization.

2.4 Resources and recommended literature

Basic principles of vibrational spectral methods

1. Smith B. Infrared Spectral Interpretation. CRC Press: Boca Raton, USA, 1999.
2. Socrates G. Infrared and Raman Characteristic Group Frequencies. John Wiley & Sons: New York, USA, 2001.
3. Griffiths P. R., de Haseth J. A. Fourier Transform Infrared Spectrometry, 2nd Edition. John Wiley & Sons: New York, USA, 2007. <https://doi.org/10.1002/047010631X>
4. Pivonka D. E., Chalmers J. M. Application of Vibrational Spectroscopy in Pharmaceutical Research and Development. John Wiley & Sons: New York, USA, 2007.

Infrared spectroscopy in mid region

5. Infračervená spektra a struktura molekul. Horák M., Papoušek D., Eds.; Akademia: Prague, Czech Republic, 1976.
6. Strauch B. Infračervená spektroskopie s Fourierovou transformací. SNTL: Prague, Czech Republic, 1988.
7. Roeges N. P. G. A Guide to the Complete Interpretation of Infrared Spectra of Organic Structures. John Wiley & Sons: New York, USA, 1994.
8. Silverstein R. M., Webster F. X., Kiemle D. J. Spectrometric Identification of Organic Compounds, 7th Edition. John Wiley & Sons: New York, USA, 2005.
9. Rouessac F., Rouessac A. Infrared Spectroscopy. In Chemical Analysis – Modern Instrumentation Methods and Techniques, 2nd Edition; John Wiley & Sons: Chichester, UK, 2007.

Infrared spectroscopy in near region

10. Dreassi E., Ceramelli G., Corti P., Lonardi S., Perruccio P. L. Near Infrared Reflectance Spectroscopy in the Determination of the Physical State of Primary Materials in Pharmaceutical Production. *Analyst*. 1995, 120 (4), 1005–1008. <https://doi.org/10.1039/an9952001005>
11. Dreassi E., Ceramelli G., Corti P., Massacesi M., Perruccio P. L. Quantitative Fourier Transform Near-Infrared Spectroscopy in the Quality Control of Solid Pharmaceutical Formulations. *Analyst*. 1995, 120 (9), 2361–2365. <https://doi.org/10.1039/an9952002361>
12. Kirsch J. D., Drennen J. K. Determination of Film-Coated Tablet Parameters by Near-Infrared Spectroscopy. *J. Pharm. Biomed. Anal.* 1995, 13 (10), 1273–1281. [https://doi.org/10.1016/0731-7085\(95\)01562-Y](https://doi.org/10.1016/0731-7085(95)01562-Y)

13. Pharmaceutical Analytical Sciences Group. Guidelines for the development and validation of near infrared (NIR) spectroscopic methods. <http://www.pasg.org.uk/NIRmay01.pdf>. May.2001.
14. Lyon R. C., Lester D. S., Lewis E. N., Lee E., Yu L. X., Jefferson E. H., Hussain A. S. Near-Infrared Spectral Imaging for Quality Assurance of Pharmaceutical Products: Analysis of tablets to Assess Powder Blend Homogeneity. *AAPS PharmSciTech*. 2002, 3 (3), 1-15. <https://doi.org/10.1208/pt030317>
15. Reich G. Near-Infrared Spectroscopy and Imaging: Basic Principles and Pharmaceutical Applications. *Adv. Drug Delivery Rev.* 2005, 57 (8), 1109–1143.
16. Cogdill R. P., Anderson C. A., Delgado-Lopez M., Molseed D., Chisholm R., Bolton R., Herkert T., Ali M. Afnan, and Drennen J. K. Process Analytical Technology Case Study Part I: Feasibility Studies for Quantitative Near-Infrared Method Development. *AAPS PharmSciTech*. 2005, 6 (2) E263–273. <https://doi.org/10.1208/pt060238>
17. Cogdill R. P., Anderson C. A., Delgado-Lopez M., Chisholm R., Bolton R., Herkert T., Ali M. Afnan, and Drennen J. K. Process analytical Technology Case Study: Part II. Development and validation of Quantitative Near-Infrared Calibrations in support of a Process Analytical Technology Application for Real-Time Release. *AAPS PharmSciTech*. 2005, 6 (2) E273–283. <https://doi.org/10.1208/pt060238>
18. Blanco M., Valdes D., Llorente I., Bayod M. Application of NIR Spectroscopy in Polymorphic Analysis: Study of Pseudo-Polymorphs Stability. *J. Pharm. Sci.* 2005, 94 (6), 1336–1342. <https://doi.org/10.1002/jps.20362>
19. Blanco M., Alcala M. Content uniformity and tablet hardness testing of intact pharmaceutical tablets by near infrared spectroscopy: A contribution to process analytical technologies. *Anal. Chim. Acta* 2006, 557 (1–2), 353–359. <https://doi.org/10.1016/j.aca.2005.09.070>
20. Matějka P. Spektrometrie v blízké infračervené oblasti. Studijní materiály. Ústav analytické chemie, Fakulta chemicko-inženýrská, VŠCHT: Prague, Czech Republic, 2007.
21. Luypaert J., Massart D. L., van der Heyden Y. Near-Infrared Spectroscopy Applications in Pharmaceutical Analysis. *Talanta*. 2007, 72 (3), 865–883. <https://doi.org/10.1016/j.talanta.2006.12.023>
22. Roggo Y., Chalus P., Maurer L., Lema-Martinez C., Jent N. A Review of Near Infrared Spectroscopy and Chemometrics in Pharmaceutical Technologies. *J. Pharm. Biomed. Anal.* 2007; 44 (3), 683–700. <https://doi.org/10.1016/j.jpba.2007.03.023>

23. Tabasi S. H., Fahmy R., D. Bensley, O'Brien C., Hoag S. W. Quality by Design, Part I: Application of NIR Spectroscopy to Monitor Tablet Manufacturing Process. *J. Pharm. Sci.* 2008, 97 (9), 4040–4051. <https://doi.org/10.1002/jps.21303>
24. Základy FT-NIR spektrometrie. Prezentace. Nicolet CZ, Thermo Scientific, 2008.
25. Vzorkovací techniky v FT-NIR spektrometrii. Prezentace. Nicolet CZ, Thermo Scientific, 2008.
26. Tabasia S. H., Moolchandania V., Fahmy R., Hoag S. W. Sustained Release Dosage Forms Dissolution Behavior Prediction: A study of Matrix Tablets Using NIR Spectroscopy. *Int. J. Pharm.* 2009, 382 (1–2), 1–6. <https://doi.org/10.1016/j.ijpharm.2009.07.029>
27. Základy NIR spektrometrie a její praktické využití. Prezentace. Nicolet CZ, Thermo Scientific, 2009.
28. Hattori Y., Otsuka M. NIR spectroscopic study of the dissolution process in pharmaceutical tablets. *Vib. Spectrosc.* 2011, 57 (2), 275–281. <https://doi.org/10.1016/j.vibspec.2011.09.003>
29. Metrohm. NIR Spectroscopy: A guide to Near-Infrared Spectroscopic Analysis of Industrial Manufacturing Processes. http://www.mep.net.au/wpmp/wp-content/uploads/2013/05/MEP_Monograph_NIRS_81085026EN.pdf. February 2013.
30. United States Pharmacopeia USP 35-NF 30, General chapter <1119> Near-Infrared Spectroscopy, 2013.
31. Pan D., Crull G., Yin S., Grosso J. Low level drug product API form analysis – A validated tablet NIR quantitative method development and robustness challenges. *J. Pharm. Biomed. Anal.* 2014; 89, 268–275. <https://doi.org/10.1016/j.jpba.2013.11.011>
32. European Medicines Agency. Guideline on the use of near infrared spectroscopy by the pharmaceutical industry and the data requirements for new submissions and variations. https://www.ema.europa.eu/en/documents/scientific-guideline/guideline-use-near-infrared-spectroscopy-pharmaceutical-industry-data-requirements-new-submissions_en.pdf. January 2014.
33. McDowall R. D., Smith P. Quo Vadis Regulated NIR Analytical Procedures? *Spectroscopy* 2015, 30 (12) 10–16.
34. Otto M. *Chemometrics: Statistics and Computer Application in Analytical Chemistry*, 3rd ed., Wiley-VCH: Weinheim, Germany, 2017. <https://doi.org/10.1002/9783527699377>
35. FDA. Guidance for Industry: PAT - A Framework for Innovative Pharmaceutical Development, Manufacturing, and Quality Assurance, <https://www.fda.gov/media/71012/download>. August 2018.

36. Miller J., Miller J. C. *Statistics and Chemometrics for Analytical Chemistry*. Pearson Education, 2018.
37. Sahoo N. K, Chandana G. M. H., Vaishnavi, G. *Pharmaceutical Applications and Importance of Near Infrared Spectroscopy*. *Med. Analy. Chem. Int. J.* 2020, 4 (1) 000155.
38. Otsuka M. *Near-Infrared Spectroscopy Application to the Pharmaceutical Industry*. In: *Encyclopedia of Analytical Chemistry: Applications, Theory and Instrumentation*, section *Infrared Spectroscopy*, Meyers R. A. (Ed.). John Wiley & Sons: 2020. <https://doi.org/10.1002/9780470027318.a9701>
39. FDA: *Development and Submission of Near Infrared Analytical Procedures Guidance for Industry*, <https://www.fda.gov/media/91343/download>. August 2021.
40. Innopharma Technology: *NIR Spectroscopy PAT Sensors*, 2022, <https://www.innopharmatechnology.com/nir-spectroscopy-pat-sensors>.

3 Raman spectroscopy

Tomáš Pekárek, Dita Spálovská

3.1 Introduction

Similarly to infrared spectroscopy, Raman spectroscopy is one of the vibrational spectroscopy techniques. It is named after the Indian sir Chandrasekhara Venkata Raman who, together with the sir Kariamanickam Srinivasa Krishnan, observed the inelastic light scattering and was awarded the Nobel Prize in 1930 for this discovery [1]. L. I. Mandelstam and G. S. Landsberg also observed this phenomenon in the former USSR [2-5].

Raman spectroscopy offers the same options as infrared spectroscopy (see chapter 2.1.). Moreover, it enables easy measurement through the package, and even water is not an obstacle here, whereas in IR spectroscopy water is a very unsuitable matrix for measurements, as explained below. The higher cost of Raman spectrometers was the main obstacle for their wider use. In recent years, the price continues to decline, and although it is not at level with infrared spectrometers, the Raman spectrometers are now more affordable.

A molecule is not of a rigid shape, but it can be compared to weights connected to a spring. All atoms of a functional group perform a permanent vibration. A non-linear and a linear molecule can vibrate at $3N-6$ and $3N-5$ vibrational degrees of freedom (normal vibrational modes), respectively, [6-9], where N is the number of atoms in the molecule. The individual vibrational modes are characterized by the quantum number n , which can acquire values 0, 1, 2, 3, etc. Transitions between individual states are linked to energy changes and the energy of these vibrational transitions is quantified according to the following equation:

$$E = h\nu \left(n + \frac{1}{2} \right) \quad \nu - \text{vibrational transition frequency}$$

h – Planck constant

If the energy quantum is absorbed by a molecule, transitions that are shown in Fig. 3.1 take place (marked as IR) and can be observed by the infrared (IR) spectroscopy. The second option is that the transitions occur during the scattering effect, which can be described as absorption of a photon and excitation of the molecule to the excited energy state (virtual levels) followed its immediate relaxation to a lower energy state linked with an emission of a scattered photon. The whole process lasts no longer than 10^{-15} second, which means that we cannot speak about true absorption or emission, but the effect is considered as a non-elastic two-

photon scattering. If the molecule returns to the ground state after its excitation, the scattered photon is of the same energy as the photon which was absorbed, and it carries no information about the vibrational states of the molecule (Rayleigh scattering) [6-9]. Stokes-Raman scattering is a process when the transition starts at the ground vibrational level and ends at a higher vibrational level, whereas anti-Stokes-Raman scattering is observed when the molecule relaxes to a lower energy level. The individual transitions are shown in Fig. 3.1.

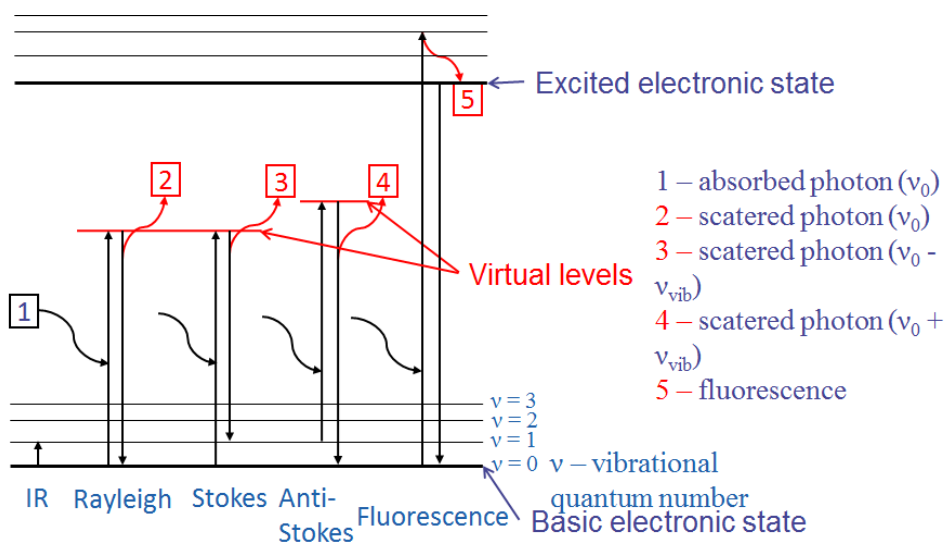


Figure 3.1. Visualization of vibrational transitions of a molecule after its interaction with radiation. Arrows up indicate a molecule excitation by radiation; arrows down indicate molecule relaxation connected with “emission” of a photon; ν_{vib} – energy differences between individual vibrational levels.

The Rayleigh radiation intensity is approximately six orders of magnitude higher than the Raman bands intensity, resulting in high energy requirements for detection of Raman spectra. The intensity of the Stokes and anti-Stokes lines is different as well. As most molecules are in the ground vibrational state at room temperature (Boltzmann distribution, see below), the anti-Stokes transitions are rare compared to Stokes transitions and their bands have therefore lower intensity.

N_0 – molecule abundance in the basic state

N_1 – molecule abundance in the higher energy state

$$\frac{N_1}{N_0} = e^{-\frac{h\nu_{vib}}{kT}}$$

h – Planck constant

ν_{vib} – vibrational frequency

k – Boltzmann constant

T – temperature

Temperature of the sample during measurement can be calculated by the following equation, which might be important especially in biological tissue analysis.

$$\frac{I_{\text{anti-Stokes}}}{I_{\text{Stokes}}} = \left(\frac{\nu_0 + \nu_{vib}}{\nu_0 - \nu_{vib}} \right)^4 e^{-\frac{h\nu_{vib}}{kT}}$$

$I_{\text{anti-Stokes}}$ – band intensity in the Stokes region

I_{Stokes} – band intensity in the anti-Stokes region

ν_0 – incidental photon frequency

As depicted in Fig. 3.1, the differences in vibrational energy levels are important for both IR and Raman spectroscopy. The IR spectroscopy observes a photon with the energy of the particular vibrational energy transition, whereas Raman spectroscopy deals with a two-photon process where the energy of the vibrational transition is equal to the shift (difference) between the absorbed and the emitted photon, and the techniques are complementary.

For the IR vibration to be active, a non-zero dipole change must occur as it moves.

p – dipole moment

$$\frac{\partial p}{\partial q} \neq 0$$

q – normal coordinate

In Raman spectroscopy, the functional group needs to change its polarizability to be Raman active.

$$\frac{\partial \alpha}{\partial q} \neq 0$$

α – polarizability – the ease of bond (electron cloud) distortion by an external energy field

The dipole moment is induced by the external electric field E given by the following relationship:

$$p = \alpha E$$

Intensity of the IR bands is proportional to the second power of the dipole change during particular vibrational motion $(\frac{\partial p}{\partial q})^2$, and Raman bands are proportional to the second power of the polarizability change $(\frac{\partial \alpha}{\partial q})^2$. The modes with the high dipole moment change that provide high intensity IR bands usually result in weak Raman bands. In contrast, vibrations of non-polar functional groups appear as intensive bands in the Raman spectra and as weak bands in the IR spectra. For instance, carboxyl and carbonyl groups usually provide very strong bands in the IR spectrum and very weak bands in the Raman spectrum. High Raman intensity bands are usually found for double and triple bonds and for symmetric vibrations of functional groups. Example is shown in Fig. 3.2 with the IR and Raman spectrum of acetylsalicylic acid. The IR spectrum is dominated by bands 1600–1700 cm^{-1} assigned to the vibrations of carboxylic group. As two nonequivalent C=O groups are present in the molecule (ester and acid), two maxima corresponding to stretching vibration are found in the spectrum. Another strong, broad band is found in the region of 2500–3500 cm^{-1} in the IR spectrum, assigned to the O–H stretching vibration. Both mentioned spectral characteristics are weak in the Raman spectrum. In contrast, Raman spectrum is dominated by the C=C aromatic ring stretching vibrations near 1600 cm^{-1} , and there are also intensive bands around 3000 cm^{-1} corresponding to the C–H stretching vibration.

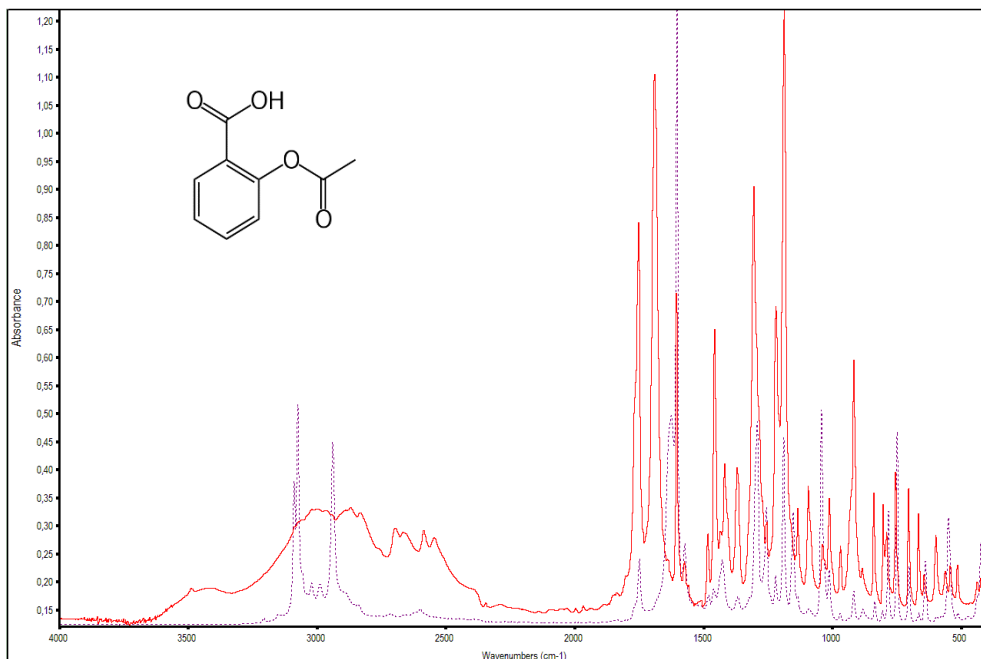


Figure 3.2. IR and Raman spectrum of the acetylsalicylic acid (IR spectrum red, Raman violet).

Raman spectroscopy is often used together with IR spectroscopy in the mid-infrared region to obtain as much spectral information as possible. Raman spectroscopy can be a supplementary technique for the structural analysis of organic molecules in combination with nuclear magnetic resonance (NMR) and/or mass spectrometry (MS).

Raman spectrometry provides the key information on the molecule structure. Band positions and intensities are employed in functional group identification of the sample or for identity confirmation [10]. Having the necessary knowledge, one can identify chemical compounds or observe intermolecular interaction by evaluation of Raman band positions and intensity changes. Spectral libraries serve as a tool which makes sample identification easier by comparing the measured and library spectra.

The time required for spectral accumulation depends on the particular Raman system, and ranges from hours to nanoseconds with a special instrumentation.

One of the biggest advantages over all other analytical techniques is that a sample can be measured directly with very easy preparation or even without any sample pretreatment. Issues with sample thickness appearing in transmission techniques do not represent a problem. On the other hand, quantitative analysis is tricky for solid-state samples as the optical pathlength is not exactly known.

In Raman spectroscopy, the ambient atmosphere (humidity and CO₂) has a weak influence on the resulting spectra, so there is no need to measure background. Samples can be measured directly in solution or suspension (as water has very weak bands) or in packaging material (glass, polyethylene, etc.), thus, contamination of both sample and operator can be avoided. Next advantage, similar to IR spectroscopy, is the possibility of connecting the Raman spectrometer to a microscope with identical technical possibilities as mentioned for IR spectroscopy, but with the advantages mentioned above (measurement through packaging materials, water suspension measurements, and so on).

3.2 Experimental setup

The basic arrangement of Raman spectrometer is depicted in Fig. 3.3. Incident radiation is emitted from the source and reaches the sample. Scattered photons are passing through the collection optics to the diffraction element (usually grating) or interferometer – based on spectrometer type – and are registered at the detector.

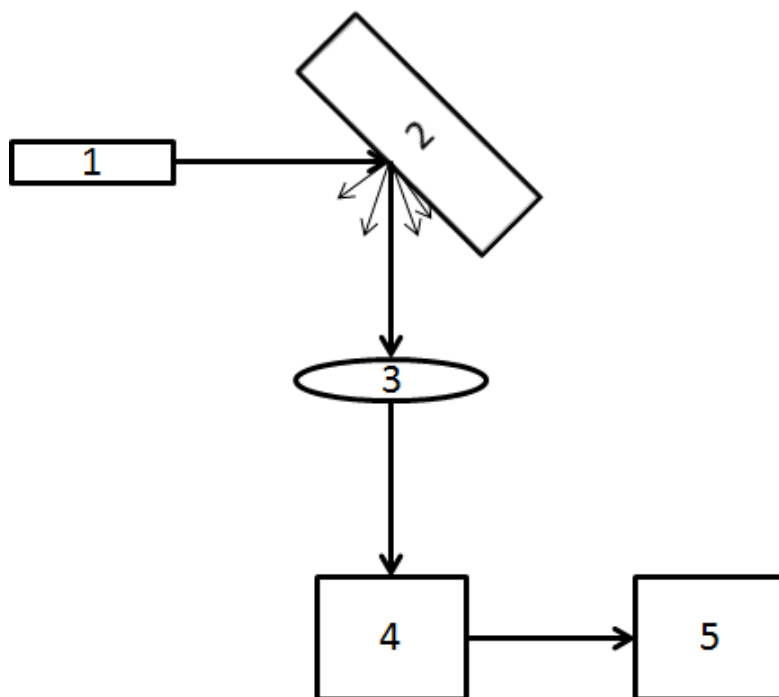


Figure 3.3. Basic arrangement of a Raman spectrometer: 1 – Source, 2 – sample, 3 – collection optic, 4 – interferometer or diffraction element, 5 – detector.

Lasers are usually used as a source for the emission of high-energy coherent radiation [9]. Wavelength of the lasers used for Raman spectroscopy varies from IR and visible to UV region. Raman signal intensity is higher with lower laser wavelengths, but this is associated with a higher risk of continual sample emission – fluorescence – which can overlap the whole Raman spectrum with its much stronger signal (Fig. 3.4). Examples of lasers commonly used in Raman spectroscopy are as follows: Nd:YAG (neodymium-doped yttrium aluminum garnet) with the wavelength of 1064 nm (NIR region) or doubled (532 nm), He-Ne gas laser (633 nm), Ar⁺ (488 and 458 nm), laser semiconductor diode (780 and 785 nm), color lasers (360–700 nm), etc., and lasers with adjustable wavelength. Most of the routine applications employ continuous lasers. Pulsed lasers are used in the research for time-resolved measurement.

Depending on the angle between the excitation and the scattered light, we can distinguish 90° and 180° arrangement (geometry). Some special applications use SORS (Spatially Offset Raman Spectroscopy) for measurement through packaging material (glass, paper, or plastic bags, etc.). Sample can be placed into a vial, NMR or UV cuvettes, on a plate or other holders. Handheld Raman systems can be used for various *in situ* measurements. Optical fibers enable collection of spectra outside of the spectrometer that can be used to monitor chemical reactions, crystallization, and other processes. Special sample pretreatment is required for Surface Enhanced (Resonance) Raman Scattering (SER(R)S), Tip-Enhanced Raman Spectroscopy (TERS) and some other techniques employed mainly in primary research [6].

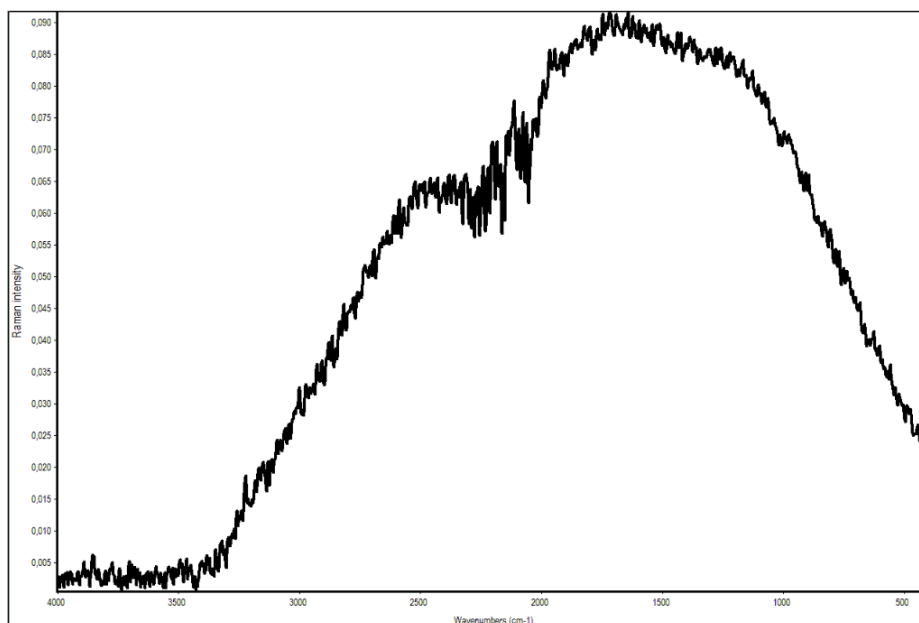


Fig. 3.4. Example of fluorescence in the Raman spectrum.

In general, measured sample must be placed in a proper distance from the collection optic (usually an objective) to collect the most scattered photons. Thus, sample is focused to reach the maximum signal. This setting is not applicable in case of immersion probes or handheld systems. Furthermore, the laser spot is usually small, and several accumulations must be obtained from different sample locations to obtain statistically representative spectrum of solid state and/or inhomogeneous samples.

In contrary to IR spectroscopy which almost exclusively employs interferometers, Raman spectroscopy uses both interferometers and dispersive elements (diffraction gratings) [6]. The grating is usually a plate with hundreds to thousands of grids per one millimeter. Fourier transformation is used for signal processing in case of systems with interferometers. Such systems are signed FT.

Interferometric setup is equipped with a laser with an excitation wavelength of 1064 nm (NIR region). Dispersive (grating) systems are utilized with excitation source in the UV, visible and NIR region. Dispersive systems provide better spatial resolution and higher Raman signal intensity, while Fourier transform systems offer lower risk of fluorescence.

FT (interferometric) systems are usually connected to high-sensitivity germanium detectors which need to be cooled by liquid nitrogen or InGaAs detectors working in ambient laboratory temperature. CCD (Charge Coupled Device) are employed in dispersive systems.

Capabilities of Raman spectroscopy can be extended by connection to microscope which enables measurement of small particles, approx. 1 μm , or mapping of surface component distribution and depth profiling [11]. Here, the basic spectrometer scheme as presented in Fig. 3.3 remains unchanged. Excitation radiation is brought through microscope objective to the sample and scattered light is collected by the same objective, i.e., 180° geometry is applied. Confocal microscopes can also be employed (basic scheme in Fig. 3.5) In this case, the sample hit by excitation radiation emits an inelastically scattered light and this light is focused by lens. Combination of focusing and slit position enables better spatial resolution and suppresses radiation from different sample layers. The Fig. 3.5 shows focusing on a layer 2, whereas radiation from neighboring layers 1 and 3 is mostly blocked by the slit shade. Only the radiation from level 2 can thus pass to the detector through the slit, almost without any restriction. Depth profiling is suitable for sample analysis where the upper level cannot be easily removed, or for mapping of components in a matrix.

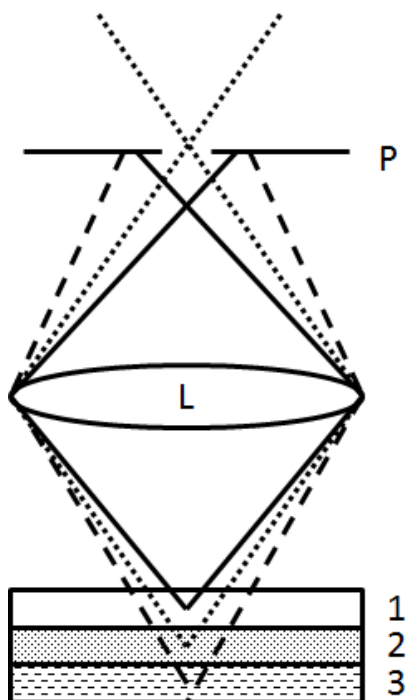


Figure 3.5. Scheme of a confocal microscope; P – slit, L – lens, 1,2,3 – individual sample levels.

Spectrometer settings, such as sample placement, laser power, accumulation time and other parameters, differ significantly between instruments and manufacturers. The sample type and requirements for spectral quality influence the instrumental setting. Therefore, neither standard procedure nor general user guide is available for every sample. One can only say higher laser energy, shorter laser wavelengths, and longer spectral acquisition can increase sample temperature and cause its destruction or degradation and also increase fluorescence risk. Thus, when analyzing sensitive materials, e.g., biological tissues, it is recommended to start with short accumulations with low laser energy. The goal is to gain maximal signal to noise ratio without sample degradation.

3.3 Application of Raman spectroscopy

3.3.1 Identification of unknown samples

Some general applications of Raman spectroscopy were stated above. This chapter will provide more detail together with case studies.

Raman spectroscopy is a non-destructive analytical method. Its complementarity with IR spectroscopy and characterization of the molecular and crystal structures enables its utilization for identification of unknown samples. As stated in the chapter on IR spectroscopy, each group vibrates at a specific frequency. These vibrations are observed, and the location of peak (band) maxima corresponds to the presence of particular functional groups. Moreover, functional group vibrations are influenced by their chemical neighbors, as some substituents can increase or decrease vibration frequency. Therefore, not only can we determine which functional groups are present in the sample, but also what substituents are present in their neighborhood, e.g., if there is only one isolated aromatic ring or if it is substituted, etc. Fig. 3.6 shows spectra of two isomers differing only in the location of one double bond.

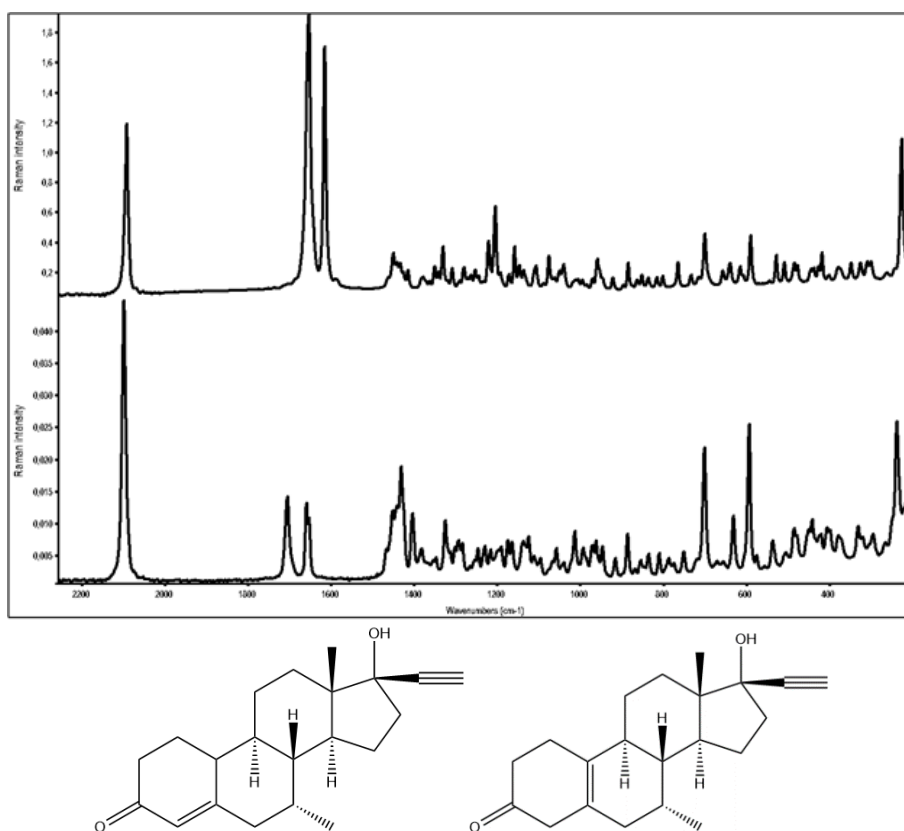


Figure 3.6. Comparison of Raman spectra of two isomers.

Similarly to IR spectroscopy, chemical structure of a sample can be determined by the assignment of spectral bands to particular functional groups. Certain knowledge and experience are required for such spectral analysis. Tables and charts with

characteristic vibration energies of specific functional groups are a useful tool. Chemical structure can be confirmed by NMR spectroscopy, comparison with a standard, spectral library search, etc. As the spectrum of a mixture is a superposition of individual components' spectra, one can identify components contained in the mixture. Individual components can be quantified with the limitation mentioned above, i.e., the exact depth of the excitation laser penetration is not known and therefore calibration curve construction can be complicated. In case of perfectly homogenized liquid samples, calibration is easily applicable.

3.3.2 Identification of polymorphs, solvates and salts

Allotropy is a property of an element to exist in different structural modifications, which can differ in their physical and chemical properties. In analogy, molecules can also exist in different modifications and this property is called polymorphism. Individual polymorphs can have different specific surface area, hardness, dissolution rate, etc. As the spatial arrangement of functional groups in different crystal lattices varies, the neighborhood of functional groups varies also. This effect influences bond vibration frequency and lattice vibrations occur at lower wavenumbers. That is why two different polymorphs of the same molecule do not have the same Raman spectrum (Fig. 3.7), but the differences between polymorphs can have various intensity. Therefore, Raman spectroscopy is not suitable for determining of a crystal structure without standards. In such case, X-Ray Diffraction (XRD) analysis will be the method of choice. Raman spectroscopy is however a fast and non-destructive technique and requires smaller amount of sample than thermal methods, e.g., Differential Scanning Calorimetry (DSC), which is used for polymorph differentiation as well. Raman spectroscopy is also cheaper compared to XRD. Thus, polymorph structure can be first identified by XRD and the reference spectra recorded by Raman spectroscopy, and the further polymorph screening of sample sets can be carried out only by Raman spectroscopy if the polymorph spectra are different enough. In that case, quantification of polymorphs is also feasible by Raman spectroscopy.

Besides the rapid identification of chemical structure and functional groups, Raman spectroscopy serves as a tool for discrimination between different salts of a single molecule. The salts can be distinguished and identified, and the ratio of dissociated and non-dissociated carboxylic groups can also be determined. Fig. 3.8 shows spectra of tartaric and succinic salts of one molecule. Even without deep knowledge of Raman spectroscopy, the difference is easily recognizable.

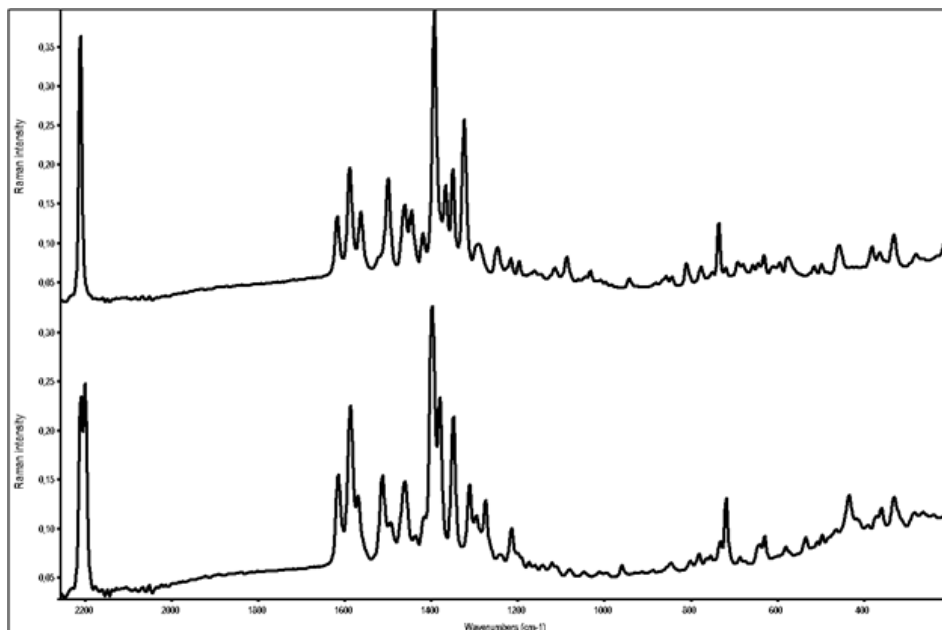


Figure 3.7. Comparison of different polymorph Raman spectra.

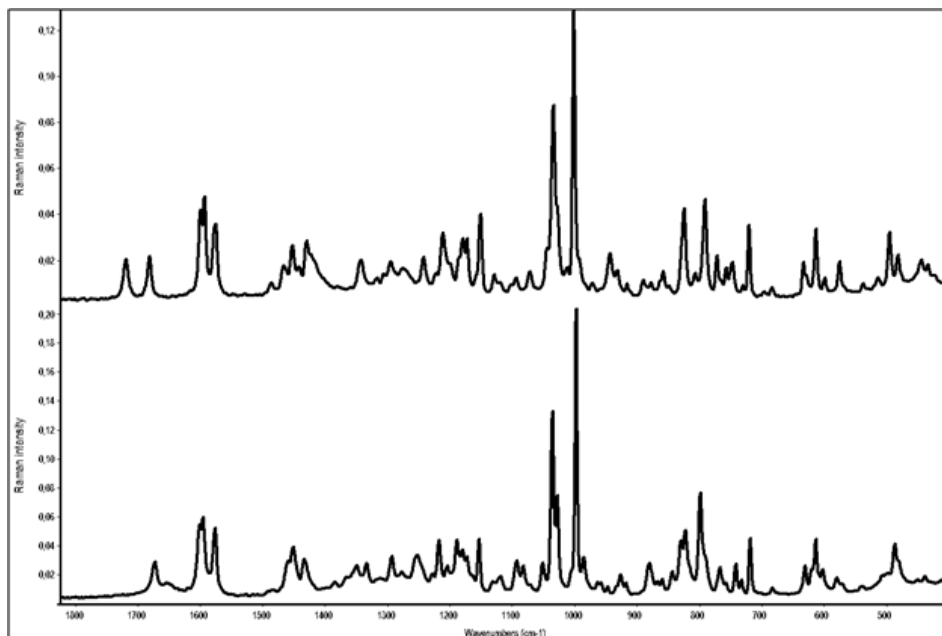


Figure 3.8. Comparison of Raman spectra of two different salts of one molecule – succinic and tartaric. Major differences occur around 1700, 1450, 1050 cm^{-1} .

Differentiation between salt, solvate or cocrystal is also feasible by Raman spectroscopy. Solvate is formed by molecules of a sample and solvent arranged in the crystal lattice. Hydrates are the special case of solvates when the solvent in the lattice is water. Cocrystal contains two or more species when all of them are solids under normal conditions, and the arrangement in the lattice is not based on ion-pairing but on weaker interactions such as hydrogen bonding, π - π stacking or van der Waals interaction.

Fiber optics and probes are used for *in-situ* reaction and crystallization monitoring. Transition of polymorphs can also be directly observed in suspension or through glass by Raman spectroscopy. Furthermore, a heating stage can be placed under the microscope objective to reveal the polymorphic changes during heating or cooling.

3.3.3 Raman mapping and imaging

Possibility to connect microscope with a spectrometer was already mentioned above. The arrangement is suitable for analysis of samples with minimal size of approximately one micrometer. With special instrumentation like TERS, a nanometer resolution can be reached, which is more often used in the primary research. The same application as in case of the “macro” settings are applied, i.e., identification of unknown samples, including fibers, small impurities, etc. One of the biggest advantages of the microscope-spectrometer arrangement is the mapping possibility. Spectra are accumulated on a sample surface in predefined points with regular spacing. When the points form a line, the mapping is called line-mapping. Line-mapping is suitable for evaluation of concentration gradient of one or more components, e.g., diffusion of one component into another. If the predefined measurement points are spread over the part or over the whole surface, it is called an “area mapping” or 2D mapping. Line- and area mapping require line and area detectors, respectively. In combination with the depth profiling, a 3D mapping can be obtained. Mappings are crucial in applications where component distribution and surface homogeneity are to be observed and checked. Fig. 3.9 and 3.10 represent Raman map of a pharmaceutical tablet.

Spectra accumulated during mapping are evaluated by multidimensional mathematical and statistic methods, such as Principal Component Analysis (PCA), and when the components are known and spectra available, maps can be evaluated by comparison with spectral library records. It is possible to observe intensity, area, bandwidth, etc., as well as distribution of only one or more bands which do not interfere with other components. The obtained map or image is consequently visualized in different colors, 2D or 3D (Fig. 3.10), demonstrating the distribution of one excipient in the tablet.

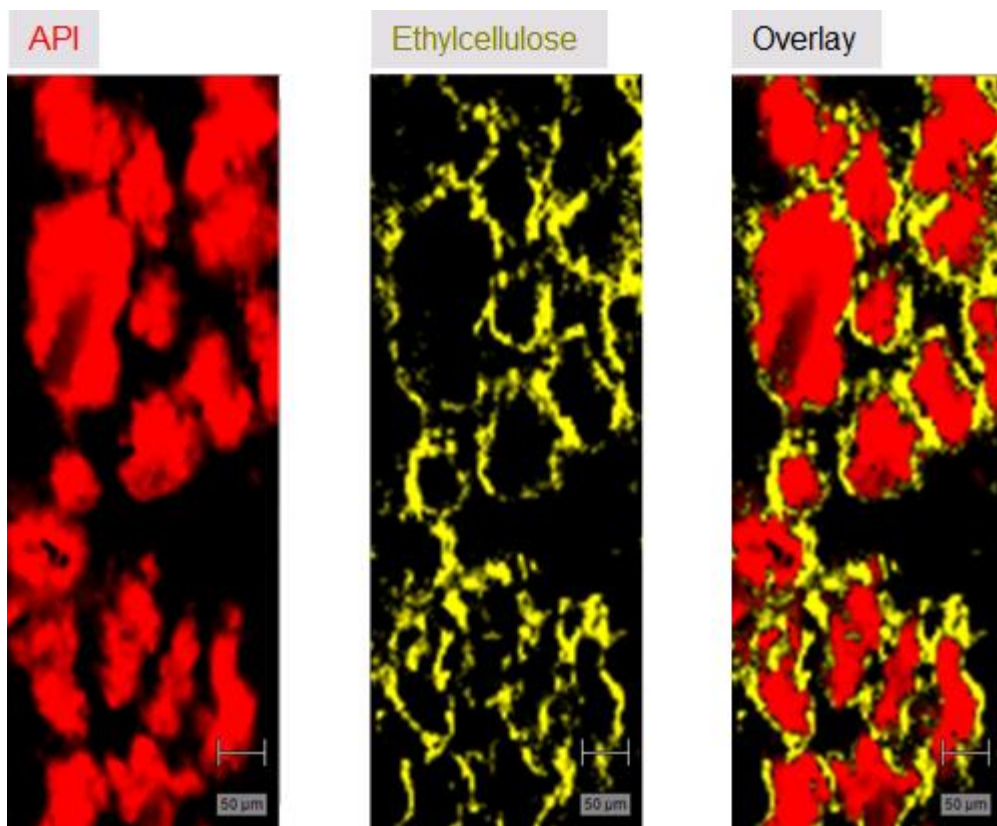


Figure 3.9. Cross-section Raman map of a pharmaceutical tablet. API particles are highlighted on the left, one excipient in the middle, and blended picture on the right.

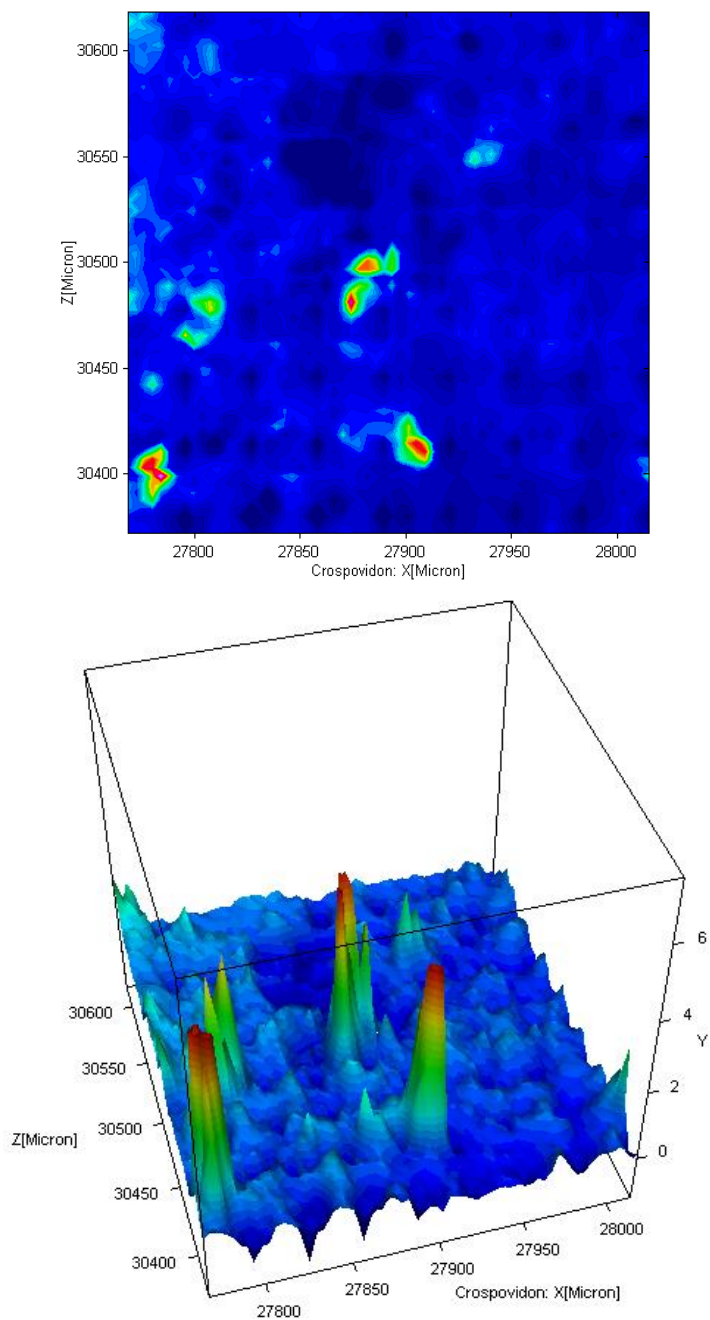


Figure 3.10. Distribution of an excipient in a tablet cross section (2D a 3D visualization).

3.4 Resources and recommended literature

1. Sodomka L., Sodomková M., Nobelovy ceny za fyziku, Prague, Czech Republic, 1997.
2. Raman C. V., A new radiation, *Ind. J. Phys.* 1928, 2, 387.
3. Landsberg G. S., Mandelstam L. I., New phenomenon in scattering of light (preliminary report), *Journal of the Russian Physico-Chemical Society, Physics Section* 1928, 60, 335.
4. Landsberg G. S., Mandelstam L. I., Eine neue Erscheinung bei der Lichtzerstreuung in Krystallen, *Naturwissenschaften.* 1928, 16, 557. <https://doi.org/10.1007/BF01506807>
5. Landsberg G. S., Mandelstam L. I., Über die Lichtzerstreuung in Kristallen, *Zeitschrift für Physik.* 1928, 50, 769. <https://doi.org/10.1007/BF01339412>
6. Ferraro J. R., Nakamoto K., Brown C.W, *Introductory Raman Spectroscopy*, Academic Press: London, UK 2003.
7. Long D. A., *The Raman Effect*, Wiley: Chichester, UK 2002. <https://doi.org/10.1002/0470845767>
8. Pivonka D. E., Chalmers J. M., Griffiths P. R. *Applications of Vibrational Spectroscopy in Pharmaceutical Research and Development*, Wiley: Chichester UK, 2007.
9. Atkins P., de Paula J., *Fyzikální chemie*, VŠCHT, Praha 2013, 978-80-7080-830-6.
10. Socrates G., *Infrared and Raman Characteristic Group Frequencies*, Wiley: Chichester, UK, 2001.
11. Salzer R., Siesler H. W., *Infrared and Raman Spectroscopic Imaging*, Wiley-VCH: Weinheim, Germany, 2009. <https://doi.org/10.1002/9783527628230>

4 X-ray diffraction

Hana Brusová and Bohumil Kratochvíl

4.1 Introduction

X-ray diffraction is one of the main solid state analytical techniques, considered as the "gold standard" not only for characterization and identification of crystalline substances, but also for their discrimination.

Originally, the X-ray diffraction was used mainly to study inorganic materials and minerals, where it was also observed for the first time, at the beginning of the 20th century. X-ray diffraction uses the ability of solids to scatter X-ray photons and thus create a diffraction pattern which characterizes the internal structure of the studied material. The main analytically usable quantities are the intensities and positions of the diffracted X-ray beams in the diffraction pattern. The theory of X-ray diffraction is based on the knowledge of crystallography, so this chapter therefore also includes the basics of crystallography.

Because the final product of many industrial technologies are microcrystalline powders, the X-ray powder diffraction technique is the most discussed in this chapter. The fact that the technique is well established in pharmaceutical industry is also demonstrated by its inclusion into the European Pharmacopoeia (Ph. Eur.). Besides, other control authorities also require this test as a standard control of polymorphic forms of active substances (APIs). ICH directive (International Conference on Harmonization – Quality) Q6A and FDA directives list X-ray powder diffraction as a basic analytical method for resolving different crystal structures (polymorphs). It can generally be assumed that different internal arrangements of molecules in a crystal are reflected by various physico-chemical properties of the crystalline substances. Furthermore, the X-ray powder diffraction enables non-destructive resolving of different forms of one API (polymorphs, salts, hydrates, solvates and cocrystals).

4.2 Crystal structure, its geometry and symmetry

External morphological symmetry of crystals has long been speculated as a manifestation of regularity of their internal arrangement. This was for example observed in crystallization of arsenates into different crystal forms depending on the crystallization conditions.

Crystalline substances are indeed characterized by regular arrangement of particles they consist of (atoms, ions, molecules or parts of molecules). The given structural motif is three-dimensionally, translationally repeated throughout the whole structure (model of the ideal crystal). If we approximate the structural motif by a point, then we get an imaginary spatial lattice which represents a regular arrangement of points in space. Nodal points lie on lines and planes creating a spatial lattice. If this regularity is maintained throughout the whole volume (e.g., 1 mm^3), the crystal is called a single-crystal. Fig. 4.1 shows the crystal structure and the spatial lattice of sodium chloride.

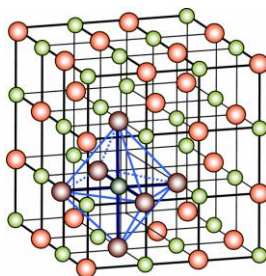


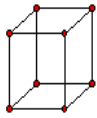
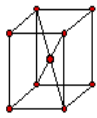
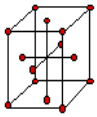
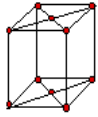
Figure 4.1. Ionic crystal structure and spatial lattice of NaCl (Na^+ ions are green, Cl^- ions are red). The structural motif is formed by a pair of Na-Cl ions, with the lattice points always lying in the position of Cl^- ions

(Source: https://en.wikipedia.org/wiki/Crystal_structure.)

The smallest parallelepiped of the spatial lattice is called a unit (elementary) cell, which fills an ideal crystal without a residue when multiplied in three dimensions. It represents a figure with parallel sides, having lattice points either only in its vertices (primitive cell) or also in centers of its sides (face-centered, see e.g., the structure of NaCl in Fig. 4.1) or in vertices and the middle of the cell (body-centered). The number of unit cell types is limited by the internal symmetry of the crystal structure. The distribution of unit cells according to the arrangement of their nodes is shown in Table 4.1.

A unit cell is characterized by lattice parameters a , b , c and α , β , γ (lengths of edges, and the angles between them, respectively). The smallest fraction of the unit cell is called the asymmetric unit, see Fig. 4.2. Thus, according to the symmetry of a crystal structure, there can be distinguished 7 crystal systems, 14 Bravais lattices (divided into crystal systems), 32 crystal classes, and 230 distinct space groups, see Table 4.2.

Table 4.1. Classification of unit cells according to the location of their lattice points.

P – primitive (simple cell) – lattice points only in the vertices of the cell	
I – spatially centered – lattice points in the vertices and the center of the cell	
F – face centered – lattice points in the vertices and centers of the sides of the cell	
C – base centered – lattice points in the vertices of the cell and the centers of its opposite sides	

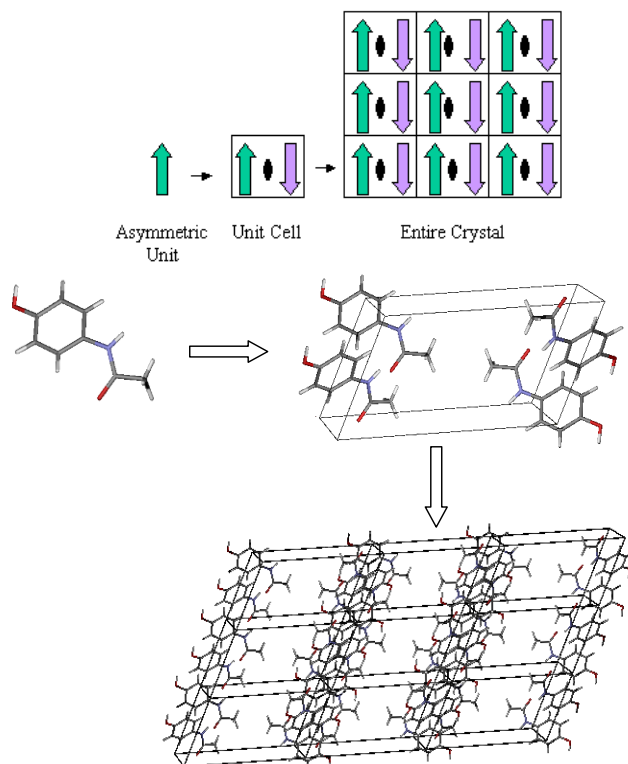
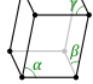
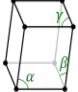
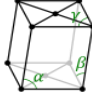
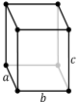
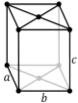
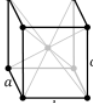
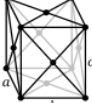
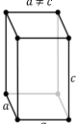
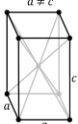
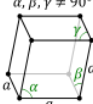
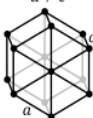
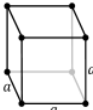
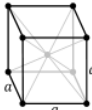
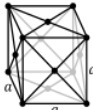
**Figure 4.2.** Scheme of an assessment of a crystal structure.

Table 20.2. List of Bravais lattices.

7 crystal systems	14 Bravais lattices			
Triclinic	P			
	$\alpha, \beta, \gamma \neq 90^\circ$ 			
Monoclinic	P	C		
	$\alpha \neq 90^\circ$ $\beta, \gamma = 90^\circ$ 	$\alpha \neq 90^\circ$ $\beta, \gamma = 90^\circ$ 		
Orthorhombic	P	C	I	F
	$a \neq b \neq c$ 	$a \neq b \neq c$ 	$a \neq b \neq c$ 	$a \neq b \neq c$ 
Tetragonal	P	I		
	$a \neq c$ 	$a \neq c$ 		
Rhombohedral	P			
	$\alpha, \beta, \gamma \neq 90^\circ$ 			
Hexagonal	P			
	$a \neq c$ 			
Cubic	P (pcc)	I (bcc)	F (fcc)	
				

4.3 X-rays

To obtain an analyzable diffraction pattern, the probing radiation must have a wavelength comparable to or lower than the distance between the scattering centers (atoms – high electron density sites). X-rays (e.g., generated by a laboratory X-ray tube, see Table 4.3) meet this requirement, and the result of a diffraction experiment is the intensities and positions of diffraction spots, which encodes information about the crystal structure and properties of the studied material.

There are generally three options for X-ray generation:

- impact of an accelerated electron onto a solid surface – X-ray tube
- alternation of flight path of a relativistic electron moving in the synchrotron (so-called synchrotron radiation in the X-ray region)
- excited fluorescence radiation

4.3.1 X-ray tube

Radiation in an X-ray tube is created by a sudden collision of very fast-moving electrons with a high mass matter (high atomic number). The cathode in X-ray tube is heated. Then, if voltage is applied between cathode and anode, the electrons, emitted from the hot cathode, start to move towards the anode. Upon their impact on the anode, around 1% of their kinetic energy converts to X-rays, and 99% converts to heat. Therefore, the anode must be cooled. Radiation is produced by 1% of the accelerated electrons penetrating K and L electron levels of the anode (levels near the core) where they knock other electrons out. Electrons from higher levels move to fill these empty spaces, and the excess energy is radiated as X-rays. The basic scheme of an X-ray tube is shown in Fig. 4.3.

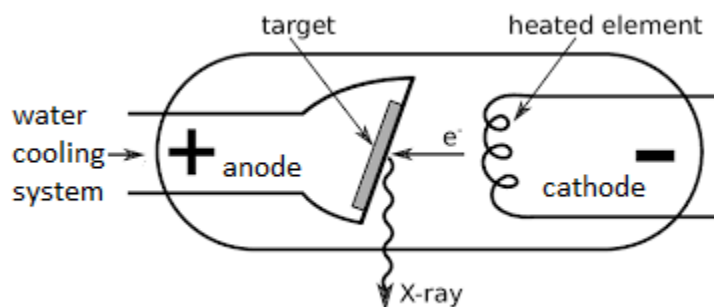


Figure 4.3. Schematic description of an X-ray tube, with fixed anode.

(Source: https://en.wikipedia.org/wiki/X-ray_tube.)

The radiation created by an impact of an electron onto a mass is divided into:

- braking radiation (Ger. Bremsstrahlung, see German nationality of W.C. Roentgen, discoverer of X-rays) – continuous, produced by electron velocity change
- X-ray fluorescence (defined by the electron energy levels of the chemical element)

Braking radiation is produced by an interaction of an electron and a nucleus anode target atom. The deceleration is one-step and has the shortest wavelength (continual braking creates longer wavelengths). By each interaction with the anode atoms, the electrons (denoted A and B in Fig. 4.4) lose part of their kinetic energy gained between the two electrodes. The lost energy converts into X-rays. Since the energy lost in the collisions has various intensities, the X-rays will be represented by a range of wavelengths from minimum value λ_{\min} to maximum value λ_{\max} . Therefore, the radiation is termed continuous.

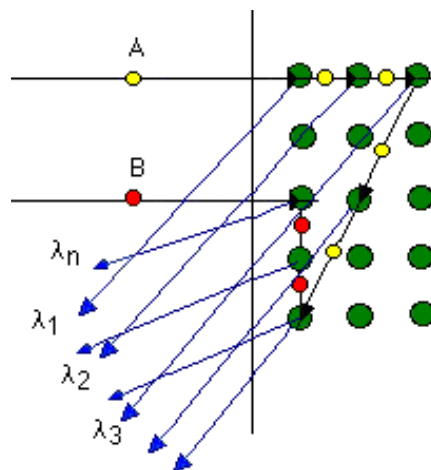


Figure 4.4. Scheme of braking radiation formation.

(Source: <https://www.sciencedirect.com/topics/earth-and-planetary-sciences/bremsstrahlung>.)

X-ray fluorescence consists of discrete wavelengths. It is produced by an electron with sufficient energy ($E = eU$), moving from cathode and knocking out an electron from outer layers K and L of the anode. The vacant space is filled by an electron with higher energy originating from level farther from nucleus. Excess energy is released in the form of X-rays, see Fig. 4.5. The wavelength λ of the X-ray radiation emitted during the transition is determined by the difference between the two energy levels. Since this wavelength is characteristic for the anode material, the resulting radiation is called characteristic.

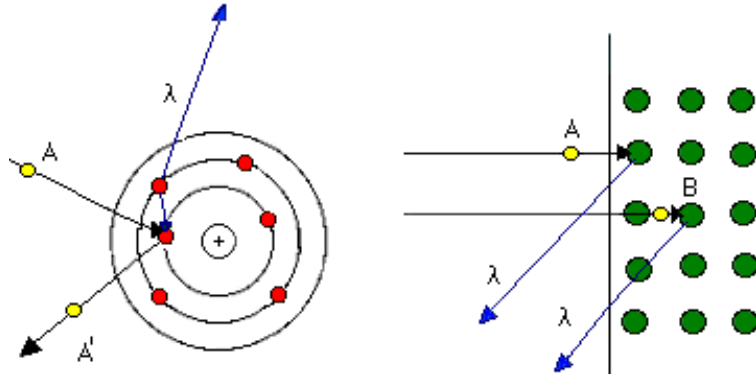


Figure 4.5. Scheme of characteristic X-ray emission.

(Source: <https://www.sciencedirect.com/topics/medicine-and-dentistry/characteristic-x-ray>.)

Fig. 4.6 shows characteristic lines of monochromatic X-rays on a background of a continuous spectrum. The wavelength of a characteristic line (denoted K_α , K_β) depends on the atomic number of the anode material.

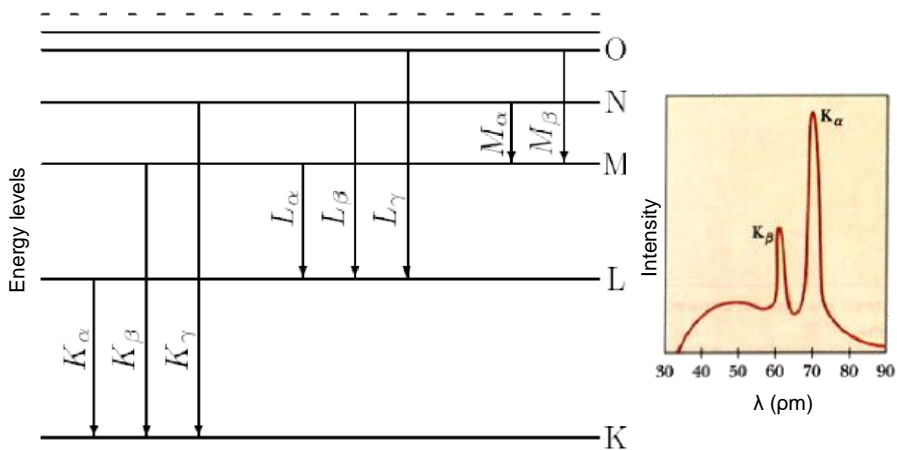


Figure 4.6. Depiction of allowed electron transmissions between the individual energy levels in an electron cloud of an atom (anode) and a wave spectrum of characteristic monochromatic radiation.

(Source: Kratochvíl B. *Chemie a fyzika pevných látek I. VŠCHT Praha, 1994.*)

4.3.1.1 Synchrotron radiation

Synchrotron radiation (Fig. 4.7), in the X-ray region, is created by radial acceleration of a relativistic electron. Its movement on a circular path emits energy in the form of a continuous spectrum with long wavelengths and with approximately constant intensity. Undulating and bending magnets are used for this purpose.

Synchrotron radiation is polarized in the orbit plane, and a deviation from this plane enables to use also elliptically polarized radiation. Other characteristics are: coherence of the radiation, its time course (particles circulate in clusters), and about two orders of magnitude higher energy than an X-ray tube.

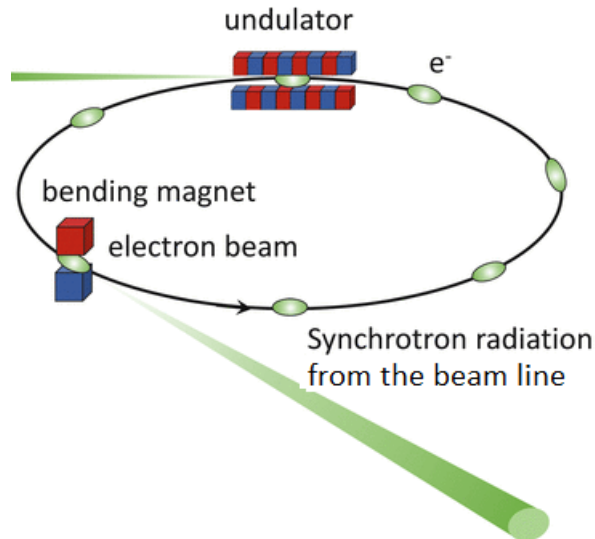


Figure 4.7. Configuration scheme of an accumulation ring of a synchrotron with undulator and bending magnets. Work stations are called „Beam Lines“.

(Source: https://www.researchgate.net/figure/A-schematic-diagram-of-a-synchrotron-radiation-accelerator-hv-photon-source-e_fig1_237806176.)

4.3.2 Characterization of X-ray radiation

- It is an electromagnetic radiation with very short wavelengths 10^{-8} – 10^{-12} m. Wavelength of 10^{-9} m is used in radiodiagnostics.
- It is invisible and passes through matter where it is partially absorbed, and the absorbed amount depends on the composition of the matter (average atomic number, density, and thickness) and the quality of the radiation (wavelength). It decreases with square of its path length. It is radiated linearly from its source.
- Its wavelength depends on the material of anode focal point. Radiation created by incidence of electrons on the focal point is called primary beam and has a conic shape.

4.4 Analytical X-ray diffraction methods

Two basic methods are discerned, based on the type of the analyzed sample:

- single-crystal X-ray diffraction (SCXRD)
- powder X-ray diffraction (PXRD)

Their basic characteristics, advantages, and disadvantages are summarized in Table 4.4a and 3.4b.

The X-ray structural analysis with single crystals allows a complete determination of crystallographic characteristics. Diffraction on a single crystal yields diffraction intensities with positions which enable determination of the complete 3D crystal structure. Number of collected diffraction spots varies between 10^2 – 10^4 . In powder diffraction, max. about 100 diffraction lines can be distinguished at most in a debyegram or in a diffractogram. Therefore, X-ray powder diffraction is mainly used to determine the phase composition of materials.

It is therefore obvious that full structural analysis of crystals with complex structures or low symmetries can be successfully performed only by diffraction on single crystals. The vast majority of crystalline substances however exist in polycrystalline forms, and the creation of single crystals is often difficult. Moreover, X-ray powder methods are irreplaceable where the polycrystalline structure plays a critical role in determination of material properties (phase composition, grain size and orientation, internal stress, etc.).

Table 20.4a. Comparison of basic diffraction methods.

Name	Single crystal X-ray diffraction	X-ray powder diffraction
Abbreviation	SCXRD	PXRD
Sample type	Single crystal	Powder
Sample amount	1 single crystal with size of 0.1–1 mm	100–500 mg
Sample preparation	Selection of a suitable single crystal and its fixation onto the goniometric head	Filling the holder cavity or possibly milling
Sample consumption	Non-destructive	Non-destructive
Measurement time	Hours/days	Minutes/hours
Analysis of obtained data	Complete information about molecule, conformation, bond lengths, chirality, spatial arrangement of molecules, interactions between molecules, determination and location of solvents.	„Fingerprint“ of the crystal structure
Method principle	Monochromatic X-rays impact a single crystal which rotates according to three axes (the principle of four-circle diffractometer).	Monochromatic radiation impacts a polycrystalline material which rotates around one axis.
Practical application	3D crystal structure determination of pharmaceutical substances, proteins, and other materials.	Phase qualitative and quantitative analyses.

Selection of an X-ray tube, i.e., wavelength, depends on the type of the studied material. Excitation of an X-ray radiation emission in the sample, called fluorescence radiation, is undesirable, as it increases the background. It can be expected in cases where the absorption coefficients of atoms of the studied material reach high values with the radiation wavelengths of the particular X-ray tube. Furthermore, a large number of diffraction lines are typical for crystals with low symmetry or large unit cell. Their number decreases and their mutual distance increases when using an X-ray lamp with longer wavelength. The most commonly used X-ray lamp is a lamp with a copper anode, whose $K_{\alpha 1}$ component wavelength is approximately in the middle of the manufactured lamp wavelengths. The middle wavelength K_{α} is used if the doublet is not discernible (Table 20.3).

Table 20.3. Selected wavelengths of the most applied anode materials.

Components of characteristic radiation ($10^{-10} \text{ m} = 1 \text{ \AA}$)				
anode	$K_{\alpha 1}$	$K_{\alpha 2}$	K_{α}	K_{β}
Cu	1.54050	1.54434	1.5418	1.39217
Co	1.78889	1.792801	1.79019	1.620703
Mo	0.70261	0.71354	0.706253	0.632253

The discovery of X-rays in 1895 is associated with the name of the German physicist W.C. Roentgen. In 1912 Max von Laue expressed a belief that the regular arrangement of atoms in crystals may act as a three-dimensional diffraction lattice. The prediction was confirmed by later experiments. These showed that X-rays provide a diffraction pattern with characteristic maxima and minima of diffraction spot intensities, after passage. Less than a year after the Laue's discovery, W. H. Bragg and his son W. L. Bragg showed how to determine crystal symmetry, mutual position of building blocks (atoms, ions), and their distances in crystal structures based on the diffraction patterns. From the analysis of diffraction spot intensities on films they interpreted the X-ray diffraction phenomenon as a reflection on the crystal planes placed one after another at certain distances, see Fig. 4.8.

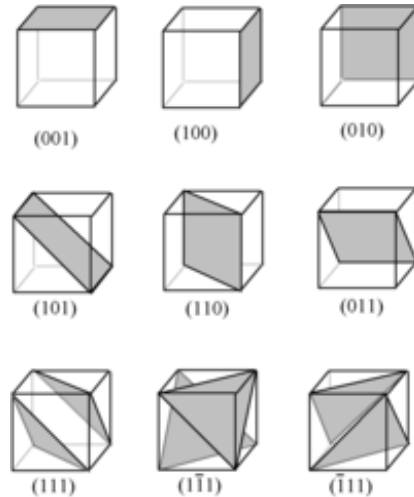


Figure 4.8. Depiction of three systems of imaginary planes with various interplanar lengths. The planes are denoted according to Miller indices hkl , depending on how they intersect the unit cell.

(Source: Kratochvíl B. *Základy fyziky a chemie pevných látek I. VŠCHT Praha, 1994.*)

Each plane scatters only a small amount of radiation, but the resulting scatter from a number of planes provides sufficient intensity for observation. If parallel X-ray beams impact any two parallel planes with distance d , an interference maximum of the diffracted beams can be detected if their path difference is equal to an integer multiple of the incident radiation wavelength, as shown in Fig. 4.9

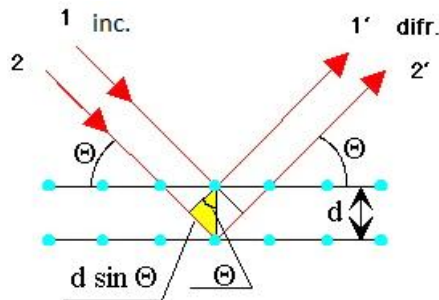


Figure 4.9. Schematic depiction of X-ray diffraction on a crystal structure showing the angle of incidence θ , interplanar distance d and phase shift of the individual rays $2d\sin\theta$.

(Source: Kratochvíl B. *Základy fyziky a chemie pevných látek I. VŠCHT Praha: Praha, 1994.*)

The path difference between beam 11' and beam 22' is equal to $2d\sin\theta$, where the angle θ is the angle held between the incident beam and the given crystal plane. The angle between the incident and diffracted beam is then 2θ . The condition for the

occurrence of diffraction maxima for beams 1' and 2' is given by the following relationship – Bragg equation:

$$2d\sin\theta = n\lambda \quad n = 1, 2, 3\dots \text{(order of reflection)}$$

If the wavelength λ and the angle θ are known, the distances d between the crystal planes can be determined, if all reflections are considered as of the first order. This principle is the basis for the whole discipline of X-ray structural analysis.

So far, only one set of planes has been discussed. By turning the crystal and changing the angle of the incident radiation, the Bragg equation – the diffraction condition – will be met by various sets of planes, enabling to obtain point diffraction pattern of a single-crystal. In case of powdered samples, the diffraction condition is simultaneously met by multiple sets of planes. By changing the diffraction angle, a resulting diffraction pattern can be obtained in the form of a system of conical areas with axes along the axis of the incident radiation and apex angles 4θ given by the interplanar distances between planes. It is therefore evident that measuring of the diffraction angle enables to determine the interplanar distances.

4.4.1 Interactions of X-rays with crystal

Many physical effects occur when X-rays impact a solid matter. The radiation incident on a crystal is called primary, and the reflected radiation (irradiated or diffracted) is called secondary. Secondary radiation is divided into fluorescent, electron emission, and scattered.

Scattering of X-ray radiation is the most important effect for X-ray diffraction, where a part of the originally parallel beam of X-rays is scattered sideways. Electrons are the scattering centers in the material. If the electrons oscillate at the same frequency as the primary radiation, the scattering of radiation is elastic (coherent). The oscillating electrons then become a source of a new secondary radiation with identical wavelength to that of the primary radiation. The diffraction result is then a set of diffracted waves which are radiated from the crystal, but only in certain directions. The spatial distribution of the diffracted waves forms a diffraction pattern of the crystal. This diffraction pattern, and especially the intensity of the diffracted reflections, carry information about the internal structure of the crystal.

The effect of elastic scattering is critical for the formation of a diffraction pattern which enables determination of the distribution of atoms or ions in the studied crystalline material. In elastic scattering, the waves scattered (emitted) by individual

atoms have an invariant phase difference – these atoms form a set of coherent sources (Fig. 4.10).

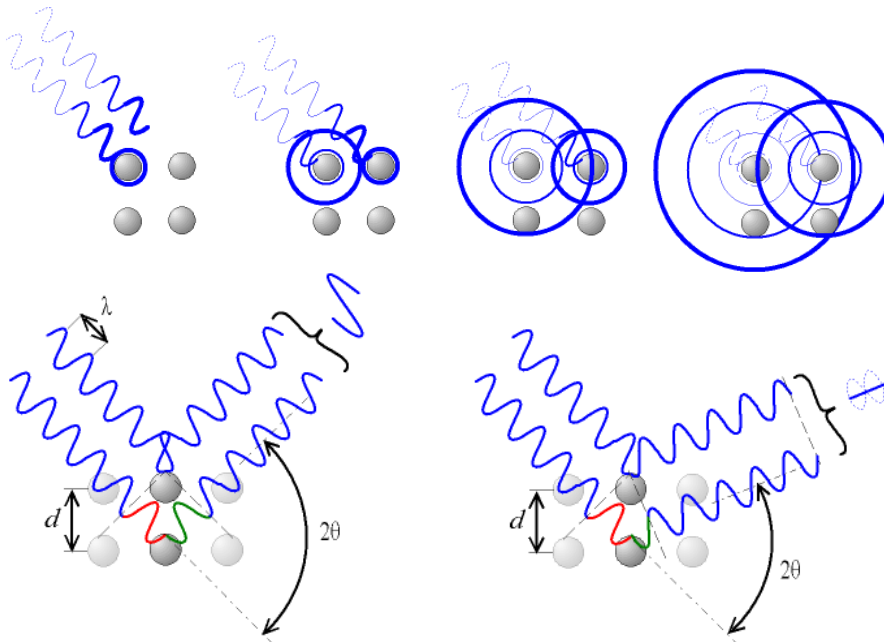


Figure 4.10. Depiction of the interaction of X-ray photons with atoms in a crystal structure.

(Source: http://en.wikipedia.org/wiki/Bragg_law.)

Interatomic distances in solids are comparable with wavelengths of X-rays, and an observable interference effect may occur between the scattered waves that manifest in certain directions, creating a diffraction pattern.

If the primary radiation is assumed to be a flow of photons from the view of the wave particle duality, then after collision of a photon and an electron, a part of the energy is passed onto the released electron and a part is radiated as a photon with a different, longer wavelength in another direction and participates on emergence of the secondary radiation. This effect is called a Compton effect, and the scattering is called inelastic (incoherent).

Besides the diffraction effects, a luminescence effect can also be observed when the impact of a radiation on a luminescent surface causes luminescence. There are two types.

- *Fluorescence* – a substance luminesces only upon incidence of a short-wavelength radiation. Photon of the primary X-ray radiation with sufficient energy can release an electron from the inner atomic layer. Its place is then

filled up by another electron from a higher layer, and an emission of a fluorescence radiation quantum occurs.

- *Phosphorescence* – a substance luminesces for some time after the impact of the radiation.

Luminescing materials called luminophores are, for example, cesium iodide, cesium sulfide, zinc, etc. During luminescence, an X-ray photon knocks out an electron from an outer shell to a shell closer to the core. Lower energy is then emitted in form of a light which has a longer wavelength than the X-rays – termed as outer layer transitions. Along with the electron transition from an outer surface to an empty inner surface space, another outer electron may be expelled from the atom. This is termed as a non-luminescent transition – Auger effect – and the emitted electrons are called Auger electrons.

Photochemical effect can be another occurring effect. It affects silver halides (AgBr), and the radiation causes a generation of individual silver and bromine atoms in this case, which is used in film development.

An important factor which must be considered when working with X-ray radiation is the biological effect as X-rays are harmful to living matter.

In the case of single crystals, it is possible to meet the condition for Bragg equation with a suitable crystal orientation towards the beam of incident radiation. In the case of polycrystalline or powdered samples, with random orientation of crystal grains, it is likely that some grains will be oriented so that the above-mentioned planes hkl will be in the diffraction position. This probability will be greater with higher number of grains in the irradiated space. The radiation diffracted by planes hkl of one grain will further be radiated in a direction which holds an angle $2\theta_{hkl}$ with the direction of the incident radiation. If the considered crystal grain is turned around an axis identical with the direction of the incident radiation, the diffraction planes hkl still remain in the diffraction position (since they still hold an angle θ_{hkl} with the incident beam), and the diffracted beams move over the circumference of a cone with apex angle $4\theta_{hkl}$ and axis in the direction of the incident radiation. Diffracted beams from all grains with planes hkl in the diffraction position will also be radiated onto this conical area.

Table 20.4b. Comparison of X-ray diffraction methods.

Information	Single crystal	Powder record
Crystal size	0.1–0.8 mm	0.2–10 μm
Number of crystals	1	From hundreds to thousands
Sample preparation	Selection of single crystal	Milling in agate mortar
Reflective positions	3 position rotation angles	1 angle (2θ)
Individual intensity of reflexions	Clear separation of each reflection	Overlapping of intensities caused by symmetry (absolute) and close position of reflexions.
Reflexion profiles	Sharp, given by the shape of the crystal	Deformed by instrument flaws, tension in small crystals, and preferred orientation
Phase purity	Always one phase	Presence of another phase cannot be excluded by simple means.
Preferred orientation	Without problem	Distorted information about intensity
Number of observed reflections ($V = 1000 \text{ \AA}^3$)	Thousands, suitable for evaluation using direct methods	Tens to hundreds. Low number for direct methods using statistics.

The basic difference between single crystal and powder X-ray diffraction methods lies in the appearance of the diffraction patterns which are obtained during the measurements. In the case of single-crystal diffraction, the diffraction pattern consists of individual points corresponding to the reflections (Fig. 4.11a), while for powder diffraction the pattern is formed by Debye-Scherrer rings (Fig. 4.11b).

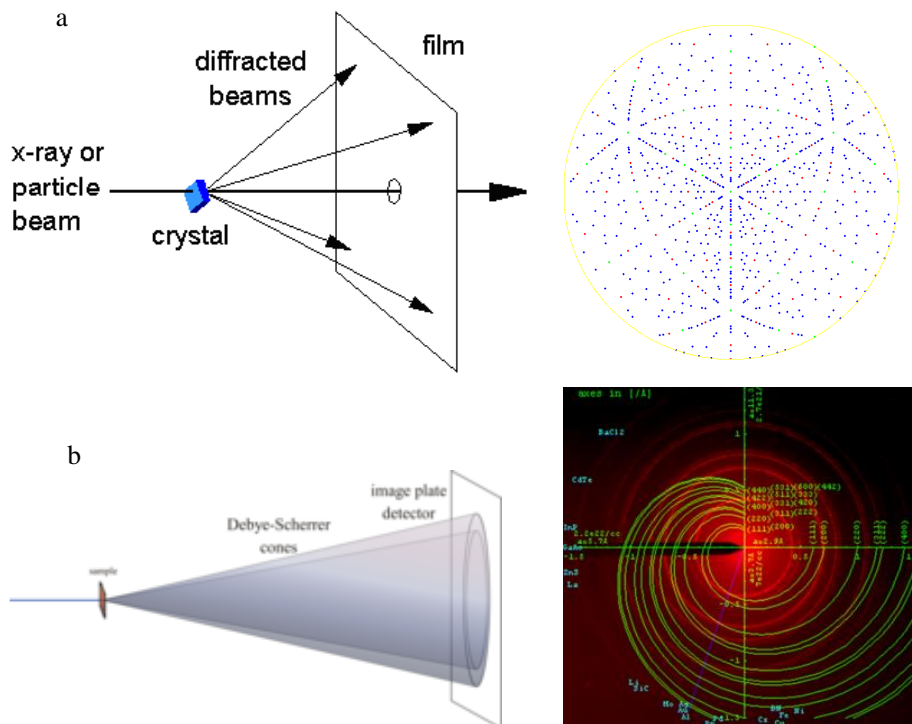


Figure 4.11. Separate point diffractions for single crystal diffraction patterns (a) and diffraction rings for powder diffraction patterns (b).

(Source: <https://www.britannica.com/science/X-ray-diffraction>.)

4.4.1.1 Structure determination methods

In pharmaceutical applications, it is essential to determine the crystal and molecular structure of active substances (polymorphs, solvates, salts, cocrystals, etc.) with high precision. Routine single crystal X-ray diffraction analysis is now available with sophisticated experimental techniques (single crystal X-ray diffractometer) and software packages for complete interpretation of measured data. The disadvantage of this method is the input material: a single crystal of sufficient size, which is difficult to obtain in some cases. Therefore, assessment of crystal structures from X-ray powder data is being developed very rapidly. In addition, the electron diffraction method which does not require such large single crystals as X-ray diffraction is also being applied. Furthermore, in electron diffraction data collection, it is not necessary to separate the single crystal from the mixture, and the structural analysis can be performed directly in the matrix (compact or powder).

4.4.1.2 Data collection on the single crystal X-ray diffractometer and the crystal structure solution

The input material for SCXRD is a single crystal, in the order of 0.01 mm^3 in size, and monochromatic X-rays are used for analysis. The single crystal is placed on the goniometric head of the X-ray diffractometer and a three-circle system allows the single crystal to be rotated to all positions where the Bragg condition is satisfied (see Bragg equation). A position-sensitive CCD detector rotates around the fourth axis and collects diffraction beams from the measured crystal. The movement of the crystal and the detector is controlled by a computer. (Fig. 4.14).

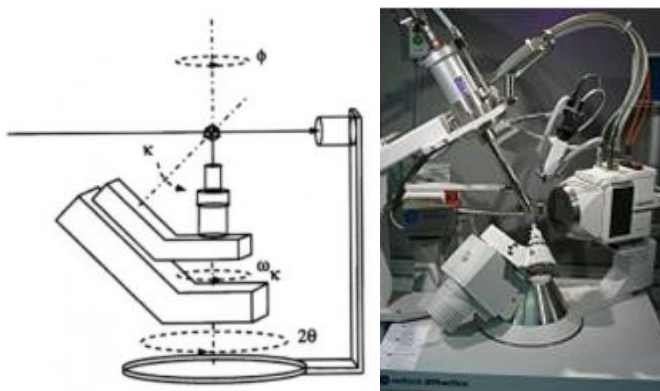


Figure 4.14. Schematic depiction and a photograph of a four-circle single-crystal diffractometer with kappa geometry.

(Source: http://serc.carleton.edu/research_education/geochemsheets/techniques/SXD.html.)

The position of atoms in a unit cell affects the intensity of the the diffracted beams from the individual crystal planes h,k,l . To determine the geometry and symmetry of the crystal structure – the lattice parameters, the space group, and the atom coordinates (x,y,z) – it is required to measure both the positions and intensities of diffraction spots in the diffraction pattern (Fig. 4.15).

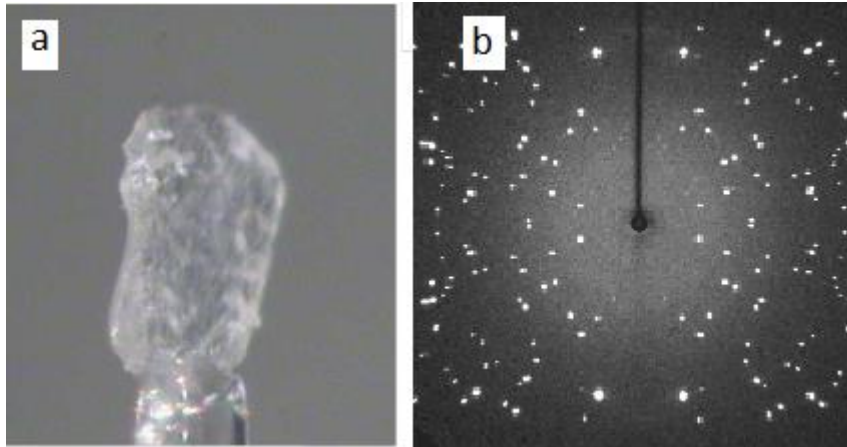


Figure 4.15. Single-crystal ready for measuring, size 0.1×0.3 mm (a); acquired single-crystal diffraction pattern (b).

(Edited according to: http://en.wikipedia.org/wiki/X-ray_Crystallography.)

The principle of finding atomic coordinates in the asymmetric part of the unit cell is described by the following equation:

$$\rho(x,y,z) = (1/V_{\text{cell}}) \sum_h \sum_k \sum_l F_{hkl} \exp[-2\pi i (hx + ky + lz)]$$

V_{cell} – unit cell volume

To determine the unknown graph of the electron density function $\rho(x,y,z)$, assuming that knowledge of a sufficiently large number of F_{hkl} values, it is required to perform a three-dimensional summation of the Fourier series over all values of the indices h,k,l in the elementary cell or its asymmetric part, respectively. The atoms lie in the found maxima of the function. However, there is one important consideration with this procedure – the structure factor F_{hkl} is a complex number, so it is necessary to know not only the amplitude but also the phase ϕ_{hkl} :

$$F_{hkl} = |F_{hkl}| \exp(i\phi_{hkl}); \quad I_{hkl} = |F_{hkl}|^2$$

The phase values cannot be obtained directly from the diffraction experiment but can be extracted by mathematical procedures. Experimentally, only the I_{hkl} intensities are available from which the F_{hkl} values needed to perform Fourier summation can be obtained. The whole procedure is described in Fig. 4.16.

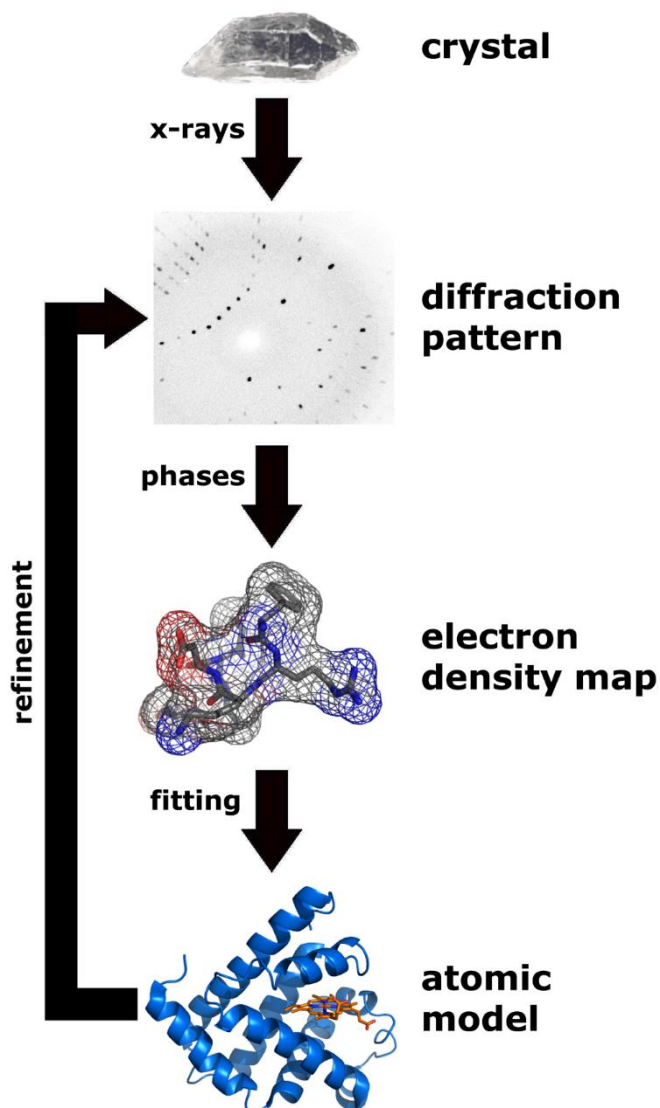


Figure 4.16. Depiction of procedure for solving of crystal structure, based on single-crystal measurements.

(Source: http://en.wikipedia.org/wiki/X-ray_crystallography.)

4.4.1.3 Standard outcome and presentation of results of a single-crystal diffraction

Molecular structure is usually presented in form of images which also show thermal movements of individual atoms in the form of thermal ellipsoids. Sets of interatomic distances, angles, and torsion angles are also exported by default.

Information on molecular packing and types of non-bonding intermolecular interactions is also attached to the solved crystal structure. From the molecular packing, it is also possible to identify intramolecular interactions and find open spaces (channels and cavities) in the structure. Plenty of molecular graphics programs can be used for visualization (e.g., Mercury, WebLabViewer). The most common input is a cif-file (contains lattice parameters, space groups, chemical composition, atomic coordinates, thermal-vibration coefficients, bond distances, etc.). A table of crystallographic parameters or a table of hydrogen bonds contained in the studied structure are parts of the report for a solved structure, based on single-crystal measurement, see Table 4.5, Table 4.6, Fig. 4.17, and 3.18.

The resolved crystal structures are usually published together with synthetic data, where the solved structure is the most illustrative confirmation. The published cif-files are saved in Cambridge Structural Database (CSD) where they undergo a verification process. In a publication, the validated structure is referred to by a CCDC code. In the CSD database, the structures are saved under another codes. According to these references, it is possible to search for a structure, and the data are publicly available *per request* (www.ccdc.cam.uk).

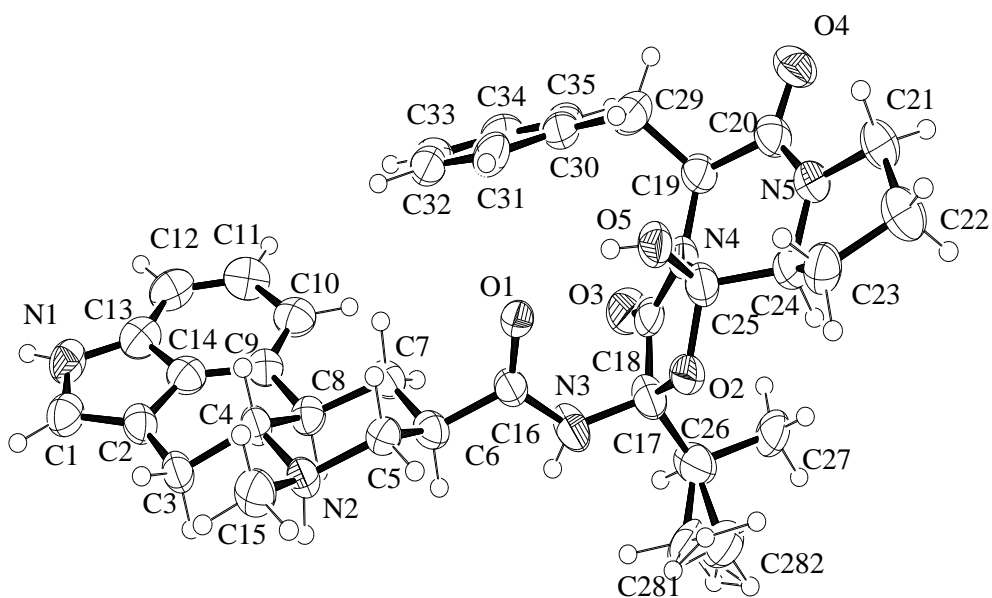


Figure 4.17. Depiction of a molecular structure of ergot alkaloid, dihydroergocristine, using thermal ellipsoids of vibrating atoms.

(Source: Petříčková H. *Structural study of morphine alkaloids and their complexes*. Dissertation. UCT Prague, 2007.)

Table 20.5. Basic crystallography (left) and measurement parameters (right) for the structure of dihydroergocristine mesylate ethyl acetate monohydrate.

Crystal parameters		Measurement parameters	
Formula	C ₃₅ H ₄₂ N ₅ O ₅ CH ₃ O ₃ S 2.C ₄ H ₈ O ₂ H ₂ O	Crystal dimensions [mm]	0.2 × 0.3 × 0.4
a [Å]	12.5090(3)	Range of h k l	-16 → 16 0 → 22 0 → 25
b [Å]	17.7480(5)	Total number of reflections measured, θ range	49251, 1.97–27.09
c [Å]	20.3050(5)	Number of independent reflections	8718
α [°]	90	Criterion for observed reflections	I > 1.96 (I _σ)
β [°]	90	Minimized function	Σw(F _o - F _c ²)
γ [°]	90	Weighing scheme	Chebyshev polynomial
Space group	P 2 ₁ 2 ₁ 2 ₁	Parameters refined	595
Z	4	Values of R R _w S	0.0721 0.0802 1.0480
Unit cell V (Å ³)	4507.9(2)	Ratio of the maximum least-squares shift to e.s.d in the 1 st cycle	0.0002
μ [mm ⁻¹]	0.142	Max. and min. heights in final Δρ map	-16 → 16 0 → 22 0 → 25
		CSDC number	56324

Table 20.6. Hydrogen bonds in the studied structure.

Distances and angles	D–H..A	D–H	H..A	D..A	D–H..A	Symmetry
	O5–H4..O1	0.9924	1.8143	2.702(3)	147.10	
	N1–H1..O _{solvent}	0.9900	2.0142	2.944(5)	155.49	
	N2–H2..O _{msf}	0.9985	1.9366	2.907(4)	163.11	
	N3–H3..O4	0.9951	2.4783	3.174(5)	126.61	$-x, 1/2 + y, -3/2 - z$
	O _{H2O} –H _{H2O} ..O _{msf}	1.0048	1.9732	2.703(7)	127.31	
	O _{H2O} –H _{H2O} ..O4	1.0118	1.8011	2.576(7)	130.50	$-x, 1/2 + y, -3/2 - z$

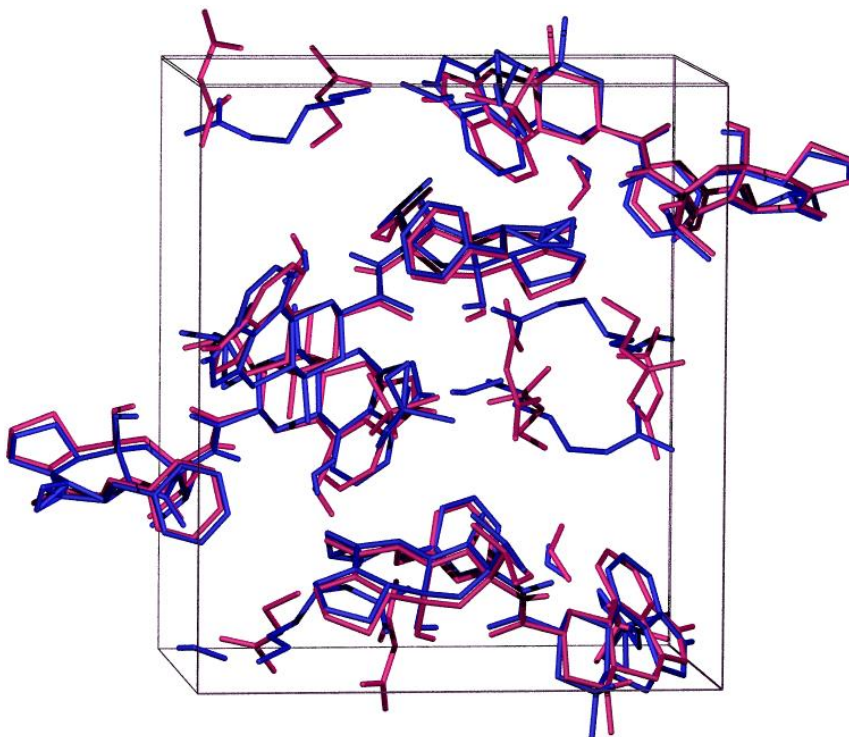


Figure 4.18. Overlap of two crystal structures of dihydroergocristine mesylate solvates, crystallized with various solvents built inside the structures. The positions of ergot alkaloid molecules are virtually identical and there is a large number of cavities in the structures where the solvent molecules (either two molecules of ethyl acetate or a single molecule of amyl acetate) can fit.

4.4.1.4 Electron diffraction

Three-dimensional electron diffraction (3D ED) is a relatively new method that is being introduced into structural analysis, and that requires only a small amount of input material (nanocrystal). It has great potential for development and is certainly interesting for application in pharmaceuticals.

Due to the wave properties of elementary particles (Louis de Broglie, 1924), electron beam incident on crystals also exhibits diffraction phenomena. At significantly higher incident electron energies, from approximately the first tens of keV onwards, relativistic electrons can illuminate a thin layer of the substance under investigation, e.g., of a nanocrystal, and diffract and provide analyzable diffraction data – diffraction intensities and positions which enable the crystal structure determination.

The 3D ED experiment is performed on a transmission electron microscope (TEM) in the diffraction mode; but specialized electron diffractometers are already being developed. Data are collected from a nanocrystal (volume $1-10^{-4} \mu\text{m}^3$). The size of the nanocrystal is matched to the width of the probing electron beam which ranges from units of nm to a few μm . Compared to X-ray single crystal analysis, the crystal size required for 3D ED is 2–3 orders of magnitude smaller, which is very significant for sample preparation.

Nanocrystals measured by ED are of course very sensitive to any mechanical instability of the TEM goniometer which can easily deflect the sample out of the irradiated area. Most often, the electron beam follows the motion of the nanocrystal according to a predetermined trajectory.

Protocols in 3D ED ensure optimal collection of integrated diffraction intensities and their positions. There is a number of data reduction software packages specifically designed for 3D ED or adapted from software for X-ray diffraction data. Compared to X-ray diffraction however, there are two experimental limitations with the 3D ED, so far: the positions of the diffractions on the detector are inaccurate, and multiple electron scattering occurs in the material under investigation, which distorts the diffraction intensities. In contrast, one of the advantages of 3D ED is that the strong Coulomb interaction between the incident electrons and the crystal mass allows a good signal-to-noise ratio even for very thin samples, making it easier to identify light atoms such as lithium and hydrogen, compared to X-ray diffraction. The 3D ED can thus determine the absolute structure more reliably.

Current pharmaceutical research is widely using the SCXRD method for structural studies of molecular crystals (substances, impurities, intermediates, etc.). The problem however is that some substances crystallize poorly – in submicroscopic crystals of inappropriate shapes (filaments, leaflets, book-like crystals, etc.), or in

imperfect crystals formed at phase interfaces. Polymorphism of substances and their unexpected polymorphic transitions are also a persistent problem in the pharmaceutical industry. It is therefore important to perform structural studies of polymorphic transitions already at the nucleation stage, and then in complex matrices, e.g., in a tablet or capsule. Recently, cocrystals have been the subject of research in pharmaceuticals. The boundary between the category of pharmaceutical cocrystals vs. pharmaceutical salts is loose and can be a subject of litigation. A recognized criterion for clear classification of a substance into the correct category is the determination of the position of the proton (hydrogen) between the donor and acceptor. The occasional problems with determining the proton positions are known in SCXRD. Knowledge of the absolute structure and the resulting chiral purity is crucial for pharmaceuticals, which no pharmaceutical manufacturer can afford to ignore today. The SCXRD method can determine the absolute structure more reliably when the structure contains a heavy atom (Fig. 4.19).

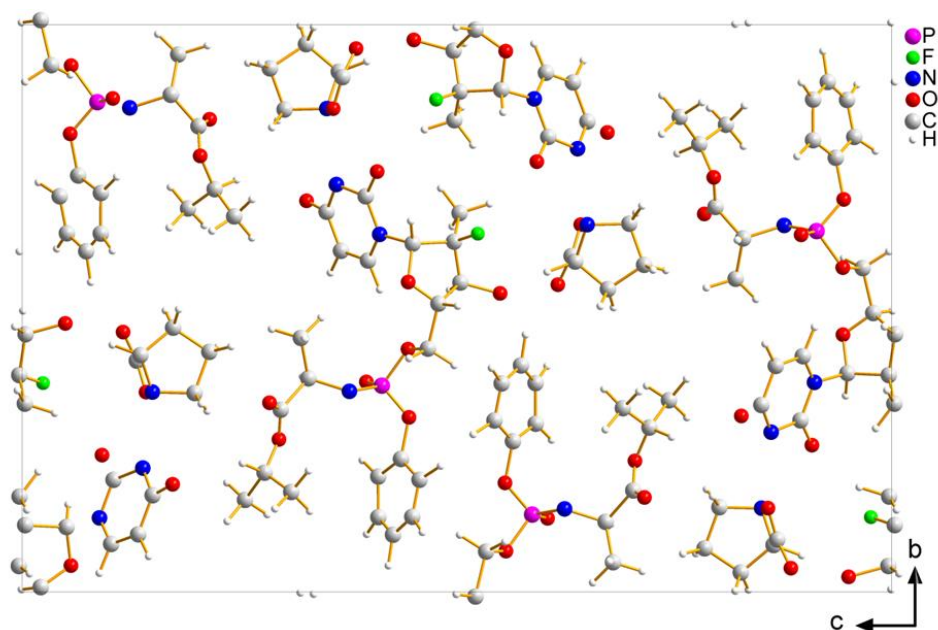


Figure 4.19. Absolute crystal structure of cocrystal sofosbuvir–L-proline determined by 3D electron diffraction method.

(Source: Palatinus et al. *Chem. Listy.*, 2021.)

In all of these pharmaceutical applications, 3D ED can be successfully applied. Even compared to SCXRD, the 3D ED method, in combination with dynamic refinement, can more easily and reliably determine the absolute structure, even when consisting of only light atoms. Other examples of pharmaceutical applications of 3D ED are the determination of the active substance structure directly in the

dosage form (compact matrix), or the structural study of rapid polymorphic transformations.

4.4.2 Powder methods

4.4.2.1 Debye-Scherrer method

Polycrystalline material consists of many small, randomly distributed, and independently diffracting single crystals. All single crystals are variously rotated towards each other. A polycrystalline sample can be a compact solid body (joint crystal grains), a loose powder, or a thin surface layer. A basic and by far the most applied method used for polycrystalline materials, is the Debye-Scherrer technique, see Fig. 4.20.

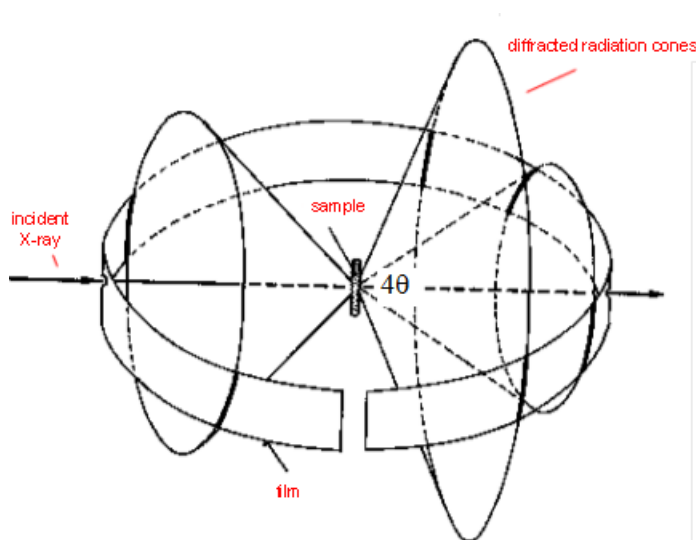


Figure 4.20. Principle of Debye-Scherrer method.

(Source: <https://encyclopedia2.thefreedictionary.com/Debye-Scherrer+Method.>)

When a monochromatic beam is incident on a polycrystalline sample, the crystal planes that satisfy the Bragg equation diffract. The diffracted beams then form a concentric cone with a vertex angle of 4θ . The intersection of the diffraction cone with a planar detection film placed perpendicular to the axis of the cone is the diffraction line which has the shape of a circle. The powder sample is spread on a glass fiber with a diameter of about 0.3 mm or is poured into a glass capillary placed in the center of a cylindrical chamber, with a film strip placed along its inner circumference. Here, the diffraction cones produced by diffraction of the incident

beam on a system of crystal planes with varying interplanar lengths d_{hkl} (and therefore different angles θ) intersect the film in circles. The unrolled film then shows a set of circular arcs with different radii. As an example, a Debye photograph of powder silver obtained with radiation from a copper anode (CuK_α radiation) is shown in Fig. 4.21.

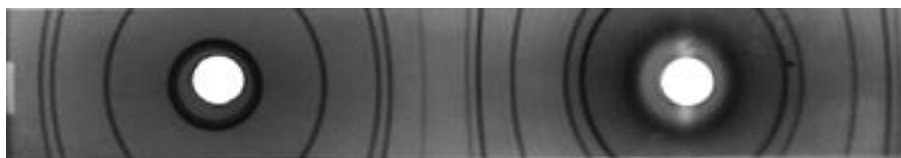


Figure 4.21. Debye photograph of powdered silver.

(Source: <http://www.xray.cz/krytalografie/str11a.htm>.)

Diffraction angles θ are determined from measured positions of the diffraction lines, and their determination enables to calculate the interplanar lengths d_{hkl} using the Bragg equation. The chamber is designed so that the distance of diffraction lines from the center of the right hole, expressed in millimeters, gives either the value of θ or 2θ in degrees.

4.4.2.2 Powder X-ray diffractometer with the Bragg-Brentano geometry

The powder diffractometer in Bragg-Brentano parafocusing geometry is currently the conventional apparatus for the study of powder diffraction on polycrystalline materials. It enables precise measurement of diffraction line positions and intensities, utilizing an extensive control and application software. A simple diagram of the most common type of a powder diffractometer is shown in Fig. 4.22. A photo of the whole instrument and its goniometer is shown in Fig. 4.23.

Sample is placed in the middle of a circular plate, see Fig. 4.22, which rotates around the main axis of the goniometer. A detector for diffracted radiation moves on the perimeter of a circle with radius given by the geometric configuration, with twice the angular speed of the sample. Diffractogram is measured either continuously, where the angular dependence of registered pulse frequency is plotted with a plotter, or in steps, with data output maintained using a printer or other recording medium.

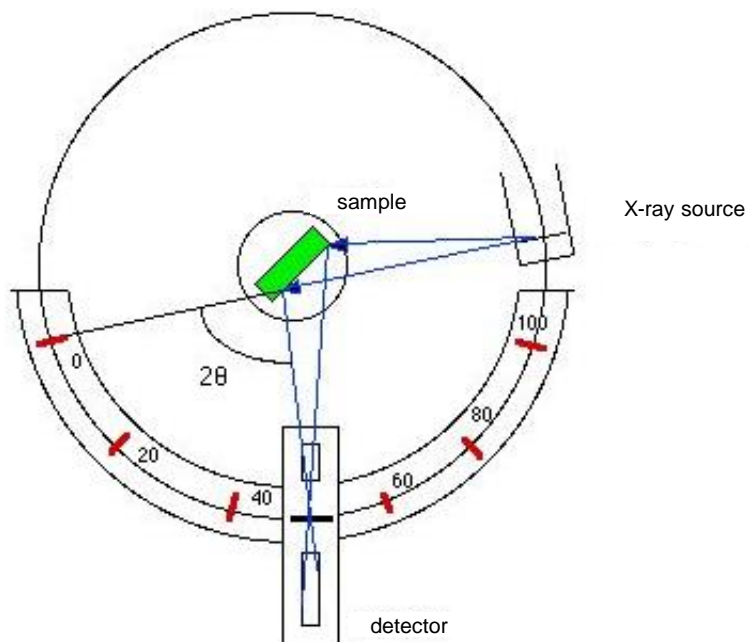


Figure 4.22. Scheme of a diffractometer in Bragg-Brentan parafocusing geometry.

The primary incident beam forms 2θ angle with the diffracted beam.

(Source: <http://pd.chem.ucl.ac.uk/pdnn/inst1/focircle.htm>.)

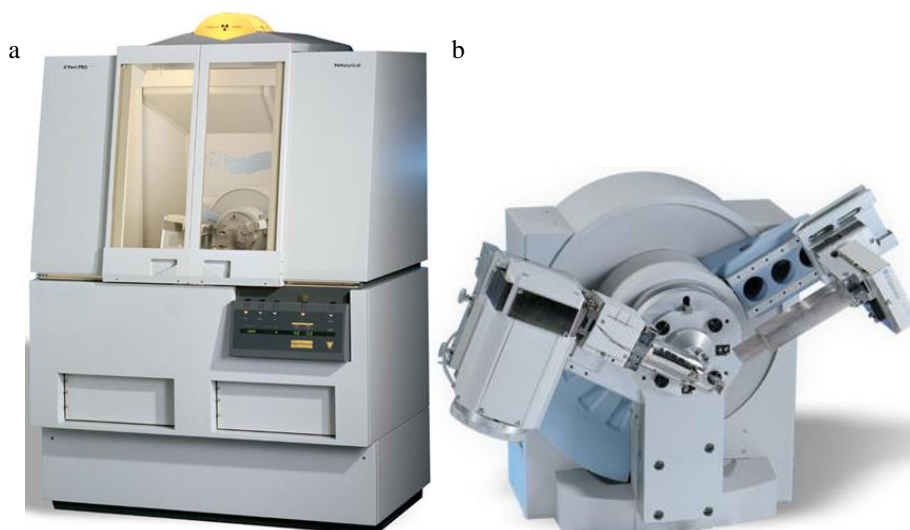


Figure 4.23. The whole X-ray powder diffractometer (a) and the separate goniometer with arms (b).

(Source: <https://www.malvernpanalytical.com/en/>.)

In this arrangement, a powder sample is filled into a flat holder located in the goniometer axis, see Fig. 4.24. Scanning is carried out as the detector moves at speed 2θ and the sample moves at speed θ . The diffraction is symmetrical as the incident angle is identical with the diffraction angle. Thus, diffraction is always registered on planes hkl which meet the diffraction condition for the particular θ and are oriented parallel with the sample surface. This means that the information for different hkl planes is obtained from different grains.



Figure 4.24. Samples prepared for measurement, placed in the most used holders in the X-ray powder diffraction with Bragg-Brentano geometry (a), raw powdered sample (b).

A significant instrument error can occur with Bragg-Brentano diffraction, where the most serious effect is the positioning of the sample away from axis. This leads to both blurring of the diffraction line and also to its shifting. Diffracted beam is thus focused in a place other than the position of the detector. A functional dependence of this shift on the diffraction angle ($\cos \frac{\theta}{R_G}$) can be derived from a geometrical sketch. This can be used when evaluating lattice parameter, as shown in Fig. 4.25

So far, only a monochromatic incident radiation was considered. Acquisition of monochromatic radiation using diffraction on a crystal – a monochromator, is associated with a decrease in intensity for the primary beam, and therefore the most common measurements use the most intense parts of the characteristic spectrum of an employed X-ray tube: doublet $K_{\alpha 1}$, $K_{\alpha 2}$. The wavelength difference of this doublet is so small that splitting of the diffractions occurs only at higher diffraction angles. This implies directly from the Bragg equation. If this splitting is observed, it is required to use corresponding wavelengths of the individual doublet components for the interpretation. It should be emphasized that in this case, there are two diffractions from the same system of planes but for two different wavelengths contained in an incident beam of X-rays. Except the two most intense components, there are also other components in the X-ray spectrum of an X-ray tube, and continuous radiation is also not negligible. These components are inhibited by absorption filters or monochromators.

4.4.2.3 Standard results of powder diffraction and their presentation

A pattern of X-ray powder diffraction, shown in Fig. 4.26, is reported in a graphical form with relative intensities (intensity of the maximum line is 100 cps and the other lines are calculated accordingly). Another addition to a graphical output is a table of peak positions (2θ) and their relative intensities (I_{rel}), value of d -spacing, and the full width at half maximum (FWHM), see Table 4.7. In case of a control pattern measurement, it is compared with a standard, and this comparison is only visual (number of peaks and peak positions), with no available algorithm, such as for FT-IR data comparison. Calibration curve and deviation are presented in case of quantification. The measurement method is also reported as it has great influence on the results, and the information is insufficient without the measurement parameters (wavelength, measurement geometry).

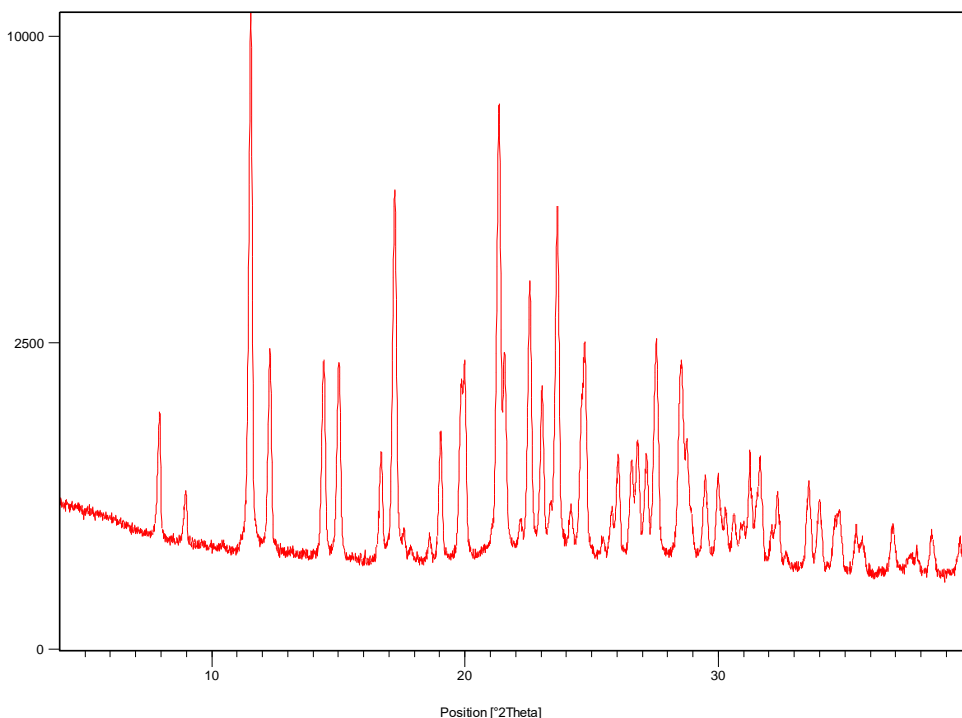


Figure 4.26. X-ray powder pattern of a studied API. Diffractogram was measured using X'PERT PRO MPD PANalytical diffractometer under the following experimental conditions: radiation: $\text{CuK}\alpha$ ($\lambda = 1.542 \text{ \AA}$); monochromator: graphite; excitation voltage: 45 kV; anode current: 40 mA; measured range: $4\text{--}40^\circ 2\theta$; step size: $0.008^\circ 2\theta$; flat sample of area/thickness 10/0.5 mm.

Table 20.7. Values of peak positions (diffraction angles) 2θ , d -spacings, and relative intensities of characteristic peaks of a crystal API form.

2θ [°]	d [Å]	I_{rel}
7.9229	11.14991	11.05
11.5267	7.67078	100
12.2892	7.19649	20.17
14.4072	6.14294	17.46
15.0082	5.8983	16.91
17.208	5.14891	49.72
19.841	4.47116	15.47
19.9785	4.4407	18.84
21.3222	4.1638	67.82
21.5503	4.12023	18.58
22.5418	3.9412	31.22
23.0286	3.85898	14.15
23.649	3.75912	46.14
24.6039	3.61534	12.33
24.726	3.59777	21.29
27.5295	3.23743	21.7
28.5065	3.12864	17.37
28.7475	3.10296	8.56
31.2385	2.86098	7.06

4.5 Applications of X-ray diffraction in pharmacy

Both single crystal and powder X-ray diffraction are widely used in pharmaceutical research, development, manufacture, and control. For example, powder diffraction is used to monitor the reproducibility of production batches or to identify and determine unknown phases. Single crystal diffraction is used, for example, for structural characterization of impurities or for absolute structure determination. In addition, data obtained from both methods are used in pharmaceutical documentation, patent litigation, etc.

4.5.1 Characterization and identification of unknown samples

After an X-ray pattern measurement, it is possible to immediately determine whether the substance is crystalline or amorphous. In the case of a crystalline substance, a database (or specifications, literature, DMF [drug master file]) can be used to compare results with reference data and identify the studied phase. With X-ray powder pattern measurement and extraction of positions of individual peaks, a set of 2θ , I_{rel} is obtained, and this set of data is then compared with available standard libraries (Fig. 4.27) and literature patents (Fig. 4.28). If a pattern library is available, the peak positions can be assigned, and the crystal phase identified.

When searching for new polymorphic forms, results of a set of crystallization experiments are considered, and similar patterns are looked up to create groups of particular polymorphs. Cluster analysis proved useful for comparison of diffraction patterns, see Fig. 4.29.

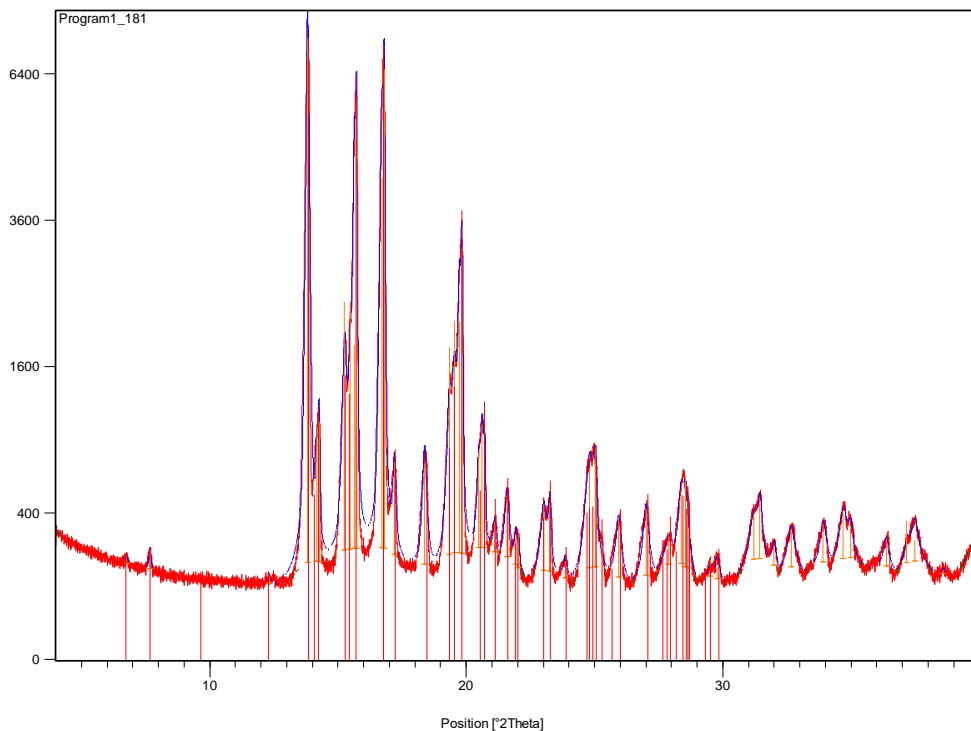


Figure 4.27. Identification of a crystalline phase using a library of X-ray patterns (database PDF-4): Finasterid, orthorhombic polymorph I, (CSD reference code: **WOLXOK02**).

(Source: <http://www.ccdc.cam.ac.uk/products/csd/>.)

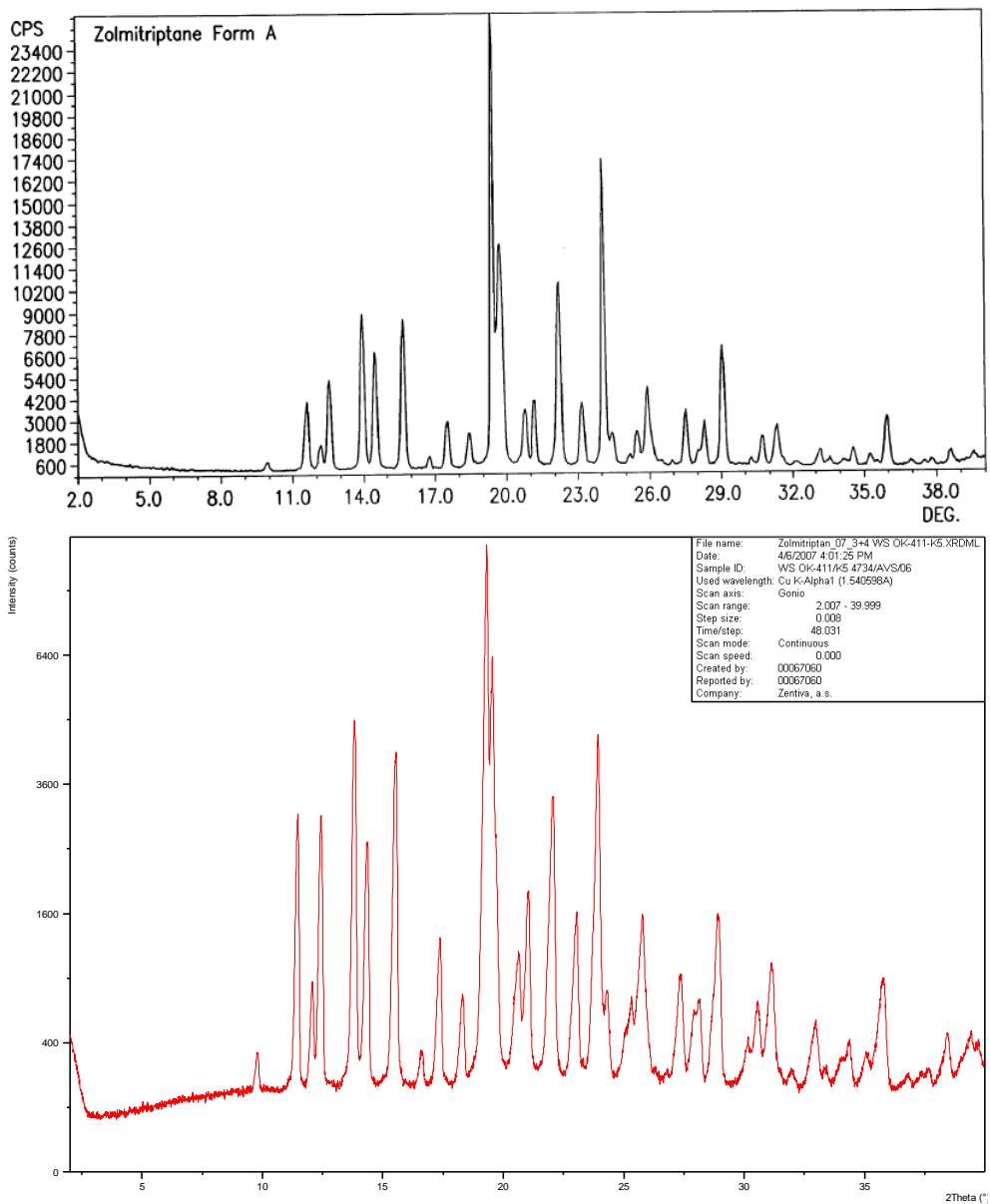


Figure 4.28. Identification of a polymorph according to a patent.

(Source: U. S. patent 2006/0148868A1.)

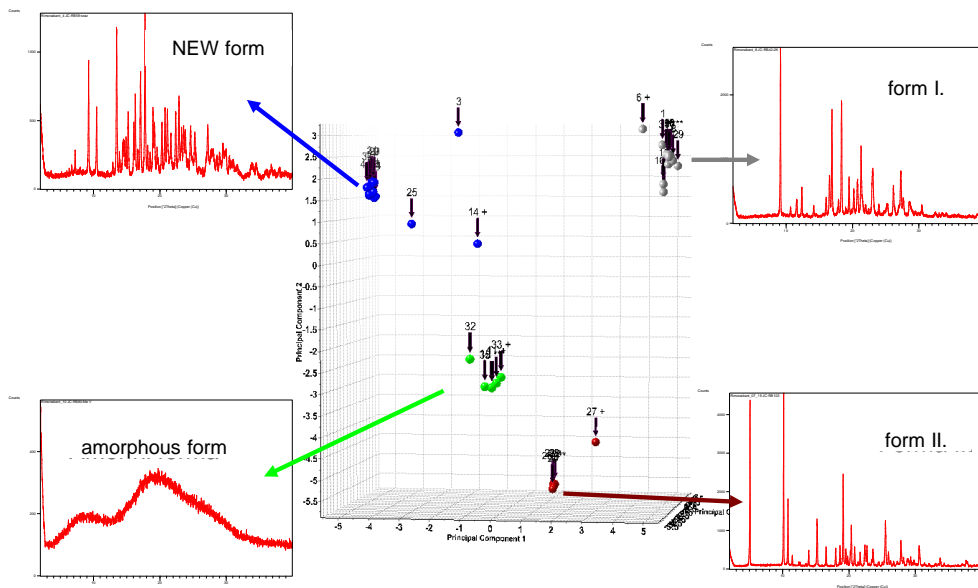


Figure 4.29. Polymorph screening using cluster analysis.

4.5.2 Crystalline phase control

X-ray powder diffraction is suitable also for routine control of the reproducibility of production batches, with the possibility to control presence of unwanted crystalline impurities (unwanted polymorphs), see Fig. 4.30 and 10.31. For this type of experiments, it is needed to find a suitable window in the diffractogram where peaks of one of the studied forms always occur. The particular polymorph modification can then be checked the same way, even after processing into a solid dosage form, see Fig. 4.32.

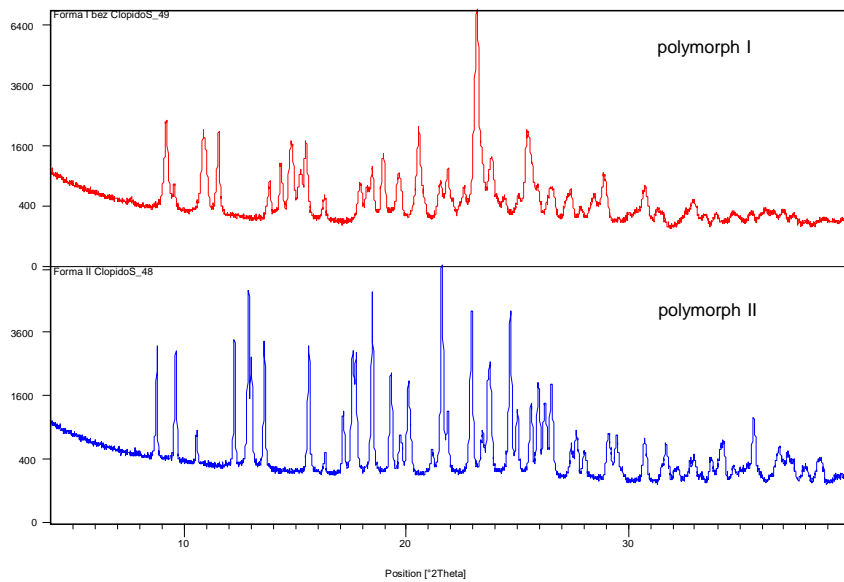


Figure 4.30. X-ray powder patterns for two polymorphs of clopidogrel hydrogen sulphate.

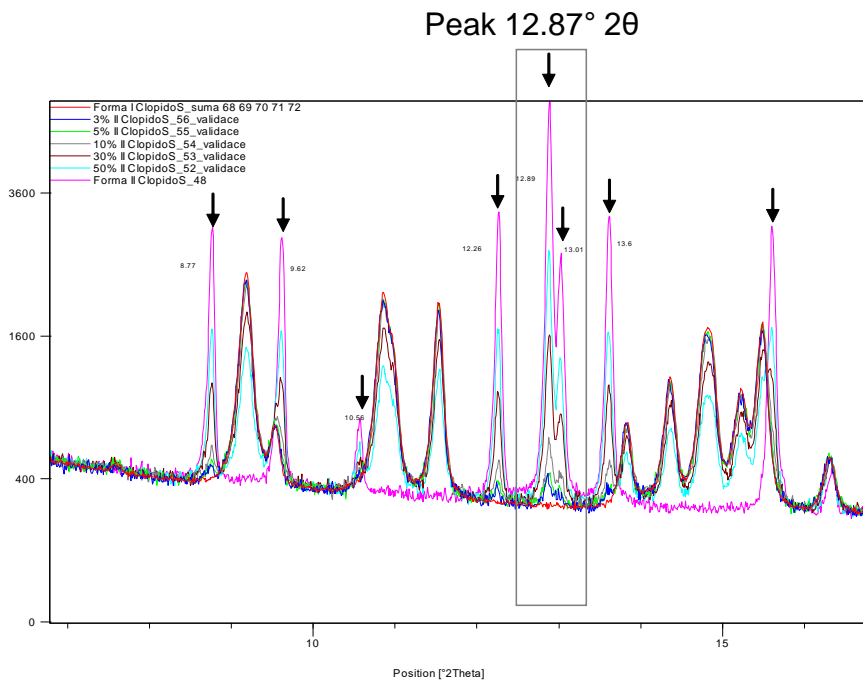


Figure 4.31. Determination of the limit of detection for clopidogrel polymorph II contained in polymorph I.

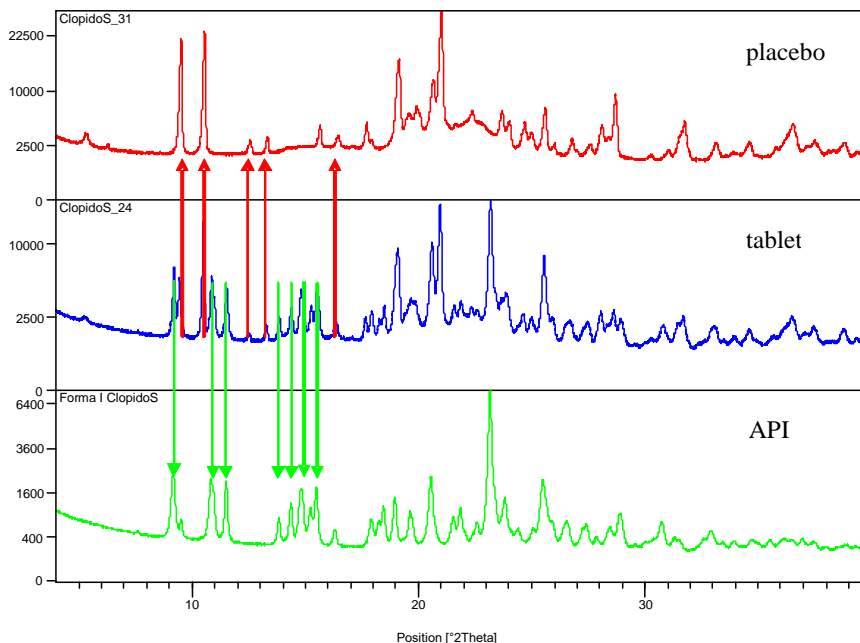


Figure 4.32. Control of crystalline clopidogrel after manufacturing into a solid dosage form.

4.5.3 Negative proof of crystalline phase – amorphous material

To obtain a diffraction pattern, the studied material must show a periodic arrangement of molecules in its structure. If the periodic arrangement is missing or present only in short distance, the X-ray powder pattern will show only wide "humps", see Fig. 4.33. As shown in Fig. 4.34 and 10.35, crystalline or amorphous phase can also be detected in a mixture.

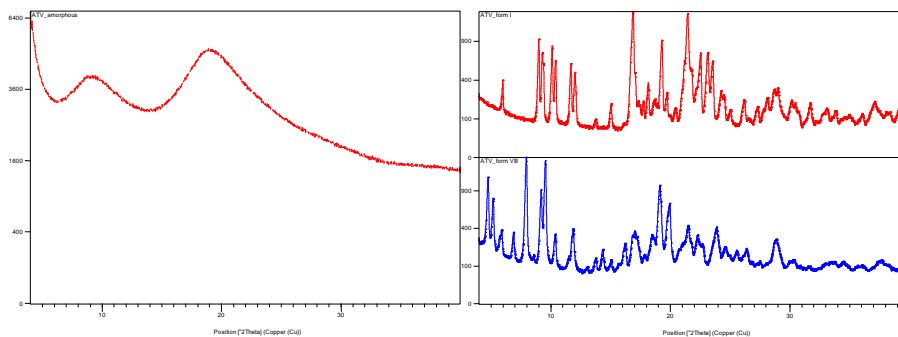


Figure 4.33. Examples of X-ray patterns of an amorphous and a crystalline phase of an API.

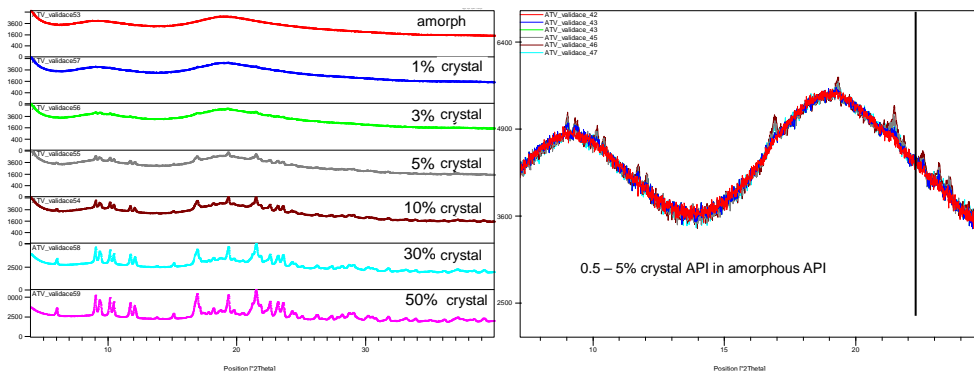


Figure 4.34. Detection of a residual crystalline phase in an amorphous sample.

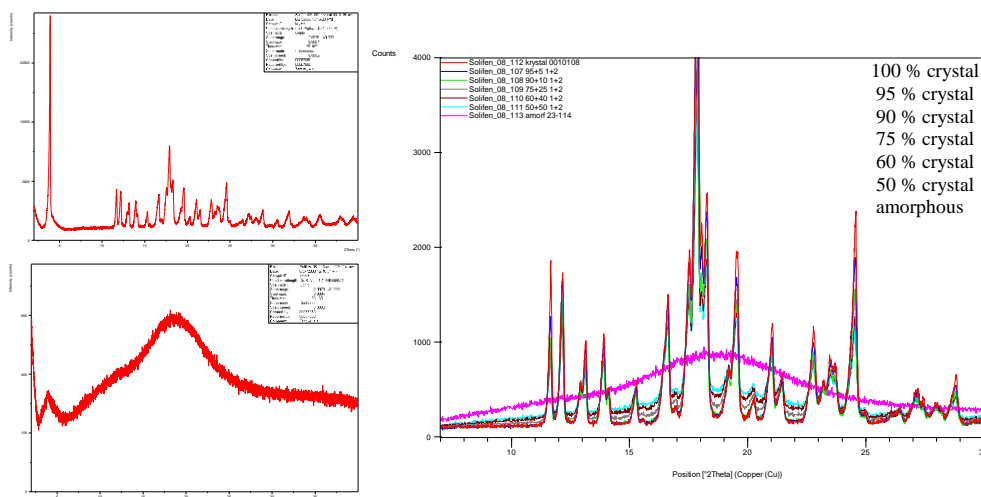


Figure 4.35. Detection of an amorphous phase mixed with the crystalline phase.

4.5.4 Observation of phase transformations

Changes in crystallization parameters of an API can produce its different polymorph, solvate, or an amorphous. Similarly, stability testing (Fig. 4.36) or processing of an API into a formulation (see Fig. 4.37 and 10.38) may lead to phase transitions mentioned above, i.e., changes in the molecular packing. These phase changes may occur due to mechanical processing (tableting, micronizing, milling), or increased temperature, relative humidity, or combination of both.

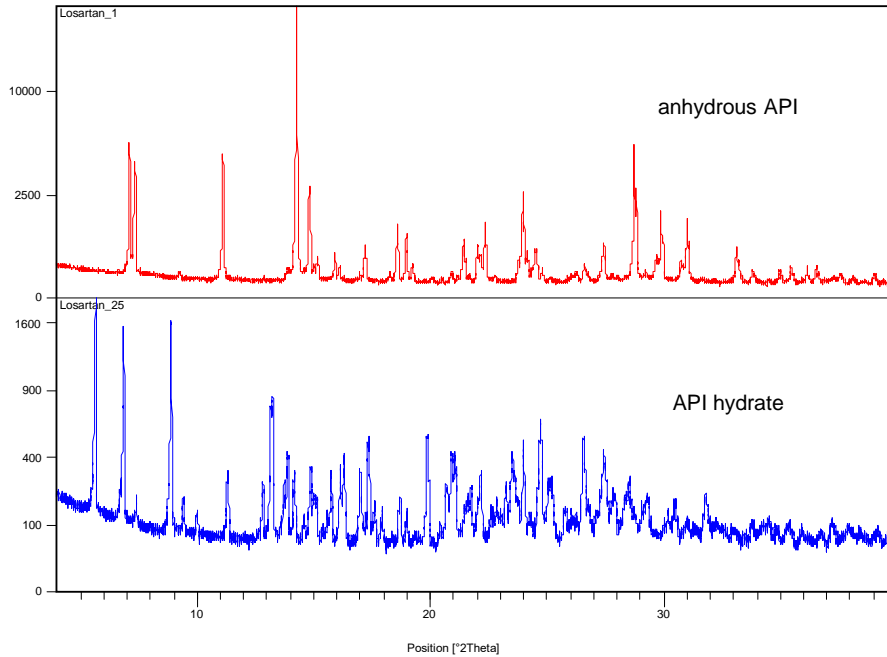


Figure 4.36. Change in a crystal form of an API – formation of a hydrate during stability testing. After three-months, under 40 °C/75% RH in PE package, the anhydrous API recrystallized into a hydrate.

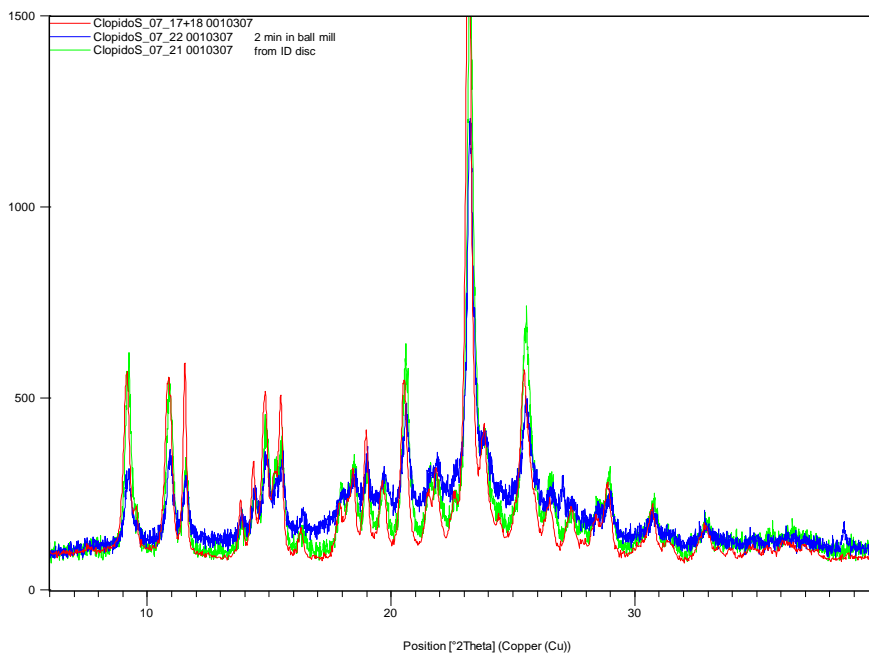


Figure 4.37. Amorphization of a crystalline sample caused by milling.

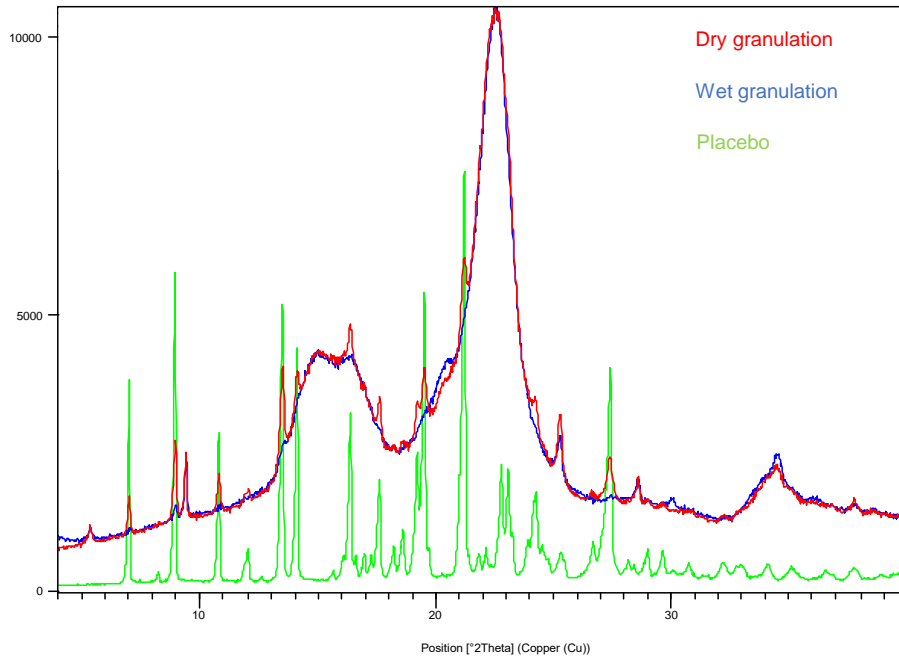


Figure 4.38. Phase conversion of a crystalline API into amorphate, caused by wetting during granulation.

4.5.5 Study of substance behavior under defined conditions

Temperature-humidity chamber, shown in Fig. 4.39, enables monitoring of powder sample behavior under different temperature and relative humidity. In this case, a sample placed in this chamber is repeatedly irradiated by X-rays. The X-ray powder monitoring of behavior of pharmaceutical substances, depending on the humidity, is shown in Fig. 4.40.

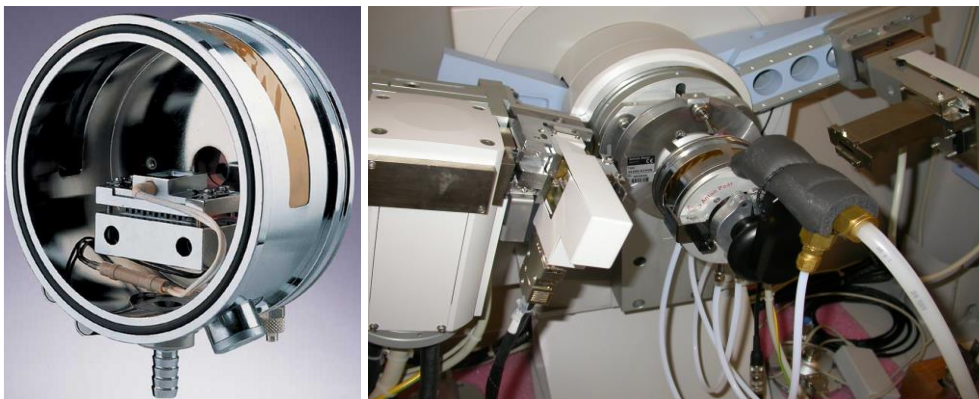


Figure 4.39. Temperature-humidity chamber.

(Source: <https://www.anton-paar.com/cz-cs/>.)

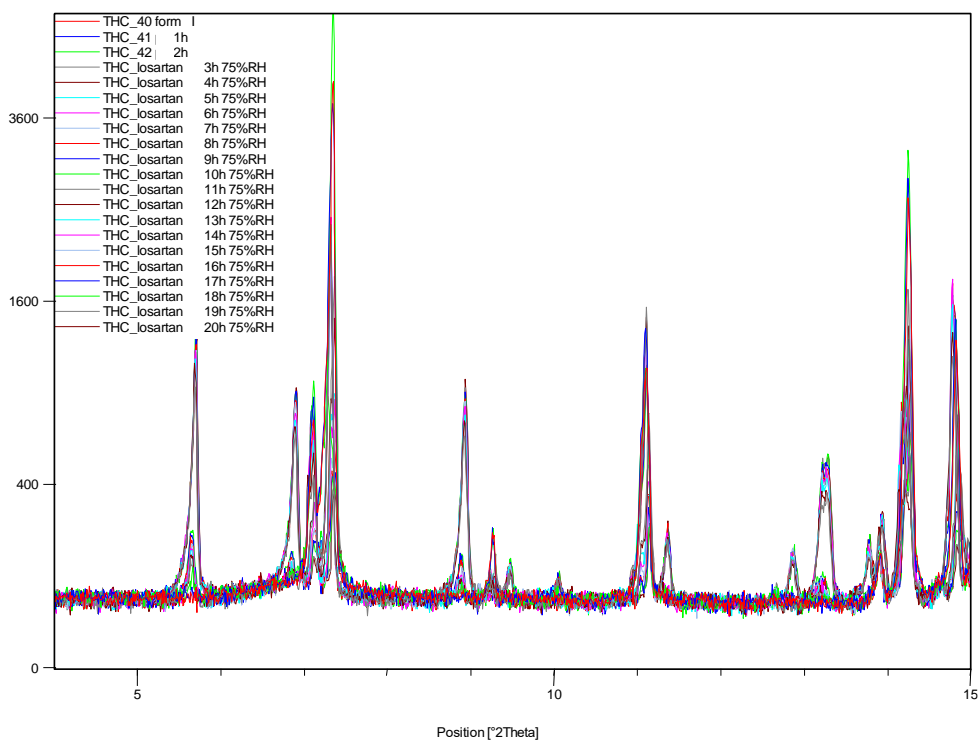


Figure 4.40. Formation of hydrates in a temperature-humidity chamber.

4.5.6 Determination of structures of unknown impurities or molecule chirality

For each API, it is necessary to characterize the impurity profile and determine impurity structures. Each impurity must be separately crystallized, and the resulting single crystal subjected to a structural analysis. In most cases, the single crystal diffraction analysis is able to determine the absolute structure, i.e., the configuration of the chiral centers in the molecule (if present), see Fig. 4.41.

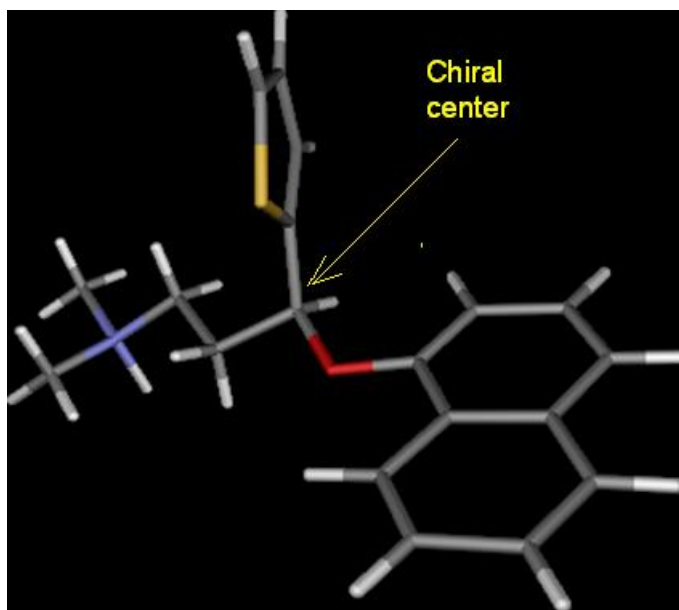


Figure 4.41. Molecular structure of an API with a determined configuration of the chiral center at the carbon atom, obtained by single-crystal X-ray diffraction.

4.5.7 Calculation of powder diffraction patterns

From the experimentally determined crystal structure (lattice parameters, space group of symmetry, atomic coordinates), the so-called calculated theoretical powder diffraction pattern of the substance can be calculated. Such a pattern is thus free from all instrument and sample influences and errors (peak asymmetry, peak extensions, preference orientation, etc.). The calculated theoretical powder pattern is ideal for setting of a substance standard (reference) X-ray pattern, see Fig. 4.42. Single-crystal structure can therefore serve as a model for calculation of a theoretical powder pattern – the optimal reference standard.

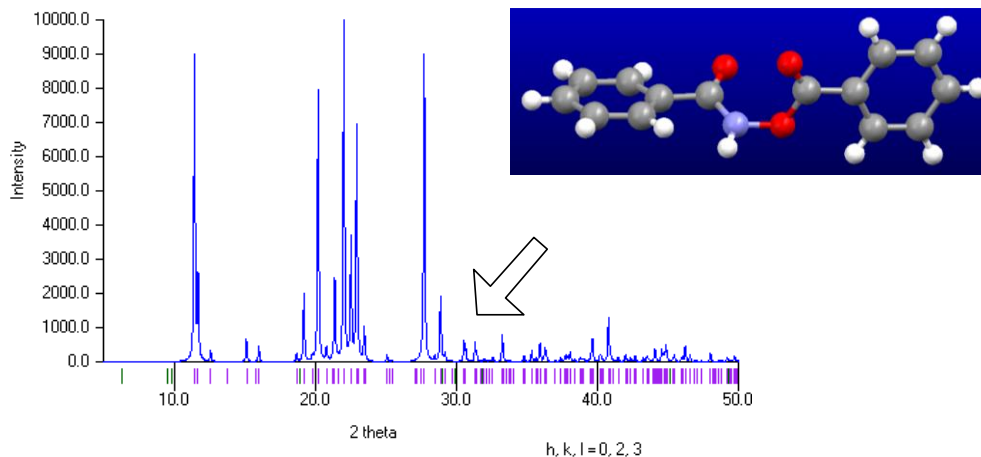


Figure 4.42. A calculated theoretical powder pattern of a known crystal structure, determined from a single crystal data.

4.5.8 Determination of a 3D crystal structure from X-ray powder data

If a suitable single crystal for SCXRD cannot be crystallized, a powder sample with a grain size of about 10^{-3} – 10^{-5} m must be used. In this case, it is recommended to solve the crystal structure from the powder diffraction data. The powder data are measured on an advanced laboratory powder diffractometer or on a synchrotron.

However, this method has its limitations and is experimentally and computationally more demanding than SCXRD. As already mentioned in Table 4.4b, a maximum of about 100 diffraction intensities can be extracted from the powder diffraction pattern. Unfortunately, these are biased because of their overlap and distorted by the preferred orientation. To get the undistorted intensities, they must be mathematically corrected and refined (Le Bail refinement). However, the number of intensities available may be lower than the number of refined structure parameters. Therefore, additional structure information is obtained by other methods, e.g., ssNMR, theoretical calculations, etc. For example, the molecule shape can be optimized by quantum-chemical calculations and the position of the molecule (or only part of it) is specified in the asymmetric part of the elementary cell as a single object (3 positional parameters and 3 angular rotation parameters), without specifying the positions of individual atoms, see Figure 4.43.

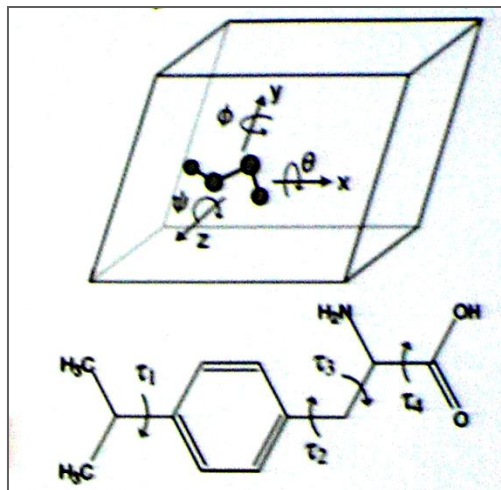


Figure 4.43. Refinement of the whole molecule position in the unit cell. DOF parameters.

In addition, only molecules that do not contain many internal rotation parameters can be resolved ($\tau_1\dots$). These parameters are called DOF (degree of freedom), and currently the limit to resolve structures from powder data is roughly $\text{DOF} < 40$.

As a result, refinement of the structure from the powder provides similar verification parameters as for single crystal (R-factors). However, these are higher for the powder than for the single crystal, and the powder structure model needs to be assessed based on chemical reality, especially intermolecular bonding (H-bridges, etc.). An example of a solved structure from powder data is illustrated in Fig. 4.44.

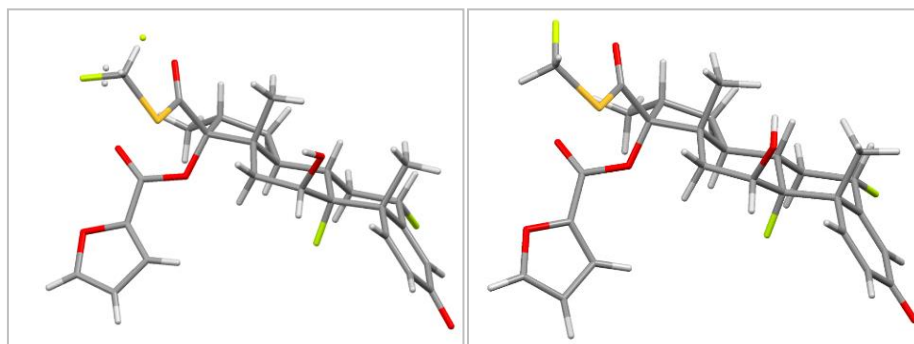


Figure 4.44. Structure of fluticasone solved from single crystal (left) and from powder (right). The differences are in the orientation of the terminal methyl groups.

(Source: The picture was kindly provided by Mr. Michal Hušák.)

4.5.9 Quantitative phase analysis

Quantitative phase analysis is currently performed using the Rietveld method. Its principle is to calculate the theoretical powder patterns for all phases present in the mixture. Their superposition is fitted to the experimental powder profile of the mixture until a match is achieved. The least squares method is used in this refinement. The theoretical fitted profile then gives the percentage of each component in the mixture (Fig. 4.45 and 10.46).

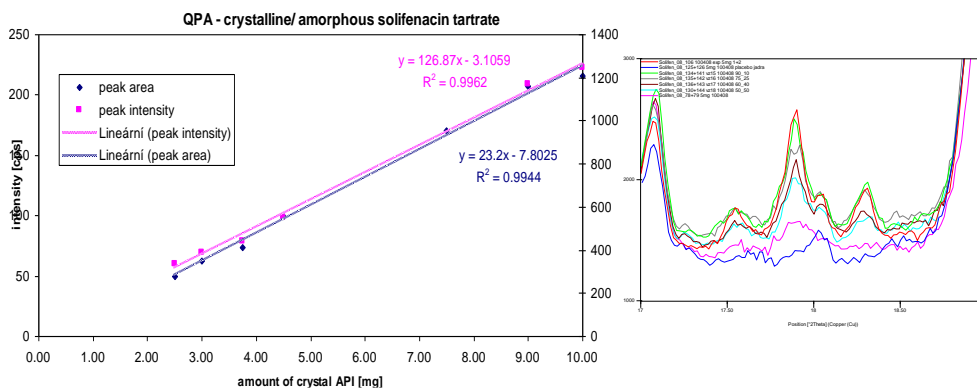


Figure 4.45. Quantitative determination of components in a mixture using a calibration curve.

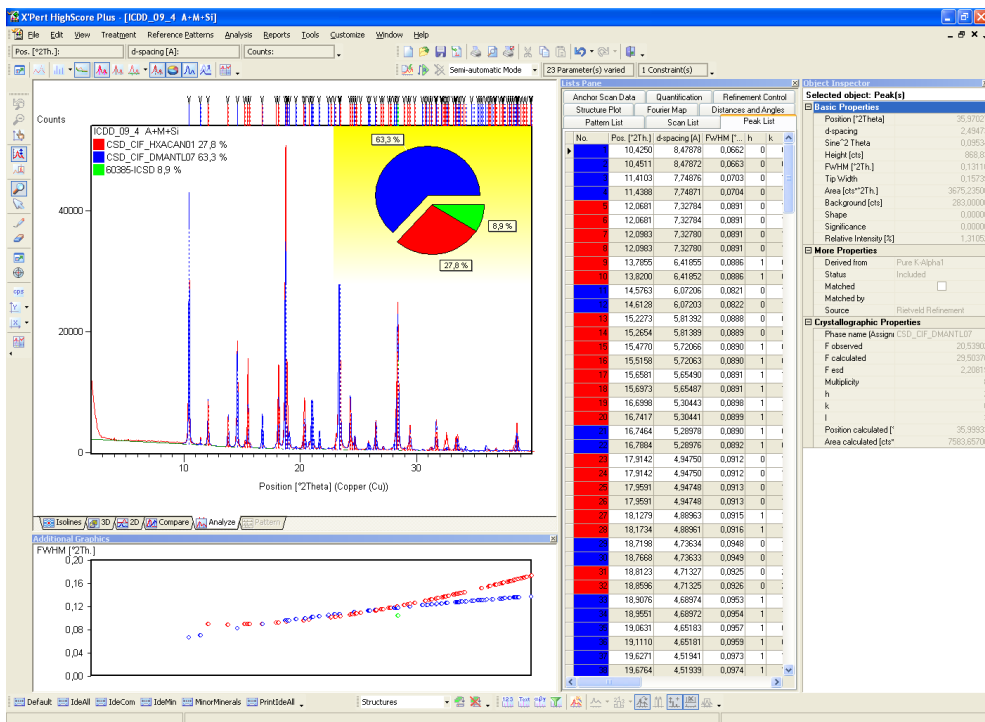


Figure 4.46. Quantitative determination of components in a mixture, using Rietveld method in HighScore Plus software.
(Source: <https://www.malvernanalytical.com>.)

4.6 Summary

X-ray diffraction is a unique analytical method for studying of inner structure of crystalline solids. X-ray powder diffraction is used mainly for quick resolution of various solid forms (polymorphs, salts, bases, acids, hydrates, solvates) and is rightly recognized as the gold standard. In its applications, it is a very powerful method, but its use is not simple and requires a certain detailed knowledge of crystallography and at least a basic understanding of elementary principles and limitations for divergent X-ray beams. For advanced users, special optics come into consideration, such as mirror optics for generating of parallel X-ray beams, as the most important one. The X-ray diffraction technique cannot be in any case used as a "black box". An obtained diffractogram reflects the molecular packing in a crystal, and therefore the individual peaks cannot be assigned to specific parts of the molecule, as in spectroscopy. Modern trends in analytical diffraction techniques are represented by electron diffraction and the further development of structure solving from powder data.

This chapter presents the principles of X-ray diffraction and its application mainly for pharmaceutical analysis. Mathematical basics, hidden under the applications themselves, are almost not mentioned in the text. There are, however, many high-quality literature sources listed, from worldwide renowned authors and "fathers" of crystallography, powder diffraction, and single-crystal diffraction.

4.7 Resources and recommended literature

1. Palatinus L., Kratochvíl B.: Electron diffraction – a new toll for crystal structure solutions. *Chem. Listy*. 2021, 115, 368-374.
2. Siegrist T. X-Ray Structure Analysis. Gruyter, Walter de GmbH: Berlin, Germany, 2021. <https://doi.org/10.1515/9783110610833>
3. Kraus I., Fiala J. Krystalografie. Nakladatelství ČVUT: Prague, Czech Republic, 2021.
4. Giacovazzo C., Monaco H. L., Viterbo D., Scordari F., Gilli G., Zanotti G., Catti M. Fundamentals of Crystallography. The second edition. Oxford University Press: New York, USA, 2002.
5. Kratochvíl B. Základy fyziky a chemie pevných látek I. VŠCHT Praha: Prague, Czech Republic, 1994.
6. Polymorphism in the pharmaceutical industry, Hilfiker R. (Ed.). Wiley-VCH: Weinheim, Germany, 2006.
7. Byrn S.R., Pfeiffer R.R., Stowell J.G. Solid state chemistry of drugs. The second edition. SSCI, Inc: West Lafayette, USA 1999.
8. The Rietveld Metod, Young R.A. (Ed.). Oxford University Press: Oxford, UK, 1993.
9. Jenkins R., Snyder R. L. Introduction to X-Ray Powder Diffractometry. Chemical Analysis. Wiley Interscience: New York, USA, 1996. <https://doi.org/10.1002/9781118520994>
10. Bruno J., Cole J. C., Edgington P. R., Kessler M. K., Macrae C. F., McCabe P., Pearson J., Taylor R. New Software for Searching the Cambridge Structural Database and Visualising Crystal Structures. I. *Acta Crystallogr.* 2002, B58, 389–397. <https://doi.org/10.1107/S0108768102003324>
11. Hovmöller S., Abrahams J. P Gemmi M., Mugnaioli E., Gorelik T. E., Kolb U., Palatinus L., Boullay P. 3D Electron Diffraction: Nanocrystallography Revolution. *ACS Cent. Sci.* 2019, 5, 1315-1329. <https://doi.org/10.1021/acscentsci.9b00394>

12. Kratochvíl B., Hušák M., Korotkova E. I., Jegorov A. The importance of X-ray crystal structure determination for pharmacy. *Chem. Listy*. 2016, 110, 40-47.
13. Solid State Characterization of Pharmaceuticals. Zakrzewski A., Zakrzewski M. (Eds.); Assa: Danbury, USA, 2006.
14. Newman A. W., Byrn S. R. Solid State Analysis of the Active Pharmaceutical Ingredient in Drug Products. *Drug Discov. Today*. 2003, 8 (19), 898–905. [https://doi.org/10.1016/S1359-6446\(03\)02832-0](https://doi.org/10.1016/S1359-6446(03)02832-0)
15. Macrae C. F., Edgington P. R., McCabe P., Pidcock E., Shields G. P., Taylor R., Towler M., van de Streek J. *Merkury: Visualization and Analysis of Crystal Structures*. *J. Appl. Cryst.* 2006, 39 (3), 453–457. <https://doi.org/10.1107/S002188980600731X>
16. Petříčková H. Structural study of morphine alkaloids and their complexes. Dissertation. UCT Prague: Prague, Czech Republic, 2007.
17. Bruker company. <https://www.bruker.com/en/landingpages/baxs/x-ray-structural-and-elemental-analysis.html>.
18. The Cambridge Crystallographic Data Centre (CCDC). <https://www.ccdc.cam.ac.uk/solutions/csd-core/components/csd/>.
19. U.S. Food and Drug Administration. <https://www.fda.gov/>.
20. The International Council for Harmonisation of Technical Requirements for Pharmaceuticals for Human Use, <https://www.ich.org/>.
21. European Medicines Agency. <http://www.ema.europa.eu>.
22. Státní ústav pro kontrolu léčiv. www.sukl.cz.

5 NMR spectroscopy

Jaroslav Havlíček

5.1 Basic principles

NMR spectroscopy (nuclear magnetic resonance) is a method, where energy state of nuclear spins is changed in a strong magnetic field, after absorption of radiofrequency radiation.

The basic building blocks of atomic nuclei – protons and neutrons, rotate around their axes and thus have a momentum p , called spin. Protons and neutrons have a spin quantum number $I = 1/2$. Nuclei of isotopes with an even number of both protons and neutrons have paired particle spins, so the resulting nuclear spin $I = 0$. Such nuclei, e.g., ^{12}C , ^{16}O , have zero spin, and do not provide NMR signals. Nuclei with an odd number of protons, neutrons, or both types of particles do not have paired spins and their $I > 0$. Because the movement of electrically charged particles on a closed path, is associated with emergence of magnetic field, the nuclei with $I > 0$ (e.g., ^1H , ^{13}C , ^{17}O) have their own magnetic moments:

$$\mu = \gamma p \quad \gamma - \text{gyromagnetic ratio, characterising each isotope}$$

If a sample containing an isotope with a non-zero magnetic moment is placed into a strong magnetic field with induction B_0 , the energy levels of its nuclear spins are split (Fig. 5.1).

The potential energy of a nucleus E is given by:

$$E = -\mu B_0$$

and for a component of magnetic moment in the direction of field B_0 applies:

$$\mu = \frac{mh\gamma}{2\pi} \quad \begin{array}{l} m - \text{magnetic quantum number} \\ h - \text{Planck constant} \end{array}$$

Magnetic quantum number acquires values $m = I, I-1, -I+1, -I$. The number of created energy levels is defined by the value of spin quantum number I (number of states = $2I+1$), therefore in isotopes with $I = 1/2$, such as ^1H and ^{13}C , the nuclear spins acquire two energy states with magnetic quantum number $m = +1/2$ and $m = -1/2$. Their energy can then be calculated by the relationship:

$$E_{+\frac{1}{2}} = -\frac{1}{2} \left(\frac{hB_0\gamma}{2\pi} \right) \quad E_{-\frac{1}{2}} = +\frac{1}{2} \left(\frac{hB_0\gamma}{2\pi} \right)$$

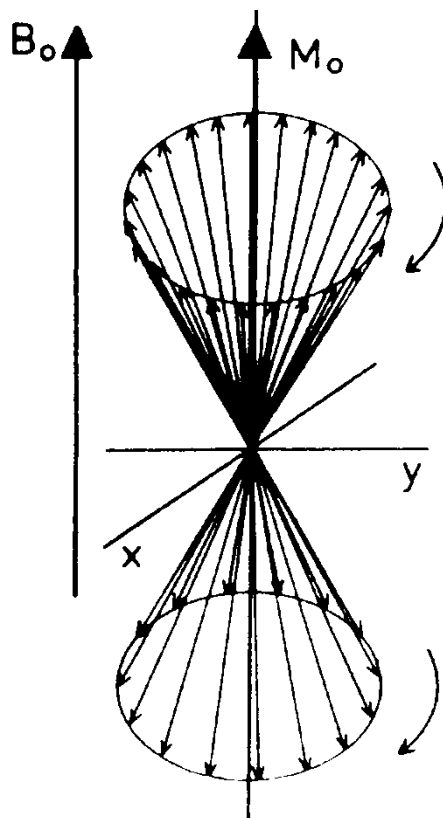


Figure 5.1. Nuclear magnetization M_0 in equilibrium. Magnetic moments that are directed according to the outer magnetic field B_0 belong to spins in $+1/2$ state, and oppositely directed moments belong to spins in $-1/2$ state.

According to the laws of quantum mechanics, each spin can permanently occupy only one energy level, and so it can only have one of two possible orientations. Transitions between these levels can be caused by radiation whose frequency meets the condition:

$$\Delta E = E_{-\frac{1}{2}} - E_{+\frac{1}{2}} = h\nu \quad \Delta E - \text{energy difference between levels}$$

Using the previously mentioned relationships, the following can be stated:

$$\nu_0 = \frac{\Delta E}{h} = \frac{\gamma B_0}{2\pi}$$

This relationship is known as the resonance condition, and the frequency ν_0 is a so-called Larmor frequency, often stated in the form:

$$\omega = \gamma B_0 \qquad \omega - \text{angular speed}$$

Since the difference ΔE between the energy levels is small, energy of radio-frequency radiation (frequency in orders of MHz) is enough to excite these nuclei.

Lower energy level is occupied by nuclei whose projection of a nuclear magnetic moment μ matches the orientation of an external magnetic field B_0 . This orientation corresponds to the magnetic quantum number $m = +1/2$. Nuclei at a higher energy level have the resulting magnetic moment oriented oppositely to the direction of the magnetic field $m = -1/2$ (Fig. 5.1).

Comment. At an equilibrium state, temperature $T = 300$ K, and magnetic field induction $B = 1$ T, the ratio of the number of proton spins at an energy level matches the Boltzmann distribution law:

$$n_{+\frac{1}{2}} \left(m = +\frac{1}{2} \right) \quad \text{and} \quad n_{-\frac{1}{2}} \left(m = -\frac{1}{2} \right), \quad \text{hence:} \quad \frac{n_{+\frac{1}{2}}}{n_{-\frac{1}{2}}} = \exp \left(\frac{\Delta E}{kT} \right) = 1.000006$$

k – Boltzmann constant

Population of nuclei at a lower energy level is therefore only slightly larger than at the higher energy level. The result of this difference is a vector sum of all the nuclear spin magnetic moments – nuclear magnetization M_0 . Its value is proportional to the excess of nuclei at the lower energy level.

When measuring NMR spectra using pulse methods, the population of both energy levels is equalized by a suitable radiofrequency pulse, and the magnetization M_0 is deflected from its equilibrium position (from the direction of the axis of the external magnetic field B_0). Since the magnetization is associated with the momentum of nuclei, it does not return to the direction of the magnetic field immediately after the termination of the pulse but behaves as a flywheel mounted outside its centre of gravity whose rotation axis is tilted towards the gravitational field. The result is a precession in which the magnetization retains its intensity and an angle towards the magnetic field and rotates around the direction of the magnetic field B_0 with Larmor frequency (Fig. 5.2).

The relaxation processes also gradually restore the disrupted equilibrium. After a certain time characterized by the period of the so-called spin-lattice relaxation T_1 , the equilibrium distribution of spins on both energy levels is once again stabilized. This restores the magnetization component in the direction of the field. A magnetization component perpendicular to the direction of the magnetic field on the

other hand decreases down to zero during the so-called spin-spin relaxation interval T_2 .

Similarly, as a rotating magnet induces an alternating current in a stator coil, rotating magnetization vector induces AC voltage in a receiver coil that is wound around a sample in an NMR spectrometer. The time course of the voltage (signal) induced by the nuclear magnetization in the coil is commonly referred to as FID (free induction decay) and is shown in Fig. 5.3. It can be thought of as a fading tone after pressing a piano key.

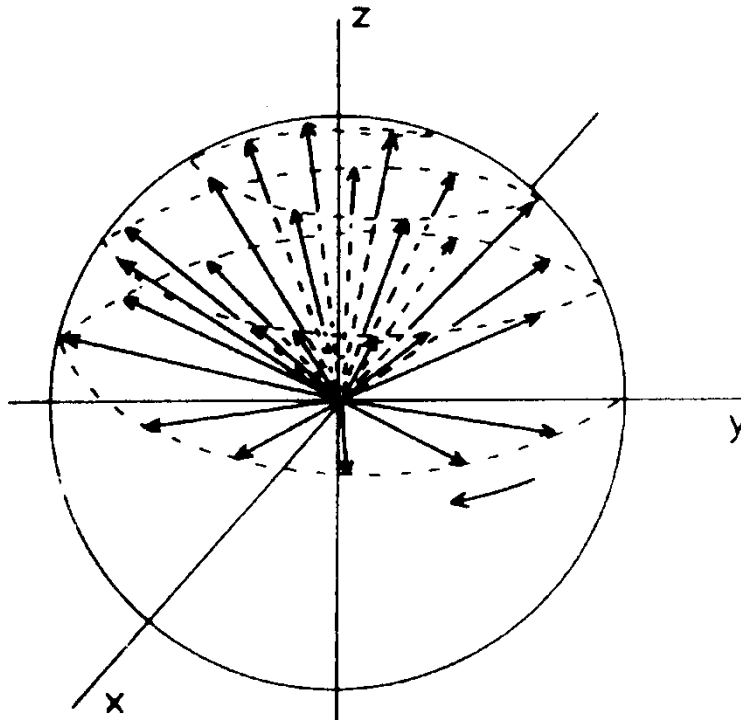


Figure 5.2. Return of magnetization M into an equilibrium position, after being tilted by a radiofrequency pulse.

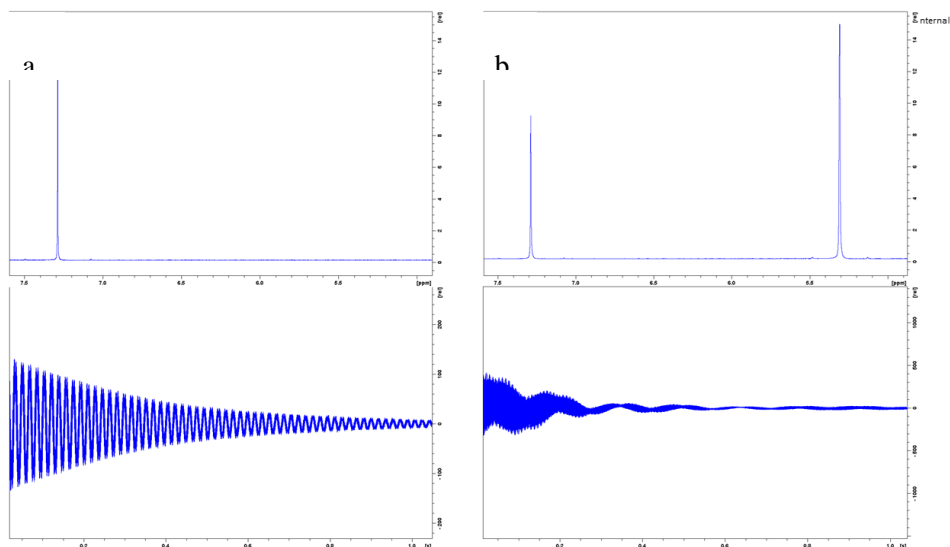


Figure 5.3. FID – dependence of signal s and time t for: one (a) and two (b) types of nuclei with one or two signals in the spectrum, correspondingly.

5.2 NMR spectrometer

A modern NMR spectrometer with Fourier transform (FT-NMR) is a very complicated device that has three basic parts:

- magnet
- electronic part of the spectrometer
- computer system with peripherals

The main part of each NMR spectrometer is a magnet with a probe. Electromagnets with iron core were used earlier. Currently, there are used superconducting magnets allowing to reach higher magnetic induction (4.7 to 28.2 T, which corresponds to a working frequency of ^1H 200–1200 MHz). Superconducting magnet is formed by a solenoid coil made of superconducting material (e.g., NbTi or NbSn alloy) which is placed in a cryostat with liquid helium that provides cooling of the solenoid to temperature of 2–4 K. Sample of a measured substance in a glass tube is placed into the so-called probe (Fig. 5.4b). The sample tube rotates in the probe to increase homogeneity. The main parts of the probe are coils and electrical circuits used to supply energy to the sample using a radio-frequency pulse from a transmitter and to detect absorption of this energy in receiver circuits (FID scan). Furthermore, the probe also contains circuits used for irradiation of a sample by another radiofrequency radiation used for decoupling (see below).

The electronics of the spectrometer provide excitation of the spin system and a subsequent detection of the signal from the sample. An NMR spectrometer usually contains three independent high-frequency channels:

- observation (measuring) – for nuclei excitation and response detection
- locking (stabilization) – for resonance condition stabilization, usually using a resonance signal of deuterium from deuterated solvents
- decoupling – for sample irradiation with another high-frequency radiation (the so-called decoupling method)

Computational system provides control of all spectrometer functions and the processing of acquired data. The experiment itself is performed by a pulse programmer or a separate acquisition processor. The computer controls the spectrometer, operation of the pulse programmer or the acquisition processor, mathematical processing of measured data (FIDs) and their Fourier transform and provides output of the acquired spectra (along with necessary parameters) onto screen and printer (Fig. 5.4).

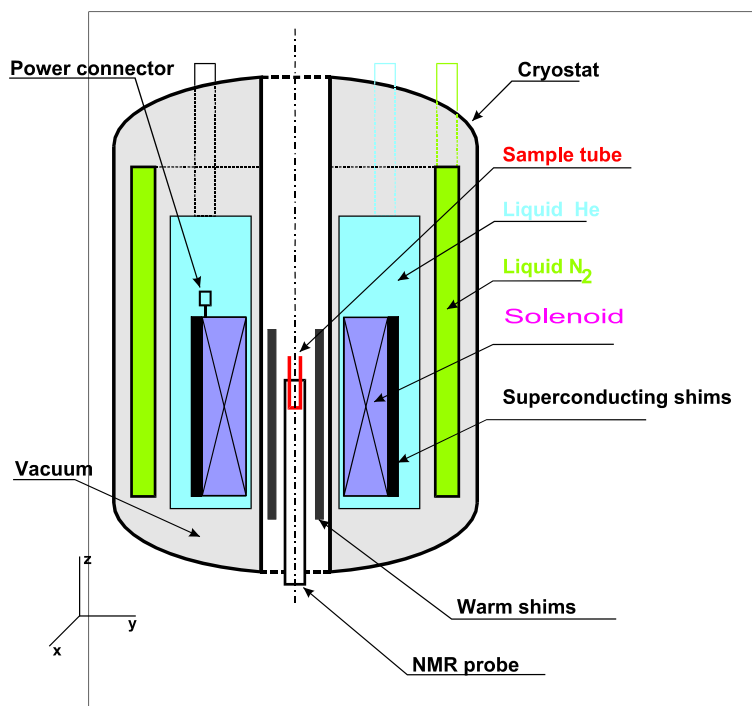


Figure 5.4a. Scheme of a superconducting magnet.

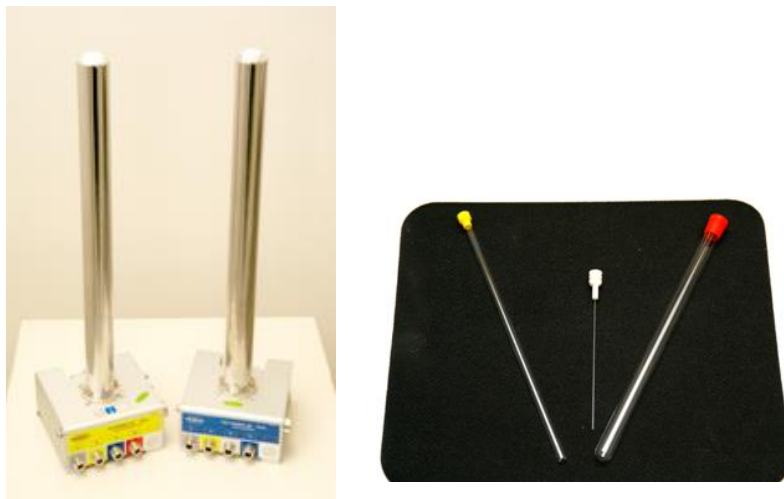


Figure 5.4b. Photo of measuring probes and NMR sample tubes for liquid state analysis (from the left: 5 mm, 1 mm and 10 mm sample tube).

If a sample contains only one type of atoms of one isotope, for example CHCl_3 (Fig. 5.3a), the decrease of amplitude of muted oscillations is exponential and is characterized by the duration of the spin-spin relaxation T_2 . The oscillation frequency is the Larmor frequency. For more complex samples, the resulting FID is an interferogram or a superposition of FIDs originating from different nuclei of the same isotope (Fig. 5.3b). To obtain the resonant frequencies and an intensity of signal response for individual nucleus types, it is necessary to first convert the FID from signal time dependence to a frequency dependence, i.e., the NMR spectrum. This conversion is done by a computer using Fourier transform.

The NMR spectrum then contains information about the structure of substances, stored in three parameters:

- position of signals (chemical shifts)
- integral intensity of signals
- multiplicity (fine structure) of signals

5.3 ^1H NMR spectroscopy

5.3.1 Signal position – chemical shift

Relationship between frequency of absorbed radiation and magnetic induction B_0 is expressed in the resonance condition:

$$\nu_0 = \frac{\Delta E}{h} = \frac{\gamma B_0}{2\pi}$$

According to this condition, resonant frequency should be constant for all nuclei of the same isotope. However, the nuclei in the molecule are bound into groups and are therefore influenced by different electron environments. The electron surrounding alters ("shields") the magnetic field at the nucleus, and the following relationship applies for magnetic induction B_{lok} :

$$B_{\text{lok}} = B_0(1 - \sigma) \quad \sigma - \text{shielding constant}$$

Determination of the shielding constant is experimentally demanding and therefore relative values are used in practice for resonant frequency, related to a frequency standard. As an internal standard, tetramethylsilane (TMS) is usually directly added to the sample. Distance length of resonance signals from the TMS signal is measured in Hz. Because this value is dependent on B_0 , a chemical shift δ [ppm] was defined as a quantity independent on magnetic field induction:

$$\delta = \frac{\nu - \nu_{st}}{\nu_0} 10^6$$

ν – frequency of measured nucleus
 ν_{st} – frequency of measured standard
 ν_0 – working frequency of spectrometer for the given isotope

Chemical shift is expressed in ppm (parts per million). The value of a chemical shift of TMS, according to the following relationship, is equal to 0 ppm.

$$E_{+\frac{1}{2}} = -\frac{1}{2} \left(\frac{hB_0\gamma}{2\pi} \right) \quad E_{-\frac{1}{2}} = +\frac{1}{2} \left(\frac{hB_0\gamma}{2\pi} \right)$$

The range of chemical shifts in hydrogen ^1H NMR spectra is usually 0–20 ppm.

Table 7.1 lists chemical shifts of protons, according to which signals can be assigned to specific structural groups. If protons are bound identically, and therefore have the same "surrounding", they show identical resonant frequencies. Such nuclei are then called magnetically equivalent and are always chemically equivalent (but not vice versa). For example, in the benzene ring of cyclohexane, all protons are chemically equivalent due to the symmetry, and in a ^1H NMR spectrum they

provide only one signal. Similarly, in the $-\text{CH}_3$ group, all three protons are equivalent due to the free rotation around the single bond, and they will match only a single signal in the spectrum. Also, the compounds tetramethylsilane $\text{Si}(\text{CH}_3)_4$ and symmetrically substituted ethane $\text{X}-\text{CH}_2-\text{CH}_2-\text{X}$ (with free rotation around single bond and also molecule symmetry) provide only one signal in a ^1H NMR spectrum, corresponding to twelve and four equivalent protons in the case of tetramethylsilane and ethane, respectively.

Chemical shift is influenced by many factors (electronegativity of substituents, magnetic anisotropy, steric effects, temperature, concentration, solvent, etc.). The most important of these is the electronegativity of substituents. A rule applies that with increasing electronegativity of neighbouring atoms or groups, shielding decreases and the value of chemical shift δ increases. Temperature, concentration, and solvent have the highest effect on the value of the chemical shift of protons bound to heteroatoms ($-\text{OH}$, $-\text{NH}$, $-\text{SH}$).

Fig. 5.5 shows a ^1H NMR spectrum of ethyl formate. The spectrum contains three signals (1.3 ppm, 4.2 ppm, and 8.0 ppm) which correspond to three groups of protons contained in the ethyl formate, i.e., CH_3- , $-\text{CH}_2-$ and $\text{H}-\text{CO}-$. They differ in their chemical shifts which are consistent with the values given in Table. 4.1. A signal with chemical shift of 7.26 ppm, which is also contained in the spectrum, corresponds to a residual signal of CHCl_3 in CDCl_3 , which was used as a solvent in this case.

Comment. Solvents used for NMR are not 100% deuterated and thus signals of non-deuterated solvents always appear in the ^1H NMR spectra.

5.3.2 Integral signal intensity

In ^1H NMR spectra, the areas of resonance signals are proportional to the number of protons in the molecule. For this purpose, an integral record is acquired, which has a shape of a wave placed over the individual signals. Height of the integral wave corresponds to the areas of individual signals, and the values of these areas are usually found in the spectrum, below the scale of chemical shifts. To know the number of protons, contained in the individual signals, the ratio of the area sizes must be adjusted to the ratio of small integers.

For example, in the case of ethylformate (Fig. 5.5), the signal area (wave height) at 1.3 ppm must be considered equivalent to three protons. In this area, there almost always appear only the signals of $-\text{CH}_3$ groups. Thus, it can be easily determined, what area size corresponds to one proton. The remaining areas can then be divided by this value, and the resulting numbers rounded. In the spectrum of ethylformate in Fig. 5.5, this ratio is 3:2:1 after rounding, from right to left. This implies that the signal with the relative intensity 3 corresponds to the group $-\text{CH}_3$, the signal with relative intensity 2 to group $-\text{CH}_2-$, and the last signal with relative intensity 1 corresponds to $\text{H}-\text{CO}-$.

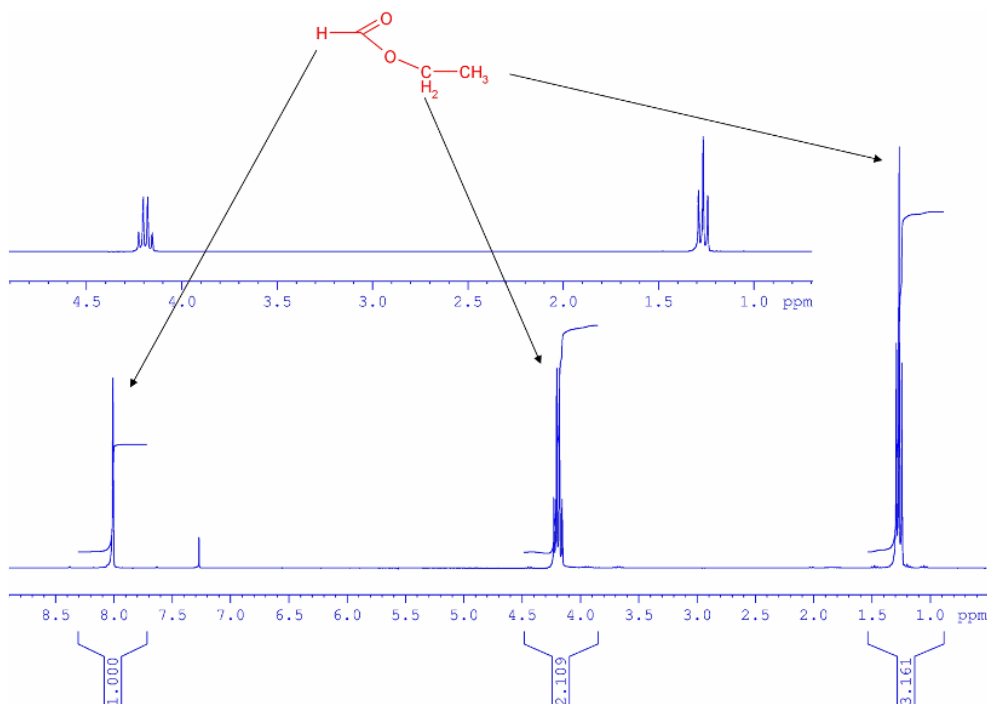


Figure 5.5. Ethylformate ^1H NMR spectrum.

5.3.3 Signal multiplicity

In ^1H NMR spectrum of ethylformate (Fig. 5.5), the signals differ not only in different position caused by different chemical shift of individual groups in the molecule and in the varying intensity given by the number of protons in the individual groups, but also in fine structure (splitting, multiplicity) of the signals. The cause of this splitting is a mutual interaction of spins of individual protons – spin-spin interaction – that is transmitted by bond electrons (not space). It is therefore most important usually for the closest neighbouring groups. Spin-spin interaction is mutual, i.e., if a signal from A protons is split by protons matching the signal B, then the signal of the B protons must also be split by protons matching the signal A.

Spin-spin interaction is characterized by the value of a spin-spin coupling constant J , whose value is expressed in Hz and is independent on induction of external magnetic field. Its value is not directly shown in the spectrum but can be calculated. The positions of lines of multiplets are stated in Hz above these multiplets. Assuming that the interpreted spectrum is a first order spectrum, i.e., it meets condition $\Delta\nu/J > 6$, where $\Delta\nu$ is the difference between resonant frequencies of interacting nuclei, the coupling constants can be calculated as the differences in the frequencies of lines of individual multiplets. Values of some spin-spin interaction constants are listed in Table 5.2.

In general, simple rules apply in the first order spectra for the shape of multiplets of protons and nuclei with spin quantum number $I = 1/2$:

- If there are groups containing different nuclei with different coupling constants than the observed nucleus in their vicinity, then the signal of the observed nucleus is split to a maximum of $(n_1 + 1) \times (n_2 + 1)$ components (lines), where n_1 and n_2 are numbers of the nuclei of the neighbouring groups with coupling constants J_1 and J_2 . However, if $J_1 = J_2$, then the signal is split to $(n + 1)$ components, where n is the total number of nuclei of the adjacent group or groups with the same coupling constant, see Table 5.3.
- For a multiplet resulting from an interaction with a group of n magnetically equivalent nuclei, the relative line intensities have ratios of binomial development coefficients $(a + b)^n$, which can be obtained from Pascal's triangle, i.e., doublet 1:1, triplet 1:2:1, quartet 1:3:3:1, etc.

In the spectrum of ethylformate (Fig. 5.5), there can be observed two multiplets, a triplet with a chemical shift of 1.3 ppm, and a quartet with chemical shift of 4.2 ppm. The triplet corresponds to $-\text{CH}_3$, as this group is directly adjacent to two equivalent protons of the $-\text{CH}_2-$ group. The quartet corresponds to the $-\text{CH}_2-$

group, because the methylene group is directly adjacent to three equivalent protons of $-\text{CH}_3$ groups. The proton in $\text{H}-\text{CO}-$ group has no proton on the adjacent carbon, and hence the signal with a chemical shift of 8.0 ppm for this group is a singlet in the spectrum of the ethylformate.

The value of spin-spin coupling constant in ^1H NMR spectra decreases with the number of bonds between the interacting nuclei. Therefore, there are distinguished geminal $\text{H}-\text{C}-\text{H}$ coupling constants, denoted with 2J , vicinal 3J constants ($\text{H}-\text{C}-\text{C}-\text{H}$), and long-range coupling constants 4J up to 9J . It is appropriate to point out the oddity of aromatic protons. In a substituted aromatic ring, the hydrogen atoms are not equivalent. Depending on the nature of the substituent present, the condition for the first order spectrum is often not met (differences in chemical shifts are often small) and spectrometers with lower working frequency cannot distinguish between these hydrogen atoms. Therefore, a series of signals with fine structures can be found in the spectrum, in 6–9 ppm range. Since these signals can be mistaken for the signals of double bonds (the ranges of chemical shifts can overlap), the relative intensities of multiplets and the values of spin-spin interaction constants (Table 7.2) which are lower than for a double bond should be considered when analysing a spectrum.

Table 7.2. The values of spin-spin interaction constant proton-proton [Hz] for selected molecular arrangements.

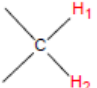
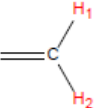
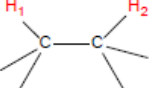
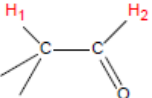
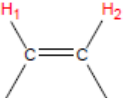
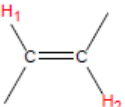
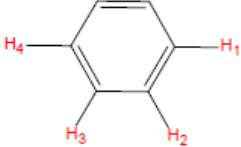
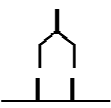
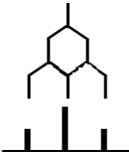
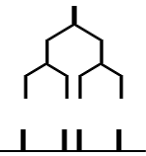
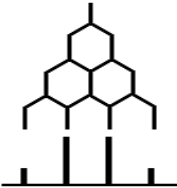
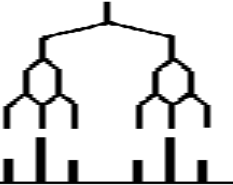
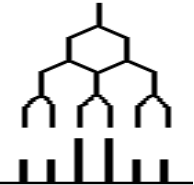
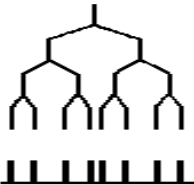
Interaction constant $J_{1,2}$			
	Maximum range	Typical range	
	0–25	10–15	
	0–3,5	2	
	0–8	7	
	0–3	2	
	0–12	7–10	
	12–18	14–16	
	$J_{1,2}$	6–10	8
	$J_{1,3}$	0–3	2
	$J_{1,4}$	0–1	1

Table 7.3. A scheme of signal splitting in ^1H NMR spectra.

J_1	$J_1 = J_2$	$J_1 > J_2$	$J_1 = J_2 = J_3$
			
doublet (d)	triplet (t)	doublet of doublet (dd)	quartet (q)
$J_1 > J_2 = J_3$	$J_1 = J_2 > J_3$	$J_1 > J_2 > J_3$	
			
doublet of triplet (dt)	triplet of doublet (td)	doublet of doublet of doublet (ddd)	

Comment. In case of more multiplets, the weakest side signals of a multiplet can be overlapped by noise (e.g., for nonet, the theoretical ratio between the weakest and the strongest signal in the multiplet is 1:70 according to Pascal's triangle).

Multiplicity	Intensity of bands
singlet	1
doublet	1 1
triplet	1 2 1
quartet	1 3 3 1
quintet	1 4 6 4 1
sextet	1 5 10 10 5 1
septet	1 6 15 20 15 6 1
octet	1 7 21 35 35 21 7 1
nonet	1 8 28 56 70 56 28 8 1

5.4 ^{13}C NMR spectroscopy

Since isotope ^{12}C is not magnetically active, only the carbon isotope ^{13}C can be measured as its spin quantum number is the same as for protons, i.e., $I = 1/2$. The carbon ^{13}C NMR spectra have several differences compared to ^1H NMR.

- The range of chemical shifts is approximately 300 ppm. Usually, the signals of carbon atoms from organic compounds appear in the interval of 0–220 ppm. This enhances the transparency and simplifies the interpretation of these spectra since overlapping of signals is not as frequent as in the case of proton spectra. Chemical shift of carbons as well as for protons is related to TMS and is also affected by many factors. Its value depends primarily on the hybridization of carbon atoms and decreases in this order: $\text{sp}^2 > \text{sp} > \text{sp}^3$.
- The greatest chemical shifts are however those of carbonyl and often of quaternary carbon atoms. The chemical shift is further affected by inductive effect of substituents. Substituents attracting electrons cause shift of C_α and C_β carbons to a lower field, i.e., to a higher chemical shift, while the effect is opposite in C_γ and usually negligible in C_δ . Chemical shift is also affected by steric, conjugation, and other effects. Basic overview of the ^{13}C chemical shifts is summarized in Table 5.4.

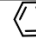
- Signal intensity A of ^{13}C nuclei depends on gyromagnetic ratio, spin quantum number I and natural occurrence of nucleus n (%) according to the relationship:

$$A = \gamma^3 n I(I + 1)$$

As a result of the natural occurrence of ^{13}C nuclei (1.11%) and a four times smaller gyromagnetic ratio than of a ^1H nucleus, the relative sensitivity for carbons is approximately 5700 times lower than for protons. Therefore, the ^{13}C NMR spectroscopy has become a common method only after the introduction of pulse FT-NMR spectrometers, which enable rapid spectra accumulation. Because the signal to noise ratio increases with square root of the number of accumulations (scans), it is necessary to perform hundreds or even several tens of thousands of accumulations to obtain quality carbon spectra, depending on the structure of the molecule and concentration of the sample.

Unlike in proton spectra, the intensities in ^{13}C NMR spectra are not always proportional to the number of corresponding carbon nuclei. This complicates the use of the ^{13}C NMR spectroscopy for quantitative purposes and sometimes also the interpretation of the spectra. The reason is the unequal relaxation times of various carbon nuclei which depend on the surroundings of the given atoms. It is useful to know that signals of quaternary carbons provide weaker signals than carbons with hydrogen atoms. The intensity of signals in ^{13}C NMR spectra is furthermore dependent on the manner (according to the pulse sequence) of spectrum acquisition.

Table 7.4. Chemical shifts of ¹³C carbons (values are related to TMS).

CH ₃ -C-	Primary C									10-25	I
CH ₃ -X										25-35	I
CH ₃ -O-										35-55	
CH ₃ -N-										40-60	
CH ₃ -S-										45-65	
-CH ₂ -C-	Secondary C									15-45	I
-CH ₂ -X										30-45	I
-CH ₂ -O-										45-65	
-CH ₂ -N-										50-70	
-CH ₂ -S-										55-75	
-CH-C-	Tertiary C									30-65	I
-CH-X										35-55	I
-CH-O-										55-75	
-CH-N-										60-80	
-CH-S-										65-85	
-C-C-	Quartry C									45-75	I
-C-X										65-85	I
-C-O-										75-95	
-C-N-										80-100	
-C-S-										85-105	
-C-C-	Alkanes									10-45	
-C≡C-	Alkynes									75-100	
-C=C-	Alkenes									110-140	
	Aromatic compounds									120-140	
-O-C≡N	Cyanates									120-135	
-S-C≡N	Thiocyanates									125-135	
-C≡N	Nitriles									120-135	
-C=N-	Azomethines									150-170	
(-CO) ₂ O	Anhydrides									160-175	
-COOR	Esters									165-185	
(-CO) ₂ NR, -CONHR	Imides, amides									165-185	
-COOH, -COCl	Acides, acid chlorides									170-185	
-CHO	Aldehydes									190-210	
-C=O	Ketones									200-220	

δ, ppm

Unlike in proton spectra, the ^{13}C - ^{13}C interaction in carbon spectra does practically not appear due to the small probability of the occurrence of two ^{13}C isotope nuclei in one molecule in proximity. The carbon spectra however show significant spin-spin interactions ^1H - ^{13}C . The most important are the direct 1J coupling constants which depend on hybridization of the carbon atom and its value which changes in the order: sp^3 (120–150 Hz), sp^2 (150–250 Hz) and sp (250–320 Hz). This fact eases the assignment of signals to carbons in a molecule, but on the other hand worsens the transparency of spectra when there is little difference in chemical shifts of specific carbons. Therefore, a method known as decoupling is used. The ^{13}C NMR spectra are measured under a constant irradiation of all protons in the molecule. This eliminates all splitting induced by spin-spin carbon-proton interactions. Moreover, it increases signal intensity of carbon atoms in a spectrum because the whole intensity is then concentrated into one signal peak. This is documented in Fig. 5.6 which shows normal (non-decoupled) and decoupled spectrum of *p*-(2-butyl)phenol. Only unsplit signals appear in the decoupled spectrum. They are characterized by different chemical shifts and correspond to the carbon atoms found in the *p*-(2-butyl)phenol molecule. In the non-decoupled spectrum, it is possible to observe two quartets matching two $-\text{CH}_3$ groups, and a triplet and a doublet matching $-\text{CH}_2-$ and $-\text{CH}-$, respectively. The signals of quaternary carbon atoms are not split by direct H-C binding interactions. This spectrum, unlike the decoupled one, also contains an information about the type of the carbon (primary, secondary, tertiary, or quaternary), but the sensitivity of this experiment is very small and there is a possibility of signal overlap. APT (attached proton test) is therefore a compromise between both techniques, where one line corresponds to each carbon in the spectrum, and carbon signals are discriminated according to the number of attached protons, odd or even by up or down oriented signals.

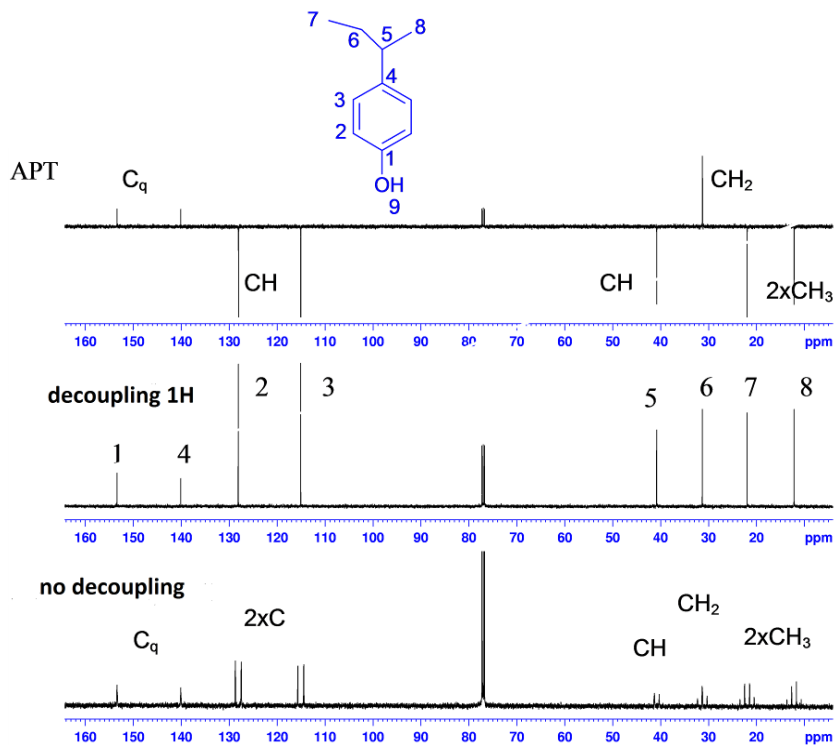


Figure 5.6. Comparison of ^{13}C NMR spectra for *p*-(2-butyl)phenol.

5.5 Two-dimensional NMR spectra

1D NMR experiment is schematically shown in Fig. 5.7. After the relaxation period which can be denoted as d_1 , a 90° radio-frequency pulse follows, and its response is detected as FID over detection time t_2 . An NMR spectrum as a function of frequency ν_2 , is obtained using Fourier transform.

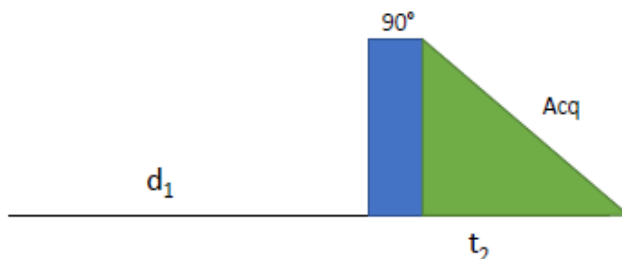


Figure 5.7. Scheme of a 1D NMR experiment.

(Source: Friebolin H. *Basic One- and Two-Dimensional NMR Spectroscopy*. Wiley-VCH, 1998.)

Addition of another time variable – evolution time t_1 , between two radiofrequency pulses, is typical for 2D NMR experiments (Fig. 5.8).

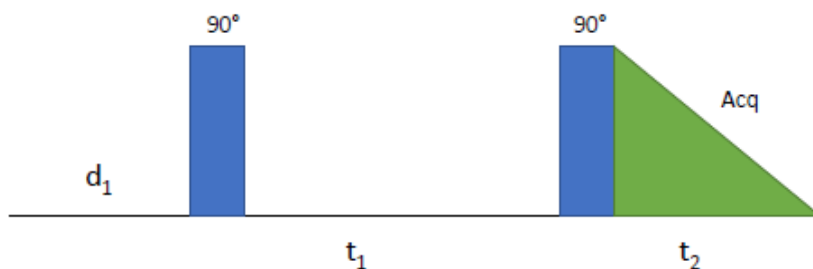


Figure 5.8. Scheme of a 2D NMR experiment.

(Source: Friebolin H. *Basic One- and Two-Dimensional NMR Spectroscopy*. Wiley-VCH, 1998.)

If the time delay t_1 between the pulses systematically changes, a dependence on time variables t_1 and t_2 is obtained and is then converted by double Fourier transform into a spectrum which is a dependency of intensity on two frequencies ν_1 and ν_2 (Fig. 5.9). The most common type is a contour plot. This view corresponds to a section of a three-dimensional view of the peaks of a 2D NMR spectrum (stacked plot) which has intensity as its third dimension (similarly as the 1D NMR spectrum has intensity as the second dimension). The advantage of the contour plots is their transparency, which simplifies interpretation.

Methods using 2D NMR are generally divided into the so-called correlated (peaks correlate with frequencies ν_1 and ν_2) and resolved (frequencies ν_2 are "resolved" according to coupling constant J (J -resolved) and the y-axis shows the coupling constant instead of frequency ν_1). Both types can then have either homonuclear or heteronuclear form.

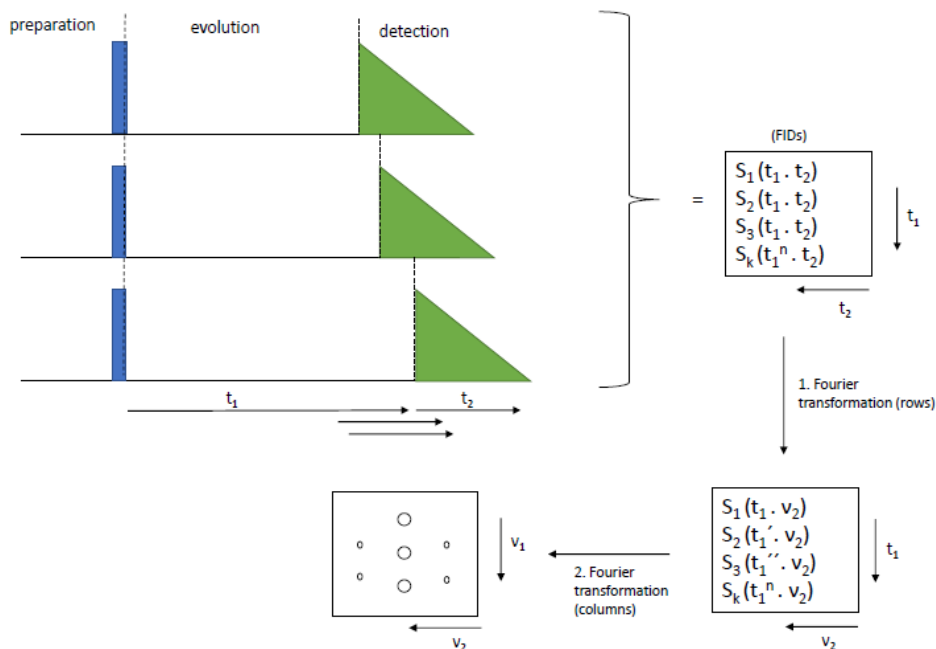


Figure 6.9. Calculation of 2D NMR spectra (contour).

(Source: Friebolin H. *Basic One- and Two-Dimensional NMR Spectroscopy*. Wiley-VCH, 1998.)

Fig. 5.8 shows a scheme of the simplest homonuclear correlated 2D method called ^1H - ^1H COSY (correlated spectroscopy). Fig. 5.10 shows a 2D COSY spectrum of *p*-(2-butyl)phenol, with chemical shifts of protons in both dimensions. It can be considered as a series of experiments with selective decoupling, during which all protons are gradually decoupled. The advantage is that all can be obtained in one step, and the protons can be selectively decoupled without a limitation, as their signals often tend to be overlapped.

Two types of signals appear in a COSY spectrum. These are the diagonal peaks representing the 1D spectrum and the so-called cross peaks indicating interactions between nuclei. The cross peaks which are usually symmetrical according to a diagonal are therefore very important for finding interactions between individual groups. A cross peak in the spectrum of *p*-(2-butyl)phenol denoted as H7-H6 represents interaction of $\text{CH}_3(7)$ and $\text{CH}_2(6)$ groups. The cross peak H8-H5 represents interaction of $\text{CH}_3(8)$ group with $\text{CH}(5)$; H6-H5 denotes interaction of $\text{CH}_2(6)$ and $\text{CH}(5)$; H2-H3 denotes interaction of aromatic protons (2) and (3).

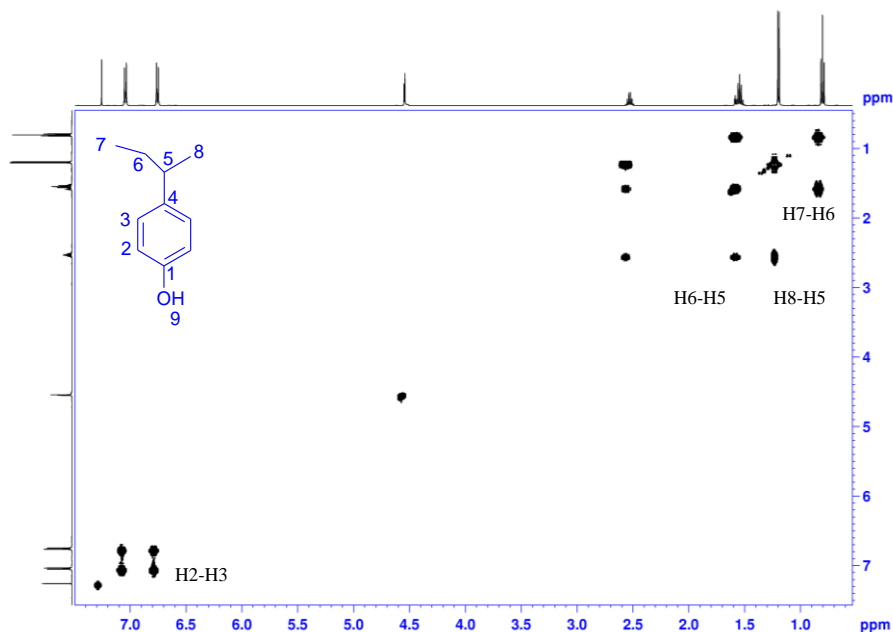


Figure 5.10. 2D COSY NMR spectrum of *p*-(2-butyl)phenol in CDCl_3 .

Diagram in Fig. 5.11 shows a pulse sequence of a heteronuclear form of a 2D COSY spectrum, known as H,C-COSY or heteronuclear H,C-correlated spectra (heteronuclear shift correlated spectroscopy, HETCOR). ¹H signals are correlated on one axis and ¹³C signals on the other axis. Similarly as in homonuclear scenario, it replaces a series of complicate ¹³C experiments with selective decoupling of hydrogens. Because on each axis there are different chemical shifts, these spectra do not have diagonal peaks nor any symmetry.

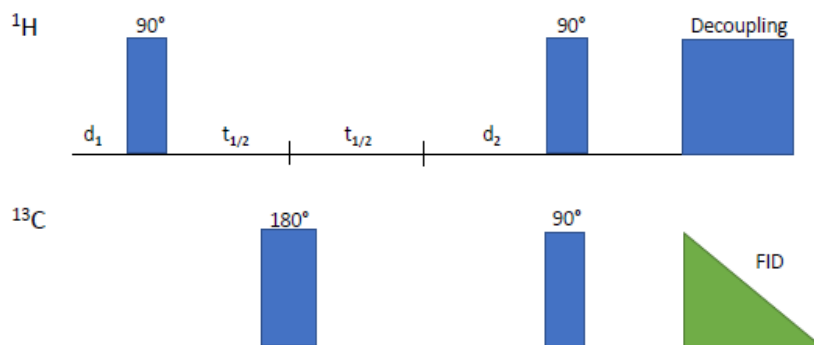


Figure 5.11. Scheme of a pulse sequence of 2D HETCOR.

(Source: Friebolin H. *Basic One- and Two-Dimensional NMR Spectroscopy*. Wiley-VCH, 1998.)

Fig. 5.12 shows a 2D HETCOR spectrum of *p*-(2-butyl)phenol. It is apparent which ^{13}C signal corresponds to ^1H signal. It is thus easy to recognize, which signal in the ^{13}C NMR spectrum corresponds to the CH_3 group 7 or 8 and which correspond to CH_2 and CH . Assignment can also be performed in a similar manner for the aromatic region. This experiment, however, cannot be used to assign signals of quaternary carbon atoms.

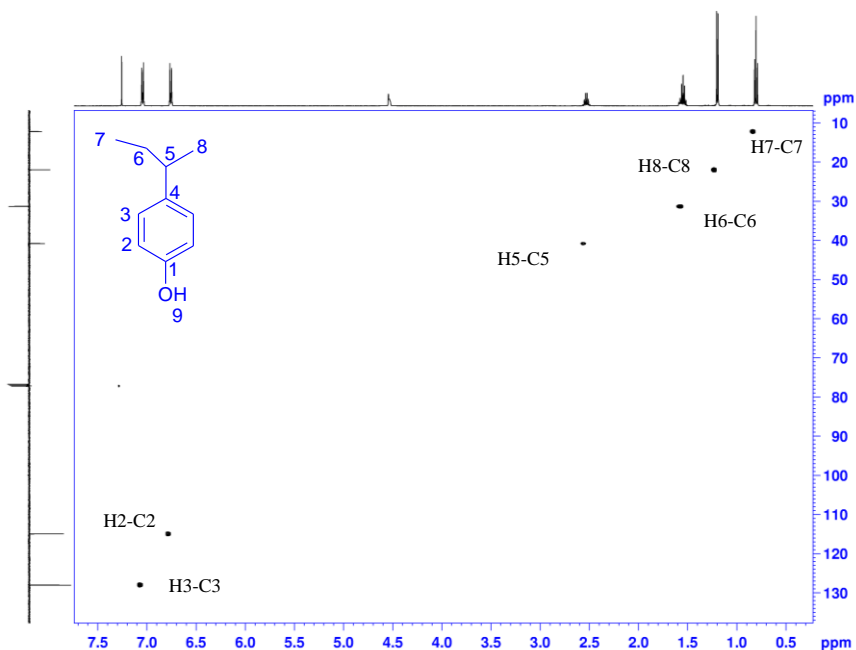


Figure 5.12. 2D HETCOR NMR spectrum of *p*-(2-butyl)phenol in CDCl_3 .

Currently, the heterocorrelated experiments are carried out in an “inverse” manner, where the protons are detected as the more sensitive of the isotopes. In this form, and especially with the use of magnetic field gradients, inversion probes, or cryoprobes, it is possible to obtain heterocorrelated experiments over several bonds within few minutes, from even few milligrams of a substance.

5.6 Application of liquid phase NMR spectroscopy in pharmacy

NMR spectroscopy is not used for routine analyses in pharmacy, but still, its role in development is indispensable and has a very wide application. The most important applications are:

- structural analysis of APIs
- structural analysis of impurities

5.6.1 Structural analysis of APIs

The use of NMR spectroscopy in liquid phase analysis of APIs will be demonstrated on acetylsalicylic acid. Fig. 5.13 comprises a ^1H NMR spectrum of this substance in $\text{DMSO-}d_6$. Except signals belonging to the solvent and water, there are five other signals in the spectrum. Assignment of all protons and carbons in the molecule was performed with the use of 2D NMR spectra.

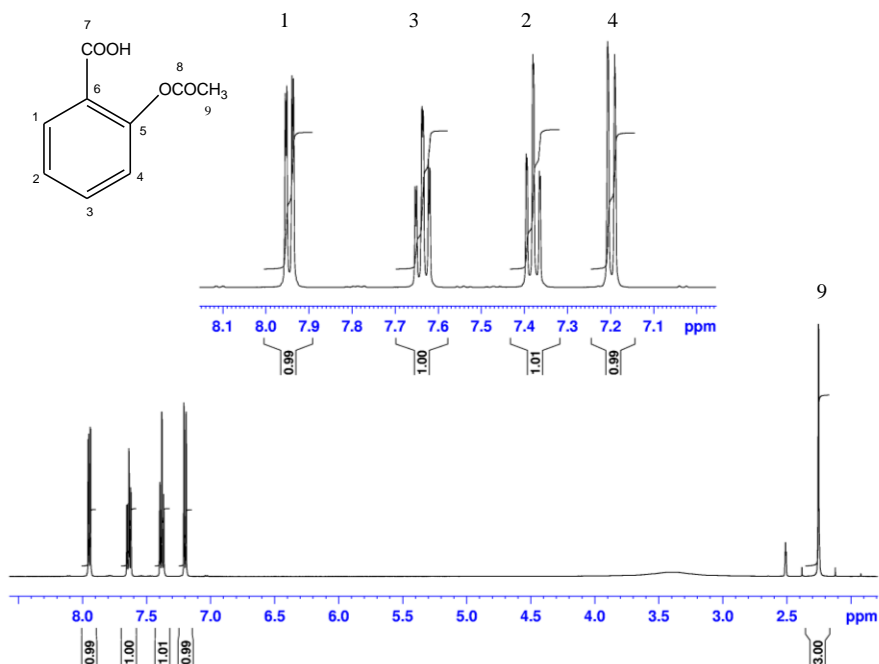


Figure 5.13. ^1H NMR spectrum of acetylsalicylic acid.

^1H NMR spectrum contains one signal in the aliphatic area at 2.25 ppm, besides the signals of solvent and water, which corresponds with a moiety from the acetyl group, in the means of position, intensity and multiplicity of $-\text{CH}_3$. In the aromatic

area, there are 4 signals that can be expected from the structure of the molecule. All signals have the same intensity, and the multiplicity of signals does not allow unambiguous assignment. It is therefore necessary to use further experiments.

Spectrum of ^{13}C APT NMR (Fig. 5.14), also allows a clear assignment of the $-\text{CH}_3$ group from the aliphatic region. Furthermore, there can be seen four signals oriented downwards, i.e., CH signals of the aromatic carbons, and four signals oriented upwards, i.e., two quaternary aromatic signals and two signals of carbonyl groups. This spectrum once again does not allow further definite assignment of all the signals.

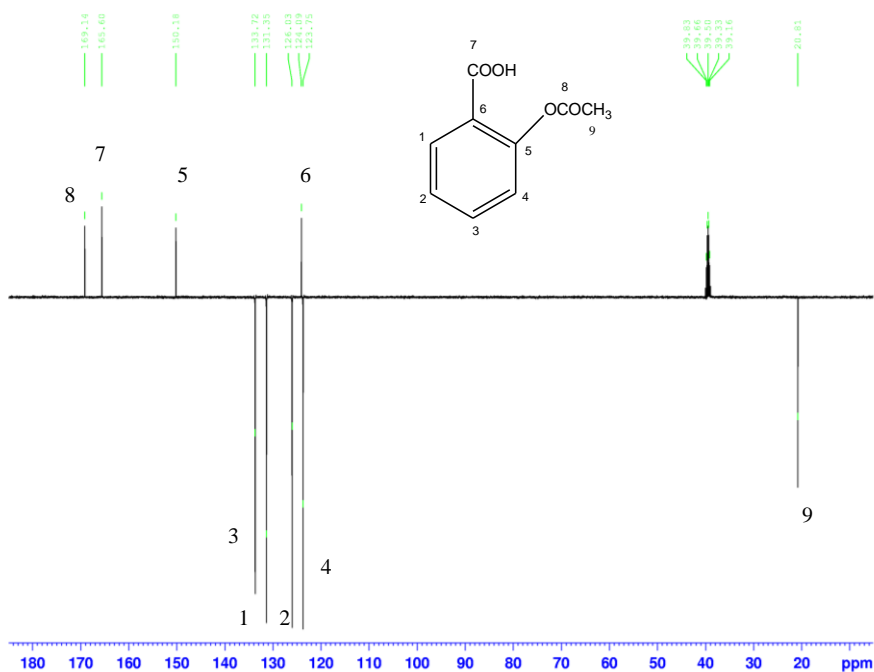


Figure 5.14. ^{13}C APT NMR spectrum of acetylsalicylic acid.

2D COSY spectrum (Fig. 5.15) contains the diagonal peaks and three cross peaks, making it apparent which signal pairs are next to each other. Again, the signals of protons 1 and 4 cannot be assigned without NMR spectra simulation or the use of ^{13}C heterocorrelated spectra.

A heterocorrelated spectrum, called heteronuclear single quantum coherence (2D HSQC), allows to form CH pairs in the aromatic region (Fig. 5.16).

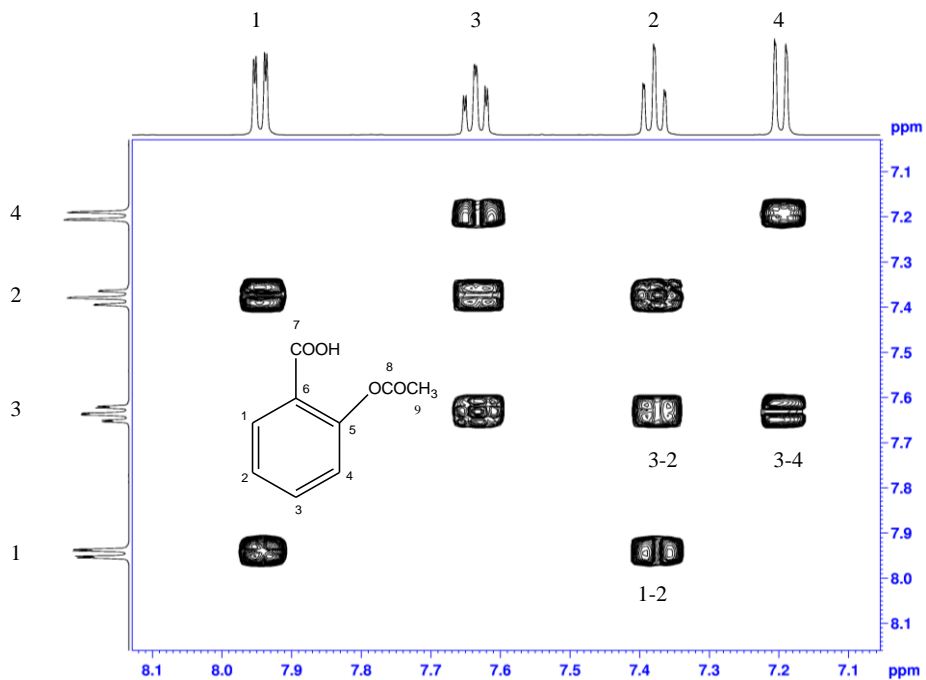


Figure 5.15. ^1H COSY NMR spectrum of acetylsalicylic acid.

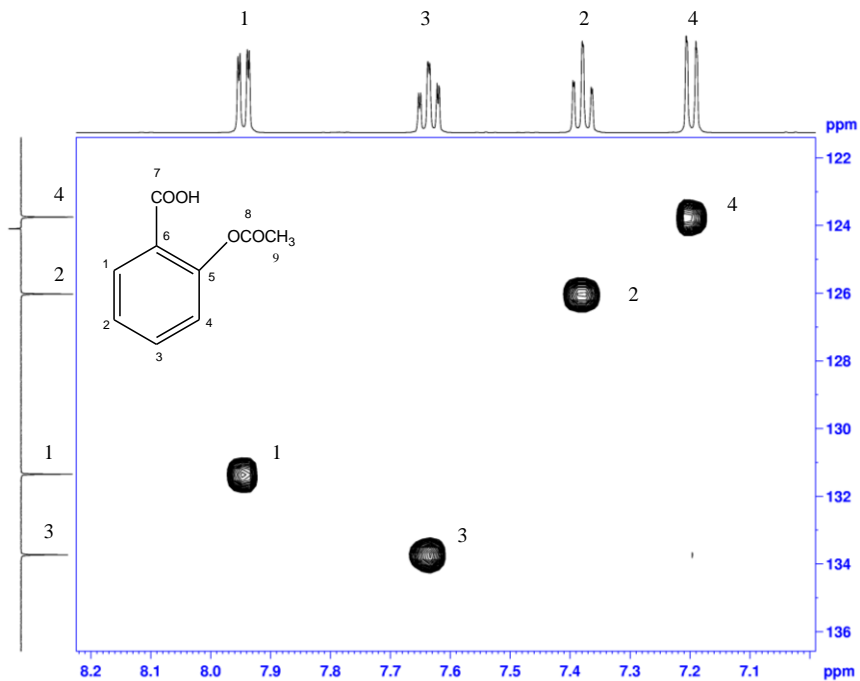


Figure 5.16. ^1H - ^{13}C HSQC NMR spectrum of acetylsalicylic acid.

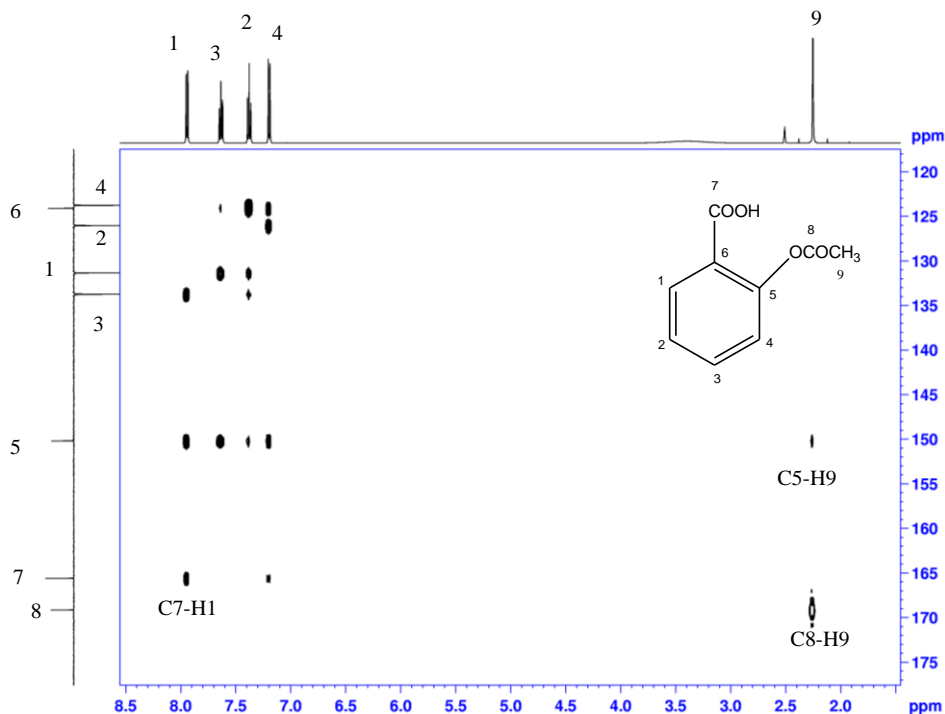


Figure 5.17. ^1H - ^{13}C HMBC NMR spectrum of acetylsalicylic acid.

Another heterocorrelated spectrum – heteronuclear multiple bond correlation (HMBC) – allows to correlate carbons and hydrogens over multiple bonds, usually over three or four bonds (Fig. 5.17). Therefore, the carbons C8 and C7, and the proton H1 can be definitely assigned. This then allows unambiguous assignment of the COSY spectrum, all protons in the molecule, and also the assignment of the remaining CH carbons from the HSQC experiment. The remaining quaternary carbon atoms can then also be assigned from the HMBC experiment.

5.6.2 Structural analysis of impurities

The next example in Fig. 5.18 will demonstrate the possibility to clearly distinguish between two positional isomers. These cannot be distinguished by common MS spectrometry – as they have identical molecular weight.

As can be seen from a heterocorrelated NMR spectrum (HSQC) and the attached 1D experiments, isotibolone has, contrary to tibolone, a signal of the proton 4 located in the proton spectrum, and the carbon 4 located in the aromatic region, which could not be provided by tibolone. The heterocorrelated spectrum contains the corresponding crosspeak. The number of cross peaks and the size of the

molecule show that a complete assignment of the molecule is not a matter of minutes.

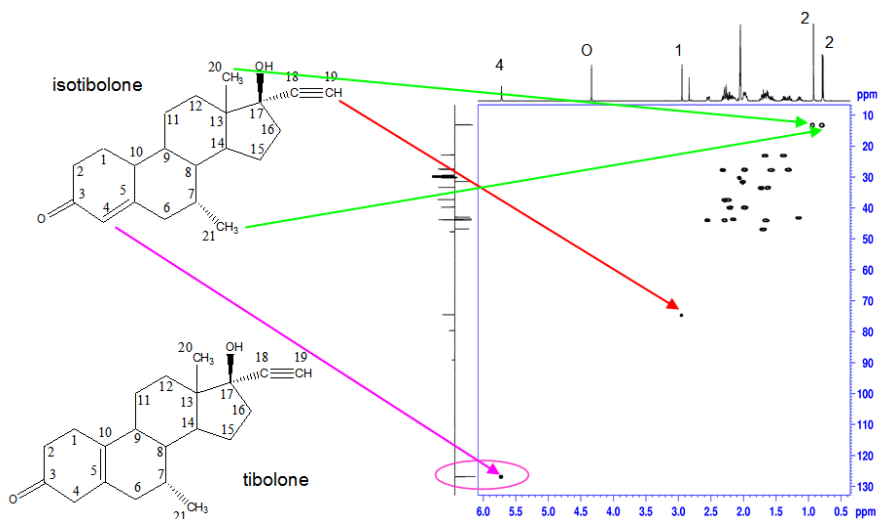


Figure 5.18. ^1H - ^{13}C HSQC NMR spectrum of isotibolone.

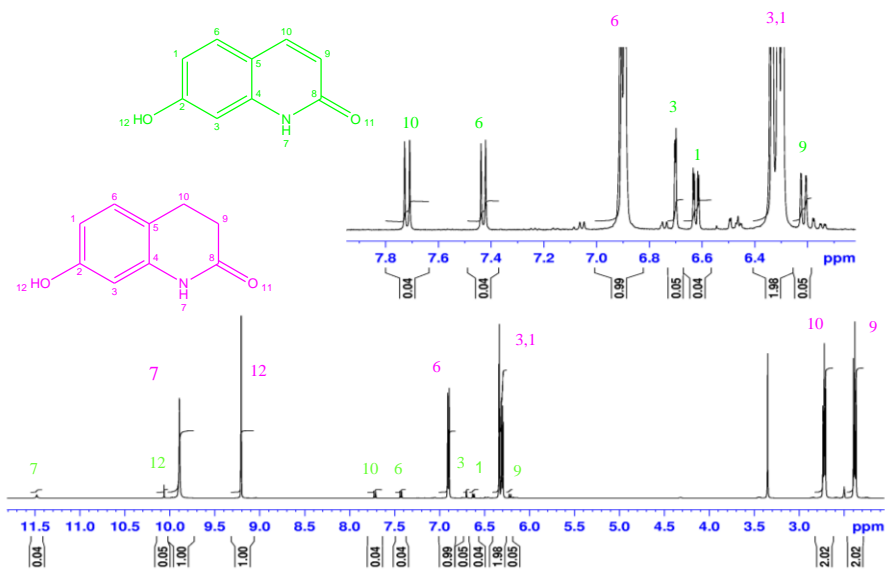


Figure 5.19. ^1H NMR spectrum of 7-hydroxy-3,4-dihydroquinolin-2(1*H*)-on and its impurities.

The last example shows and impurity analysis. Molecule of 7-hydroxy-3,4-dihydroquinolin-2(1*H*)-on, as the main component, does not have both rings unsaturated and thus provides two signals in the aliphatic region, corresponding to CH₂ groups 9 and 10. Aromatic region indicates a presence of an impurity, with a content around 5%. From the expanded proton spectrum and multiplicity of signals, a clear assignment of the molecule of 7-hydroxyquinolin-2(1*H*)-on can be provided.

5.7 Solid state NMR spectroscopy

5.7.1 Theoretical introduction

NMR spectroscopy in liquid phase and its indisputable advantages have been explained in the previous chapter. This extensive chapter will focus exclusively on the NMR spectroscopy in solid phase on nuclei with spin quantum number $I = 1/2$. Unlike in liquid phase, where signals are very narrow due to isotropic movement of molecules, in solid state the signals are significantly wider due to interactions that cannot be observed in the liquid phase. While in the liquid phase half-width of signals is often less than 1 Hz, in solid state the half-width can reach several thousand Hz. Fig. 5.20 shows ¹³C NMR spectrum of a 1-¹³C (10%) marked glycine measured in aqueous solution. Signal of CO group is split by C(α) protons into a triplet, CH₂ carbon is split to a td-triplet of a doublet (α protons cause splitting into a triplet and the carbon from carbonyl group to a doublet).

¹³C NMR spectrum of the 1-¹³C (10%) marked glycine in solid state is shown in Fig. 5.21. While the CO group signal in solution is very sharp, in solid state it is approx. 200 ppm wide and the spectrum is virtually not interpretable.

Two major factors that cause the broadening of bands in solid state are:

- dipolar interaction
- anisotropy of chemical shift

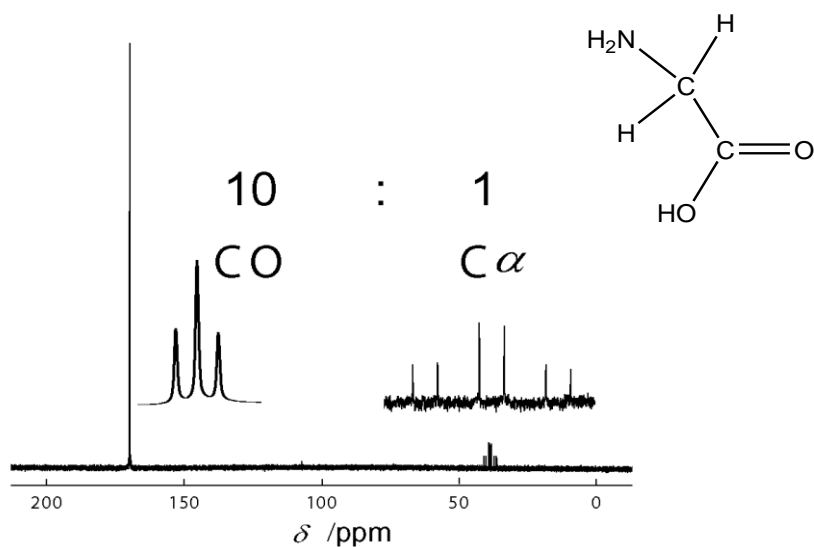


Figure 5.20. ^{13}C NMR spectrum of 1- ^{13}C (10%) marked glycine in $\text{H}_2\text{O}/\text{D}_2\text{O}$.
(Source: Laws D.D. et al. *Angew. Chem. Int. Ed.*, 2002.)

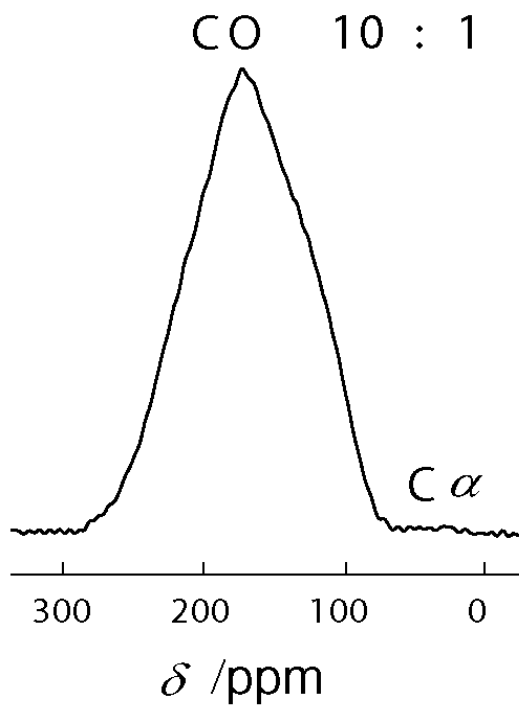


Figure 5.21. ^{13}C NMR spectrum of 1- ^{13}C (10%) marked glycine in solid state.
(Source: Laws D.D. et al. *Angew. Chem. Int. Ed.*, 2002.)

Dipolar interactions

In solution, free movement of molecules eliminates interactions of nuclei. In solid state, this interaction is very important and is characterized by dipolar interaction constant D given by relationship:

$$D = \left(\frac{\mu_0}{4\pi} \right) \left(\frac{h}{2\pi} \right) \frac{\gamma_A \gamma_X}{r_{AX}^3}$$

Dipolar interaction constant is proportional to gyromagnetic ratios (gyromagnetic ratio of hydrogen is 4 times higher than of carbon) and decreases with the third power of the distance between nuclei. The quantity μ_0 is permeability of vacuum. In contrast to liquid phase, dipolar interaction constant in solid state depends also on orientation of the nuclei connecting line to the magnetic field and is proportional to a factor $(3 \cos^2 \theta - 1)$, as shown in Fig. 5.22.

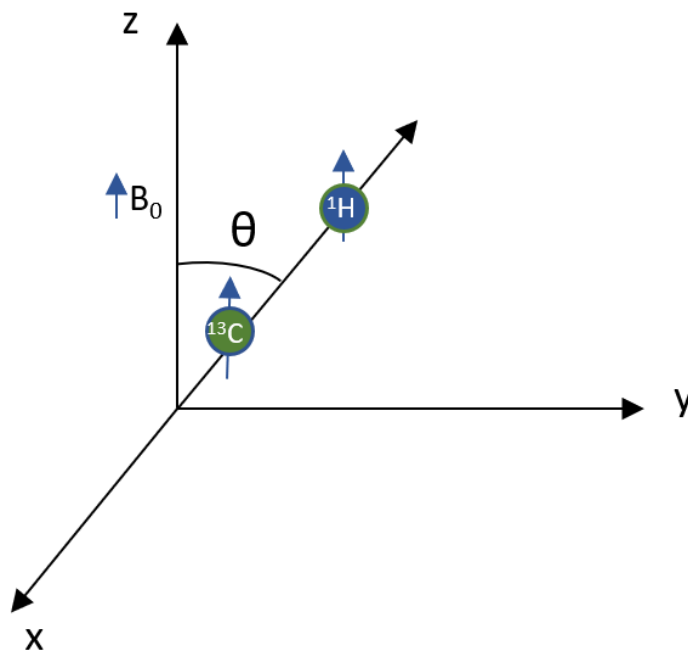


Figure 5.22. Angle θ is held between internuclear vector C–H and direction of magnetic field B_0 .

(Source: Laws D.D. et al. *Angew. Chem. Int. Ed.*, 2002.)

Unlike bond scalar interaction which requires a chemical bond, the dipolar interaction is a spatial interaction and often occurs also between nuclei of different

molecules. It exists either between nuclei of the same type – homonuclear, or between various types of nuclei – heteronuclear.

And when the following applies – $(3 \cos^2 \theta - 1) = 0 \Leftrightarrow \theta = 54.74^\circ$ – then, at this precise angle (the magic angle which corresponds to the angle between a body diagonal and the edge in a cube), the dipolar interaction is eliminated. The second option, how to eliminate the dipolar interaction, especially the heteronuclear one, is by using a decoupling technique.

Chemical shift anisotropy

Orientation dependence, or chemical shift anisotropy, on a magnetic field (CSA) is shown in Fig. 5.23. It is based on the fact that distribution of electron density around nuclei or molecules is not spherical (ball) but ellipsoidal. The value of CSA is also proportional to the factor $(3 \cos^2 \theta - 1)$ and is thus also eliminated by the magic angle. Otherwise, it may reach values of up to several hundred ppm.

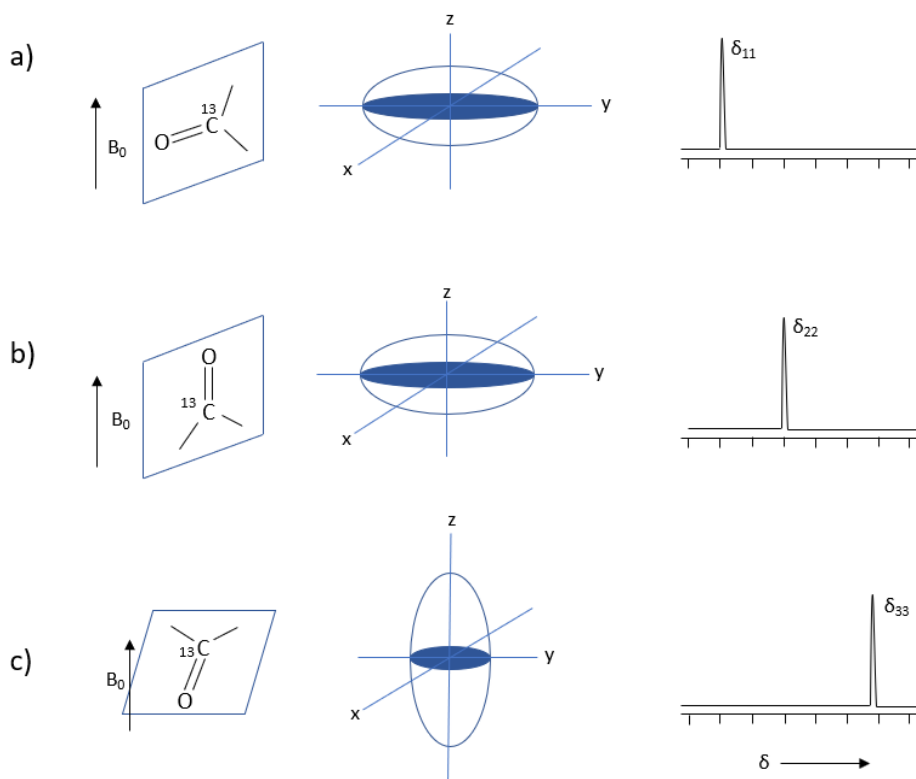


Figure 5.23. Schematic depiction of the CSA principle. Position of each resonance depends on the orientation of an ellipsoid of chemical bond electron density to the magnetic field axis.

(Source: Laws D.D. et al. *Angew. Chem. Int. Ed.*, 2002.)

The value of the isotropic chemical shift, observed in a solution, is then defined by the relationship:

$$\delta_{iso} = \frac{1}{3}(\delta_{11} + \delta_{22} + \delta_{33})$$

In a powder sample, with many random orientations, it is possible to obtain the “powder pattern” which has basically no practical importance, and in real-life, the chemical shift anisotropy must be eliminated.

Magic angle spinning

If a sample is placed at an angle of 54.74° towards the magnetic field (Fig. 5.24), the elimination of the element $(3 \cos^2 \theta - 1)$ occurs, and if the rotation is sufficiently high, it leads to elimination of the heteronuclear dipolar interactions and of the chemical shift anisotropy.

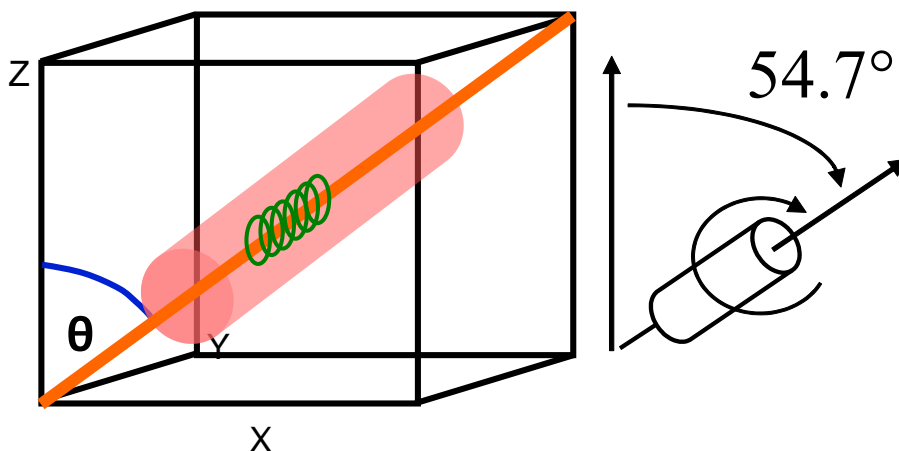


Figure 5.24. Magic angle spinning.

Magic angle spinning (MAS) is then combined with the heteronuclear decoupling technique and the result is an NMR spectrum with a very good resolution (Fig. 5.25).

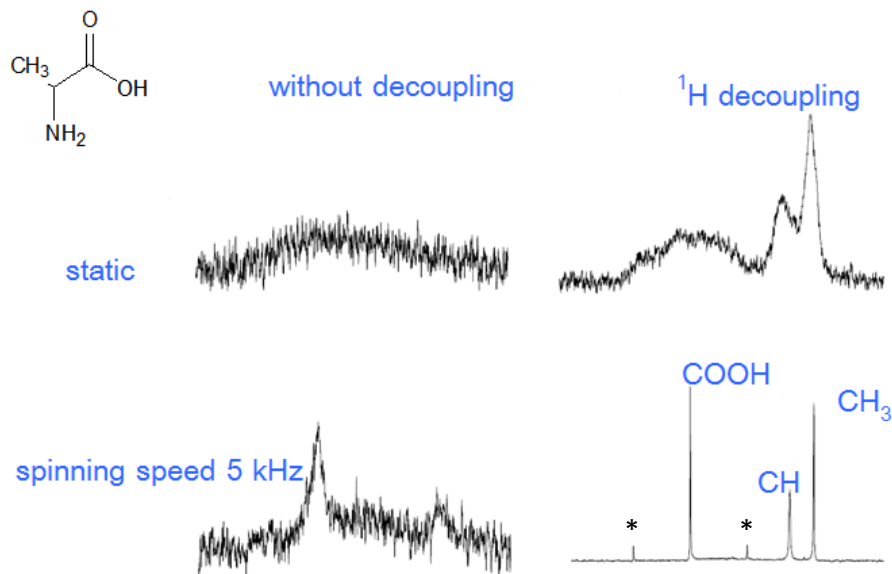


Figure 5.25. Comparison of ^{13}C NMR spectra of alanine under static conditions (no rotation), and magic angle spinning without and with heteronuclear decoupling. Symbol * denotes the spinning sidebands.

A necessary addition is a technique called cross-polarization (CP/MAS), which is used to transfer polarization from protons to isotopically poor nuclei, such as ^{13}C , ^{15}N , or ^{29}Si . This required the fulfilment of the Hartmann-Hahn condition. The result is a significant increase in sensitivity of the NMR experiment. Spinning sidebands appear in the spectrum if the rotation is not high enough, which often complicates the interpretation of NMR spectra (Fig. 5.26). Only when the speed is sufficient, the spectrum has a signal count corresponding to isotropic chemical shifts. If it is not possible to achieve adequate rotation speed due to technical reasons, the rotational sidebands can be suppressed by pulse techniques, such as a TOSS sequence (total sidebands suppression).

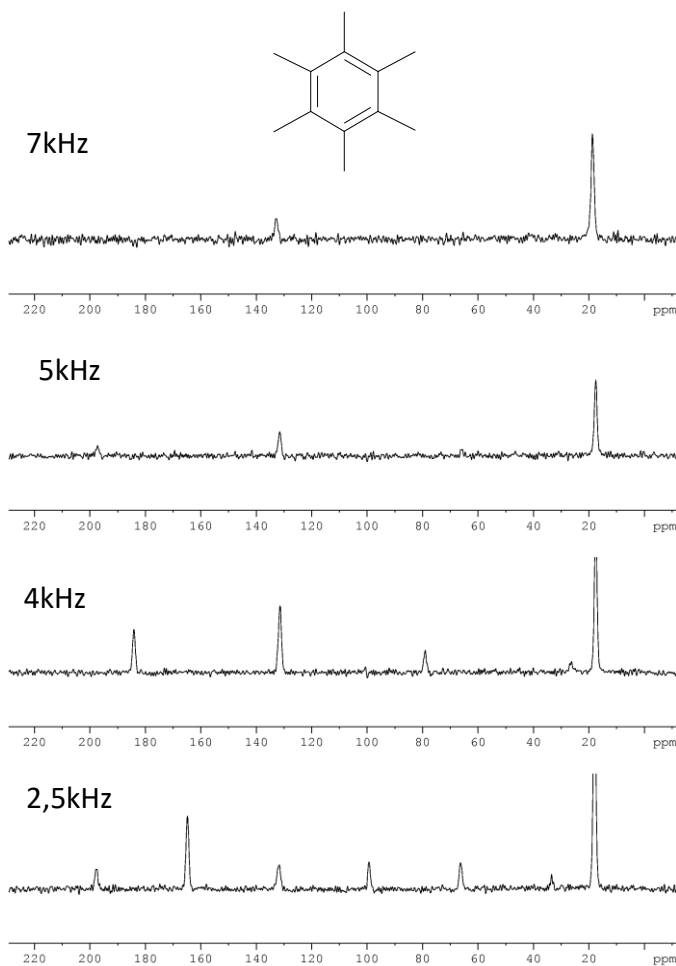


Figure 5.26. ^{13}C CP/MAS NMR spectrum of hexamethylbenzene under various spinning speeds.

Spinning speed is determined by rotor size (Fig. 5.27). The smaller the diameter of an NMR rotor, the higher the possible spinning speed but the lower the sensitivity of measurement. Maximum spinning speed of a 4 mm rotor is 15 kHz, for 2.5 mm rotor the speed reaches up to 35 kHz.



Figure 5.27. NMR rotors designed for solid state measurements.

Currently, there are already available probes with cell size of 1.3 mm, enabling rotation of 70 kHz. Yet, the rotation speed is still not sufficient for suppression of strong homonuclear dipolar interactions and acquisition of well-differentiated proton NMR spectra. The technical realization is shown in Fig. 5.28, where the rotor is spun by air flow and the velocity is detected by optical fibre.

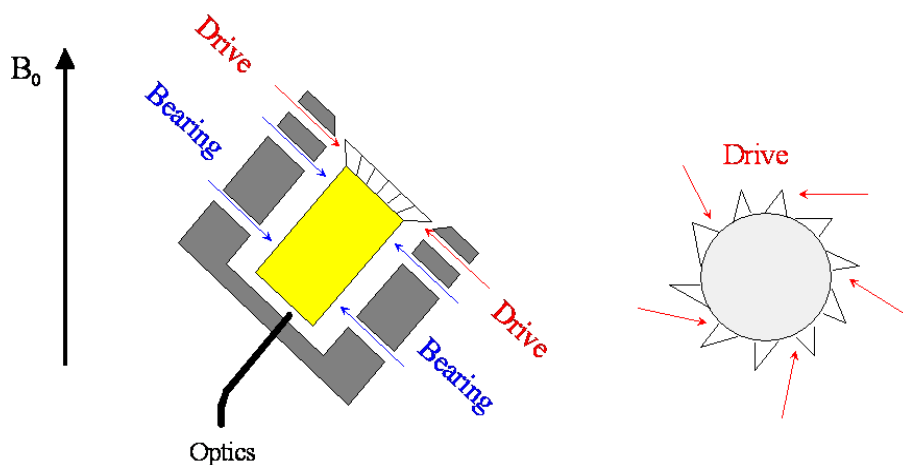


Figure 5.28. Technical realization of rotor spinning, under magic angle.

(Source: *Short CP/MAS. Presentace. Varian, 2001.*)

5.7.2 Application of solid state NMR spectroscopy in pharmacy

Solid state NMR spectroscopy is not used for routine analyses in pharmacy, but its role in development is indispensable. It has a very wide application. The most important applications can be divided into the following groups:

- API structural analysis
- polymorphism
- dosage form analysis
- solvate analysis
- salt analysis

5.7.2.1 API structural analysis

Similarly as in liquid phase, many types of solid state NMR experiments can be performed to obtain information about the molecule structure. The most common is the measurement of ^{13}C CP/MAS NMR spectra, which provides basic information about a molecule. As in liquid phase, this can then be complemented by other experiments performed to obtain information on the types of carbons included in the molecule. One of the experiments is a NQS experiment (non-quaternary suppression). Signals of carbon atoms with directly bound protons, especially CH and CH_2 are suppressed in the spectra. The CH_3 signals remain unsuppressed due to free rotation, which also applies for acetylsalicylic acid (Fig. 5.29).

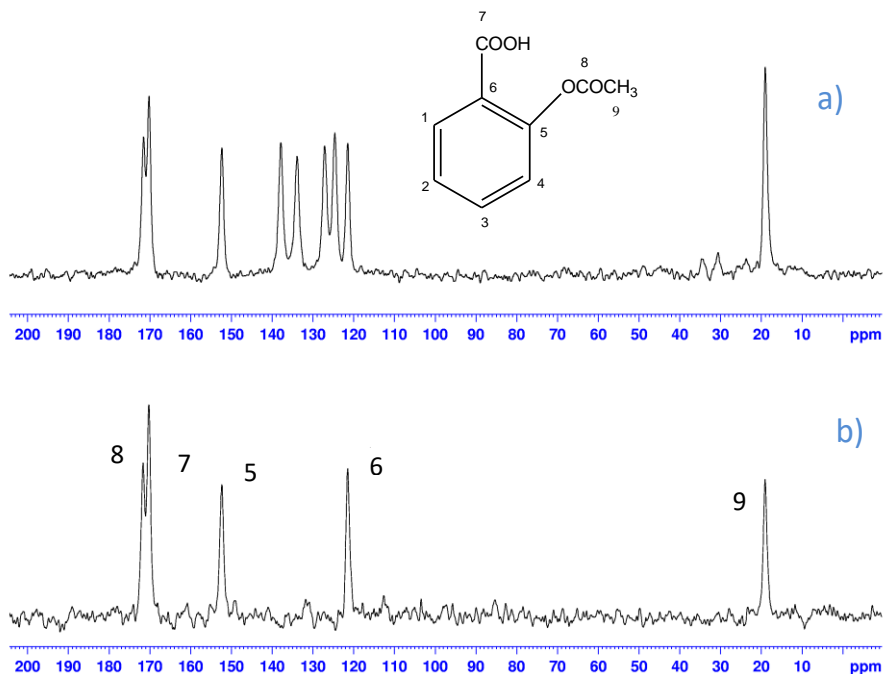


Figure 5.29. Comparison of a ^{13}C CP/MAS NMR spectrum (a) and a ^{13}C NQS (b) spectrum of acetylsalicylic acid.

As already mentioned, measurements of proton spectra in solid state are not common. Therefore, a suitable complement to a ^{13}C CP/MAS experiment is a heterocorrelated NMR spectrum, from which it is indirectly possible to acquire information about chemical shifts of protons (Fig. 5.30).

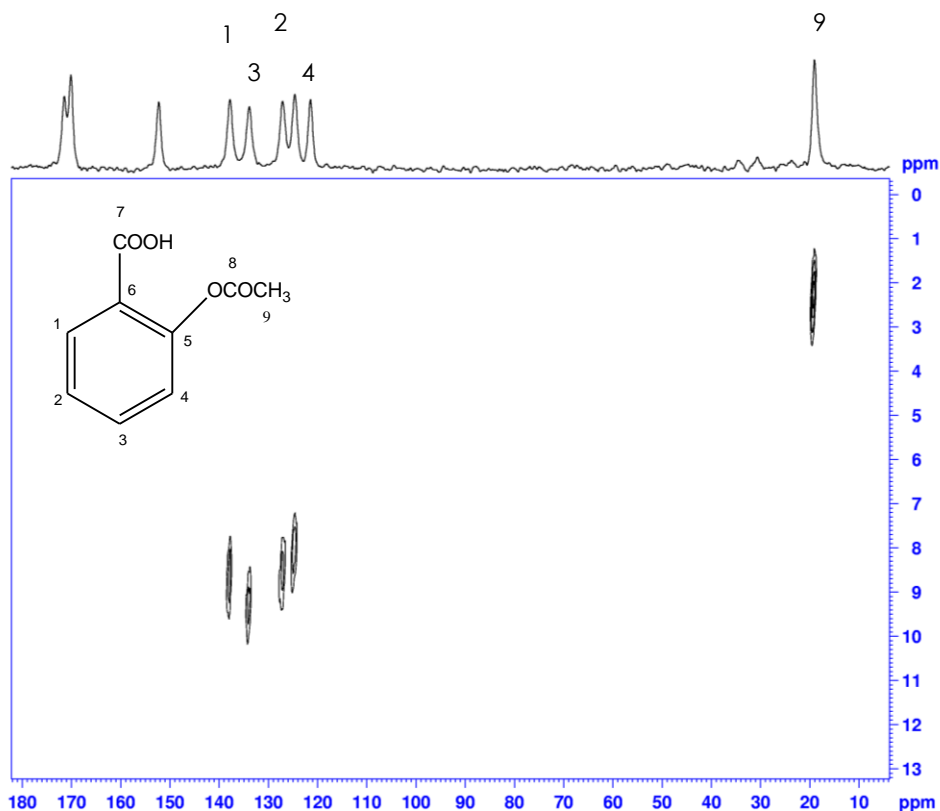


Figure 5.30. 2D heterocorrelated NMR spectrum of acetylsalicylic acid.

5.7.2.2 Polymorphism

Polymorphism can be defined as an ability of compounds to exist in more than one crystalline state, each differing in arrangement or conformation of molecules in the crystal structure. Polymorphs are chemically identical but differ in their physical (spectral) properties. The NMR spectroscopy in solid state is one of the few methods that allows clear identification of polymorphs and detection of polymorphic purity. In addition, one of the biggest advantages of NMR spectroscopy is the possibility to measure spectra of different isotopes, which provides complementary information. Usually, measuring of ^{13}C CP/MAS NMR spectra is the first and the most common choice.

Fig. 5.31 shows comparison of two crystalline polymorphs and one amorphous form. The spectra, particularly of the crystalline forms, can be clearly interpreted, and the duplication of lines indicates the presence of two symmetrically inequivalent molecules.

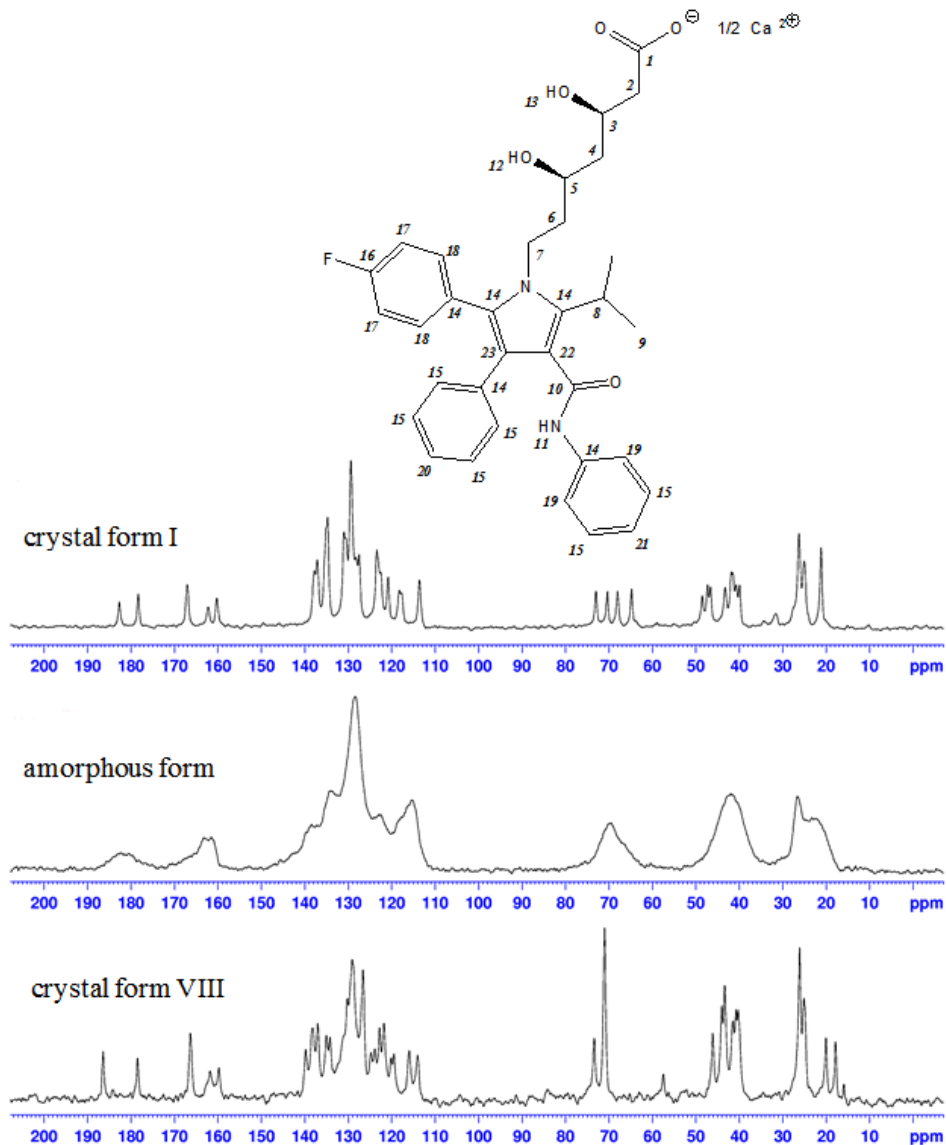


Figure 5.31. Comparison of ^{13}C CP/MAS NMR spectra of three polymorphic forms of calcium atorvastatin.

Molecule of atorvastatin contains two nitrogen atoms. Fig. 5.32 shows a comparison of ^{15}N CP/MAS spectra of the same molecule in different polymorphs. Sensitivity of the ^{15}N nucleus is however 50-fold lower, and acquisition of such spectra requires appropriate equipment and sufficient experimental time. Duplication of signals again indicates the presence of two symmetrically inequivalent molecules in one unit cell.

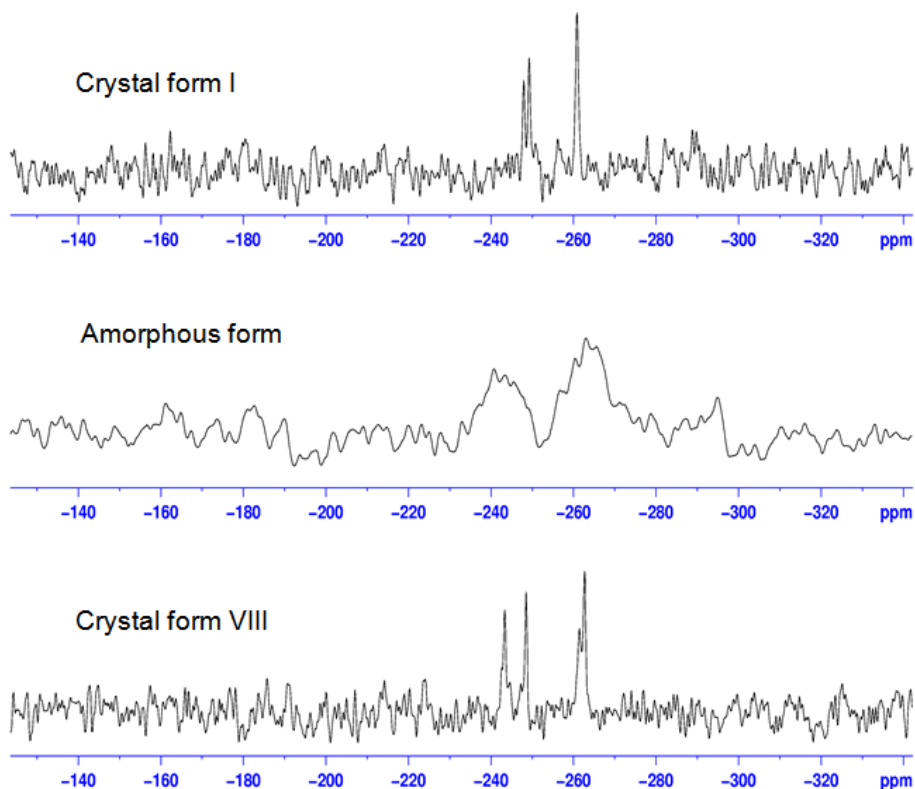


Figure 5.32. Comparison of ^{15}N CP/MAS NMR spectra of three polymorphic forms of calcium atorvastatine.

Atorvastatin molecule also contains a fluorine atom. This allows measurement of the ^{19}F isotope, which has a natural occurrence of 100%, enabling quality ^{19}F NMR spectra measurement in a relatively short time. Fig. 5.33 compares the same three atorvastatin forms, as previously. The duplication of lines is similar as in the previous cases.

The advantage of the presence of a fluorine atom can be applied in quantitative analysis or in detection of polymorphic purity of APIs. Fig. 5.34 shows ^{19}F CP/MAS NMR spectra of atorvastatin form I, its amorphous form, and their model mixture. Similar spectra can be obtained when measuring dosage forms. In this case, the fluorine atom represents an advantage not only for sensitivity but also for selectivity, since no excipient contains fluorine atoms and thus the polymorphic purity of the API can be studied also in formulations, without signals of API being overlapped by signals of excipients, which can be the case in ^{13}C CP/MAS NMR spectra.

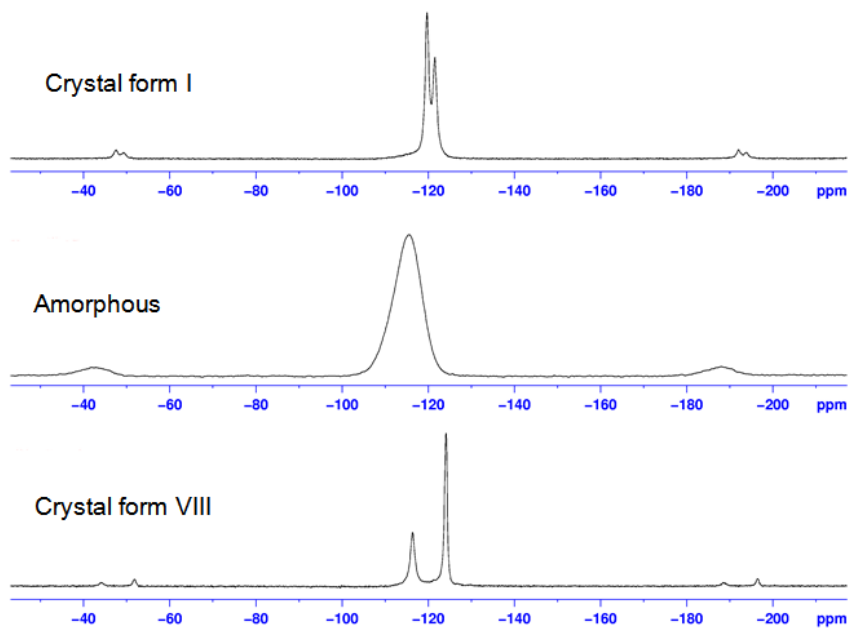


Figure 5.33. Comparison of ^{19}F CP/MAS NMR spectra of three polymorphic forms of calcium atorvastatine.

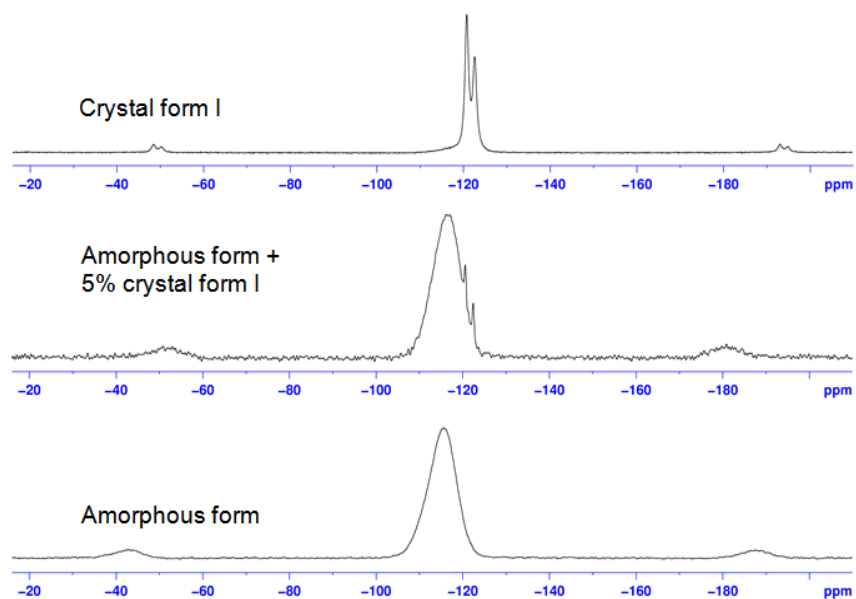


Figure 5.34. ^{19}F CP/MAS NMR spectra of a model mixture of calcium atorvastatine (5 % of form I and 95 % of amorphous form), and of pure crystalline and pure amorphous forms.

For comparison, the Fig. 5.35 contains an example of a measurement of a similar model mixture in a dosage form but using the carbon spectra. The time required for this experiment is much longer than for the fluorine NMR spectra.

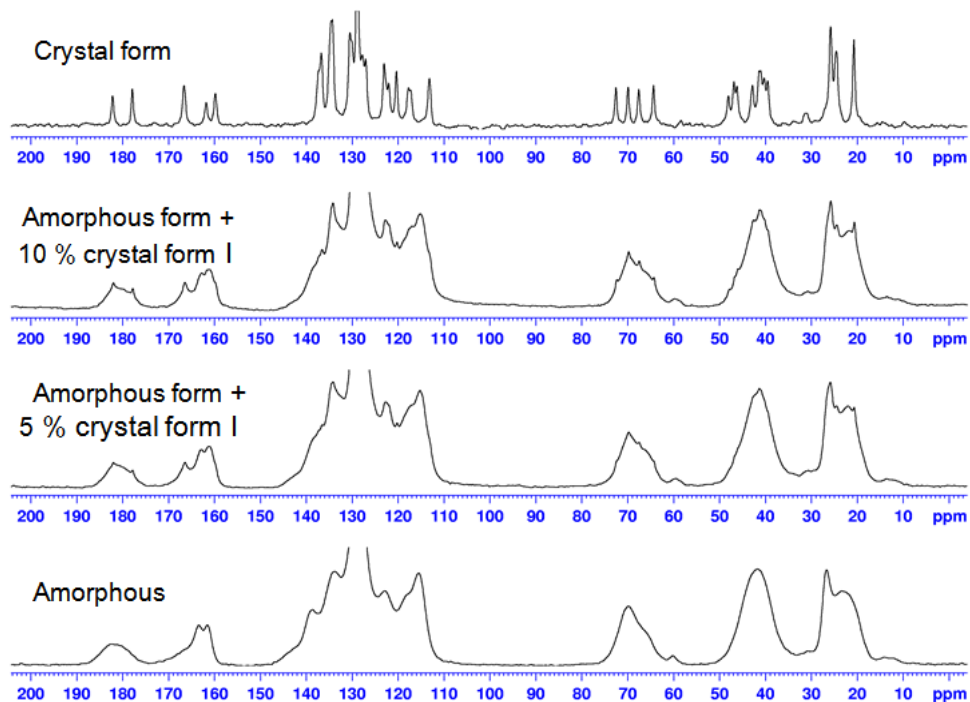


Figure 5.35. Comparison of ^{13}C CP/MAS NMR spectra of model mixtures of calcium atorvastatine (5% of form I and 10% amorphous form) with spectra of pure crystalline and amorphous forms.

5.7.2.3 Dosage form analysis

The ^{13}C CP/MAS NMR spectra are very often used for identification of polymorphs in formulations. The comparison can be carried out only in those parts of the NMR spectra which do not contain signals of excipients. If the API content in a dosage form is low, the acquisition of this information can be very time consuming and sometimes lasting several tens of hours. Fig. 5.36 shows comparison of an atorvastatine formulation containing crystalline form I with two pure atorvastatin forms.

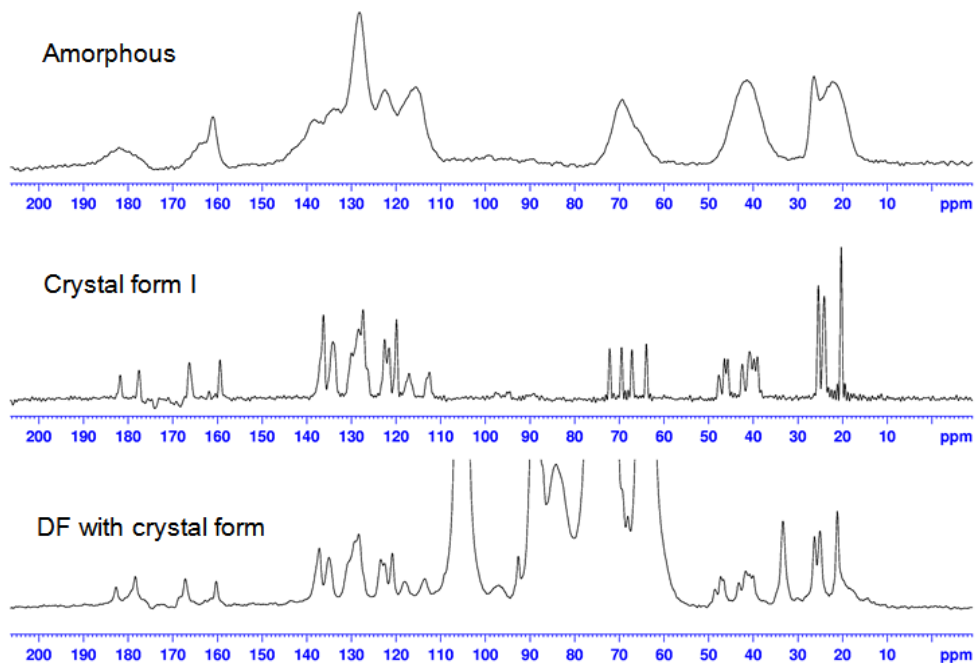


Figure 5.36. Comparison of a ^{13}C CP/MAS NMR spectrum of atorvastatin as a pure amorphous form, pure crystalline form I, and a dosage form containing calcium atorvastatine as crystalline form I.

If a dosage form contains an API with a hetero atom, such as fluorine or phosphorus, the identification of the API form is significantly easier. An example with fluorine was already shown in Fig. 5.34. Fig. 5.37 shows a situation where it is possible to find out whether dosage form contains an amorphous form of risedronate sodium polymorph A, H, or a mixture of the polymorphs A and H, in a few minutes. To determine whether a sample represents a pure API form or a dosage form, the ^{31}P spectra are not sufficient, and the ^{13}C CP/MAS NMR spectra must be measured, or the results must be complemented by other methods, such as X-ray diffraction, IR or Raman spectroscopy. In both cases, the ^{31}P CP/MAS NMR spectra will not differ, and the difference will only lie in the sensitivity of the experiment, especially when the API content in the formulation is low.

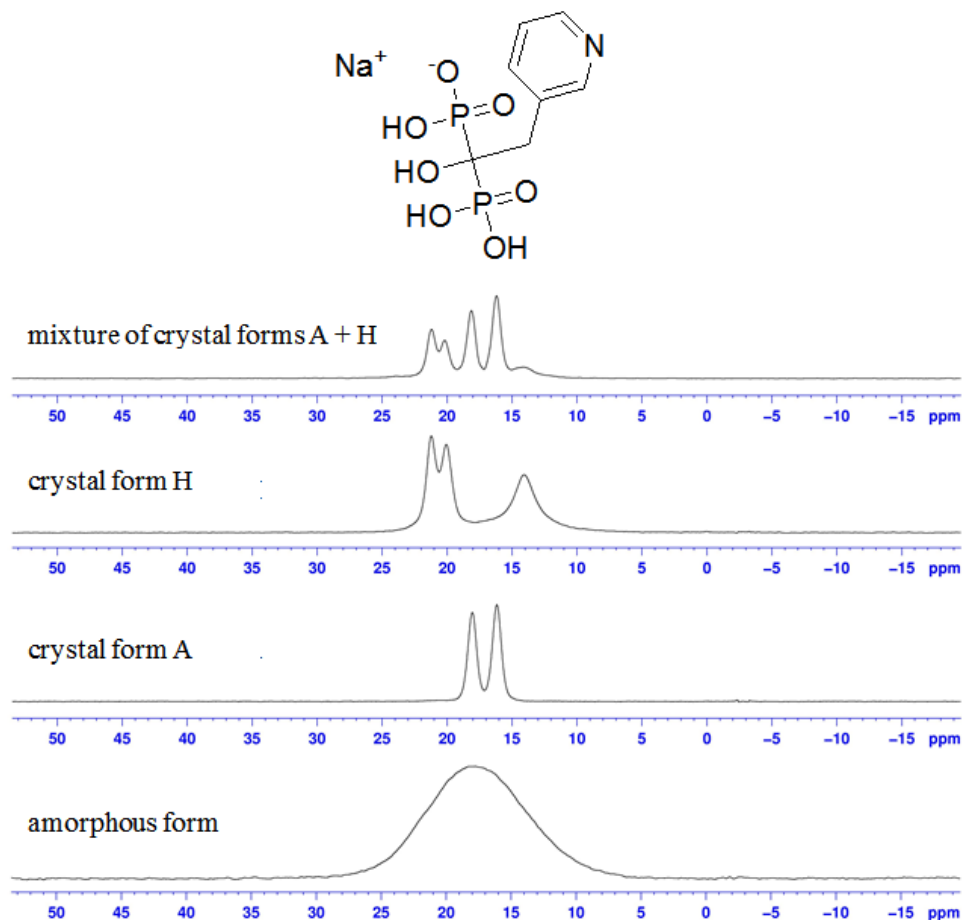


Figure 5.37. Comparison of ^{31}P CP/MAS NMR spectrum of an amorphous form of sodium risendronate and its polymorphs A and H, and a mixture of polymorphs A and H.

Analysis of dosage forms does not include only identification of API forms, but also qualitative and quantitative analysis of excipients. In this case, it is necessary to analyse also the ^{13}C CP/MAS NMR spectra. The analysis of dosage forms can sometimes be very difficult because the signals of excipients and APIs very often overlap. Usually, however, it is possible to identify the excipients at least according to some of the signals (Fig. 5.38 and 6.39). Fig. 5.40 shows, how well it is possible to distinguish some types of cellulose.

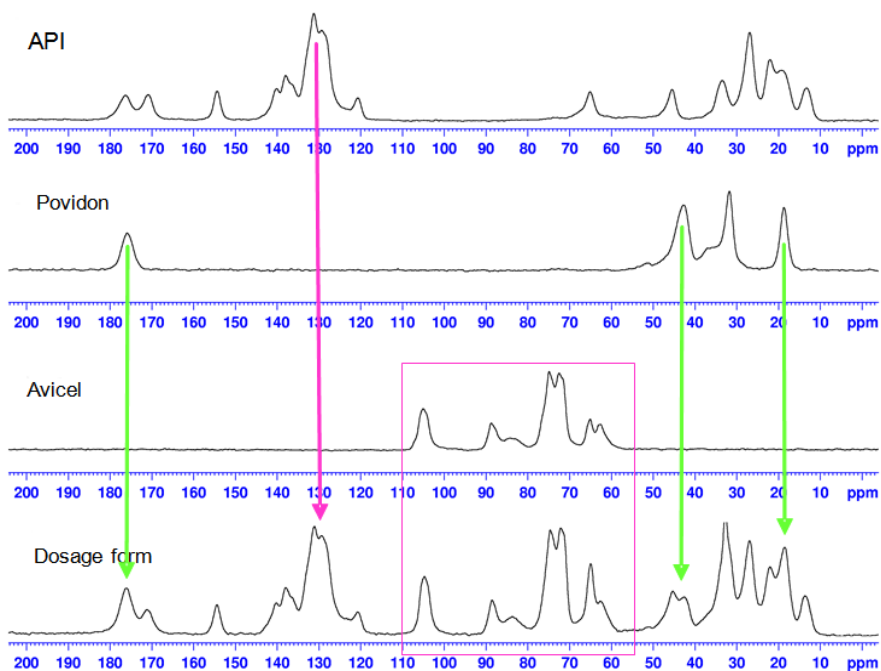


Figure 5.38. ^{13}C CP/MAS NMR spectrum of a dosage form containing excipients – microcrystalline cellulose Avicel and Povidone.

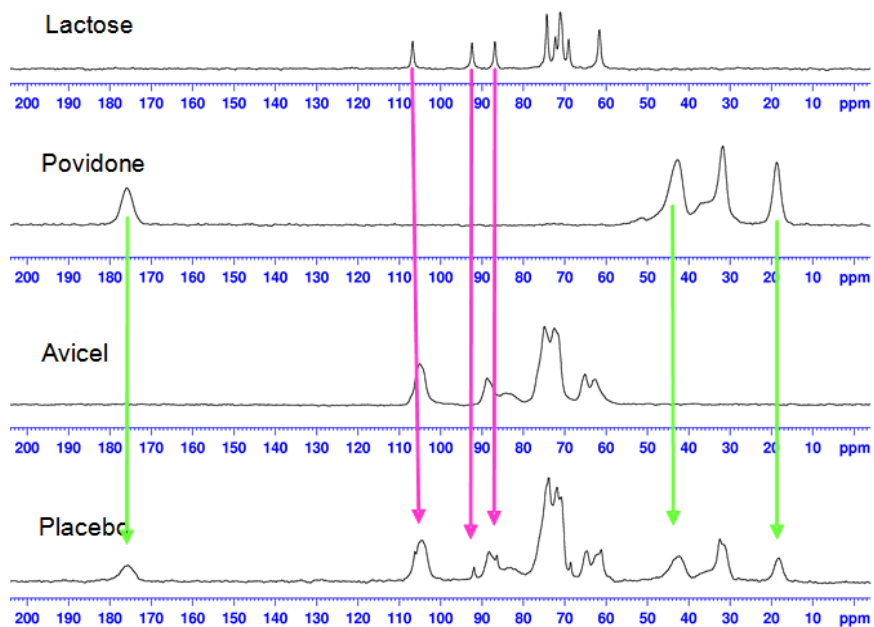


Figure 5.39. Comparison of ^{13}C CP/MAS NMR spectra of a placebo containing excipients – microcrystalline cellulose Avicel, Povidone, and Lactose monohydrate.

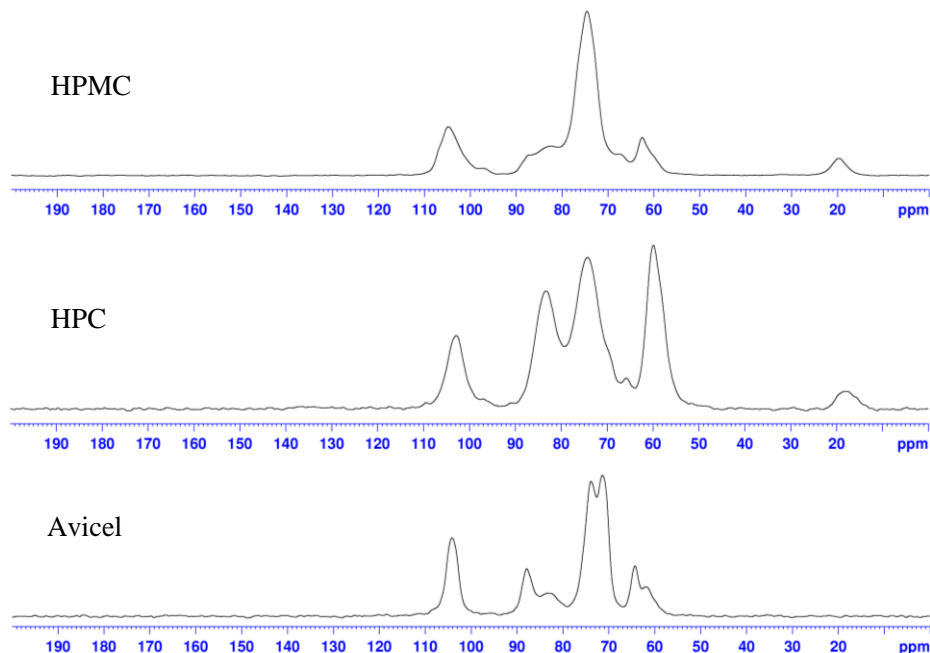


Figure 5.40. Comparison of ^{13}C CP/MAS NMR spectra of excipients – microcrystalline cellulose (Avicel), hydroxypropylcellulose (HPC), and hydroxypropylmethylcellulose (HPMC).

5.7.2.4 Solvate analysis

Analysis of solvates is nowadays a common requirement. The reason is that solvents are very often incorporated in crystal structures. Such compounds are then called solvates, pseudopolymorphs, or solvatomorphs. Hydrates are another special group, and the hydration process can be very well monitored. Desolvation, in some cases, goes easily and does not change the crystalline form of the API, but sometimes it leads to a collapse of the crystal structure. Since desolvation can also occur during production, formulation, and storage of drugs, its monitoring is very important.

Most solvents are of organic nature, and therefore it is suitable to use ^{13}C CP/MAS NMR spectra. Fig. 5.41 shows a comparison of spectra of three different solvates of one API.

The ^1H NMR spectroscopy in a solution may be a good addition, since it can both identify and quantify the solvent by comparing the signal intensities for the API and the given solvent (Fig. 5.42).

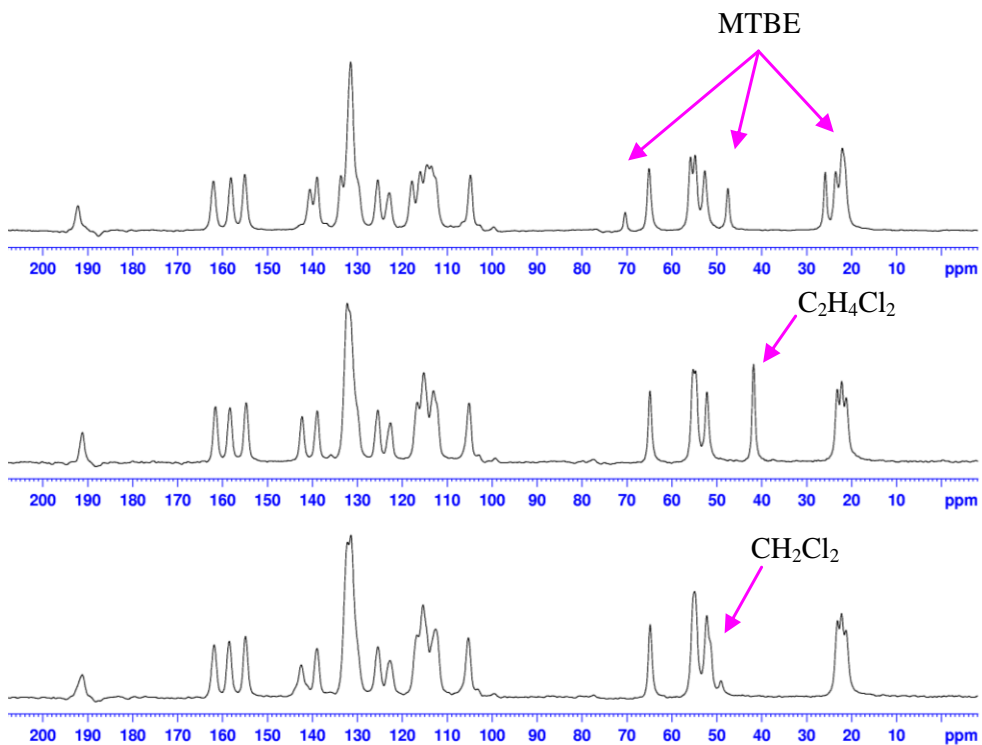


Figure 5.41. Comparison of ^{13}C CP/MAS NMR spectra of three solvates formed with dichloromethane, 1,1-dichlorethane, and methyl-*terc*-butyl ether (MTBE).

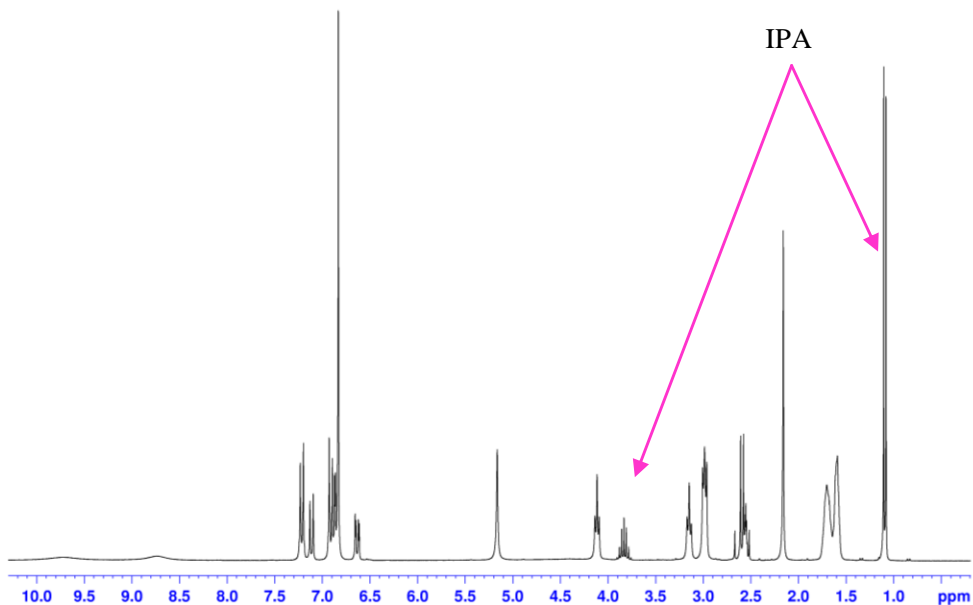


Figure 5.42. ¹H NMR spectrum of a solvate of a studied API with propane-2-ol (IPA).

5.7.2.5 Salt analysis

NMR spectroscopy is of great importance in salt analysis. Salts can basically appear in two types, either as salts of organic acids (API) with metal cations (Na^+ , K^+ etc.) or with organic cations (e.g., meglumine), or salts of organic bases (API) with inorganic anions (e.g., hydrochloride) or organic anions (e.g., maleate). Fig. 5.43 shows differences between ¹³C CP/MAS spectra of sodium and ammonium salts and a pure API.

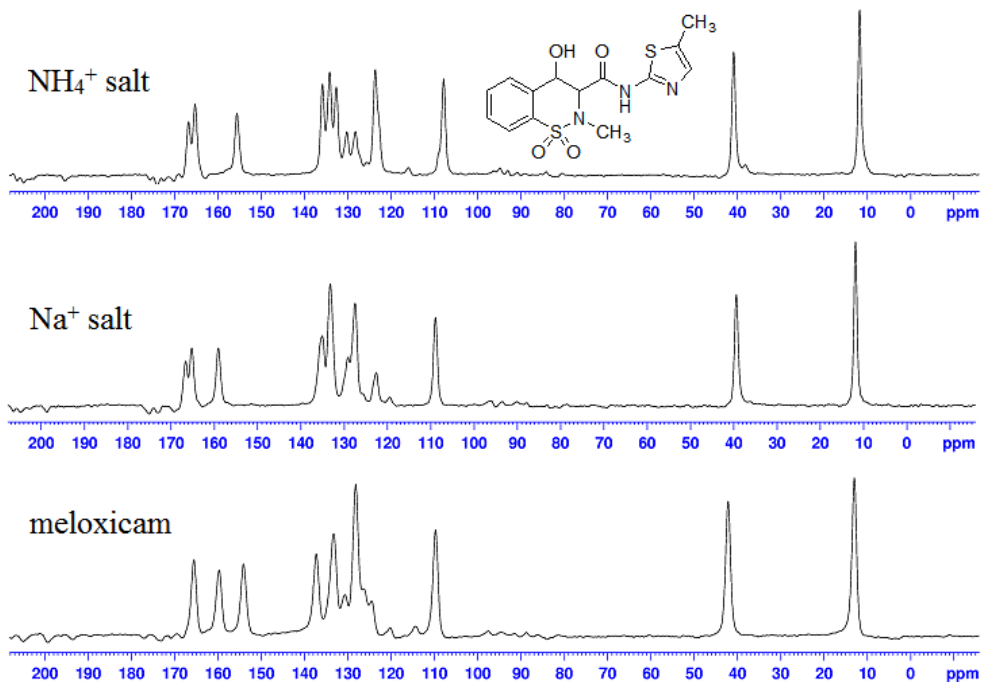


Figure 5.43. Comparison of ^{13}C CP/MAS NMR spectra of meloxicam and its sodium and ammonium salts.

^{15}N CP/MAS spectroscopy can be a good addition in case of ammonium salts, as it allows identification of ammonium salts in pure API samples and also in formulations. This is documented in Fig. 5.44 where three nitrogen atoms can be found in an NMR spectrum of meloxicam, while in the case of its ammonium salt, a signal of the NH_4 group also appears.

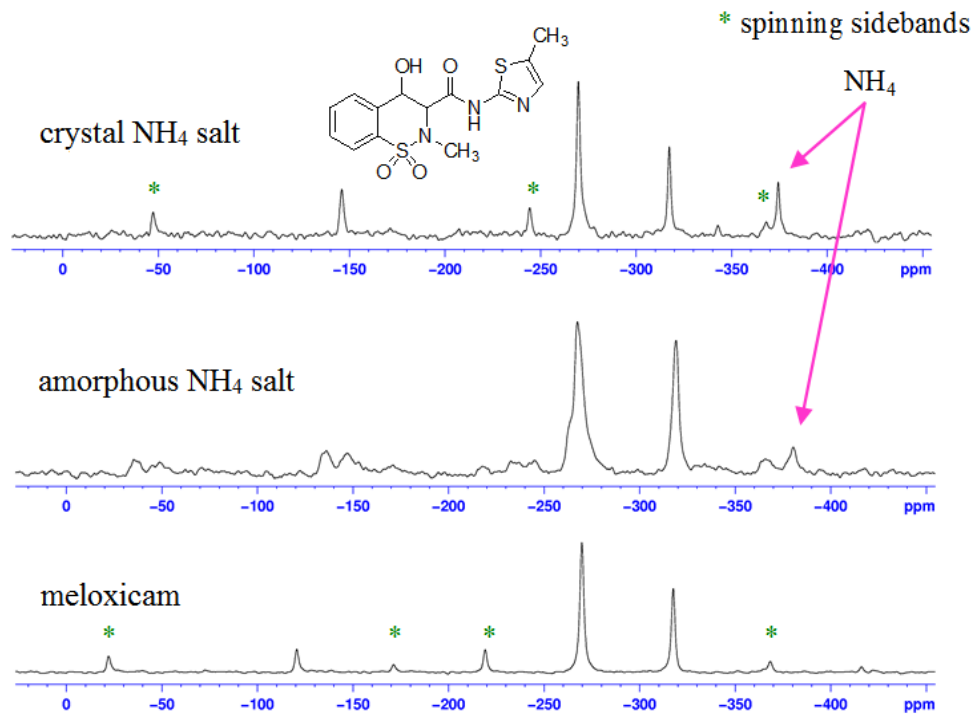


Figure 5.44. ¹⁵N CP/MAS NMR spectra of meloxicam and its amorphous and crystalline ammonium salts.

¹³C CP/MAS NMR spectroscopy is very useful for measuring of salts of bases with organic acids. This is documented in Fig. 5.45, which contains spectra of one base and three organic salts.

A good complement for determination of the base/acid ratio can be the ¹H NMR spectroscopy in solution.

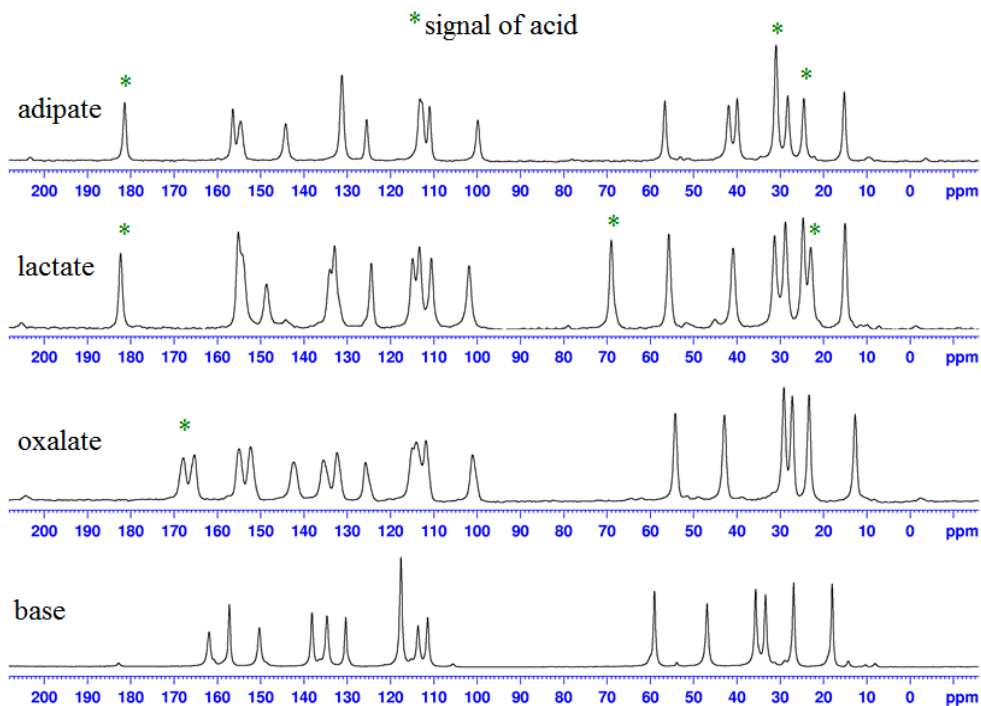


Figure 5.45. Comparison of ^{13}C CP/MAS NMR spectra of a base and salts of three of organic acids – oxalic, lactic, and hexanedioic.

5.8 Conclusion

The text provides a brief demonstration that the use of ssNMR spectroscopy in pharmacy is very broad and can be conveniently combined with other spectroscopic techniques, including NMR spectroscopy in liquid phase.

5.9 Resources and recommended literature

Principles and basics of NMR

1. Holzgrabe U., Wawer I., Diehl D. NMR Spectroscopy in Drug Development and Analysis. Wiley-VCH: Weinheim, Germany, 1999. <https://doi.org/10.1002/9783527613649>
2. Buděšínský M., Pelnař J. Fyzikálně chemické metody – NMR, 25. svazek cyklu Organická chemie. ÚOCHB: Prague, Czech Republic, 2000.
3. Keller J. Understanding NMR Spectroscopy. John Wiley & Sons: Chichester, UK, 2005.
4. Rouessac F., Rouessac A. Nuclear Magnetic Resonance Spectroscopy. In Chemical Analysis – Modern Instrumentation Methods and Techniques, 2nd Edition; John Wiley & Sons: Chichester, UK, 2007, pp. 327–365.
5. Holzgrabe U., Wawer I., Diehl D. NMR Spectroscopy in Pharmaceutical Analysis. Elsevier: Amsterdam, The Netherlands, 2008. <https://doi.org/10.1016/B978-0-444-53173-5.00005-6>

Application of NMR in liquid phase

6. Pretch C., Seidle S. Spectral Data for Structure Determination of Organic Compounds, 2nd Edition. Springer-Verlag: Berlin, Germany, 1989.
7. Friebolin H. Basic One- and Two-Dimensional NMR Spectroscopy, 3rd Revised Edition. Wiley-VCH: Weinheim, Germany, 1998.
8. Silverstein R. M., Webster X. F., Kiemle D. J. Spectrometric Identification of Organic Compounds, 7th Edition. John Wiley & Sons: New York, USA, 2005.

Application of NMR in solid state

9. West A. R. Basic Solid State Chemistry. John Wiley & Sons: Chichester, UK, 1999.
10. Duer M. J. Solid-State NMR Spectroscopy, Principles and Applications. Blackwell Science: Oxford, UK, 2002. <https://doi.org/10.1002/9780470999394>
11. Laws D. D., Bitter H. M. L., Jerschow A. Solid-State NMR Spectroscopic Methods in Chemistry. Angew. Chem. Int. Ed. 2002, 41 (17), 3096–3129. [https://doi.org/10.1002/1521-3773\(20020902\)41:17%3C3096::AID-ANIE3096%3E3.0.CO;2-X](https://doi.org/10.1002/1521-3773(20020902)41:17%3C3096::AID-ANIE3096%3E3.0.CO;2-X)
12. Klinowski J. New Techniques in Solid-State NMR. Springer-Verlag: Heidelberg, Germany, 2005. <https://doi.org/10.1007/b94544>
13. Zakrzewski A., Zakrzewski M. Solid State Characterization of Pharmaceuticals. Eds.; Assa: Danbury, CT, USA, 2006.

14. Hartus R. K. NMR Studies of Organic Polymorphs & Solvates. *Analyst* 2006, 131 (3), 351–373. <https://doi.org/10.1039/b516057j>

6 Terahertz time-domain spectroscopy

Filip Kadlec, Christelle Kadlec

6.1 Introduction

The terahertz (THz) spectral region is one of the still relatively little known parts of the electromagnetic spectrum, situated in the zone adjacent to the infrared (optical) region, on one side, and to the microwave (electronic) region on the other. Like other spectral regions, the range of the THz region is not defined precisely exactly, but its use associated with several specific experimental techniques. These techniques cover a wide interval, which can be roughly delimited by frequencies of 100 GHz and 3 THz, corresponding to wavelengths between 3 and 0.1 mm, *i.e.*, wave numbers from 3 to 100 cm^{-1} . The THz region hence partially overlaps with the far-infrared region. The characteristic frequency of 1 THz can be equivalently expressed in other spectroscopic units, as shown below.

$1 \text{ THz} \leftrightarrow 33 \text{ cm}^{-1} \leftrightarrow 0.3 \text{ mm} \leftrightarrow 48 \text{ K} \leftrightarrow 4.1 \text{ meV}$
frequency wavenumber wavelength temperature photon energy

The boom of the THz research occurred gradually in the nineties of the 20th century, after the invention of THz time domain spectroscopy. The decisive factor was the development of optical femtosecond lasers which present the basis for most current laboratory and commercial THz spectrometers. Until then, there had been only limited options for generation and detection of THz radiation since there is no access to the THz field measurements using either classical optical spectroscopy (intensity of optical radiation sources declines, similarly as blackbody radiation) or traditional electronic sources (electronic components are not capable of operation at such high frequencies).

The attractiveness of the THz field is linked to several specific possibilities of using the electromagnetic radiation with these frequencies. The applications can be divided into three main categories: spectroscopy, imaging, and data transfer (telecommunications). The applications from the first two groups are gradually finding their way into the pharmaceutical industry, mostly in analysis of solid active ingredients. In most cases, however, these are only pilot studies, designed to demonstrate the suitability of a certain method for a specific purpose. It can be

therefore expected that some other applications of the THz radiation in pharmacy will only be discovered in upcoming years.

Solid substances often exhibit specific interactions in the THz region. While some crystals are transparent in this range, many others show low-frequency oscillations of the crystal lattice (called phonon bands), with characteristic frequencies determined by short-range inter-atomic interactions and regular long-range arrangement of atoms. Since amorphous materials have significantly different atomic arrangements, the THz spectra of amorphous and crystalline phases are significantly different even with identical chemical composition.

In the cases of molecular crystals, liquids, and gases, the THz region includes molecular movements – particularly the intermolecular motions, when entire molecules or their large parts vibrate, librate, or rotate together. The vibrational frequencies of molecules are only slightly affected by their incorporation into a crystal lattice and thus the shifts of the absorption bands are relatively small compared to shifts of free molecules.

The THz properties of weakly doped semiconductors are related mainly to the movement of free electrons. The THz radiation is continuously and very strongly reflected by metals and strongly absorbed by liquid water. On the other hand, isolated water molecules, such as water vapor or crystal water, show characteristic narrow absorption bands.

6.2 Overview of experimental techniques in THz spectroscopy

Due to the interest in the THz spectral region and its specific features and expected applications, there was a rapid development of the appropriate sources, detectors, and measurement approaches, in the recent decades. By now, there are so many experimental techniques that it would be pointless to describe them all in detail in this text. Therefore, only the main options will be briefly discussed.

One of the most intensive THz radiation sources are synchrotrons. These are large and very expensive instruments working on the principle of acceleration of charged particles (mainly electrons) on an approximately circular trajectory with a diameter of tens to hundreds of meters. The irradiation of electromagnetic waves occurs due to bending of particle trajectories in a magnetic field, thus generating a broad continuous spectrum of which the THz radiation constitutes only a very small part. Since the synchrotron measurement time is limited and highly demanded, the

studies of substances using synchrotron radiation are limited to well justified cases with the aim of making breakthrough discoveries.

Gas lasers working in the THz region have been used for many decades. Their active media consist of some selected gases (e.g., methanol, formic acid, ammonia) with rotational levels that enable to choose the appropriate lines. Their output spectra are very narrow, and their performance can typically reach a few mW. A disadvantage of the THz lasers is their size and complex operation. Since their output wavelengths are practically not tunable, these sources are not suitable for spectroscopic purposes.

Backward wave oscillators were mainly developed in the Soviet Union since the fifties of the 20th century. They are composed of electron-tubes placed in a strong magnetic field where an accelerated electron beam passes through a so-called slow-wave structure, creating a monochromatic THz radiation. It is possible to tune the frequency by changing the accelerating high voltage. To cover the whole THz spectral range, it is necessary to use several different oscillators and thus a wide-spectrum measurement can prove quite lengthy. The advantage is high resolution (the width of a frequency line is typically several units of MHz).

Quantum cascade lasers belong to the so far less applied sources, but also the most promising ones. They constitute optoelectronic components based on a series of alternating thin layers of semiconductors with larger and smaller band gap energies and with well-chosen thicknesses (on the nanoscale). Applying a suitable low voltage to such structures creates a cascade of radiation transitions. They cause moving electrons to lose their energy, and to emit photons in the THz region. Although the quantum cascade lasers operating in the infrared region are very reliable, they have a fundamental limitation in the THz region, which is the operating temperature of their components. If the thermal energy of particle oscillations is greater than the target photon energy (the room temperature corresponds to the energy of 26 meV, about 6.3 THz), the energy losses are increased to such an extent that no laser amplification is possible. So far it is therefore necessary to cool the THz quantum cascade lasers to low temperatures. If this limitation can be overcome in the future, these lasers will likely be used commercially, as they are very compact and their operation is simple.

One of the most versatile and most widely applied techniques in the THz region is the THz time-domain spectroscopy. It is a set of methods based on nonlinear conversion of energy from ultrashort laser pulses into the THz region. Their rapid development began around the early nineties, when the first THz semiconductor switch was developed. These methods enable relatively poor frequency resolution (maximum of units of GHz) and operate with low output (typically units of μW).

However, their advantages include namely the possibility of a simultaneous measurement over a wide spectral range, phase sensitivity of detection, and time domain measurement (possibility to distinguish reflections of pulses from individual interfaces). The time-domain THz spectroscopy methods are discussed in the following section. More detailed information can be found for example in the monograph [1].

6.3 Principles of THz time-domain spectroscopy

Most often, the THz time-domain spectroscopy uses transmittance measurements; the usual experimental arrangement is shown in Fig. 6.1. A sequence of ultrashort pulses is generated using a femtosecond laser (oscillator), usually a titanium-sapphire oscillator, which provides pulses with a wavelength of approximately 800 nm and duration of approx. 20–100 fs at a repetition rate of around 80 MHz. The beam is then split into two parts using a semitransparent beamsplitter, with the largest part of the output impacting the THz emitter (see below). The THz radiation is emitted in a pulsed mode, in forward direction, and the pulses have duration of approximately 1 ps.

Radiation pulses with a waveform $E_o(t)$ are focused using a metallic mirror into a focal point where the sample can be placed, and the pulses passed through the sample have a waveform $E(t)$. The radiation spreading farther is focused by a second mirror onto a sensor. The detection of THz electric field intensity requires that two pulses fall simultaneously onto a detection sensor – the terahertz pulse and the femtosecond laser pulse. The waveform of the THz field $E(t)$ is measured point by point; the length of one of the laser beam branches is changed for this purpose using an exactly positioned delay line (with a sliding mirror retroreflector). An electronic synchronous detection is typically used to increase the signal to noise ratio. It is also advantageous if the entire optical path of the THz beam is placed in a vacuum chamber, since, when the measurement is performed in ambient air, an absorption on the rotational lines of water vapor molecules occurs, which complicates the subsequent interpretation of the spectra.

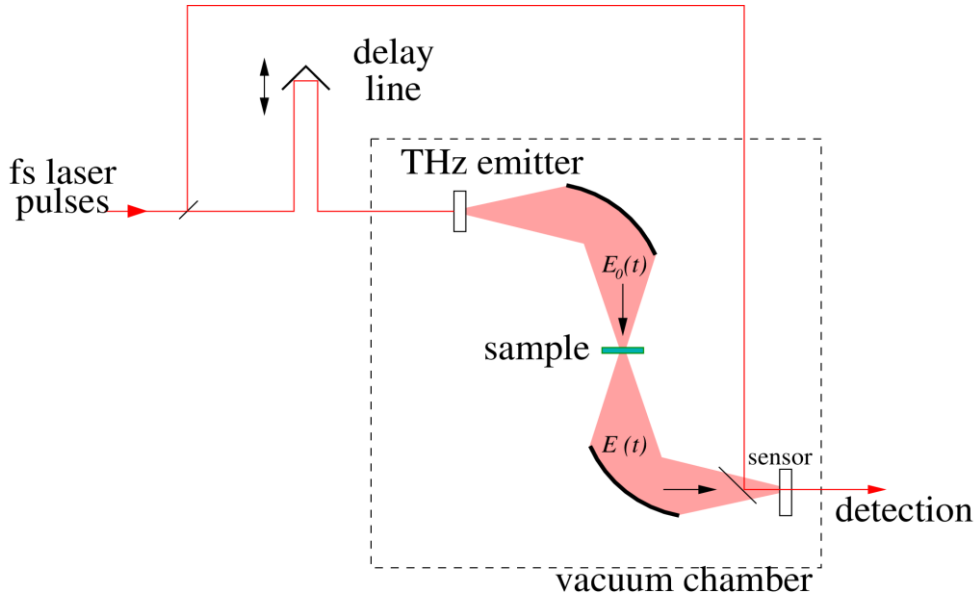


Figure 6.1. Typical experimental configuration for THz transmittance measurements.

6.3.1 Principle of THz pulse generation

The principle of THz pulse generation is schematically shown in Fig. 6.2a. The emitter consists of a thin plate made of a semiconductor with transversely applied DC voltage. In unlit state, the emitter has high resistance, therefore no current can pass through it.

If an ultrashort laser pulse comprising photons with energy higher than the band gap energy of the semiconductor impacts the emitter, free electron-hole pairs are generated near its surface. These are then immediately accelerated by the applied electric field into mutually opposite directions. The semiconductor material is fabricated in a way that the lifetime of these electric charge carriers is very short – usually less than 1 picosecond.

Thus, after the arrival of the femtosecond pulse, a very short current impulse occurs in the direction of the applied voltage, in the semiconductor. The THz pulse emitted by the accelerated charges has a shape corresponding approximately to one cycle of the electric field (Fig. 6.2b). The spatial emitting characteristic is closely related to the size of the laser beam, and in some cases a silicon lens is attached to the emitter for a better focusing of the THz beam.

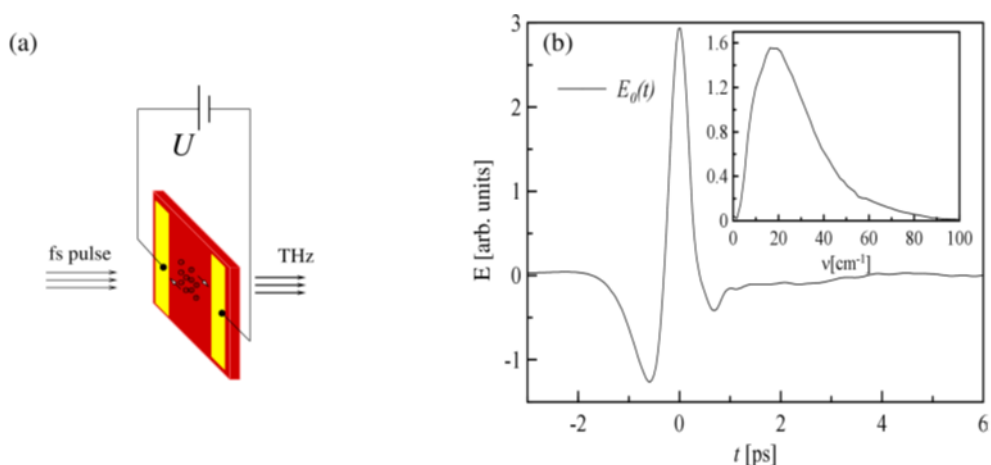


Figure 6.2. Principle of THz pulse generation. (a) function of a semi-conducting emitter, (b) typical time course of a THz pulse electric field (spectrum of an amplitude obtained by Fourier transformation of the curve $E_0(t)$).

6.3.2 Detection of THz pulses

As already mentioned, a great advantage of the THz time-domain spectroscopy is the possibility to use a phase-sensitive detection. In other words, while optical methods in the infrared, visible, and ultraviolet regions mainly use power detectors, in the THz region, it is possible to directly detect the intensity of the electric field E . Two different techniques can be used for this purpose. The common feature of both is that the THz pulse (with a duration of usually a few ps) and the optical (femtosecond) pulse simultaneously impact the detection element.

The first method is based on the use of a semiconductor receiver antenna, similar to the emitter shown in Fig. 6.2a. In this case, however, there is no bias voltage applied on the antenna. If an optical pulse impacts the antenna, free charge carriers are generated. If the THz pulse impacts the antenna during the short time period when the charge carriers move in the conduction band of the semiconductor, then the electric component $E(t)$ of the pulse, oriented in the direction t connecting the electrodes, accelerates the charge carriers. A small but easily detectable current with magnitude directly proportional to the output of the optical pulse and to the intensity of the THz field $E(t)$ then passes through the external circuit containing the antenna.

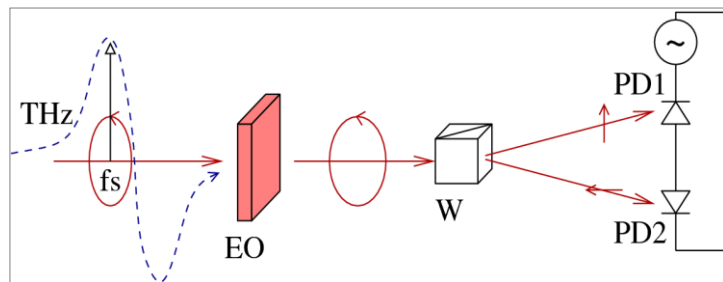


Figure 6.3. Principle of electrooptic detection of THz radiation. THz – propagating field $E(t)$; fs – femtosecond pulse with circular polarization; EO – electrooptic crystal (sensor); W – Wollaston prism; PD1,2 – detection photodiodes with a slow response (typically μs).

The second option (Fig. 6.3) is to use the electro-optic effect, also called the Pockels effect, during which a change in the polarization state of optical radiation occurs in a so-called non-linear environment (in a crystal, for example ZnTe), due to an applied electric field. The applied femtosecond pulses are always linearly polarized but can be easily converted to circularly polarized pulses. If these pulses impact an electro-optic crystal simultaneously with the THz pulse, their polarization changes to a slightly elliptical one, due to instantaneous value of the intensity of the electric (THz) field.

The size and the sign of the ellipticity are directly proportional to the size of the field E . Using a Wollaston prism, the optical beam can be split into a vertical and a horizontal component which have the same intensities in the absence of the THz field. The value of the THz field E at a given time point (i.e., for a given mutual position of the optical and THz beam) then corresponds to the voltage difference on the detection photodiodes. The $E(t)$ function is measured point by point in a wide range for different values of the delay t , corresponding to the shift of the delay line.

6.4 THz spectra measuring techniques and data processing

6.4.1 Transmittance measurements

Transmittance measurements belong to the most frequently used techniques in THz spectroscopy. A diaphragm is placed into the beam focal point, and two measurements are performed: $E_0(t)$ corresponding to the reference waveform and $E(t)$ carried out with the sample which has a shape of a homogeneous plane-parallel plate. Compared to measurement without a sample, the interaction of the THz pulse with the sample generally leads to a signal delay, its broadening in time and a

reduction of its amplitude. While a part of the pulse passes directly through the sample, reflections will occur on both its surfaces. The reflected pulses are propagating backwards, which leads to further multiple reflections. At every reflection, a part of the THz wave passes through the outer surface toward the detector (see Fig. 6.4).

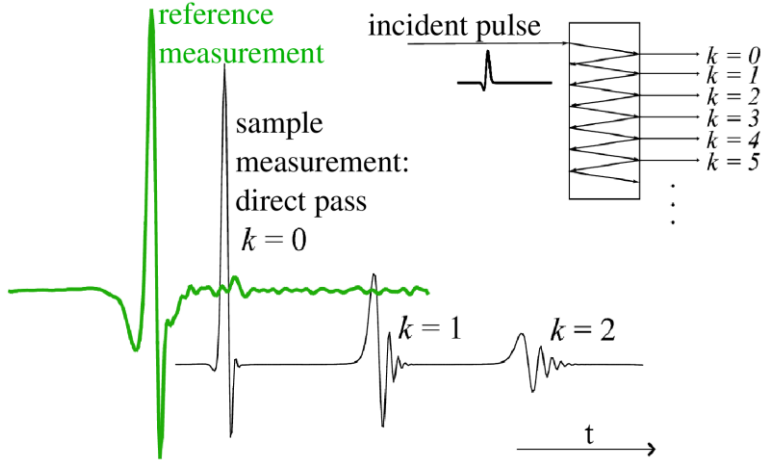


Figure 6.4. Interaction of THz radiation with a sample in a transmittance measurement. While the reference waveform contains a single pulse, multiple reflections on the sample surfaces appear as a sequence of pulses at regular intervals in the waveform $E(t)$.

Using Fourier transform, the two complex spectra are calculated, and their ratio yields the spectrum of a complex transmittance:

$$\hat{t}(\omega) = \frac{\mathcal{FT}(E(t))}{\mathcal{FT}(E_0(t))}$$

At the same time, the transmittance of a homogeneous plane-parallel plate is given by the relationship:

$$\hat{t}(\omega) = \frac{4N}{(N+1)^2} e^{i\omega(N-1)d/c} \sum_{k=0}^m \left[\left(\frac{N-1}{N+1} \right) e^{i\omega Nd/c} \right]^{2k}$$

where $N = n + i\kappa$ denotes the complex refractive index of the sample, d its thickness, c the speed of light, and m the number of measured reflections in the time domain. The task of finding the spectrum of a sample $N(\omega)$ from the experimentally measured transmittance $\hat{t}(\omega)$ must be solved numerically.

The permittivity (dielectric function) of the material can then be determined from the complex refractive index spectrum as:

$$\hat{\epsilon}(\omega) \equiv \epsilon'(\omega) + i\epsilon''(\omega) = \sqrt{N(\omega)}$$

The above-described procedure for evaluation of experimental data is straightforward and easily applicable to homogeneous solid samples.

The situation is somewhat different in the case of powder samples. Their measurement requires the use of cuvettes with parallel windows transparent in the THz region and a reference measurement performed with an empty cuvette. If the grain size is much smaller than the wavelength of the THz radiation, i.e., if the grains do not exceed several tens of microns, then the sample can be considered homogeneous. Obtaining of quantitatively correct THz spectra of a powder substance itself is however complicated by the fact that the sample behaves as an effective medium – a mixture of the substance with air. The measured refractive index is then determined not only by the properties of the solid phase, but also by the porosity of the sample, and also by the shape of the grains. Hence, if it is needed to determine the refractive index of the sample itself, it is necessary to use expressions describing the response of an effective medium. These expressions are always based on certain assumptions, corresponding to the specific microscopic arrangement of a mixture. These assumptions, however, are not always entirely valid in practice, and the choice of an appropriate mixture model can be difficult.

When measuring powdered substances with grain sizes comparable with the wavelength of the THz radiation (greater than approx. 50 μm), the quantitative evaluation of the spectra is practically impossible to perform, as scattering of the radiation passing through the sample plays a significant role, especially at higher frequencies. Even then, however, it is possible to identify in the spectra the absorption maxima, characteristic for the particular substance.

6.4.2 Reflectance measurements

In general, THz reflectance measurements of solid samples in the THz region are performed less often than the transmittance measurements, as the possibility to exactly determine the phase of a reflected radiation is critically dependent on a perfect reference measurement. This is very difficult compared to the transmittance geometry. In fact, the mirror replacing the sample in the reference measurement must not only show a perfect reflectance; at the same time, its surface must be in the same position as the surface of the measured substance, with an accuracy better than 1 μm [2]. Otherwise, the phase of the reflected radiation is increased by a phase

corresponding to free-space wave propagation at a small but unspecified distance, which impedes the determination of complex optical constants from the measured data.

Nevertheless, in certain cases, the phase sensitivity can be achieved also in the reflectance measurements. The simplest way is to place the sample behind a transparent window, where the reflection from its front side can serve as a reference signal, while the second interface includes also the measured sample, the spectrum of which can then be easily determined. This procedure is particularly suitable for measuring of liquids, which will perfectly adapt their shape to the surface of the window. By contrast, for both bulk and powdered solids, it is not easy to ensure their full contact with the window, and even a small air gap can cause significant errors in the measurement.

In practice, the reflectance measurements are mostly used in cases when it is sufficient to measure the reflected amplitude. An indisputable advantage of the method is its suitability for measuring of thick samples, where transmittance measurements would not be feasible.

6.4.3 Attenuated total reflection

Basics of the attenuated total reflection (ATR) method are described in the section 2.2.1.3, within the chapter on infrared spectroscopy. Also in the THz region, the advantage of the method is an easy sample preparation, as it suffices to place the sample on the reflective surface of the ATR prism. If the sample exhibits vibrational modes in the THz region, it is possible to identify them as absorption maxima in the ATR spectrum, which can then be unambiguously assigned to a particular substance.

Unlike the geometry for transmittance measurements, the common ATR method variant does not allow determination of complex spectra of optical constants. This can be achieved when the measured substance (a bulk sample or a tablet) is separated from the ATR prism, with a thin layer of air, the thickness of which is defined with micron accuracy and is gradually changed [3].

ATR spectra of powder samples can be obtained from amounts of less than 1 mg [4]. At the same time, however, it is necessary to ensure that the amount of the studied substance is not too small, as the penetration of the THz radiation $1/a$ rises towards low frequencies and, in the THz region with the longest wavelengths, it can reach hundreds of μm . To obtain spectra with visible absorption maxima and with

optimal contrast, it is necessary to use a sufficient compression force (of around 5 MPa [4]). At the same time, it is necessary to verify that the pressure does not result in changes of the structure of the studied substance.

Modules for the ATR measurements are offered among products supplied by commercial suppliers of THz spectrometers (e.g., TeraView company).

6.4.4 Time of flight measuring method

Thanks to high time resolution, the THz spectroscopy in reflectance mode can employ time of flight measuring method. The method utilizes the fact that every planar interface of two materials, with different refractive indexes, reflects a part of the radiation. The time of flight, for the reflected radiation, is longer for those parts of the pulse that penetrate deeper into the sample. The reflections from various interfaces can then be distinguished in the curves of electric field $E(t)$ waveforms, and the thickness of the respective layers (i.e., presence of interfaces) can then be determined from their positions in time.

6.4.5 Imaging measurement

All the aforementioned THz spectroscopy methods can be, in principle, performed in imaging arrangement. In this case, the radiation is spatially restricted by a relatively small diaphragm (minimum approx. 0.5 mm), the sample is mounted on a sliding table, and the spectra are recorded depending on its position. When a spatial resolution significantly better than 0.5 mm is needed, the use of smaller diaphragms would lead to a substantial signal decrease and to the prolongation of the measurement time. Therefore, in these cases, a special class of methods, called near-field imaging, is chosen.

6.5 Applications of THz spectroscopy in pharmacy

6.5.1 Identification of substances using THz spectra

Similarly as in the mid-infrared region, many crystalline substances show structured spectra, characteristic for the given chemical composition. In cases when the absorption of a substance is too high, and the sample transmits only very little of the radiation, it is suitable to use a powder mixture of the substance with grains of

polyethylene. After compaction of the mixture into tablets, it is appropriate to check, by using X-ray diffraction, that the compression did not adversely affect the crystal structure of the sample. Since the THz spectrum of polyethylene is flat, only absorption maxima of the studied substance will appear.

In principle, for samples prepared this way, it is possible to directly measure complex optical constants of the mixtures. However, the porosity of the sample, which leads to radiation scattering on the grains, may adversely influence the measured spectra, but this is usually neglected. The impact of porosity on the obtained data can be estimated for example by using Kramers-Kronig relations that allow to transform the real part of a complex refractive index to the imaginary part, and vice versa [5] and thus allow to verify the consistency of the spectra.

By contrast, in porous tablets with a known composition, the dependence of the refractive index on the air volume content can be used to determine their porosity, which may be directly linked to tensile strength of the sample. Measuring the tablet reflectance appears as the most appropriate method, allowing to map their surface refractive index which may be influenced for example by the compressive force in tablet production [6]. This may be important e.g., in tablets with a convex surface, as their tensile strength is not based on a well-known empirical dependence on the manufacturing compression force.

In many cases, the THz spectra also reflect crystal polymorphism of APIs (active pharmaceutical ingredients) [7] besides their chemical composition. A pilot study [8] has shown that THz spectroscopy can also be used for real-time monitoring of changes occurring in crystal structures. Transmission THz spectra of an active substance (Carbamazepine) were measured at 165 °C, for approximately 2 hours. After this period, a complete conversion of polymorphism has been detected. Due to good sensitivity of THz spectroscopy, and short acquisition time for each spectrum, it is possible to observe even significantly faster changes, occurring at the scale of minutes, or even tens of seconds.

It is known that vibrational modes of amorphous and crystalline substances are very different. This was experimentally proven in THz spectra, for example, of samples of crystalline and amorphous saccharides [9]. The absence of sharp vibrational modes that can be observed in crystalline form was later also confirmed in THz spectra of indomethacin [7]. A comparison of spectra of a complex refractive index of atorvastatin is shown in Fig. 6.5. Although the spectra of the crystalline phase do not contain any distinct vibrational bands, there is an obvious contrast between the spectra of the crystalline and the amorphous phases, respectively. It is evident that the differences in the real and the imaginary parts are much higher than the

experimental inaccuracies associated with grain size and deviations caused by imperfect compaction of powdered samples.

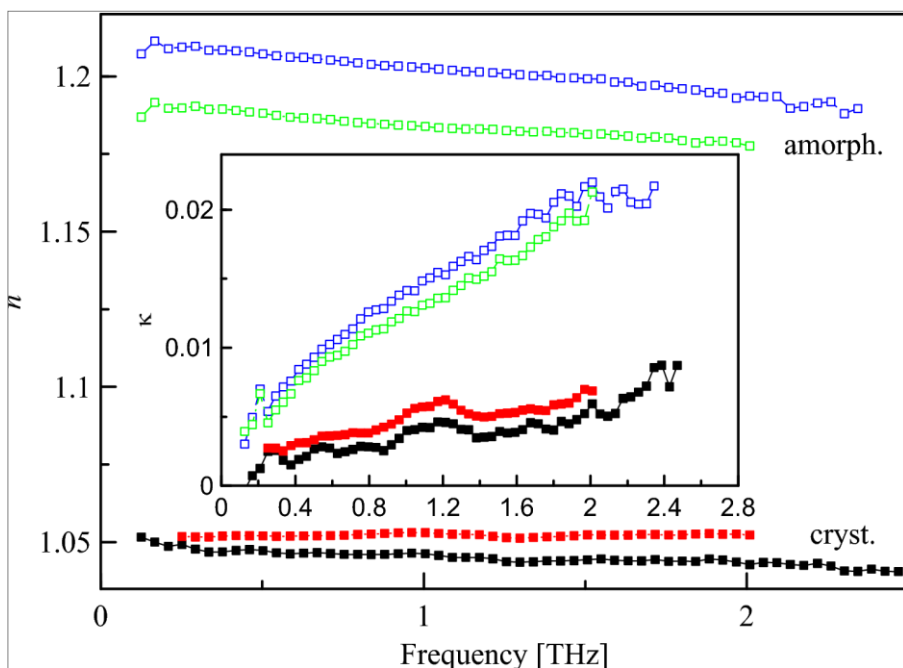


Figure 6.5. THz spectra of the complex refractive index of atorvastatin powder samples. Full symbols: crystalline phase, open symbols: amorphous phase. Measurements were performed in cuvettes, and with different grain sizes.

6.5.2 Determination of hydration state of substances

Interaction of the THz radiation with molecules of water is generally very strong. Furthermore, it is usually possible to clearly determine the phase of the water present, as the spectra are different in the case of water vapor molecules (very narrow bands), liquid water (broad absorption), or crystal water (which usually causes shifts of existing lines and changes in their intensity). Therefore, during the measurements, as mentioned above, the THz beam is usually enclosed in a space with controlled atmosphere, to eliminate the effects of ambient humidity.

In the liquid phase, water absorbs the THz radiation so strongly that for transmittance measurements of aqueous solutions, it is necessary to use special cells, where the optical path of the radiation passes through the solution with a

thickness not exceeding 100 μm . If a sufficient sample volume is available, it is possible to use for such measurements a special nozzle with freely flowing water [10].

Likewise, the presence of small quantities of water in solid samples is also very strongly apparent in THz spectra. Therefore, the THz spectroscopy is a very suitable method for determination of hydration state of samples [11]. It is suitable for analysis of raw active substances, as well as for monitoring of production processes, where it is possible to determine gradual changes in the drug water content.

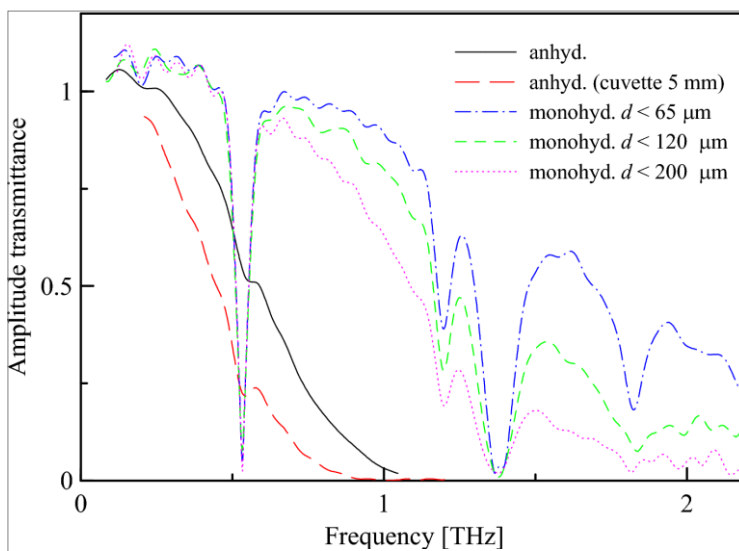


Figure 6.6. THz spectra of relative amplitude transmittance of powder lactose. Unless stated otherwise, the samples were placed in a cuvette with 2 mm thickness. Transmittance can exceed value of 1, since it is related to a spectrum of an empty cell, and inserting the studied substance reduces reflection losses at internal interfaces. The d variable denotes the grain size of the monohydrate.

An example of the difference between the spectra of anhydrous and hydrated substances is shown in Fig. 6.6. The spectra belong to powder lactose samples with different grain sizes. Two anhydrous samples and three monohydrate samples were measured. The spectra are visibly separated into two groups according to their water content. Within these groups, there are also differences based on some other factors – optical path length of the cuvette, and grain size (see section 6.5.4), but these are clearly smaller than the effect of hydration.

6.5.3 Determination of tablet coating thickness

An important parameter, ensuring a correct dissolution profile, is the thickness of coating, which is particularly important in tablets with sustained release. THz spectroscopy provides a non-destructive way of measuring of coating thickness, with the use of time-resolved detection of THz waves (time of flight of reflected radiation, see section 6.4.4). It is possible to detect the presence of hidden defects in the coating of a tablet that would be otherwise difficult to detect. A study was performed where coating thickness of separate tablets was measured [12], and the results could be partly linked to their dissolution performance. It was also proven that due to a relatively large penetration depth of the THz radiation, it is possible to analyze multilayer coatings [13] with this method.

Because of considerable time-demands of imaging measurements, the analyzes of this type that involve surface mapping are not suitable for production process monitoring. However, analysis of a small group of tablets with different parameters may help to optimize the production technology. By contrast, measuring of coating thickness in one point or small area can be very fast (< 100 ms), which, in principle, provides the potential for a technology of simplified control of coating thickness in the production process.

6.5.4 Determination of grain size

As already mentioned, for powder crystalline substances with grain sizes exceeding tens of μm , the scattering of THz radiation plays an important role, as it prevents accurate quantitative evaluation of the measured spectra. On the contrary, the average particle size can be determined based on the dependence of the intensity of scattering on particle size. Fig. 6.6 shows an example of spectra of the same substance, but with different grain sizes. The sample is lactose monohydrate, the transmittance of which is significantly dependent on grain size, especially in the region of higher THz frequencies where the radiation wavelength is comparable with the size of the grains. The scattering mechanism can be generally described using the Mie theory. In practice, however, it can be expected that this description will be usually difficult to use, as the shape of grains and their size distribution can be very varying. Therefore, the most appropriate approach seems to be a calibration of spectra for several known samples of a substance, enabling subsequent determination of the grain size of unknown samples, based on the calibration curves.

6.6 Resources and recommended literature

1. Terahertz Spectroscopy, Dexheimer S. L., (Ed.). Principles and Applications CRC Press: Boca Raton, USA, 2008.
2. Pashkin A., Kempa M., Němec H., Kadlec F., Kužel P. Phase-sensitive time-domain terahertz reflection spectroscopy, *Rev. Sci. Instr.* 2003, 74 (11), 4711–4717. <https://doi.org/10.1063/1.1614878>
3. Hirori H., Yamashita K., Nagai M., Tanaka K. Attenuated Total Reflection Spectroscopy in Time Domain Using Terahertz Coherent Pulses, *Jap. J. of Appl. Phys.* 2004, 43 (10A), L1287–L1289. <https://doi.org/10.1143/JJAP.43.L1287>
4. Newnham D. A., Taday P. F. Pulsed Terahertz Attenuated Total Reflection Spectroscopy, *Appl. Spectroscopy*. 2008, 62 (4), 394–398. <https://doi.org/10.1366/000370208784046731>
5. Tuononen H., Gornov E., Zeitler J. A., Aaltonen J., Peiponen K.-E. Using modified Kramers–Kronig relations to test transmission spectra of porous media in THz-TDS, *Opt. Lett.* 2010, 35 (5), 631–633. <https://doi.org/10.1364/OL.35.000631>
6. May R. K., Su K., Han L. H., Zhong S. C., Elliott J. A., Gladden L. F., Evans M., Shen Y. C., Zeitler J. A. Hardness and density distributions of pharmaceutical tablets measured by terahertz pulsed imaging, *J. Pharm. Sci.* 2013, 102 (7), 2179–2186. <https://doi.org/10.1002/jps.23560>
7. Strachan C. J., Rades T., Newnham D. A., Gordon K. C., Pepper M., Taday P. F. Using terahertz pulsed spectroscopy to study crystallinity of pharmaceutical materials, *Chem. Phys. Lett.* 2004, 390, 20–24. <https://doi.org/10.1016/j.cplett.2004.03.117>
8. Zeitler J. A., Newnham D. A., Taday P. F., Strachan C. J., Pepper M., Gordon K. C., Rades T. Temperature dependent terahertz pulsed spectroscopy of carbamazepine, *Thermochim. Acta.* 2005, 436, 71–77. <https://doi.org/10.1016/j.tca.2005.07.006>
9. Walther M., Fischer B. M., Jepsen P. U. Noncovalent intermolecular forces in polycrystalline and amorphous saccharides in the far infrared, *Chem. Phys.* 2003, 288, 261–288. [https://doi.org/10.1016/S0301-0104\(03\)00031-4](https://doi.org/10.1016/S0301-0104(03)00031-4)
10. Tauber M. J., Mathies R. A., Chen X., Bradforth S. E. Flowing liquid sample jet for resonance Raman and ultrafast optical spectroscopy, *Rev. Sci. Instr.* 2003, 74 (11), 4958–4960. <https://doi.org/10.1063/1.1614874>
11. Zeitler J. A., Kogermann K., Rantanen J., Rades T., Taday P. F., Pepper M., Aaltonen J., Strachan C. J. Drug hydrate systems and dehydration processes studied by terahertz pulsed spectroscopy, *Int. J. of Pharm.* 2007, 334, 78–84. <https://doi.org/10.1016/j.ijpharm.2006.10.027>

12. Spencer J. A., Gao Z., Moore T., Buhse L. F., Taday P. F., Newnham D. A., Shen Y., Portieri A., Husain A. Delayed Release Tablet Dissolution Related to Coating Thickness by Terahertz Pulsed Image Mapping, *Pharm. Technol.* 2007, 97, 1543–1550. <https://doi.org/10.1002/jps.21051>
13. Zeitler J. A., Shen Y., Baker C., Taday P. F., Pepper M., Rades T. Analysis of Coating Structures and Interfaces in Solid Oral Dosage Forms by Three Dimensional Terahertz Pulsed Imaging, *J. of Pharm. Sci.* 2006, 96 (2), 330–340. <https://doi.org/10.1002/jps.20789>

7 Mass spectrometry

Lukáš Plaček

7.1 Basic principles

Mass spectrometry (MS) is a physico-chemical method that uses separation of accelerated ionized particles (ions) based on their mass during their passage through a magnetic and an electric field in vacuum. The main processes occurring in the mass spectrometer are ionization of the analyte, separation of the resulting ions, and subsequent detection. It is a destructive but highly sensitive method with very low sample consumption. The method can be used for many purposes such as identification of unknown compounds, quantification of known compounds, structure determination of ions in a gas phase, and determination of physical and chemical properties of ions and molecules. The method is formally categorized as a spectral technique, although it does not belong to this category by definition. Spectral techniques observe interaction of radiation and matter and describe the energy differences between quantum states. MS was categorized as a spectral method only for the similarity of obtained records – mass spectra – and for similar application in structural analysis. The mass spectrometry is traditionally not a solid-state analysis method as most of the ionization techniques require a solubilized sample (sample preparation requirements are discussed separately for each ionization technique, see below). The solid-state analysis is now much easier with the newer, so-called ambient ionization techniques.

Mass spectra are usually displayed in a normalized form, which means that the most intense peak in the spectrum is assigned a 100% relative intensity and the intensities of other peaks are then normalized accordingly. Normalized form is used for both diagram and the tabular form which is mainly found in literature dealing with spectra of electron ionization (Fig. 7.1). Mass spectrum is a relationship between intensity and mass/charge ratio (m/z). The charge is equal to one, except for some cases such as electrospray ionization (ESI – explained below), which implies that the value on the x axis corresponds to molar mass.

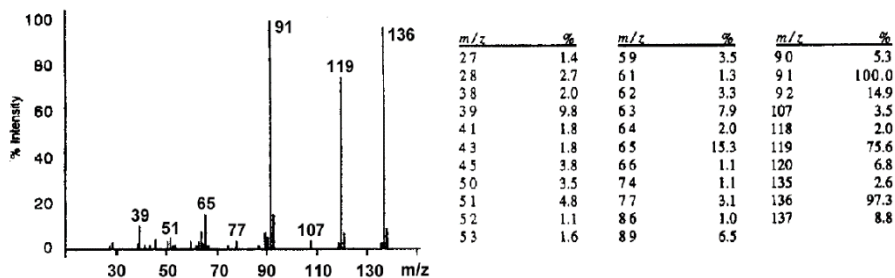


Figure 7.1. Record of a mass spectrum of *p*-methylbenzoic acid, obtained by electron ionization, with included table of intensities.

Mass spectrometer is an ion-optical device that consists of three main parts (Fig. 7.2), which are:

- ion source
- mass analyzer
- detector

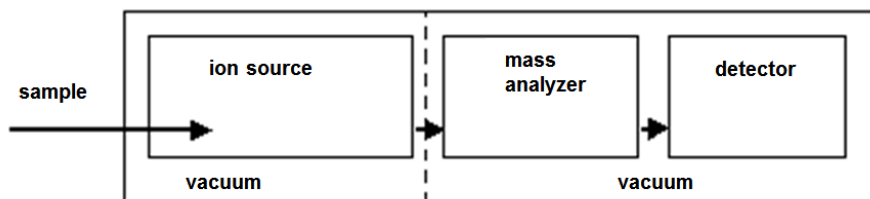


Figure 7.2. Scheme of a mass spectrometer.

Besides the main components, the operation of a spectrometer requires other parts. In case of direct measurements without a preceding separation technique, it is mainly the input system or a probe that serves as a device for injection of a sample into the ion source. Heated cartridges are used for both liquid and solid samples. In combination with separation techniques (GC-MS, HPLC-MS, CE-MS, etc., – explained below) special interfaces are used, according to the applied ionization technique. Another important part is a vacuum system since the separation of ions based on the m/z ratio in a gas phase is carried out under high vacuum (10^{-3} – 10^{-6} Pa, depending on the type of the analyzer). Ion cyclotron resonance – as the most demanding – needs even higher vacuum of about 10^{-7} – 10^{-9} Pa. Some ion sources also operate under vacuum (EI, CI, MALDI, etc., see below). The employed vacuum prevents collisions with neutral atoms and thus maintains ions with sufficiently long mean free path. Development of the combination of LC-MS

resulted in ionization techniques operating at atmospheric pressure (e.g., ESI, APCI, APPI – explained below).

The vacuum is created by a multistep pumping, using different types of vacuum pumps. The pumps can be generally divided into positive displacement, momentum transfer, and entrapment pumps. Positive displacement pumps include rotary vane pumps, diaphragm, and scroll pumps. Momentum transfer type includes diffusion pumps. Entrapment pumps include sorption pumps, cryopumps, etc. An important part of the vacuum system is a vacuummeter, which must have sufficient range, sensitivity, and minimal effect on the measured environment (temperature increase, formation of chemical compounds in discharges, etc.). Ionization gauge and thermal conductivity vacuummeters may be stated as an example. Ion optics for focusing and accelerating of ions are also indispensable, as is high-performance electronics and a control unit.

7.2 Ionization techniques

Ion source is used in a mass spectrometer to convert neutral analyte to charged particles (ions), which are subsequently separated by the mass analyzer. Ionization techniques can be divided into soft and hard techniques, according to the input energy, as shown in Fig. 7.3. Hard techniques form primarily molecular radical cations $M^{\bullet+}$ which are subjects to further fragmentation, due to large excess of internal molecular energy obtained within the ionization process. This may also result in an absent molecular ion in some cases.

Soft ionization techniques form only ions with even number of electrons. Because of ion-molecular reactions, these ions are, e.g., $[M+H]^+$, $[M+Na]^+$, $[M+NH_4]^+$, $[M-H]^-$ or others, depending on the particular ionization technique. Lack of structural information is compensated by collision-induced dissociation in the ion source, or by using MS^n techniques (tandem mass spectrometry). The ionization techniques can be approximately arranged according to their "hardness", = according to an excess of internal energy leading to fragmentation of ionized molecules, as follows: ESI < MALDI < TSI < FAB/FIB < APCI < CI < EI; individual abbreviations are explained further in the text.

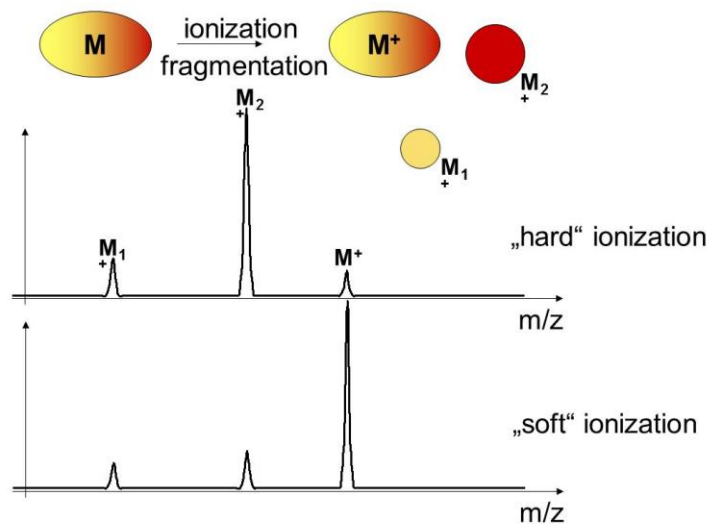


Figure 7.3. Soft and hard ionization.

Selection of an ionization technique (Fig. 7.4) depends on sample properties such as volatility, polarity, thermal stability, and molecular weight which is partly related to volatility. An important consideration for selection of an ionization technique is whether the sample is a single compound or a mixture. Polarity of the ionization techniques can be set by software. While negative ions are mainly provided by sulfonic and carboxylic acids, or also polyhydroxylated analytes, positive ions can be recorded for most substances.

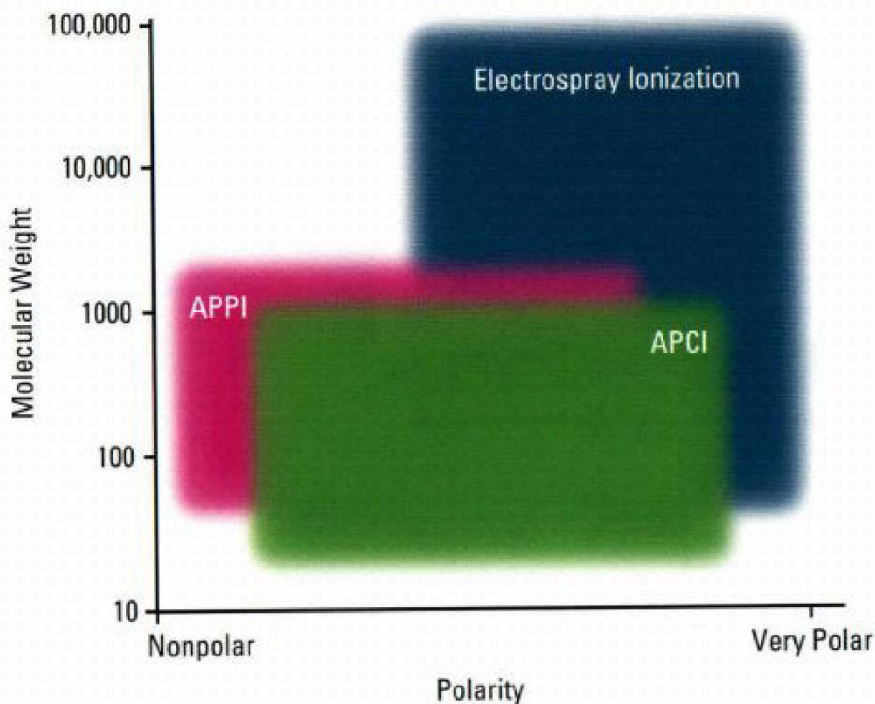


Figure 7.4. Application options for ionization techniques ESI, APCI and APPI depending on analytes.

(Source: <http://holcapek.upce.cz/teaching.htm>, 10. 12. 2009.)

7.2.1 Electron ionization (EI)

Electron ionization is the hardest and the oldest ionization technique. The requirement for measuring mass spectra with electron ionization is a sufficient sample volatility, and because the ionization occurs in gas phase at temperatures typically around 150–400 °C, also a sufficient thermostability. Heated cathode (W or Re filament) emits electrons which are detected at anode upon their passage through the ion source (Fig. 7.5). As the emitting electron approaches the valence electrons of a sample molecule, their magnetic fields are affected, which can lead to release of a valence electron and thus creation of a radical cation $M^{+\bullet}$. The created ions are expelled from the ion source by a repeller. The ion beam is then further focused and accelerated by other electrodes towards the analyzer. Accelerating potential between cathode and anode determines the energy of the electrons and is expressed in electronvolts. To be able to create libraries and compare MS spectra, it was necessary to choose an established and generally accepted value, and thus the accelerating energy of 70 eV was chosen. This provides highest sensitivity, but since the energy needed to ionize most organic compounds is between 7–16 eV, the

excessive internal energy leads to a massive fragmentation or eventually transformation and subsequent fragmentation of the molecule. Such spectra can be too complicated, but they carry valuable information about substance structure.

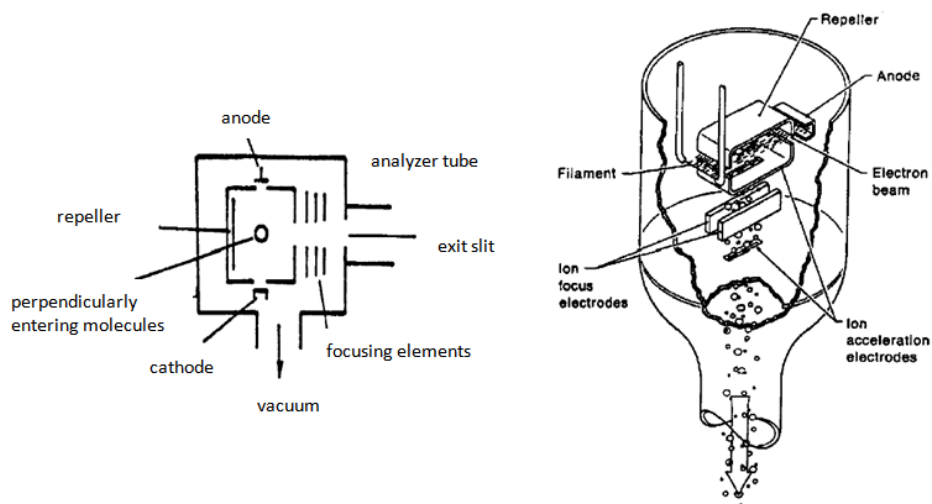


Figure 7.5. Scheme of an electron ionizer.

(Source: <http://holcapek.upce.cz/teaching.htm>, 10. 12. 2009.)

7.2.2 Chemical ionization (CI)

Chemical ionization was developed as an alternative to EI which is a very hard technique that causes strong fragmentation, making some substances impossible to identify. Design of a CI ion source is analogous to EI, and the analyte is also converted to gas phase. The source, however, contains a reaction gas which is present in excess amounts compared to the analyte, approximately 10000:1. Pressure, around 100 Pa must guarantee sufficient number of collisions. The ionizing electrons first ionize molecules of the reaction gas which then ionize the analyte molecules *via* ion-molecular reactions and form $[M+H]^+$ or $[M-H]^-$ ions. The reaction gas is often methane, isobutene, or ammonia. Examples of the reactions may be protonation, hydride abstraction, charge exchange, or condensation.

The examples in Fig. 7.6 and 7.7 show differences between the electron and the chemical ionization.

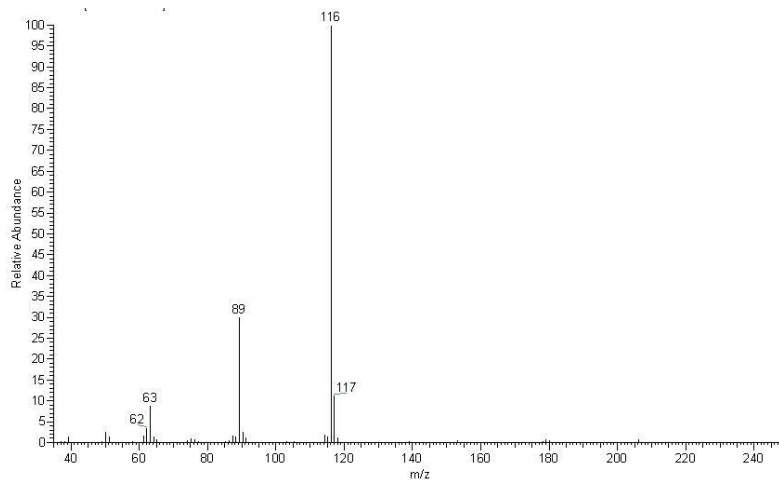


Figure 7.6. EI spectrum of 2-bromo-2-phenylacetonitrile; molecular M^+ ion is missing in the spectrum.

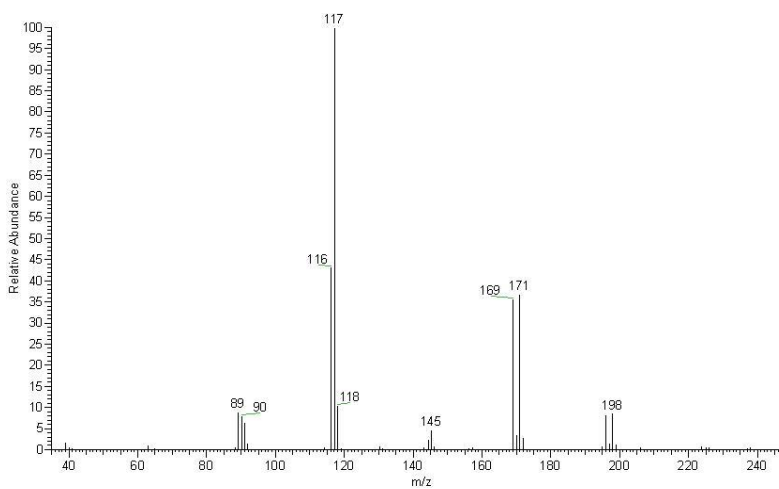


Figure 7.7. CI (methane) spectrum of 2-bromo-2-phenylacetonitrile; $[M+H]^+$ ions 196 of ^{79}Br isotope and 198 of ^{81}Br isotope are present in the spectrum.

7.2.3 Fast atom or ion bombardment ionization (FAB, FIB)

These two techniques are very similar to each other in their principle, application, sample preparation, and acquired results, and differ only in the presence or absence of a charge of the bombarding particles. FAB (fast atom bombardment) uses high-energy, neutral molecules of rare gases, usually argon or xenon, in a viscous matrix which extends the life of the resulting ions. The matrix must meet some specific requirements. The sample must be soluble in the chosen matrix, the matrix should have low volatility, and should be chemically inert to the analyzed samples. It is also important that the ions coming from the matrix do not have the same m/z values as the analyte ions. The most used matrices are glycerol, thioglycerol, and triethylamine. Nevertheless, other special matrices, such as liquid metals (Ga, In), can be employed. Accelerated atoms are obtained using a so-called ion cannon. First, the atoms are ionized by electron ionization and then accelerated by voltage of around 8–10 kV.

The accelerated ions are then introduced into a chamber with high pressure, where they collide with neutral atoms. The charge exchange does not cause loss in kinetic energy, which results in a stream of high-energy accelerated atoms. These are led onto a target with the sample placed in the matrix. Charged particles cannot get into the ion source as they are diverted by an electrode. In the case of FIB (fast ion bombardment), accelerated Cs^+ ions are used most often. Their formation can be described as follows. Alkali aluminosilicates are heated to about 1000 °C, triggering a thermal desorption of ions from surface. The resulting ions are then accelerated by an electric field and focused onto a target with the sample placed in a matrix.

7.2.4 Matrix assisted laser desorption/ionization (MALDI)

MALDI (Fig. 7.8), is one of the softest ionization techniques, which enabled mass spectrometry analysis of such molecules as peptides, proteins, oligonucleotides, nucleic acids, and biopolymers, up to $\text{MR} \approx 10^6$, triggering a rapid development in the field of biochemistry. The sample is first dissolved, mixed with a suitable matrix, and finally deprived of the solvent. Its surface is then bombarded under vacuum by short laser pulses lasting in orders of nanoseconds or microseconds at maximum. Energy absorbed by the matrix is then transferred on analyte and causes ionization, desorption of sample ions, and ion-molecular reactions. It is a pulsed ionization technique which is most often associated with time of flight analyzer (TOF).

UV lasers such as 337 nm nitrogen laser, 355 nm Nd:YAG, less frequently IR 2.94 μm Er:YAG, are the most common sources of laser pulses. Matrix choice considerably affects the quality of ionization as the matrix must absorb the

wavelength of the laser and must form the desired crystal with the analyte. Furthermore, the matrix must be sufficiently stable, non-reactive with the analyte, and not very volatile. The most commonly used matrices are organic aromatic carboxylic acids, e.g., dihydroxybenzoic acid, cinnamic acid, etc. Sample preparation also plays a key role, with several methods that have been developed. Samples are prepared on targets which can be stored for a long time.

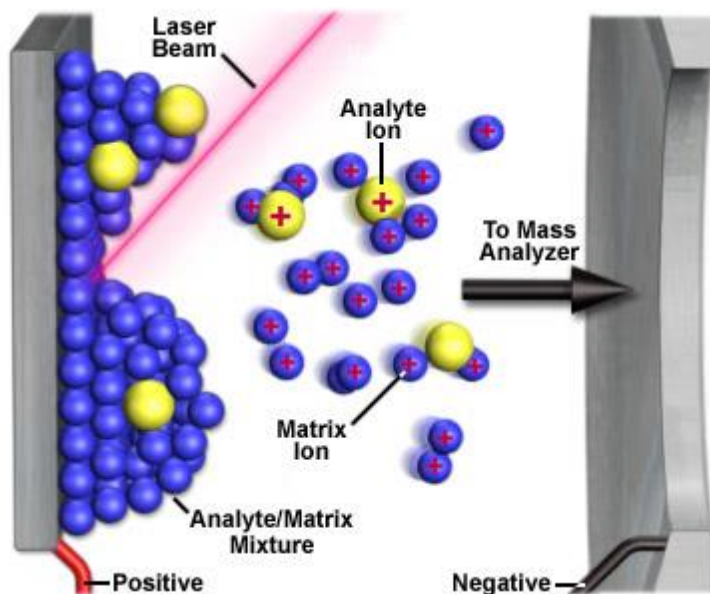


Figure 7.8. Matrix assisted laser desorption/ionization – MALDI.

(Source: <http://www.magnet.fsu.edu/education/tutorials/tools/images/ionization-maldi.jpg>, 7. 1. 2008.)

7.2.5 Thermospray ionization (TSI)

TSI (thermospray ionization) was the first ionization technique developed for the HPLC-MS connection but is now receding. It can be used with flow rates reaching 1 ml/min and with mobile phases having high water content. Since it is a very soft technique, fragmentation occurs only very rarely, and most ions have an even electron number. Analyte dissolved in a suitable solvent is brought *via* metal capillary into the ion source. The capillary end is heated in a thermostat to 150–300 °C, triggering a partial evaporation of the solvent in the capillary and thus creating a supersonic flow of the solvent vapors and small droplets containing the analyzed substance. Evaporation of the solvent from the surface of the droplets decreases their surface area and volume and increases their surface charge density. When the charge density reaches a critical limit, it causes a so-called Coulomb explosion, i.e., shattering of the charged droplet into a number of smaller droplets also with a

charge. This is repeated until the droplets are small enough to enable desorption of protonated or deprotonated molecules from their surface. This effect is called ion evaporation. Temperature of the heated capillary depends on the volatility of the analyzed compound, mobile phase flow, and the solvents applied. Therefore, for increased water content, it is necessary to use a higher temperature. An overall optimization is necessary, but in theory TSI can be used for any molecule that is present in the form of ions when already in the solution. TSI is generally not suitable for low-polar substances and large molecules.

7.2.6 Electrospray ionization (ESI)

ESI (electrospray ionization) is currently the most applied ionization technique for the HPLC-MS connection, which is due to its compatibility with a wide range of chromatographical conditions. It is suitable for moderately polar to ionic compounds with low- to high-molecular mass. It is considered the softest technique and is therefore preferably used also in analysis of thermolabile substances and biopolymers. An analyte, dissolved in a suitable solvent, is brought to the ion source *via* a metal capillary with high voltage of 3–5 kV. As a result, the created droplets possess a high number of charges after they are sprayed at the end of the capillary (Fig. 7.9). Dispersion of the eluate is maintained by coaxial inflow of nitrogen gas, serving as a nebulization gas. Afterwards, the solvent evaporation causes Coulomb explosion as in TSI. Evaporation of droplets and ion formation are facilitated by formation of small starting droplets. Therefore, mobile phases with high surface tension and/or high viscosity are not suitable. The droplets created by this method carry high number of charges on their surface, which enables formation of ions with multiple charges, currently used in analysis of biopolymers (large value of z allows display in a smaller m/z range). Fig. 7.10 and 7.11 show examples of ESI spectra.

ESI in HPLC-MS connection use flow rates reaching 1 ml/min. With such high flow rates, a flow divider is used to decrease the amount of eluent entering the ionizer. Inflowing liquid is split into two flows according to pressure resistance ratios of both flows. Therefore, microcolumn or capillary HPLC are ideal for connection with ESI, as their flow rates are consistent with the optimal flow rates for ESI. Moreover, in this case there is no sensitivity reduction as with the flow divider. There is also a special ESI modification, without the nebulizing gas and with lower temperature of the drying gas, called nanoelectrospray. Mobile phase flow rates range from units to hundreds of nl/min, in this method. The nanoelectrospray uses a specially adjusted end of the spraying capillary. Extremely low sample consumption allows *in vivo* experiments. This method has very high sensitivity (concentrations in orders of attomoles and zeptomoles, i.e., only hundreds of molecules). Nanoelectrospray is more tolerant to salt content in the

sample, reducing the requirements for sample preparation. The disadvantages are high experimental demands, and low robustness.

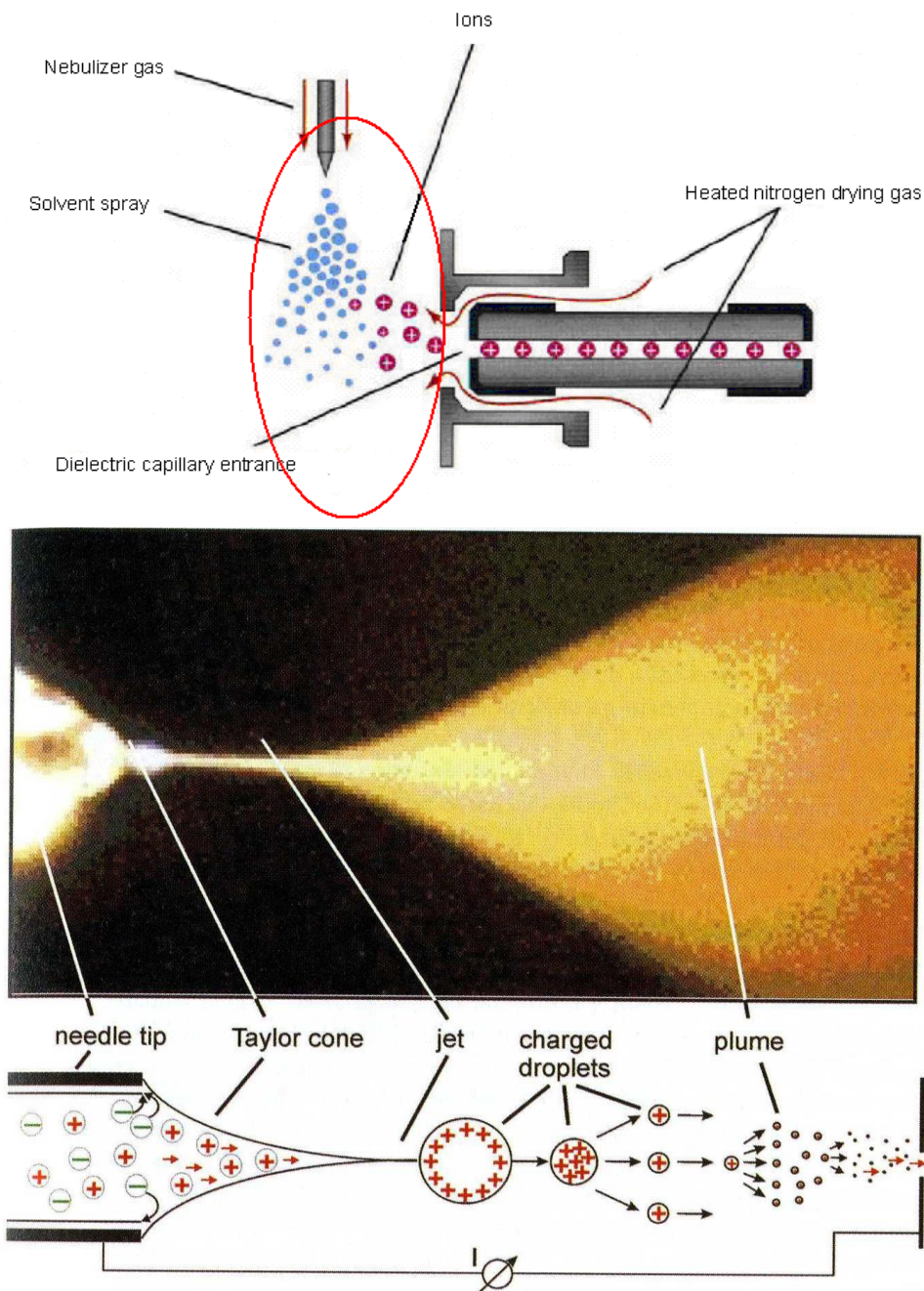


Figure 7.9. Scheme of an electrospray.

(Edited according to: Schalley C. A. *Analytical Methods in Supramolecular Chemistry*. Wiley-VCH, 2006., and <http://holcapek.upce.cz/teaching.htm>, 10. 12. 2009.)

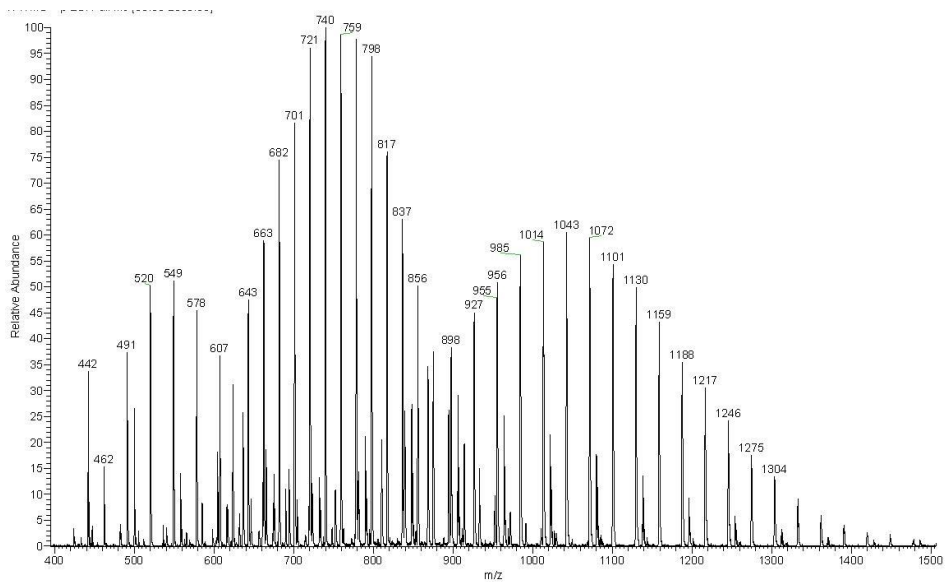


Figure 7.10. ESI spectrum of polypropylene glycol in positive mode.

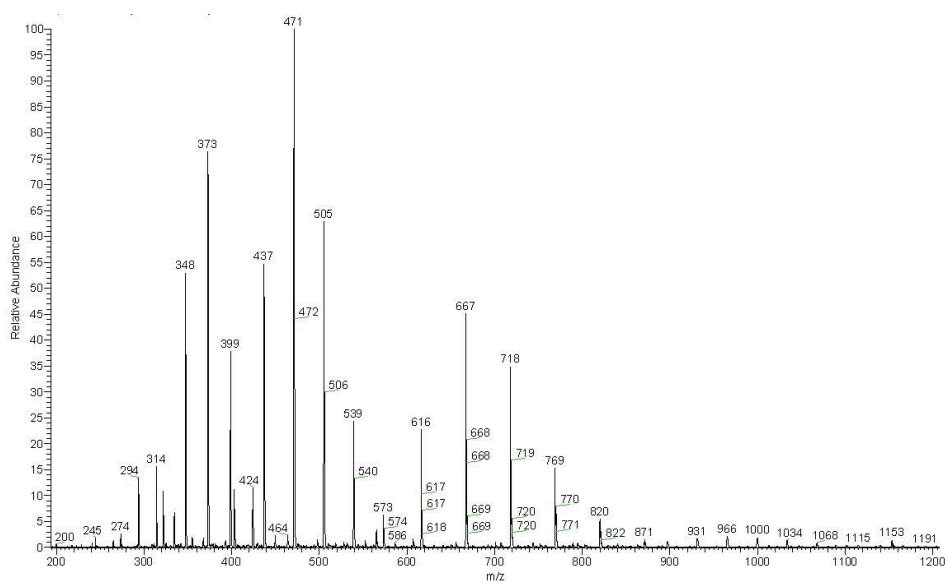


Figure 7.11. ESI spectrum of a highly sulfated α -cyclodextrin in negative mode.

7.2.7 Atmospheric pressure chemical ionization (APCI)

APCI (atmospheric pressure chemical ionization) is currently one of the standard ionization techniques for the HPLC-MS. It is a gentle technique, except for certain very unstable molecules. Electrode is placed near a heated column end and has a high voltage pulse input of 3–4 kV, resulting in corona discharge which first ionizes molecules of the mobile phase, because of their great abundance. The subsequent ion-molecular reactions cause ionization of the analyte molecules. Counter-current of drying gas, usually nitrogen, is used in a heated chamber to evaporate the carrier liquid and to break any non-covalent clusters and associates. This technique is not suitable for ionic and low volatility substances. Due to its suitability for ionization of medium- and low-polar compounds, it is *de facto* a complementary technique to ESI. It may be used with flow rates of up to 2 ml/min that is directly compatible with conventional HPLC columns. It is tolerant to the presence of buffers in mobile phases and to changes in experimental conditions including gradient elution. Its limitation is the impossibility of use at very low flow rates. A scheme of the interconnection between HPLC and MS detector is shown in Fig. 7.12, and an example of a spectrum is given in Fig. 7.13.

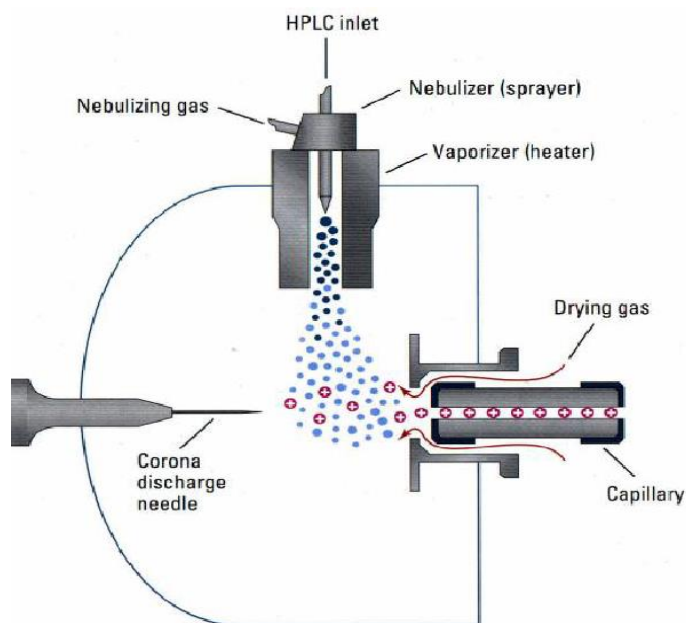


Figure 7.12. Scheme of the interface of atmospheric pressure chemical ionization.

(Source: <http://holcapek.upce.cz/teaching.htm>, 10. 12. 2009.)

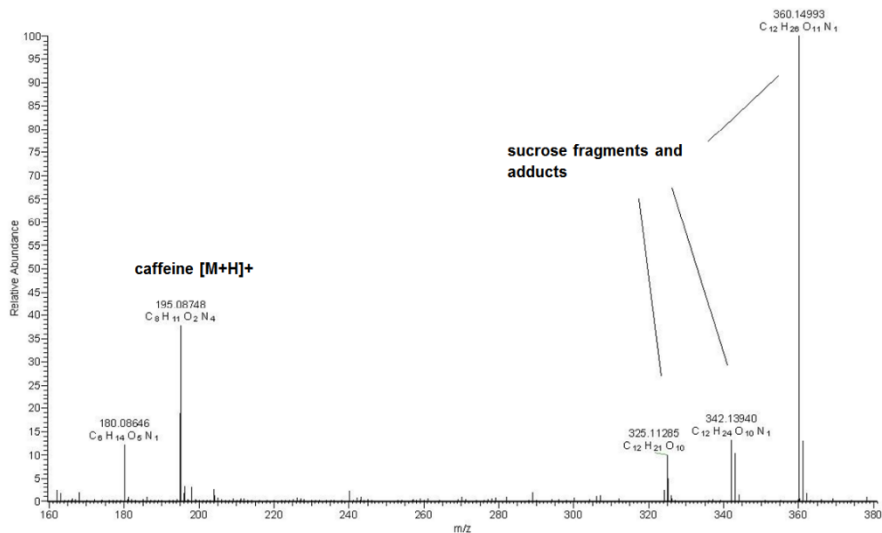


Figure 7.13. APCI spectrum of coffee with sugar.

7.2.8 Atmospheric pressure photoionization (APPI)

APPI (atmospheric pressure photoionization) is analogous to APCI, with the only difference of ultraviolet radiation used instead of corona discharge (Fig. 7.14). The source of UV radiation is usually a krypton lamp with photon energies of 10 or 10.6 eV. This energy is higher than ionization energies of most organic molecules, but lower than the energy needed to ionize atmospheric oxygen or molecules of a mobile phase such as acetonitrile, methanol, or water. This enables selective ionization of the analyte. Unlike in APCI and ESI, there may emerge ions with an odd number of electrons, which can complicate the interpretation. Thus, it is preferable to use dopant, which is usually toluene or benzene, or methoxybenzene for RP-HPLC for nonpolar substances. Dopant is a substance with ionization energy of less than 10 eV. Dopant molecules react by ion-molecular reactions with the analyte but not with the mobile phase, which increases sensitivity. Combined alternative APCI/APPI ion sources are now commonly used.

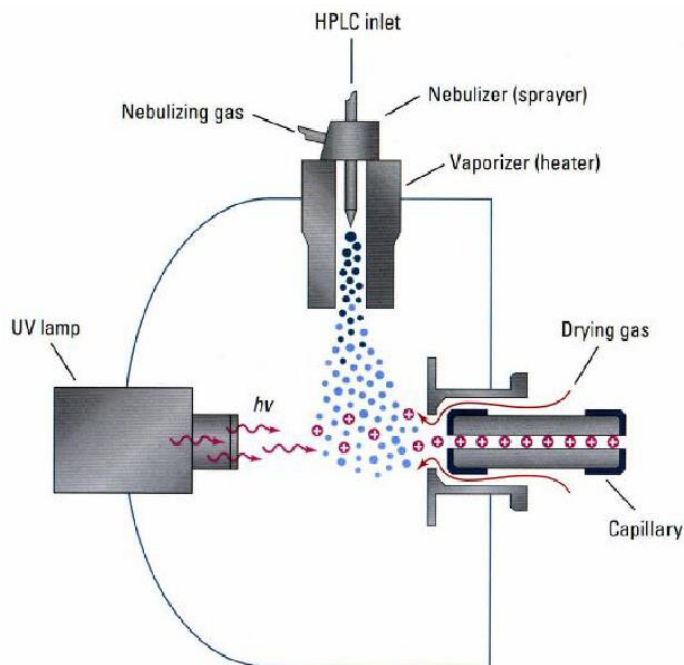


Figure 7.14. Scheme for interface of atmospheric pressure photoionization.

(Source: <http://holcapek.upce.cz/teaching.htm>, 10. 12. 2009.)

7.2.9 New ionization techniques

With the expansion of mass spectrometry in biological disciplines during the last years, there are growing demands for minimum preparation and treatment of native samples. This led to a development of *ambient* ionization techniques where the surface of often untreated sample is exposed to desorption medium under laboratory conditions. The ambient techniques are undergoing a turbulent evolution, and the unnecessary for sample preparation means that MS can now be more widely used for a solid-state analysis. Some of the commercial ambient techniques are listed below, while many others are currently in development:

- ionized spray in the case of electrospray desorption ionization (DESI)
- current of charged gas in the case of direct analysis in real time (DART)
- charged agent produced by nano-electrospray in Super Secondary electrospray ionization (SESI)
- nano ESI

Ions desorbed by these methods are then led to the analyzer (Fig. 7.15).

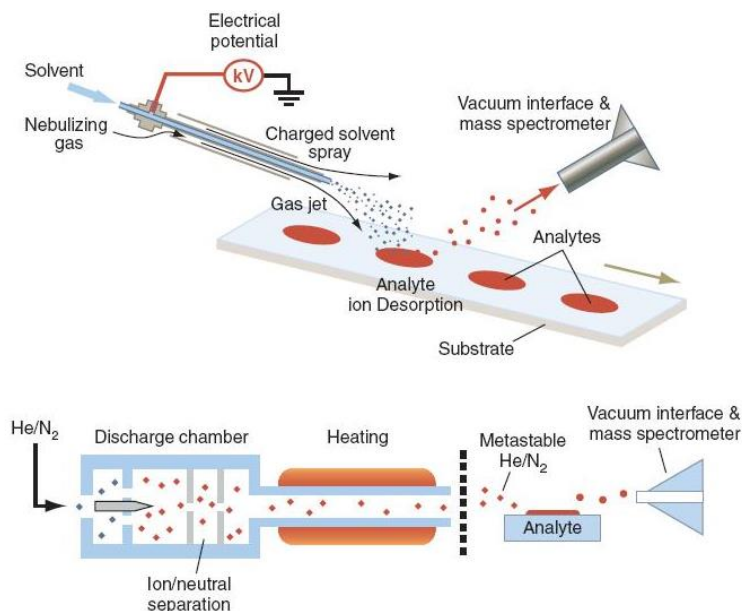


Figure 7.15. Principle of DESI (upper part) and DART ionization (lower part).

(Source: Cooks R. G. et al. *Science*, 2006.)

7.3 Mass analyzers

A mass analyzer separates ions according to m/z ratio. It is located behind the ion source so the incoming molecules are already converted into ions. The ions can be separated based on their m/z according to several physical principles:

- flight trajectory bending in magnetic or electric field
- different oscillation stabilities of ions in two- or three-dimensional combination of DC and high-frequency AC voltage
- different time of flight in an area without a field
- different energy absorption during cycloidal movement of ions in combined magnetic and electric field

An important parameter for evaluation of analyzer properties is mass resolving power (RP) which is expressed as a ratio of mass of ion m_1 and the difference in mass of ions m_1 and m_2 which have a unit charge, while the peaks of both ions are equally high and the gap between the peaks is 10%.

$$RP = \frac{m_1}{(m_1 - m_2)}$$

An alternative definition of RP applies especially for quadrupoles and ion traps – a ratio of ion mass m and the width of the peak of this ion Δm at its mid height.

$$RP = \frac{m}{\Delta m}$$

Analyzer type significantly affects both the quality of acquired mass spectra and the price of the mass spectrometer. High-resolution spectra obtained by sector analyzer with double ion focustion or by a spectrometer with ion-cyclotron resonance allow to determine elemental composition. On the other hand, low-resolution spectra only allow resolution of ions differing at most by a unit of m/z . Several basic types of analyzers can be distinguished, but there are also hybrid devices that use combinations of different types of analyzers. Examples of spectra of a single compound obtained by various types of analyzers are provided in Fig. 7.16.

7.3.1 Magnetic analyzer with simple magnetic focusing

This type of analyzers operates on the principle of bending the flight path of ions which pass through magnetic field. Positive ions with a certain value of m/z are accelerated by a negative potential V and enter the magnetic field with magnetic induction B , which results in bending the ion trajectory to a trajectory with a certain radius r . Stronger trajectory bending occurs for ions with lower m/z value as heavier ions have greater inertia and their trajectory is bent less. A continuous change, i.e., scanning of B (magnetic scan) or V (potential scan) at a constant radius given for the particular device forces all the ions to pass successively through the exit slot and continue to the detector where the intensities of the ions with specific m/z are recorded, resulting in a mass spectrum.

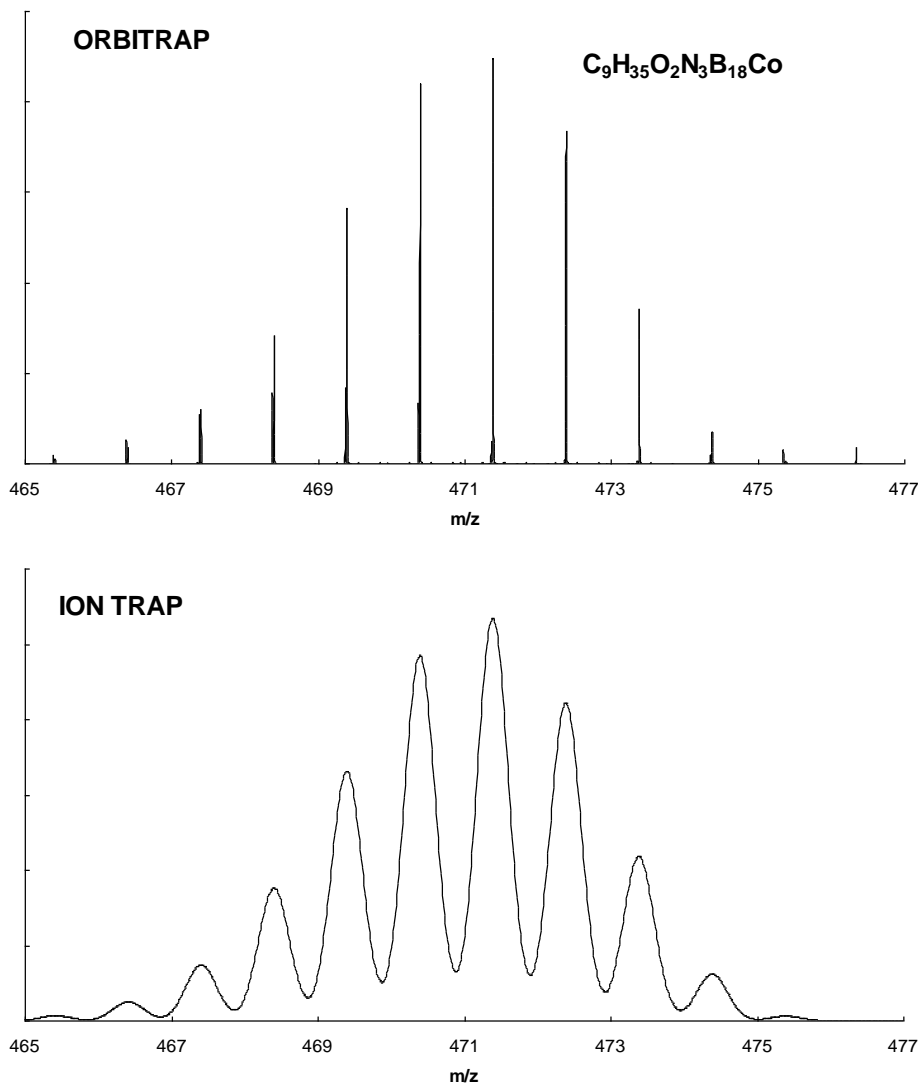


Figure 7.16. Comparison of resolution capabilities of Orbitrap and Ion trap demonstrated on mass spectrum of a cobalt-boron cluster.

7.3.2 Sector analyzer with double ion focusing

Sector analyzer with double ion focusing works on a similar principle as the previous analyzer. In addition to the magnetic focusing, it also features electrostatic focusing which significantly increases RP. If ions with different E_k and m/z enter an electric field, their paths bend according to their E_k , regardless of m/z . Since ions generated in the ion source have a certain energy distribution, explaining the width

of the obtained peaks, it is necessary to energetically unite the ions to achieve a greater resolution. This can be achieved by an electric analyzer which yields a mono-energetic beam. The combination of magnetic and electric ion focusing can achieve RP above 10^5 . There are four basic types of geometric arrangement of the magnetic and the electric focusing in sector analyzers: according to Mattauch and Herzog, Nier and Johnson, Matsuda, and inverse geometry. The advantage of this type of analyzers is the possibility of high-energy activation and especially the possibility of measuring also the so-called metastable ions. These are ions with lifetime around 10^{-4} – 10^{-6} s, which means that they break down on their way between the ion source and the detector. Their presence causes formation of broad diffuse peaks at non-whole m/z values. Their detection is important because it enables to study the fragmentation pathways.

7.3.3 Quadrupole (Q)

Quadrupole analyzer consists of four identical metal rods of circular or better hyperbolic cross-section shape, 20–30 cm long. Two opposite bars have a positive DC voltage U applied and the two other bars have a negative DC voltage U applied. All four bars are then superimposed with high-frequency AC voltage V (Fig. 7.17). An ion introduced into the center of the axis of the quadrupole begins to oscillate. At a certain time and a certain U/V ratio, the oscillations are stable only for ion with a particular value of m/z . Only this ion passes through the quadrupole and reaches the detector. All other ions are captured on the quadrupole bars. Continuous change – scanning – of the ratio of DC voltage and AC voltage amplitude U/V allows for successive release of all ions into the detector, being a mass filter by its nature. For maximum RP, the ideal cross-section of bars is hyperbolic. At the same time, higher sensitivity can be achieved by reducing the range. Quadrupole is a simple and relatively inexpensive mass analyzer which has become widespread also for GC-MS and HPLC-MS combinations.

7.3.4 Triple quadrupole analyzer (QqQ)

The triple quadrupole analyzer is probably the most commonly used MS/MS instrument. It consists of three quadrupoles arranged in a line where the middle one (q) serves as a collision cell. The first quadrupole serves for isolation, the second for dissociation, and the third for analysis of the resulting fragments. Introduction of a collision gas into the second quadrupole causes a collision activation of ions selected by the first quadrupole, and their subsequent fragmentation. Unlike in ion trap, this method can lead to repeated activated collisions, which means that it is possible to observe more fragmented ions than in MS/MS measurements performed

with ion traps. Triple quadrupole also allows measurements of precursor scans and neutral loss scans. MS^3 measurements would require connecting of five quadrupoles (QqQqQ), which is used very rarely. For high resolution MS measurements, it is usually better to connect ion trap or cyclotron resonance with Fourier transform.

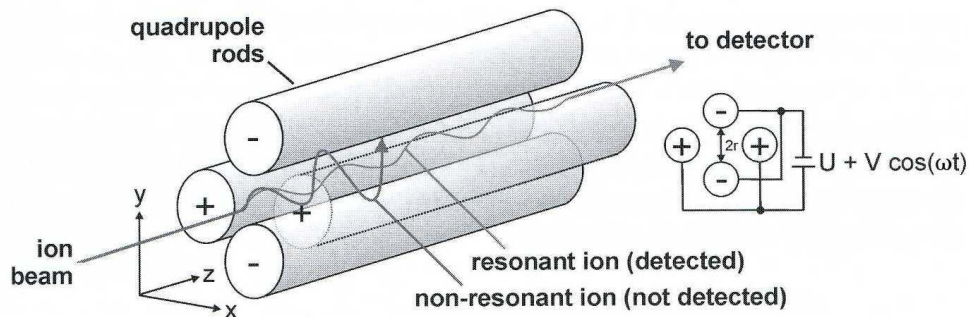


Figure 7.17. Scheme of a quadrupole analyzer.

(Source: Hillenkamp F. et al. *MALDI MS: A practical Guide to Instrumentation, Methods and Applications*. Wiley-VCH, 2007.)

7.3.5 Ion trap (IT)

Spherical 3D ion trap is composed of two end cap cylindrical electrodes and a central ring electrode, as schematically depicted in Fig. 7.18. Ions are delivered into the trap by a short voltage pulse through an inlet opening of the end cap electrode. Here, they are captured and successively expelled towards the detector according to their m/z . It is possible to use external ionization (ESI, APCI), as well as internal ionization in the ion trap. Accumulation times for ion capturing range approximately from 10 μs to 200 ms, depending on the amount of the introduced ions. Time of excitation and collisions in the trap is around 20–60 ms. The ions are retained inside the ion trap by using appropriate ratios of DC and AC voltage applied on the ring and the end cap electrodes. The ions are forced to move inside the ion trap in closed orbits. With gradually increasing voltage amplitude, the ions with increasing m/z get to unstable trajectories and leave the ion trap through an outlet towards the detector. Helium is introduced into the trap as a dumping gas at a pressure of around $5 \cdot 10^{-2}$ Pa to moderate unwanted oscillations and resulting in a significant increase in RP and improved ion capture. The number of ions let into the trap must be regulated because trap overfilling may lead to a discharge known as a “space charge”, which results in worse resolution and sensitivity. Ion traps can perform tandem mass spectrometry without any other connected analyzer. Selected precursor ion is retained in the trap and all other ions are expelled. This leads to collision activation with helium atoms present in the trap and thus also to ion fragmentation. Subsequently, an MS/MS spectrum is recorded. The same procedure

can be repeated many times, but in reality, it is limited by lifetime of the ions and sensitivity. It is practically used up to MS^5 , which is entirely sufficient for structural analysis. The process is of course fully automated. Ion trap often yields only one step fragmentations, i.e., the spectrum contains less fragments, which simplifies interpretation. On the other hand, fragment ions may be missing in the low molecular region, called "cut-off", in one-third of the m/z of the precursor ion.

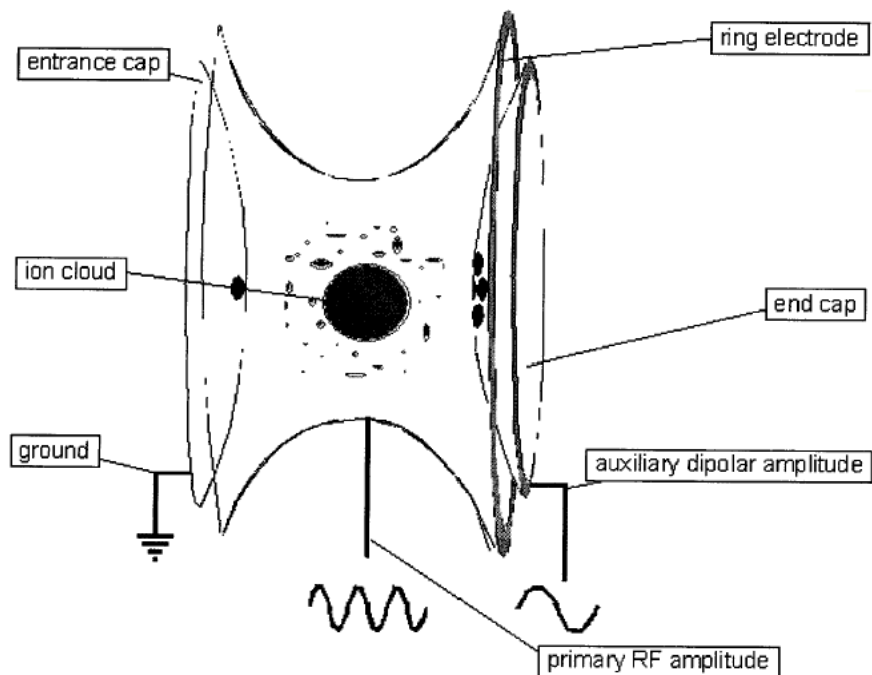


Figure 7.18. Scheme of an ion trap.

(Source: <http://holcapek.upce.cz/teaching.htm>, 10. 12. 2009.)

7.3.6 Linear ion trap (LIT)

LIT (linear ion trap) consists of four parabolic bars, similarly as quadrupole, which are however divided into three parts – front, center, and back (Fig. 7.19). These parts with appropriately selected DC and AC voltages are analogous to cylindrical end cap and ring electrodes in the 3D trap. During scanning, the ions in unstable states are expelled from the trap through slots which are parts of two opposite bars of the central part of the trap. The advantages over 3D trap are obvious: because of its length, the linear trap excels in better ion entrapment (about 70% of the injected ions are stabilized in the trap compared to 30% in 3D) and higher sensitivity, because of the presence of two exit slots and two ion detectors.

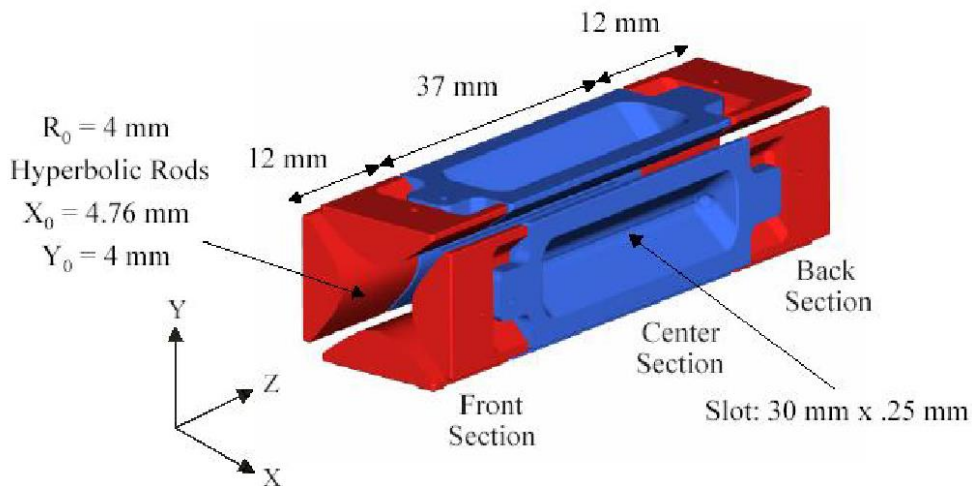


Figure 7.19. Scheme of a linear ion trap.

(Source: <http://holcapek.upce.cz/teaching.htm>, 10. 12. 2009.)

7.3.7 Orbitrap

Orbitrap is a type of analyzer somewhere between ion trap and ion cyclotron resonance. Ions with different m/z values rotate around a central asymmetric electrode that is placed in an inhomogeneous electric field which forces the ions not only to circle, but also to oscillate. The frequency of oscillation is proportional to the ratio of mass and charge of the given ion. Oscillating ions induce alternating current in the external electrodes, and this current is then further amplified and digitized. Dependence of the passage of the ions through the left and the right part of the orbitrap on time is recorded as an electric current. After Fourier transform (FT), the time domain is converted to frequency (and to mass, after calibration), which makes the spectrum much more transparent. Since the electric current measurement in time can be done very accurately and quickly, as well as the FT processing, the resolution reaches values of up to 10^6 . Orbitrap does not reach the accuracy and resolution of a cyclotron, but its cost is significantly lower and it also does not require a sophisticated magnet/magnetic field accommodation and maintenance. An orbitrap is shown in Fig. 7.20.

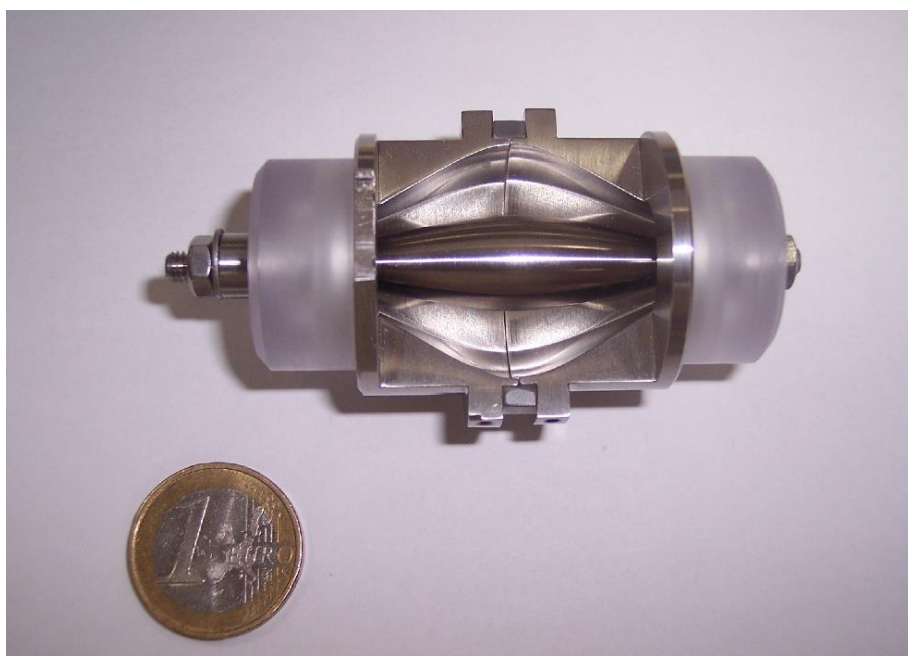
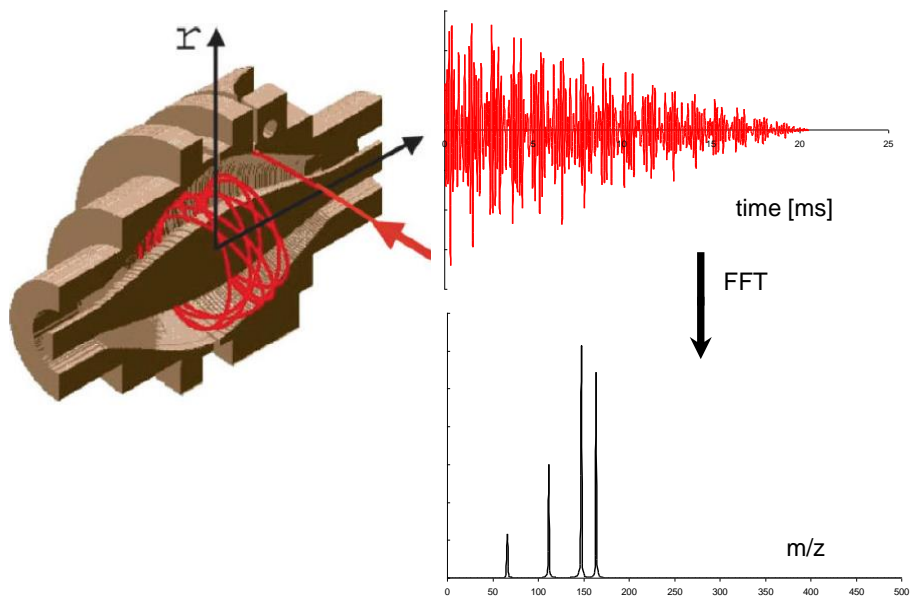


Figure 7.20. Orbitrap.

(Edited according to: <http://aston.chem.purdue.edu/files/images/research/orbitrap1.png>, 7. 1. 2008.)

7.3.8 Time of flight analyzer (TOF)

TOF analyzer is the simplest mass analyzer. It works on a principle that ions with smaller m/z , but the same kinetic energy, move faster and reach the detector sooner. It is a typical pulse analyzer. Ions are first accelerated by a very short pulse at entrance into the analyzer tube, and afterwards the time required for the ions to reach the detector is measured, determining their m/z . The scanning is fast, and the mass range is in theory not limited and depends only on the time during which the impact of the ion occurs, which can be up to 10^6 m/z . Several TOF modifications are used to increase resolution.

Reflection time of flight (r-TOF) uses an ion mirror (reflectron) which equalizes different kinetic energies of ions with the same m/z (Fig. 7.21). As already mentioned above, during ionization, the ions gain kinetic energy with a certain distribution, which leads to a widening of their peaks and thus to decrease in RP. The principle of the ion mirror, which is a system of circular electrodes with increasing voltage, is based on proportionality of E_k of ions (but not m/z) and the depth of their penetration into an electric field of the reflectron. Ions with greater kinetic energy penetrate deeper into the reflecting electric field before they are bounced back, and thus they are delayed in comparison with the ions with lower E_k , leading to levelling of total paths for ions with different E_k .

Another method is the delayed extraction which is based on delayed activation of extraction voltage. A laser pulse at a time $t = 0$ causes an expansion of ions in a deactivated extraction field, followed by a delayed rapid field activation. The MS/MS analysis can be performed also with the TOF analyzer. The repelling electrode deflects all the unwanted ions, and the chosen precursor ion is selected for the following collision-induced fragmentation. The ion can be fragmented during its flight – thus forming ions with the same speed, but lower kinetic energy. In devices without reflectron, all these ions reach the detector at the same time and are therefore not separated. However, with a reflectron, ions with different energies are distinguished and can be separated according to their m/z . This is termed a "post-source decay", as the fragments are formed only after extraction of the ions from the ion source.

Connection of quadrupole with the TOF analyzer, i.e., QqTOF (quadrupole/quadrupole/TOF) is also advantageous. The device is partially based on a triple quadrupole, but the last quadrupole is replaced by a TOF analyzer.

TOF analyzer can analyze all the ions that enter the analyzer at a given moment, unlike the other analyzers which successively scan the given m/z region. Therefore, the instrument allows continual full MS/MS spectrum measurement of products of

each ion coming from the source. The only disadvantage can be its inability to provide precursor scans and neutral loss scans as the QqQ.

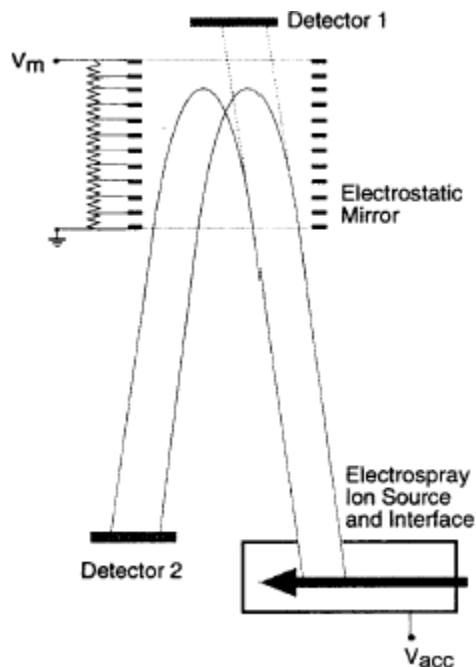


Figure 7.21. TOF analyzer scheme.

(Source: <http://holcapek.upce.cz/teaching.htm>, 10. 12. 2009.)

7.3.9 Ion cyclotron resonance with Fourier transform (FT-ICR)

Ion cyclotron resonance with Fourier transform (Fig. 7.22), completely differs from the other analyzers in its parameters, price, resolution, and applied vacuum. A bulk of ions is injected by a short pulse from the ion source into the cyclotron trap which is placed in a strong magnetic field with induction up to 7 T. The ions rotate in a plane perpendicular to the magnetic induction vector, at a frequency which is a function of their m/z . If a potential radio-frequency signal, with a frequency of any of the present ions, is inserted on a transmitter plate which forms the cyclotron trap, the given ion starts to resonate. The radius of its trajectory increases, and its rotation can be detected on a receiver plate as an induced current. If the frequency of the inserted voltage is scanned (frequency value of the inserted voltage increases linearly), all the present ions will successively resonate. After mathematical processing with Fourier transform a highly resolved mass spectrum with $RP > 10^6$ is obtained.

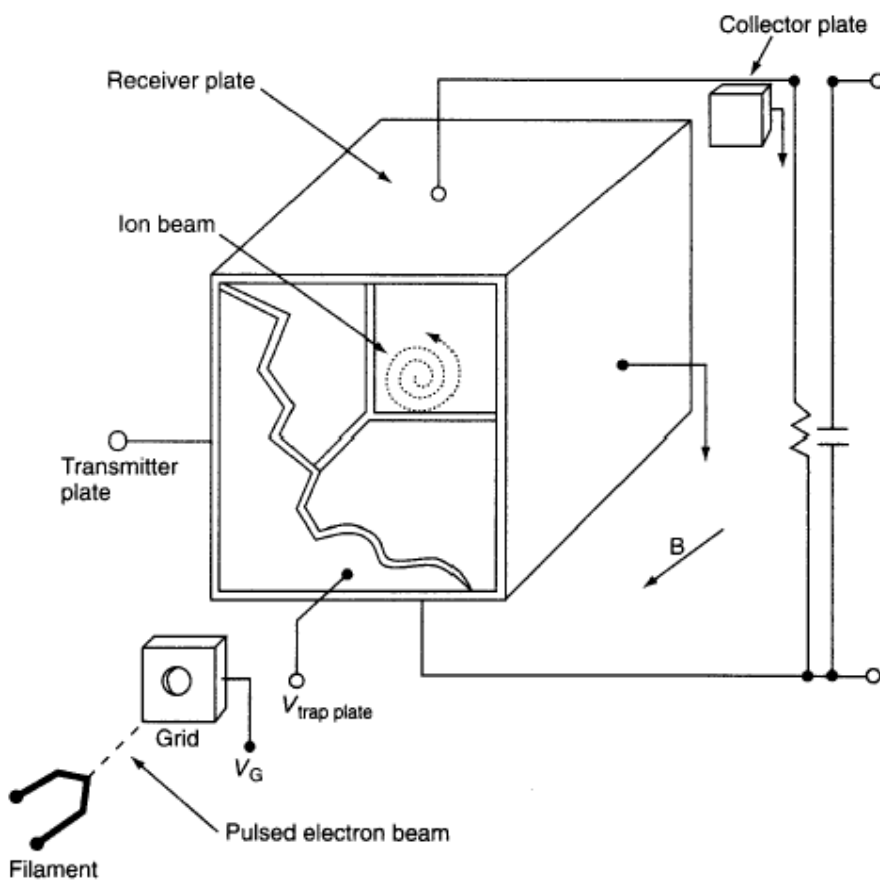


Figure 7.22. Scheme of ion cyclotron resonance with Fourier transform.

(Source: <http://holcapek.upce.cz/teaching.htm>, 10. 12. 2009.)

7.4 Ion detection techniques

Ion detector detects ions after their separation, based on their m/z , and it also determines the relative intensities of the individual ions. Detectors for mass spectrometry can be categorized into two groups:

1. Detectors for direct measurements: detect electric current generated by direct incidence of ions. These detectors are necessary for determination of the exact isotopic representation of elements and are used in specialized systems.
 - photographic plate – used in the past. Intensity was assessed according to the intensity of blackening.

- Faraday cups – ions are captured and discharged, and the current decrease is detected and amplified. It is a very accurate measuring used for the above-mentioned isotopic measurements.
2. Amplifying detectors: use amplification of electrons released from the first conversion dynode after an ion impact. This is the most often applied type of detectors in mass spectrometry, as they can yield a sufficiently measurable signal for individual ions.
- discrete dynode electron multipliers – consist of a series of metal electrically connected dynodes. After the voltage is applied between the first and the last dynode, the electrons are successively accelerated towards the following dynodes and are finally captured by collector. The incidence of ions on the first conversion dynode causes secondary emission of electrons from its material, and the number of electrons is multiplied after incidence on the following dynodes. The multipliers with discrete dynodes can even have twenty steps and can achieve amplification values of 10^7 – 10^8 .
 - continual dynode electron multipliers – consist of a curved tube from lead glass with a high electrical resistance. The tube is covered on the inside with a layer of beryllium or aluminum oxide. Contacts at the entrance and at the end of the tube are connected to a high voltage source. After an ion impacts, there are electrons emitted from the material of the tube which are further accelerated by the electric field in the direction towards the collector. Repeated collisions of the electrons on the tube wall cause further emissions and their number grows exponentially. Dimensions of the multipliers with continuous dynodes can be advantageously reduced. The effectiveness of these systems is comparable to the discrete systems, but their life and sensitivity to ions with higher mass is lower.
 - electron multiplier – is probably the most used currently. Its lifetime is one or two years, and it also exists in an arrangement with a field, which offers a higher amplification.
 - scintillation photomultiplier detector – impacting ions are converted to photons on a scintillation material and then detected by a common photomultiplier. A thin metal film on the scintillation surface prevents the growth of a surface charge, which prevents free ion incidence. Photomultiplier is also a very frequently used detector, with a longer life. Its great advantage is the possibility of measuring outside of high vacuum.

7.5 Identification and determination of compounds

Mass spectrometry is used for identification and quantification of substances. In the former case, the spectrometer becomes a tool of structural analysis, and in the latter case, the spectrometer serves as a detector, the signal of which is proportional to the amount of the monitored substance. Mass spectrometer can be used for both tasks, but it is worth mentioning that in structural analysis, it is important to scan a spectrum with a suitable range, while for the selective and sensitive quantitative analysis with low detection limit, it is useful to monitor only the selected ion of a known structure, or its fragment (especially in chromatographic separation; Fig. 7.23).

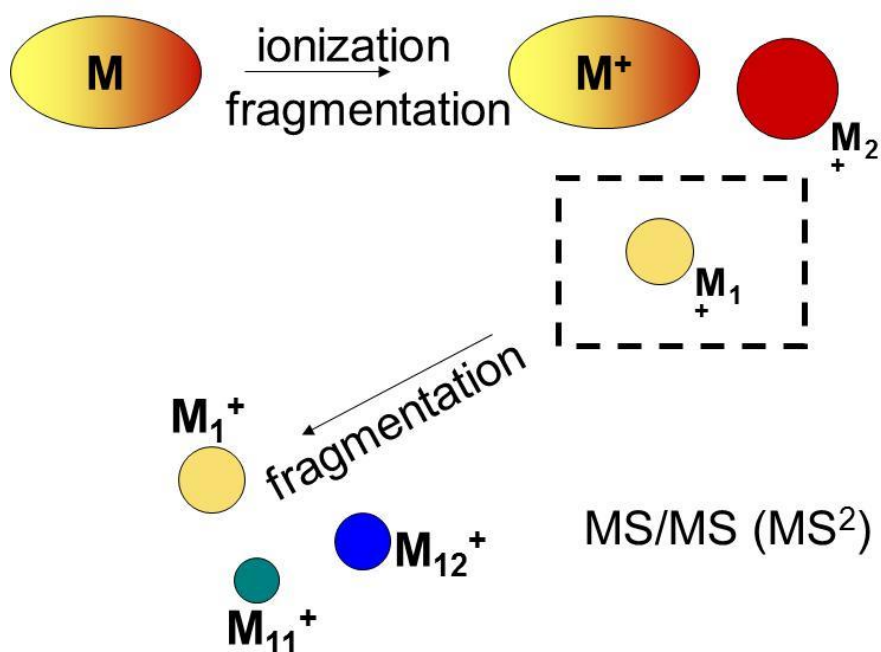


Figure 7.23. Schematic depiction of an MS/MS technique.

Various scan types are distinguished in mass spectrometry (Fig. 7.24 and Fig. 7.25):

- Full scan is a measurement of a mass spectrum in the whole studied m/z range; in the case of pre-connected separation technique, the scanning is done periodically during the whole separation and the mass spectra are recorded in time; after the measurement, it is possible to display the chromatogram as a dependence of a software selected ion on time, or as total ion current in time (TIC).

- Selected ion monitoring (SIM) measures only dependence of a selected ion signal on time; only one or few ions are selected, which significantly increases the signal/noise (S/N) ratio.
- Product ion scan results from measuring MS/MS spectrum of a chosen precursor.
- Precursor scan monitors original precursor ions for a selected fragment (typical for triple quadrupoles).
- Neutral loss scan monitors characteristic ion pairs of precursors and fragments, for which a cleavage of a selected structural unit occurred; for example $\Delta m/z = 18$ is characteristic for water molecule cleavage.
- Selected reaction monitoring (SRM) uses a selection of a precursor ion by first analyzer and its following fragmentation in a collision cell. It does not record a full spectrum as in the case of production ion scan, but only the selected fragmented ion or several ions (transitions – several successive fragments). Along with SIM, the SRM is particularly suitable for trace analysis of HPLC-MS or GC-MS. It is not a measurement of mass spectra, but only a recording of a signal corresponding to a selected ion, or a fragmented ion in SRM. The selected transition, or more transitions, markedly increase the S/N ratio and selectivity of the detection.

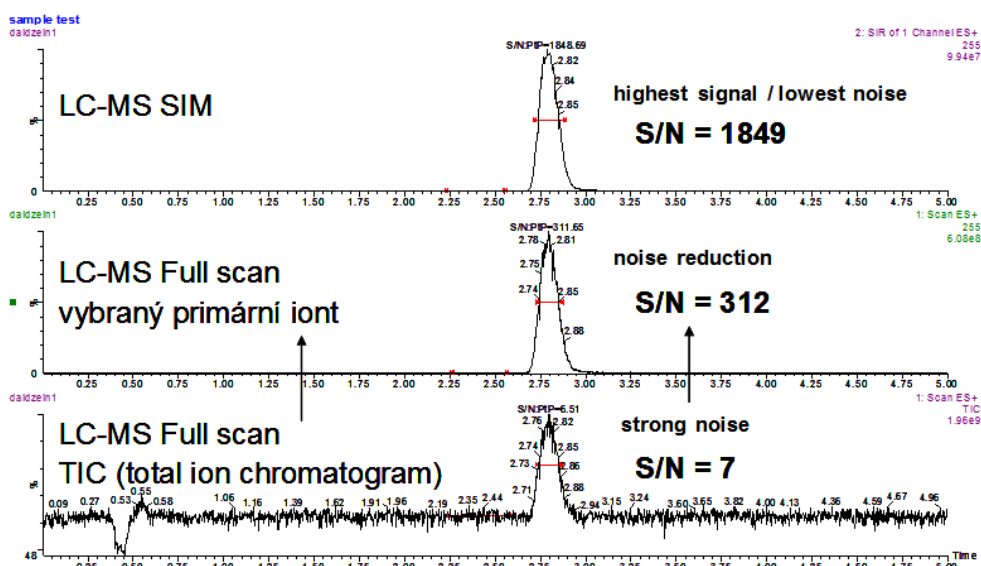


Figure 7.24. Comparison of a LC-MS technique depending on the scan type.

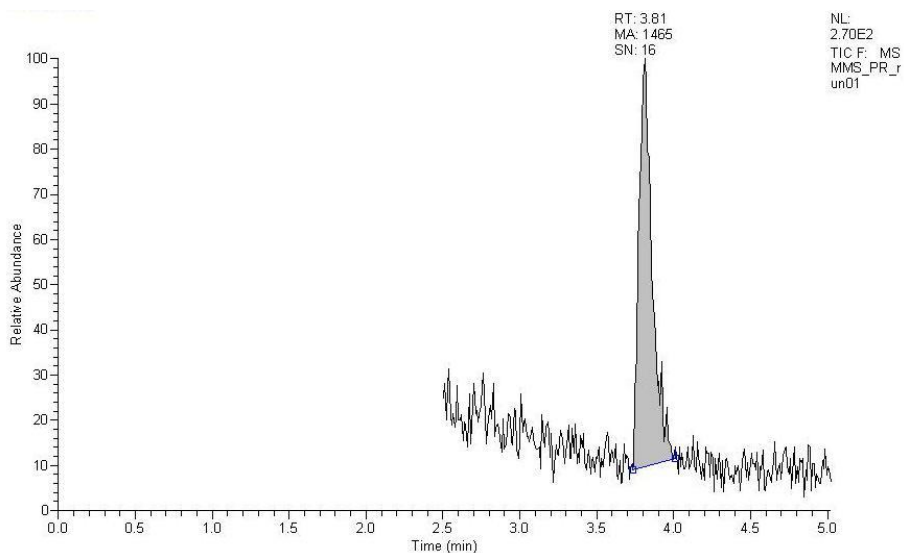


Figure 7.25. Chromatographical record of determination of methylester of methanesulfonic acid, at 15 ppm in an API, by GC-MS method (SIM mode).

A separation preceding a quantitative MS, despite high selectivity of the determination, is used to overcome a so-called “matrix effect” – an effect where the analyte signal is not only a function of its concentration but can be influenced by other substances in the sample. If the analyte signal is not affected by the matrix, a flow injection analysis (FIA) technique can be applied, where the sample is injected into a flow-through system without a separation column (Fig. 7.26).

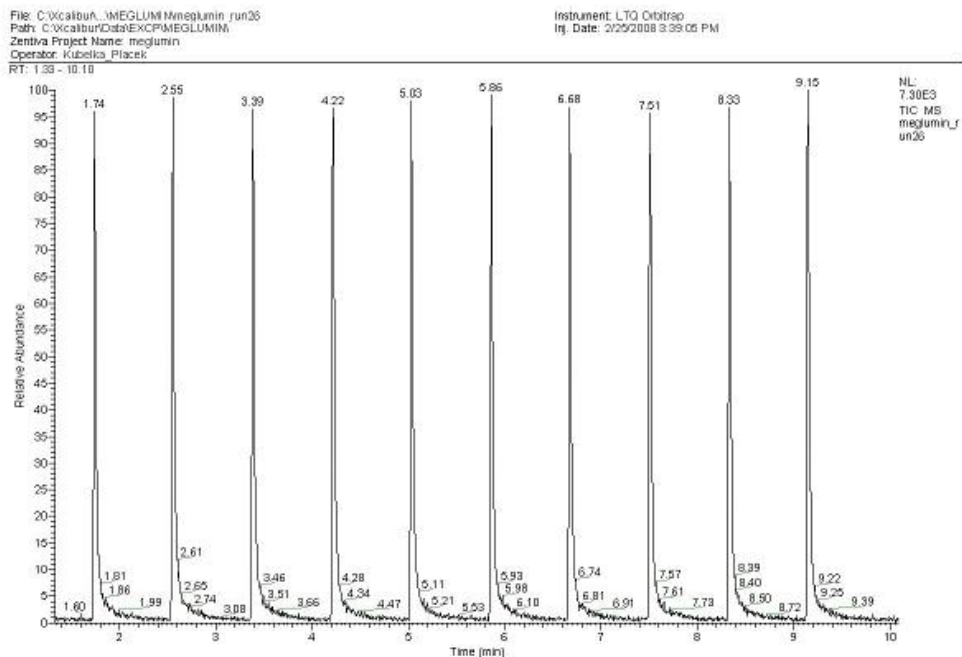


Figure 7.26. FIA-MS/MS; determination of meglumine in a dosage form, ten sample injections.

7.6 Structural MS analysis in pharmacy

The field of pharmaceutical structural analysis includes tasks as identification of main substances and impurities, from small organic molecules such as residual solvents, through synthetic active pharmaceutical ingredients (API) and their impurities with relative molecular mass of approximately 200–600, to macromolecular substances, e.g., determination of amino acid sequence of an isolated peptide or other biopharmaceuticals. Pure and isolated substances can be injected directly into the MS system, while the spectra of minor impurities should be measured after a chromatographical separation. Selection of an appropriate technique for acquisition of mass spectra for subsequent identification of substances plays a key role. Recommendations for selection of techniques are provided in Table 7.1.

Interpretation of the obtained spectra depends on the ionization and the measurement technique – each has its own specifics and possible methods of detection or clarification of the given structure. In case of any doubts, it is appropriate to operatively choose another ionization technique, perform MSⁿ, or obtain elementary composition of the molecular ion or its fragments.

Table 7.1. Options for MS technique selection and connection with separation.

Substance type	Separation technique	Ionization technique	MS analyzer
Solvents	GC, headspace	EI, CI	IT, LIT, Q
Volatile substances	GC, split/splitless	EI, CI	IT, LIT, Q, Orbitrap
API, excipients	HPLC	ESI, APCI, APPI	IT, LIT, Q, TOF, Orbitrap, ICR
Macromolecules /Biopharmaceuticals	HPLC	ESI, MALDI	Orbitrap, TOF, ICR

Despite great variability of techniques, it is possible to outline basic rules for spectra interpretation:

- finding the molecular ion and molecular adducts
- estimation of elementary composition based on the m/z of the molecular peak and the intensities of its isotopic satellites
- assessment of the most probable elementary composition if a value of highly resolved molecular ion mass is available (also from estimation in the previous step)
- fragment mapping and neutral loss calculation (possible performing of MSⁿ)

Based on the information from the assignee, and the knowledge gained from the interpretation, a possible structure is suggested, and it should be confirmed or specified by another structural analysis technique.

7.6.1 Modern MS systems in pharmacy

As mentioned above, MS systems in laboratories of pharmaceutical structural analysis should enable measurements of spectra of a wide range of sample types. GC-MS system can be appropriately set with a headspace gas injector or with a split/splitless injector for liquid samples. Capillary columns should not have an

overly thick layer of a stationary phase, so that it does not contaminate the ion source – commercial manufacturers differentiate between the use of GC columns for MS and other detector types, and the information is provided in their catalogues. Ion source of choice for GC-MS is EI in combination with CI, and as analyzer, it is useful to apply ion trap (3D or linear), triple quadrupole for easy tandem MS or orbital trap for structure elucidation. The inlet interface into an MS system may not only be from a separation technique, but it is also practical to expect direct heated probe use.

HPLC systems for MS identification of substances contain a stable gradient pump with a wide flow rate range, quality injector, sample magazine and a column space with thermostat. For practical reasons, it is recommended to include a UV detector for substance elution and impurity monitoring, as shown in Fig. 7.27. The mobile phase should be easily evaporated and contain water or aqueous solution of ammonium formate or acetate, in a gradient with methanol or acetonitrile. Any parameter reversed-phase columns can be used, when providing the desired quality of separation and ionization. For direct introduction of solutions into the ion source, it is suitable to connect a syringe pump to the MS system. ESI and APCI ionization techniques should not be missing in a standard LC/MS apparatus arrangement, either as separate interchangeable units or combined robust sources. The analyzer should be chosen with regards to the range of the m/z region (traps, quadrupoles, and orbitrap only up to approx. 2000 m/z), simplicity of tandem MS, and the use of high resolution. Although DESI and DART ionization techniques are not common, they may be desired in structural analysis and MS imaging techniques.

The biopharmaceutical industry is increasing the development of protein-based biotherapeutics (such as monoclonal antibodies or vaccines). Complexity of these drugs and their biological production by living cells requires their thorough analysis to guarantee safety and efficacy. Intact protein analysis, peptide mapping, charge variants, oligonucleotides, glycans or host cell protein analysis are important characterization steps for biotherapeutic proteins and they confirm that product with the correct molecular weight has been expressed. High-resolution, accurate-mass (HRAM) Orbitrap mass spectrometry has been shown to be essential for this technique.

However, the suitability of techniques applied for a specific purpose should always be considered and the equipment selected according to the analysis requirements assigned by the client.

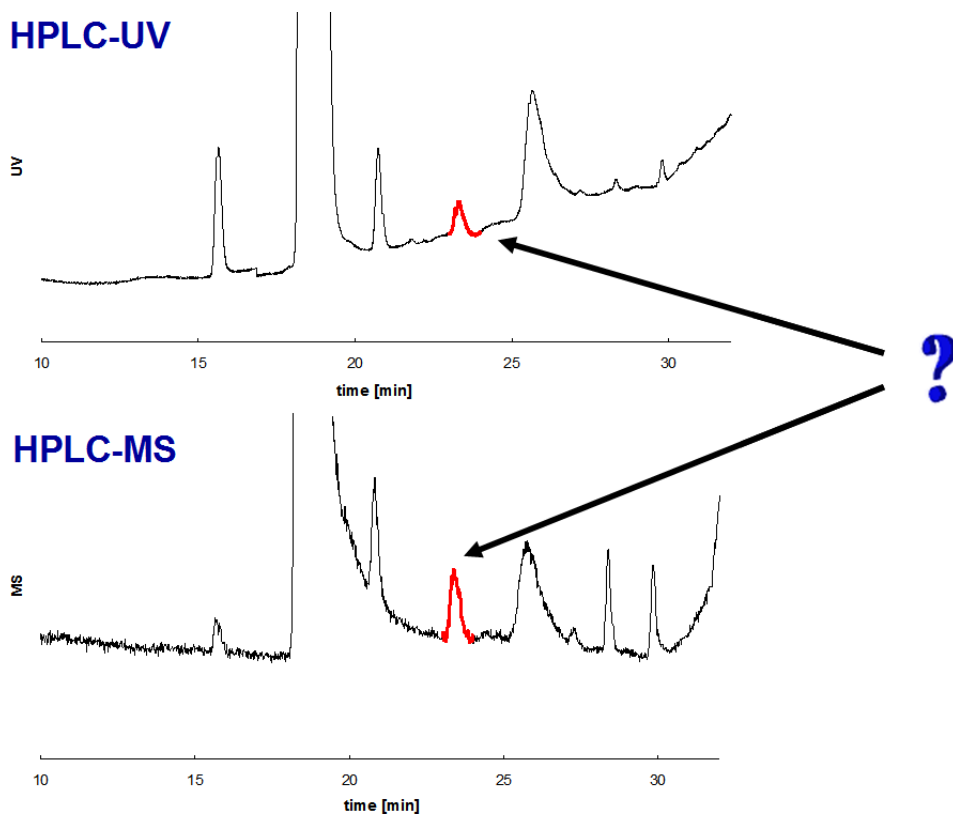


Figure 7.27. In identification of impurities by LC-MS, it is useful to connect an UV detector before the mass spectrometer.

7.7 Resources and recommended literature

1. McLafferty F. W., Tureček F. Interpretation of Mass Spectra, 4th Edition. University Science Books: Sausalito, USA, 1993.
2. Cole R. B. Electrospray Ionization Mass Spectrometry, Fundamentals, Instrumentation and Applications, John Wiley & Sons: New York, USA, 1997.
3. Willoughby R., Sheehan E., Mitrovich, S. A Global View of LC/MS. Global View Publishing: Pittsburg, USA, 1998.
4. Ardrey R. E. Liquid Chromatography – Mass Spectrometry: An introduction, Analytical Techniques in the Science. John Wiley & Sons: Chichester, UK, 2003. <https://doi.org/10.1002/0470867299>
5. Kolektiv autorů. Sborník přednášek 3. ročníku školy HPLC-MS. Doubice, 2005.
6. Analytical Methods in Supramolecular Chemistry. Schalley C. A. (Ed.). Wiley-VCH: Weinheim, Germany, 2006.
7. Cooks R. G., Ouyang Z., Takats Z., Wiseman J. M. Ambient Mass Spectrometry. Science 2006, 311 (5767), 1566–1570. <https://doi.org/10.1126/science.1119426>
8. Kogej M., Schalley C. A. Mass Spectroscopy and Gas Phase Chemistry of Supramolecules. In: Analytical Methods in Supramolecular Chemistry, Schalley C. A., (Ed.). Wiley-VCH: Weinheim, Germany, 2007, pp. 104–162.
9. MALDI MS: A Practical Guide to Instrumentation, Methods and Applications. Hillenkamp F., Peter-Katalinic J., (Eds.). Wiley-VCH: Weinheim, Germany, 2007.
10. Rouessac F., Rouessac A. Mass Spectrometry. In Chemical Analysis – Modern Instrumentation Methods and Techniques, 2nd Edition; John Wiley & Sons: Chichester, UK, 2007, pp. 369–418.
11. Aplikační listy. Thermo Fisher Scientific.
12. Hmotnostní spektrometrie (MS), http://tomcat.bf.jcu.cz/sima/analyticka_chemie/vybranemet.htm. December 2009.
13. Hillenkamp F., Katalinic J. P. MALDI MS: A practical Guide to Instrumentation, Methods and Applications. Wiley-VCH: Weinheim, Germany, 2007. <https://doi.org/10.1002/9783527610464>
14. Holčápek M. – Mass Spectroscopy Group, <http://holcapek.upce.cz/teaching.htm>. December 2009.

8 Thermal analysis

Lucie Krumbholcová, Jiří Dohnal, Izabela Jendrzewska

8.1 Definition of thermal analysis methods

The principle of thermal analysis is heating a solid sample and recording the physical changes and chemical reactions that occur under the influence of the supplied heat. During the heating, several physicochemical phenomena characteristic for the tested substance occur, such as:

- change of the physical state (melting, crystallization, sublimation)
- phase transformations (formation of a crystal lattice, polymorphic transformations)
- chemical reactions (thermal dissociation, reactions between substrates in the solid phase)

These phenomena are accompanied by a change in enthalpy ($\pm \Delta H$). If we are dealing with an endothermic reaction ($\Delta H > 0$), heat is absorbed, e.g., dehydration, reduction. An exothermic reaction ($\Delta H < 0$) is related to heat release, e.g., crystallization or oxidation.

Each substance can be characterized by free enthalpy content (ΔG), which is given by the relationship:

ΔH – change of enthalpy

$$\Delta G = \Delta H - T\Delta S$$

T – temperature

ΔS – change of entropy

Each system attempts to achieve a state corresponding to a lower free enthalpy content at a given temperature. The heating or cooling of a substance leads to reversible or irreversible changes in its size, depending on its initial dimensions and temperature. Also, analysis of gaseous products of chemical reactions and monitoring other physico-chemical parameters, such as electrical and thermal conductivity, optical properties, dielectric constant, thermoelectric voltage, magnetic properties, etc., are the principles of thermal analysis methods. Since a chemical reaction or a phase change is accompanied by simultaneous changes in several physico-chemical parameters, various complementary thermal analysis

methods can be used to obtain more results to ensure a better match of experimental conditions.

One of the oldest thermal analysis methods is thermogravimetry analysis (TGA) and differential thermal analysis (DTA). First works with thermogravimetry character were already carried out in 1893 and 1914, even if the scales used at that time were not termed thermobalances. Thermobalance is a device allowing to express or graphically record weight changes of a sample subjected to heating or cooling, depending on temperature or time. The beginnings of DTA date back to the same period as the thermogravimetric method itself. In 1886, it was first used by Le Chatelier for studying calcite and later for studying clay materials. The technique was advanced in 1891 by Roberts-Austen by introducing differential thermoelectric cells which measured thermoelectric voltage difference between a cell located in the studied sample and a cell located in the standard sample which was not subject to changes.

8.2 General principle of thermal analysis methods

Thermal analysis belongs to experimental material analysis. New methods for monitoring material changes depending on temperature are still developed. Generally, there are three quantities of interest:

- Time – changes in time are observed during isothermal heating. In practice, the isothermal heating of a studied material is combined with non-isothermal heating. In non-isothermal heating, a heating rate is determined, and the time is then given by the heating rate and the temperature interval.
- Temperature – besides isothermal conditions, the variable temperature is often used in thermal methods. Primarily, a constant heating rate is used, but the current level of regulatory and information technology also allows other types, such as periodic temperature increase or decrease in a chosen temperature range where the temperature rise can have a constant rate. The decrease may be spontaneous or controlled along with the heating. Another option is a periodic heating rate change with a sinusoidal or another period.
- Material properties – thermal analysis techniques are classified according to the observed property type. An overview of the essential techniques is listed in Table 8.1.

Table 8.1. A list of the most common thermal analysis techniques.

Method name	Studied quantity
Differential thermal analysis (DTA)	thermal difference between the studied and a standard sample
Differential scanning calorimetry (DSC)	thermal energy provided for compensation of temperature between the studied and a standard sample
Thermogravimetry analysis (TGA)	weight change
Differential thermogravimetric analysis (DTGA)	the first derivation of weight change
Thermomechanical analysis (TMA)	mechanical property change (module, hardness)
Dilatometry	volume change
Effluent gas analysis	studied gas volume
Pyrolysis	pyrolysis products
Thermal luminescence analysis	light emission
Electric conductivity analysis	electric conductivity change

8.3 *Thermal methods*

Thermal analysis is a broad term referring to methods that measure the physical and chemical properties of a substance, a mixture, or a reaction mixture as a function of temperature or time during a controlled temperature program. The sample may also be exposed to other effects (e.g., reactive atmosphere, static or dynamic mechanic load). The application field of thermal analysis in pharmacy is wide.

8.3.1 Basic measurement factors

The variables affecting measurements can be divided into the three following groups.

- Instrumental factors:
 - thermal source and the thermoregulatory system
 - temperature measuring system
 - thermoanalytical curve recording system
 - detection system
- Methodical factors:
 - temperature program
 - the geometrical arrangement of the measuring system
 - atmospheric effect
 - sample placement and preparation
- Properties of measured substances:
 - physical and chemical properties of the measured sample
 - particle size and shape
 - sample thermal conductivity
 - density and thermal capacity
 - the effect of humidity and (residual) solvents
 - crystallinity and sample purity degree

8.3.2 Measuring procedure

8.3.2.1 Instrument calibration

Accurate temperature determination is crucial, and because of the different instrument construction and temperature measuring systems, there must be internationally accepted temperature calibration standards. The international confederation for thermal analysis and calorimetry (ICTAC) includes a scientific committee coordinating standardization and nomenclature activities. There exist some standards that have been comparatively measured in laboratories worldwide. These standards are high purity, low molecular substances with precisely defined thermal characteristics: boiling point, melting point, solidification temperature.

The calibration is performed by inserting a standard sample into the measuring cell, and an empty capsule is used to prepare the standard into the reference cell. The phase transition is sharp and can be accurately read. The standards are supplied with the instruments. Calibration is performed in the same range and intervals as the following measurements, as the instrument properties may change over time. For some methods (DSC), enthalpy is also calibrated as one of the outputs. In thermogravimetry, calibration of scales is essential, making it necessary to determine whether the measured weight of the standard at different temperatures corresponds to the actual weight.

8.3.2.2 Sample preparation before analysis

Due to the different nature of the thermoanalytical measurements, it is clear that the sample weight and dimensions are important for measurement outcomes, as they affect the heat flux between the environment and the measured sample. Generally, it is good to use identically large samples spread evenly over a pan or a measuring cell to achieve reproducibility.

8.3.2.3 Measurement atmosphere

The type of gas used for creating the measuring environment depends on the measurement type. Inert nitrogen is used for melting temperature measurements, polymorph screening, glass transition temperature measurement, etc. The nitrogen flow also removes gaseous products formed during the heating. Oxygen is used to measure degradation products during oxidation or other processes. The oxygen must then have access to the sample, i.e., the lid of the closed pan is pierced.

8.3.2.4 Heating rate

The heating rate depends on the information that is to be obtained. Typical measurements are performed at a rate of 10 °C/min. However, to determine glass transition temperature, it is often preferable to choose a higher rate of up to 500 °C/min. High sensitivity measurement changes, at speeds of up to 1.2° C/min, are enabled by microcalorimetry. In practice, an unknown sample is recommended to be measured at several heating rates to better interpret the ongoing processes. Instrument calibration must be performed after every heating rate adjustment. Different behavior of one substance at different heating rates is documented in Fig. 8.1.

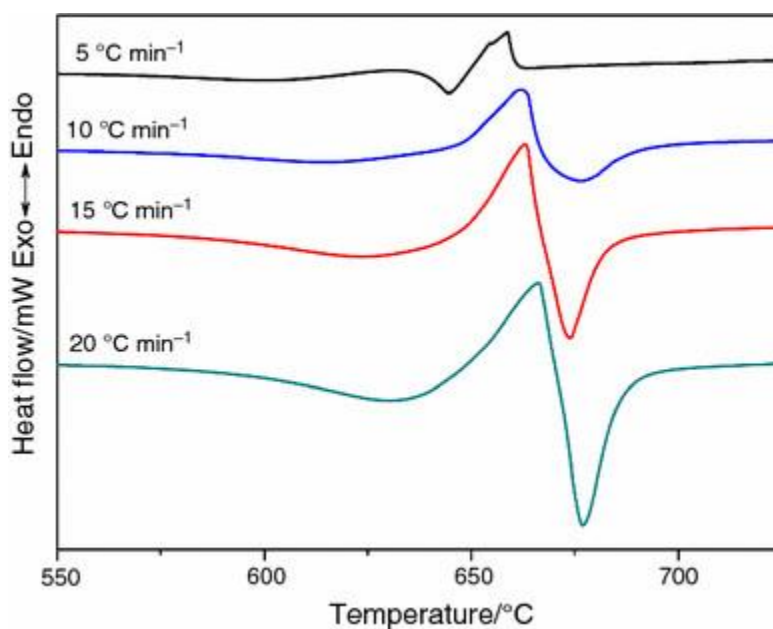


Figure 8.1. DSC for one sample measured at different heating rates.

(Source: Nicoara, et al., *J. Therm. Anal. Calorim.*, 2016.)

8.3.3 Evaluation of thermoanalytical measurements

Two curve characteristics are typically evaluated in thermoanalytical measurements:

- Thermal process position, i.e., the temperature at which the process occurs. Peak value and onset (tangent line to the curve) is obtained. Next, the

inflection point is determined – typically for glass transitions of polymers or amorphous materials (Fig. 8.2 and 8.3.).

- Peak area proportional to weight change in TGA and enthalpy process in DSC; generally determined by integration, see Fig. 8.4a and 8.4b.

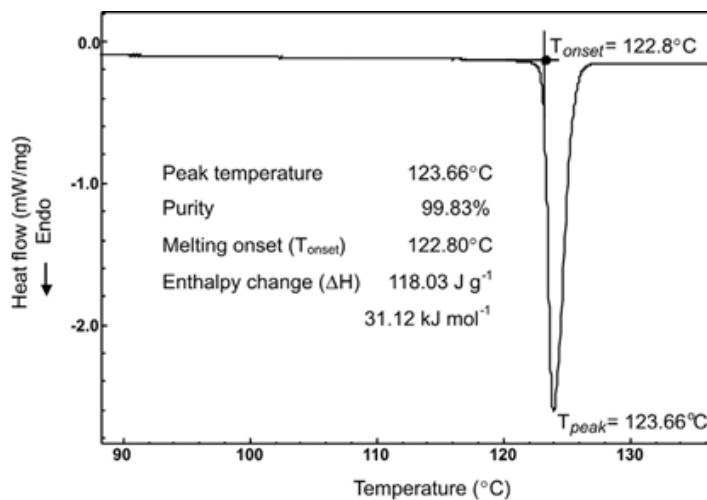


Figure 8.2. A typical record of a DSC curve for crystalline substance melting.

Evaluation – peak, onset and ΔH .

(Source: Araujo et al. *Braz. J. Pharm. Sci.*, 2010.)

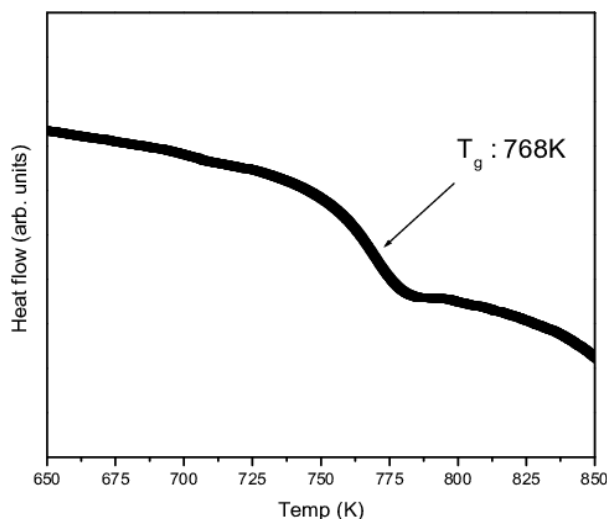


Figure 8.3. Glass transition curve record for an amorphous substance.

Evaluation – T_g .

(Source: Joseph et al. *Energy Procedia*, 2011.)

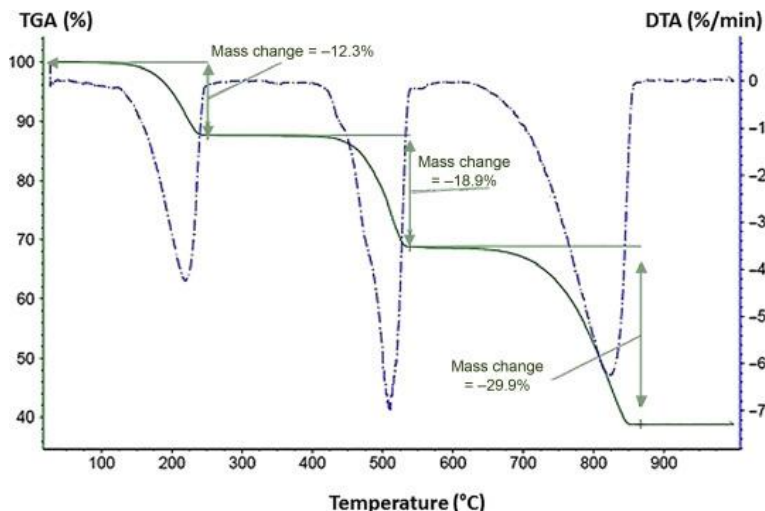


Figure 8.4a. TGA curve record for a pharmaceutical substance hydrate ($\text{CaC}_2\text{O}_4 \cdot \text{H}_2\text{O}$). The curve with a distinct minimum represents the first derivation of a TGA curve. Evaluation – water content.

(Source: <https://www.sciencedirect.com/topics/materials-science/differential-thermal-analysis>, 6.02.2022.)

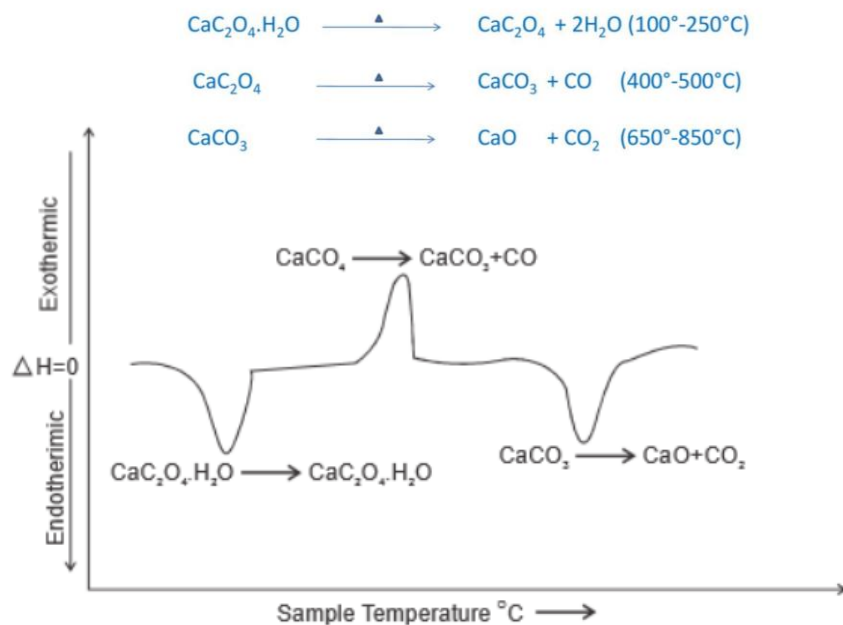


Figure 8.4b. DSC record of the substance from Fig.8.4a, showing decomposition of hydrated calcium oxalate ($\text{CaC}_2\text{O}_4 \cdot \text{H}_2\text{O}$) in three stages. The ignition temperature of 838–1025°C is evident.

(Source: <https://www.sathyabama.ac.in/sites/default/files/course-material/2020-10/SCY2.pdf>, 6.02.2022.)

8.3.4 Differential scanning thermal analysis (DSC)

8.3.4.1 Theoretical basics of DSC

Differential scanning thermal analysis (DSC) is one of the most applied thermal analysis methods in pharmaceutical development. In DSC, the sample is subjected to linear heating, and the heat flux rate in the sample is proportional to the actual specific heat and is continuously measured. Two symmetrical containers are placed inside the measuring jacket, typically maintained at room temperature. The primary temperature control system consists of a resistance thermometer and a heating unit embedded in the sample holder. The secondary temperature control system measures the temperature difference between both carriers, and this difference is adjusted to zero value by controlling the measured heat flux. In other words, the sample temperature is maintained isothermally with the comparative sample (or block) supplied with heat. The amount needed to maintain isothermal conditions is recorded as a measure of time or temperature. The electric input required to maintain the isothermal conditions is measured instead of differential temperature as in classical DTA. The use of small samples (milligram quantities) placed on metal foils reduces the thermal gradient to a minimum. The small heat capacity of the whole system allows the use of high heating rates (tens to hundreds of °C/min) and provides a high-resolution capability. The amount of released (seized) heat is thus proportional to the amount of electric energy used to heat the sample (standard). It is, therefore, a calorimetric method. Devices and their principles are shown in Fig. 8.5–8.7.



Figure 8.5. DSC Pyris 1 and TGA6 by Perkin Elmer company.

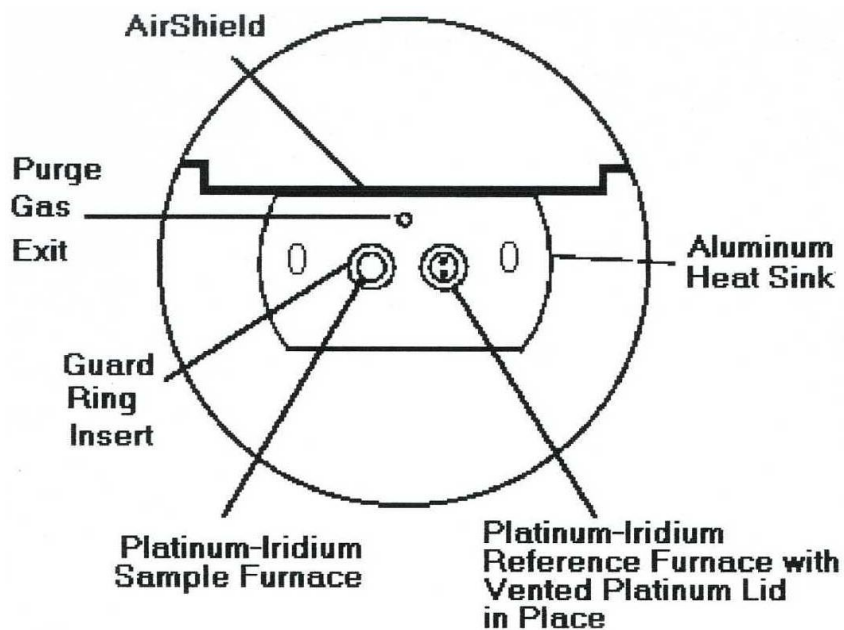


Figure 8.6. Measuring cell in DSC Pyris 1.

(Source: Aplikace DSC Pyris1. Perkin Elmer, 1997.)

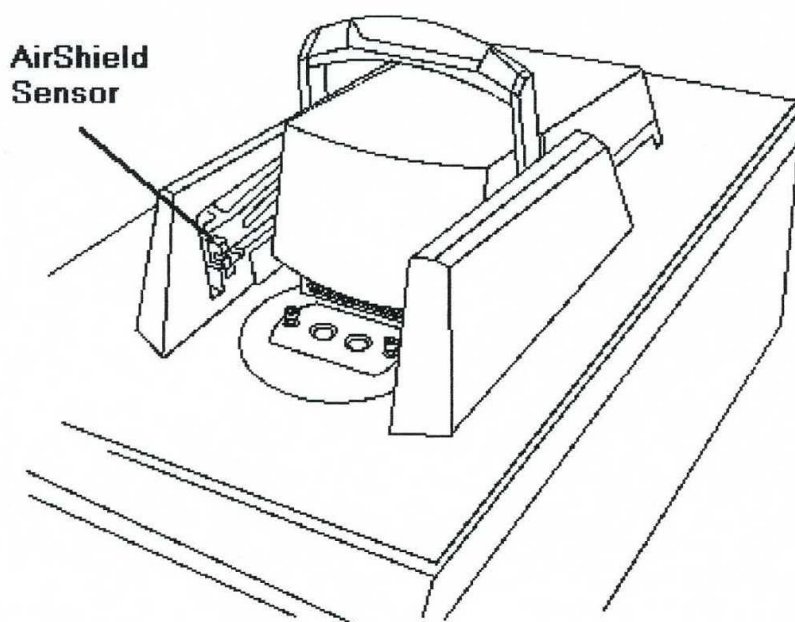


Figure 8.7. Closing of measuring room for its isolation from extraneous influence.

(Source: Aplikace DSC Pyris1. Perkin Elmer, 1997.)

Besides the measured quantity, methods can be characterized based on thermal balance also by the basic thermal flow between:

- sample and surroundings
- reference and surroundings
- sample and reference

The following applies for sample enthalpy change:

ΔH_s – measured quantity

q_s – enthalpy term

$$\Delta H_s = q_s + \Delta q + Q_s$$

Δq – thermal conductivity term

Q_s – inertion term + (supplement term)

8.3.4.2 *Sample preparation*

It should always be kept in mind that a sample is heated or cooled during its preparation through direct contact with the platform on which it is placed. Good thermal contact with the platform is therefore necessary. The sample must be placed evenly on the bottom of the crucible or tamped onto it, and it should have a minimum thickness. Weight depends on the expected thermal effect. In general, greater sample weight reduces the instrument sensitivity. When studying subtle effects (glass transition, heat capacity measurements, etc.), the sample amount should be greater than 10 mg. The sample mass should be about 2–6 mg when determining purity or phase transition enthalpy. The scales should be selected accordingly when weighing samples for the DSC measurements.

The selection of an appropriate pan, see Fig. 8.8, is another crucial step in sample preparation before measurement. The crucibles are made of different materials, and according to the sample characteristics, they may be non-hermetic and hermetic or high-pressure. The most common crucibles are aluminum that can be used for measurements up to 550 °C. Less common crucibles for special applications can be made of, e.g., graphite, copper, gold, alumina or platinum crucibles. Generally, non-hermetic aluminum crucibles can be used for non-volatile samples, and hermetic or high-pressure crucibles must be used for liquid samples and organic materials.



Figure 8.8. DSC measuring crucibles.

8.3.4.3 Application of DSC

The most common applications of DSC in pharmaceutical analysis include the determination of API purity and the study of API polymorphism and excipients. Some examples are shown in Fig. 8.9–8.11.

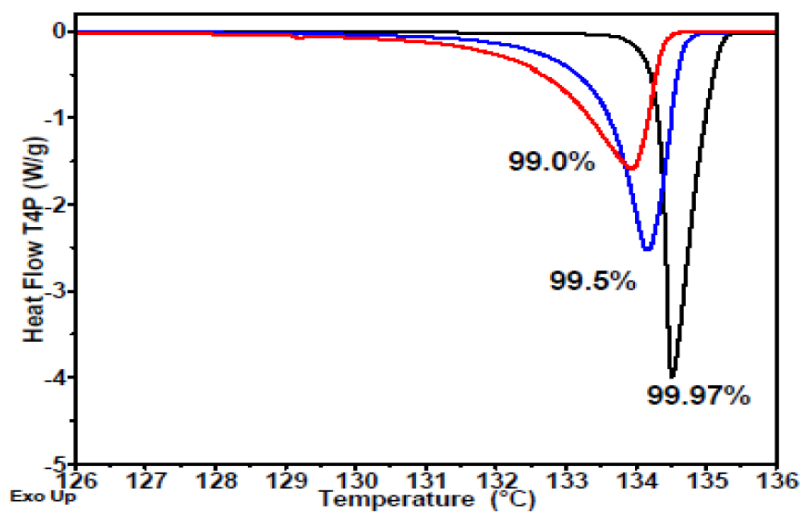


Figure 8.9. Purity of phenacetine.

(Source: TA Instruments, Cassel RB, Purity determination and DSC Tzero™ Technology)

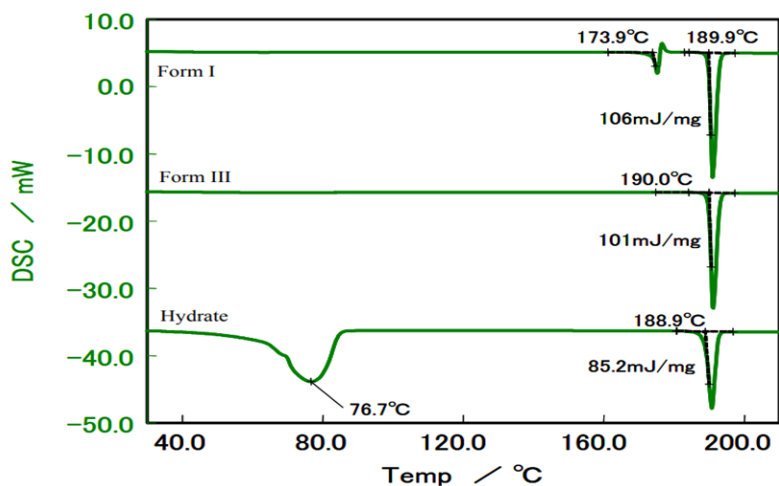


Figure 8.10. DSC sample curves for polymorphic forms of carbamazepine.

(Source: https://www.hitachi-hightech.com/file/global/pdf/products/science/appli/ana/thermal/application_TA_079e.pdf, 20. 02. 2022.)

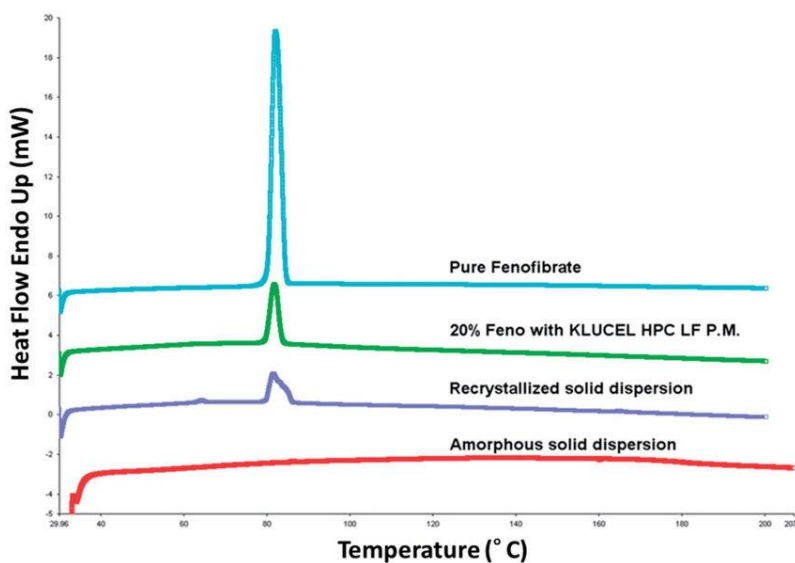


Figure 8.11. Evaluation of crystallinity using DSC: pure fenofibrate (blue curve), physical mixture of 20% fenofibrate with Klucel LF (green curve), recrystallized solid dispersion (purple curve), amorphous solid dispersion (red curve).

(Source: Feng et al. *Drug. Dev. Ind. Pharm.*, 2014.)

8.3.5 Hyper DSC

Hyper DSC offers a much more sensitive evaluation of changes during rapid temperature increase to up to 500 °C/min (Fig. 8.12). This technique provides additional and often crucial information about the tested material.

Advantages of Hyper DSC:

- speed, simplicity
- lower occurrence of effects typical for lower temperature increase rates that may lead to incorrect result interpretation (water evaporation, recrystallization, or chemical degradation)
- detection of effects with lower kinetic energy (glass transition or melting)

Disadvantages of Hyper DSC:

- calibration for every individual heat rate

Application of Hyper DSC:

- more accessible study of polymorphism
- improved identification of glass transition
- realistic simulation of polymorphism behavior
- protein analysis

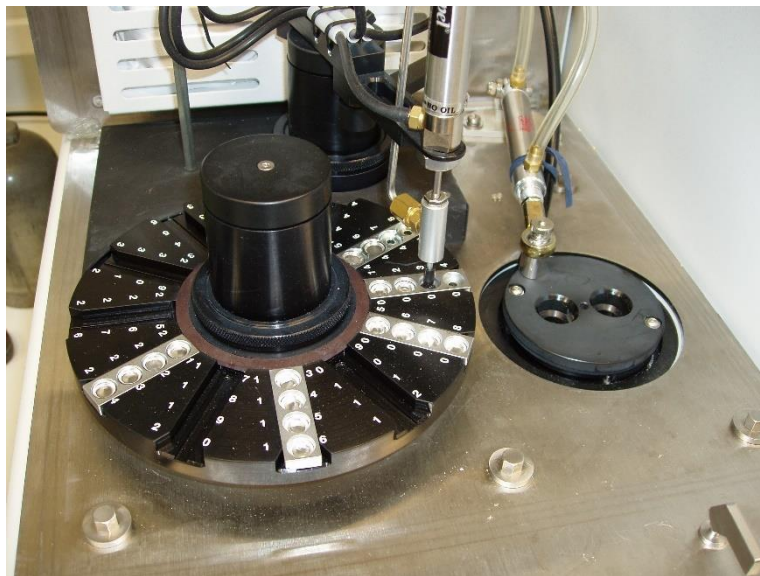


Figure 8.12. Diamond Hyper DSC by Perkin Elmer company (with autosampler).

8.3.6 Micro DSC

Another thermal analysis technique used in pharmaceutical development is a purely calorimetric method. It monitors the enthalpy and thermal capacity of processes during the measurement, and it also enables the measurement of mixtures of two substances and observation of their reactions. The sample is heated or cooled, resulting in structural and chemical composition changes. These changes are usually associated with heat exchange. Micro DSC is a highly sensitive technique with a special place among other DSC techniques.

8.3.6.1 *Micro DSC III (SETARAM)*

Micro DSC III device by SETARAM (Fig. 8.13) has a temperature range of 20 ~ 120 °C. Its detection limit is significantly lower than in commonly applied DSC techniques, and it can detect calorimetric changes of less than 1 μ W, allowing analysis of small sample amounts, with a very low temperature increase rate from 0.001 to 1.2 °C/min.



Figure 8.13. Micro DSC by SETARAM (from left: external cooling, unit with a calorimetry block, and CS 32 unit for collection and data transfer to PC).

Technical arrangement

The calorimetric block consists of gold-coated cylinders with high thermal conductivity. This arrangement provides excellent temperature homogeneity and precise control. There are two cavities in a block that serves as a measuring space for experimental cells. A three-dimensional thermal flow sensor (3D sensor) enables the Micro DSC III to achieve high sensitivity (detection limit of 0.2 mW) with perfect precision.

The calorimetric block (Fig. 8.14) is very well protected against thermal influences from the external environment, which ensures the ability to detect minimal thermal effects in the sample.

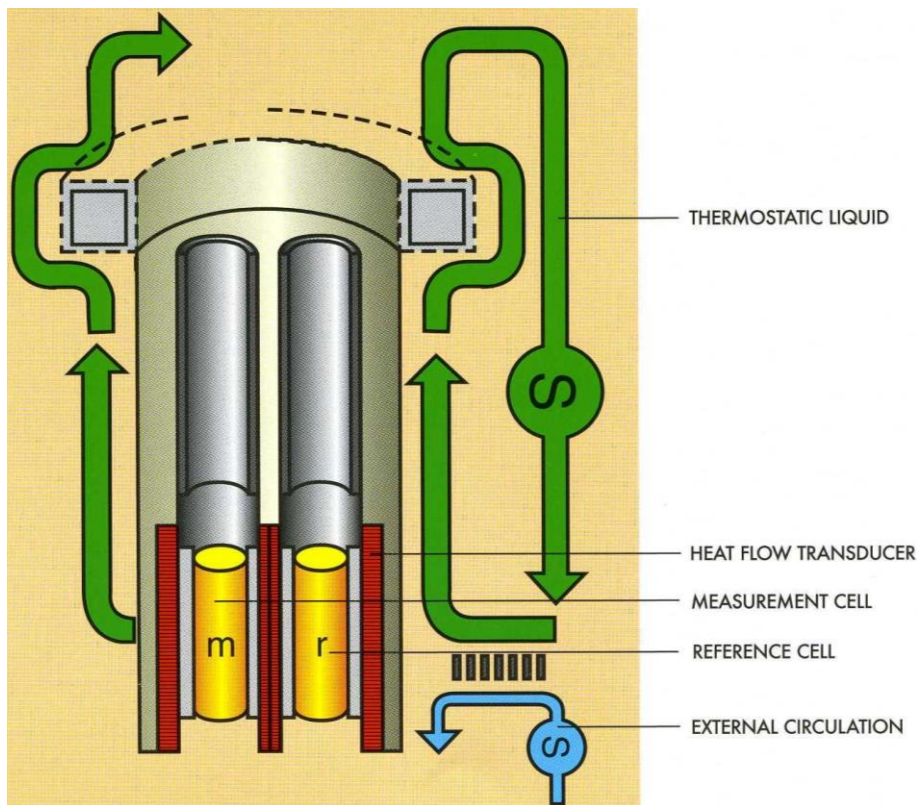


Figure 8.14. Calorimetry block.

(Source: Aplikační listy. SETARAM Instrumentation.)

Types of measurement cells

Several experimental cells ensure the flexibility of Micro DSC III. There are insertion "Batch" types or flow-through types of measuring cells. All cells can be used for isothermal as well as for DSC measurements. They are made of unique "Hastelloy C" (brand name) steel, have a volume of 1 cm³, and are quickly changeable and easy to clean.

The most common cells in pharmaceutical development are closed "Batch" cells and mixing "Batch" cells.

A closed "Batch" cell (Fig. 8.15a) for analysis of raw solid and liquid samples. A screw-on ensures good sealing with a gasket that can withstand the maximum internal pressure of 20 bar. The cell is used for studies of protein denaturation, phase transitions, gelling processes, and compatibility studies for active substances with excipients.

The mixing "Batch" cell (Fig. 8.15b) has two separate compartments for the insertion of substances for which the mixing processes are to be observed. The cell also allows manual mixing and is used for studying reactions between solid and liquid substances.

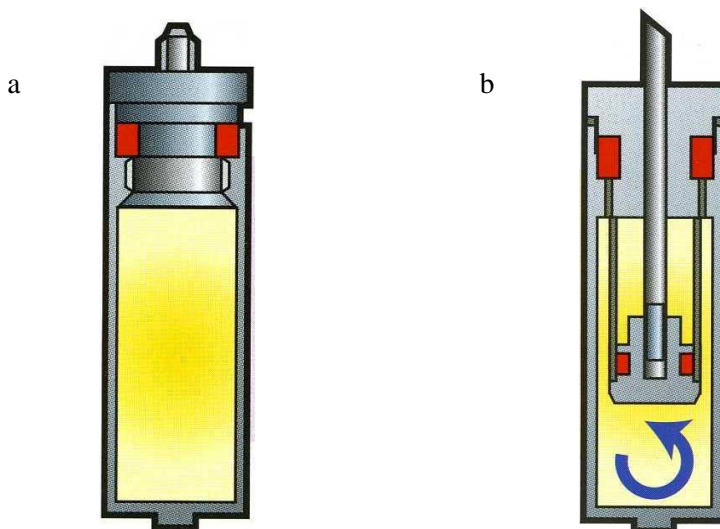


Figure 8.15. Closed "Batch" cell (a); mixing "Batch" cell (b).

(Source: Aplikační listy. SETARAM Instrumentation.)

8.3.6.2 Application of Micro DSC III

DSC mode

- Denaturation – aggregation of collagen solutions. Collagen is a fibrous protein with three chains bound in a triple helix. Like other proteins, it denatures when heated. At the same time, a subtle endothermal effect occurs, which can be measured only by sensitive methods, such as micro DSC (Fig. 8.16).

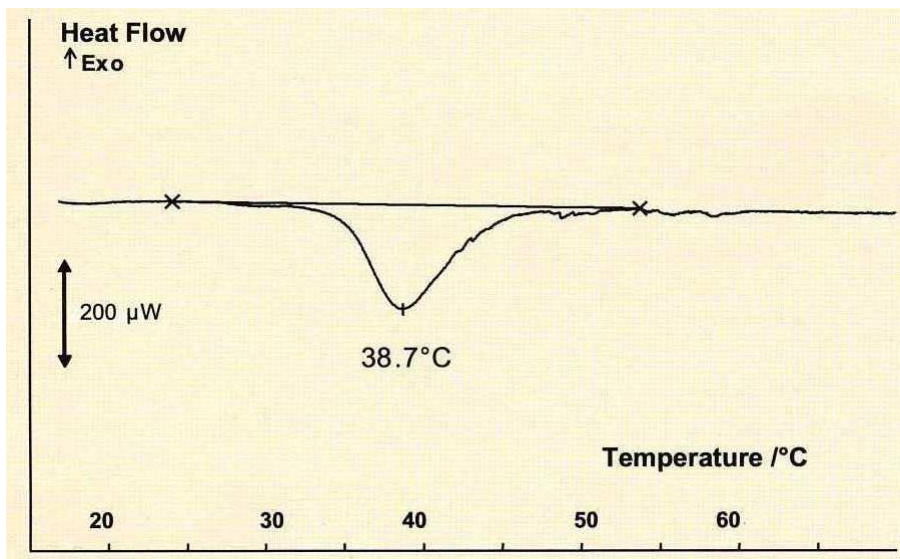


Figure 8.16. Denaturation – aggregation of collagen solutions.

(Source: Aplikáční listy. SETARAM Instrumentation.)

- Starch gelatinization. Starch is a hydrocompatible polymer, naturally forming water-insoluble crystalline granules. If such suspension is heated, a transition of crystalline state occurs, and a gel is formed. It is once again accompanied by a small endothermic effect that is detectable by micro DSC (Fig. 8.17).
- Phase transformations of phospholipids. Phospholipids are one of the cell membrane building blocks. Upon their dispersion in water, two thermal effects can be observed: i) gel/gel transition appearing at a lower temperature, accompanied by a molecular rearrangement, ii) and the following transition between the gel and the crystalline phase, accompanied by melting hydrocarbon chains (Fig. 8.18).

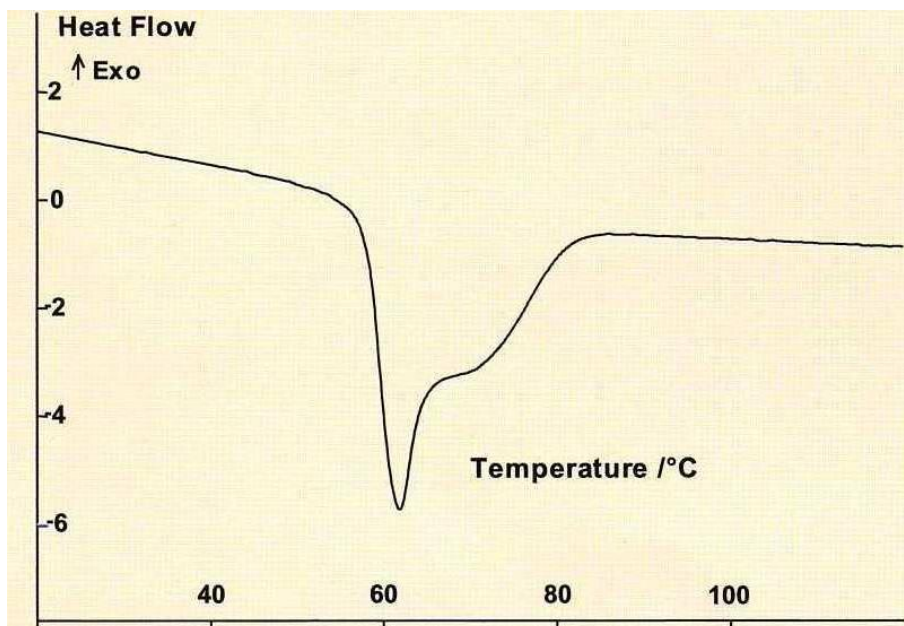


Figure 8.17. Starch gelatinization.
(Source: Aplikační listy. SETARAM Instrumentation.)

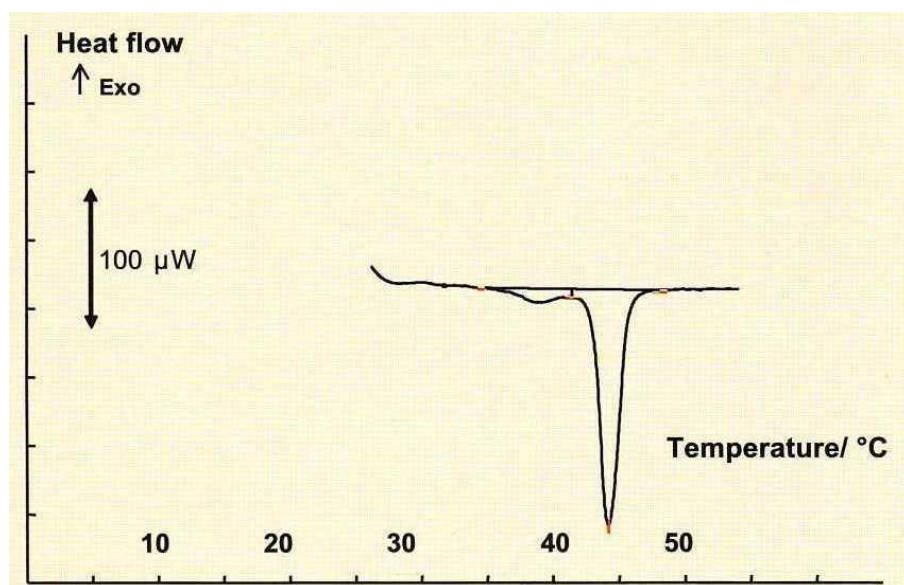


Figure 8.18. Phase transitions of phospholipids.
(Source: Aplikační listy. SETARAM Instrumentation.)

- Denaturation and aggregation of immunoglobulin solution. Immunoglobulin is a protective protein in blood plasma, the lymphatic system, and some other body fluids. Like other protein structures, immunoglobulin solution begins to denature during heating. An endothermal effect accompanies denaturation, and the temperature characterizes the protein's thermal stability. A higher denaturation temperature means a more stable protein. Fig. 8.19 shows an aggregation accompanied by an exothermal effect.

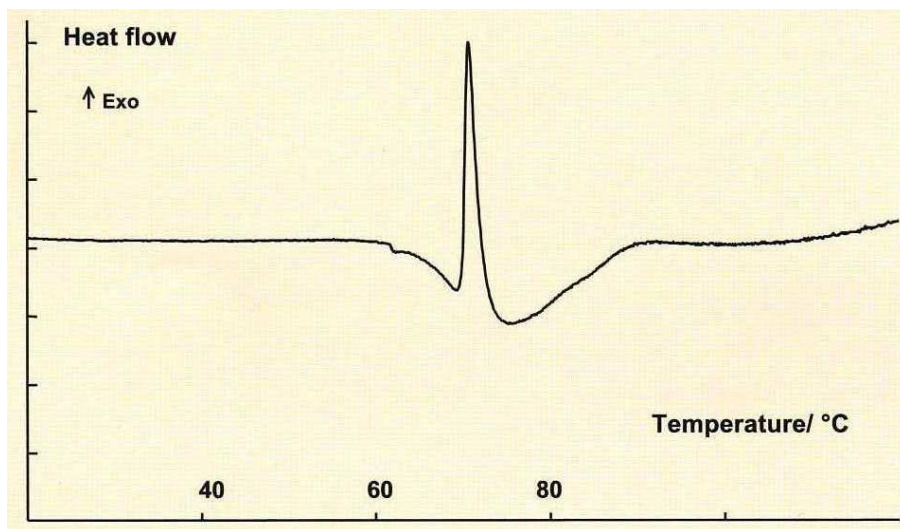


Figure 8.19. Denaturation and aggregation of an immunoglobulin solution.

(Source: *Aplikační listy. SETARAM Instrumentation.*)

The examples mentioned above show that micro DSC can measure minimal thermal changes which cannot be measured by classical thermal analysis methods, such as DSC.

Isothermal mode

- Compatibilities between active substances and excipients. Whether in original or generic products, selection of proper excipients in pharmaceutical development is necessary. Micro DSC can speed up the selection by revealing possible reactions between an excipient and an active substance (Fig. 8.20). The information could otherwise be obtained later from long-term stability tests where product degradation will likely occur by, e.g., formation of similar undesirable substances after a long time (at least three months). The micro DSC measurement is relatively simple, and it is based on measurements of two-component mixtures at predefined ratios and gradually

increasing temperature. The mixture is heated for at least 4 hours at each selected temperature point.

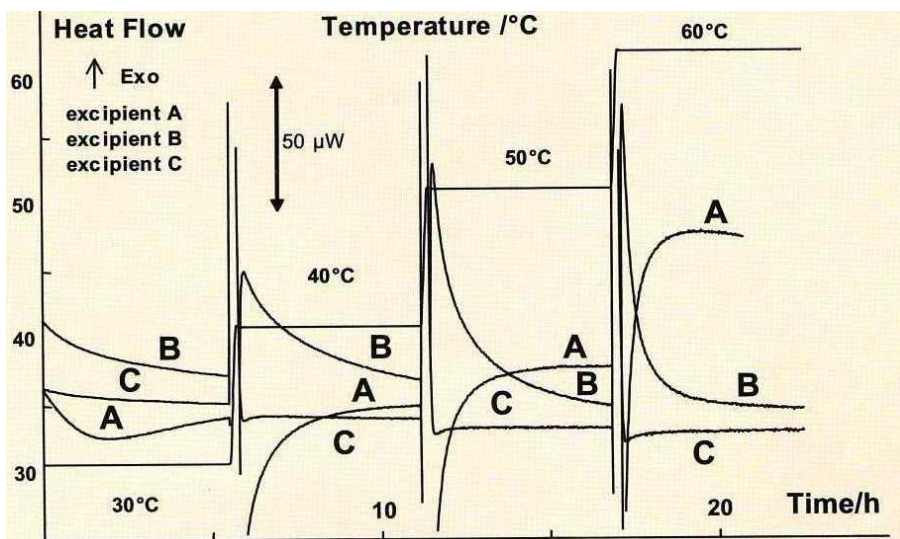


Figure 8.20. Compatibilities of an active substance and excipients. The curve of excipient C remains at zero heat flux value, showing no interaction with the active substance, demonstrating compatibility of the substances. Another two excipients A and B deviate from zero heat flux value and are thus incompatible with the active substance and not suitable for product formulation.

(Source: *Aplikační listy. SETARAM Instrumentation.*)

- Stability of pharmaceutical products. Stability tests are one of the main tests for pharmaceutical, and micro DSC can accurately and rapidly predict their outcome. Fig. 8.21 shows an analysis of two different formulations with the same active ingredient at 80 °C. PREP 1 exhibits a thermal reaction during the test, as a degradation process occurs. This formulation is not acceptable and would be unsatisfactory in long-term stability tests.
- Enzyme reactions. Micro DSC can also be used to determine optimum temperatures for enzymes and to model enzyme reactions. Such a reaction is continually monitored using a mixing cell. Fig. 8.22 shows a study of the transformation of maltose by glucoamylase in water.

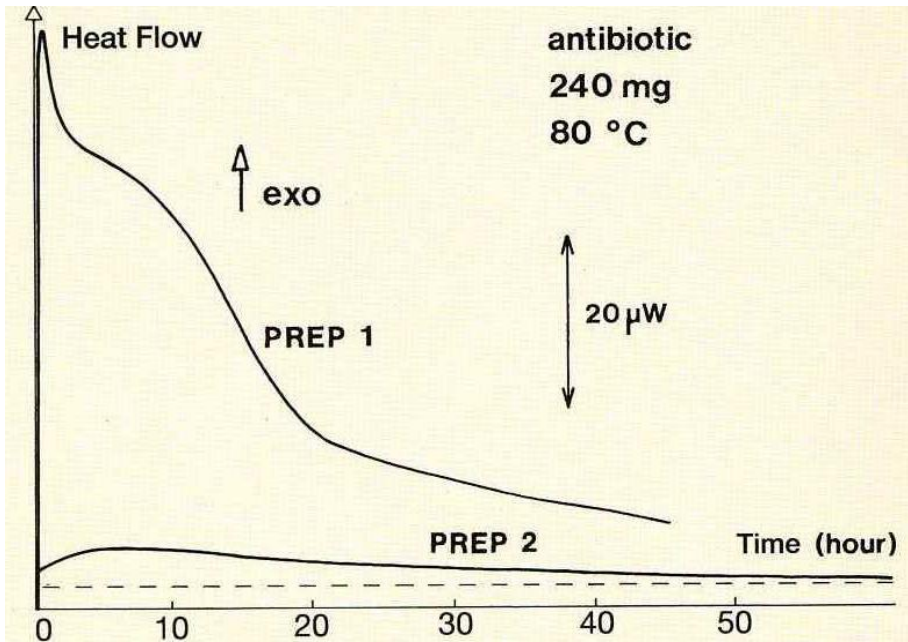


Figure 8.21. Stability of pharmaceutical products.
(Source: Aplikační listy. SETARAM Instrumentation.)

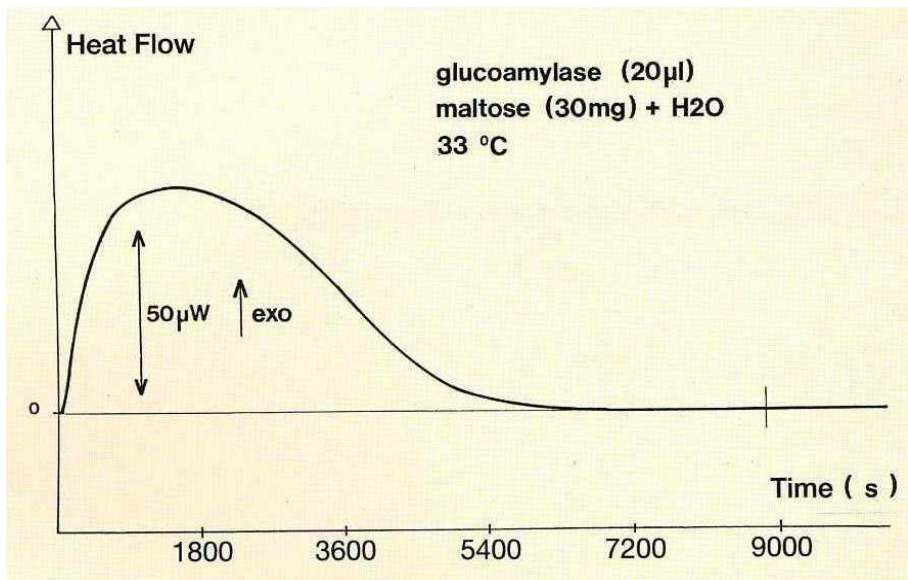


Figure 8.22. Study of glucoamylase induced maltose transformation in water.
(Source: Aplikační listy. SETARAM Instrumentation.)

8.3.7 Temperature modulated differential scanning calorimetry (TMDSC)

8.3.7.1 Nomenclature and method origin

The method came into use in the early nineties of the 20th century and has no established name. Besides temperature modulated differential scanning calorimetry (TMDSC), also other terms are used, e.g., modulated differential scanning calorimetry (MDSC), alternating differential scanning calorimetry (ADSC), or dynamic differential scanning calorimetry (DDSC). The same heating process can be similarly used for thermal gravimetry, thus getting modulated differential thermogravimetry analysis (MDTA). Because the principle is the same, only TMDSC will be discussed.

8.3.7.2 Method principle

As mentioned before, the temperature and the heat flux associated with phase changes are measured in DSC as a function of time and temperature in a defined atmosphere. The heating of the sample is performed at a constant rate. The measuring principle is the same as in classical DSC, but the sample undergoes modulated heating by a periodically changing heat flux. It has a sinusoid shape and superimposes the heat flux from classical DSC, and it linearly varies with time. The result of a classical DSC is a total heat flux. In TMDSC, the total heat flux is interpreted by two terms that characterize reversible (e.g., melting) and irreversible (e.g., crystallization) processes that occur during the measurements. TMDSC allows a more specific study of substance properties or analysis of mixtures that usually cannot be interpreted using DSC.

This measurement provides qualitative and quantitative information about physical and chemical changes with either exothermal or endothermal character or only the thermal capacity of the material changes.

The measurements start by heating at least 2 minutes before a phase transformation, e.g., with 10 °C/min heat rate, the start should be at least 20 °C below the expected transformation. The heating is performed for at least two minutes to reach the phase transition. Table 8.2 shows the effect of heating rate on analysis.

Table 8.2. Effect of heat rate on the course of T_g .

Heating rate [$^{\circ}\text{C}/\text{min}$]	Sensitivity	Reproducibility
5	low	very good
20	good	good
40	very good	low

8.3.7.3 Division of TMDSC curve into reversible and irreversible part

A comparison of heat flux in DSC and TMDSC is shown in Fig. 8.23 and 8.24.

Heat flux consists of sample heating and the following phase transition. DSC is, however, only able to measure their sum. TMDSC can separate these two components.

For all TMDSC experiments, the signal is derived from three measured parameters:

- time
- modulated temperature (as a stimulator)
- modulated heat flux (as a response)

The average value of the modulated heat flux is qualitatively and quantitatively consistent with the average flow value in a conventional DSC method. A calculation using Fourier transform yields an average value.

Reversible heat flux is a capacitive component of the total heat flux. The conversion of specific capacity gives a component corresponding to a classical heat flux.

$$\text{Reversible heat flux} = -C_p \cdot \text{average heat rate}$$

Irreversible heat flux is a kinetic part of the total heat flux.

$$\text{Irreversible part} = \text{Total} - \text{Reversible}$$

Thus:

dQ/dt – total heat flux

C_p – measured capacity

dT/dt – average rate

$C_p (dT/dt)$ – reversible part

$f(T,t)$ – irreversible part

$$\frac{dQ}{dt} = C_p \frac{dT}{dt} + f(t, T)$$

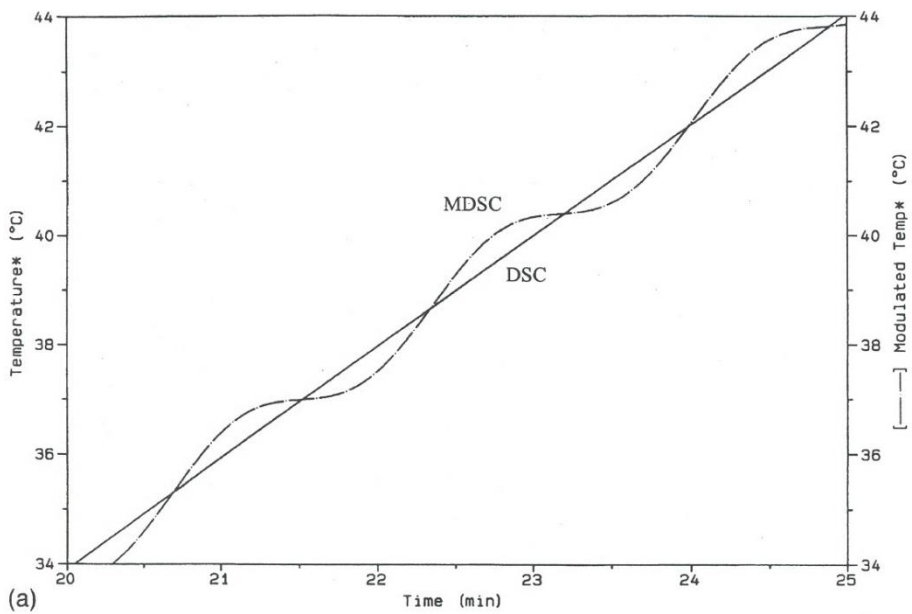


Figure 8.23. Continued.

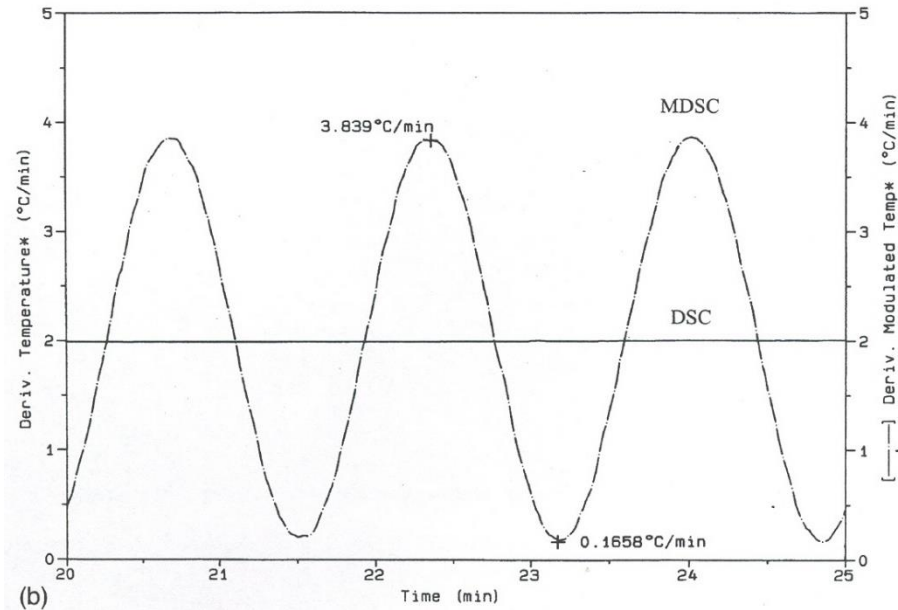


Figure 8.23. Input signal in DSC and TMDSC, (a) temperature as a function of time for a typical DSC and TMDSC experiment; (b) temperature increase (heating rate) as a function of time for a typical DSC and TMDSC experiment.

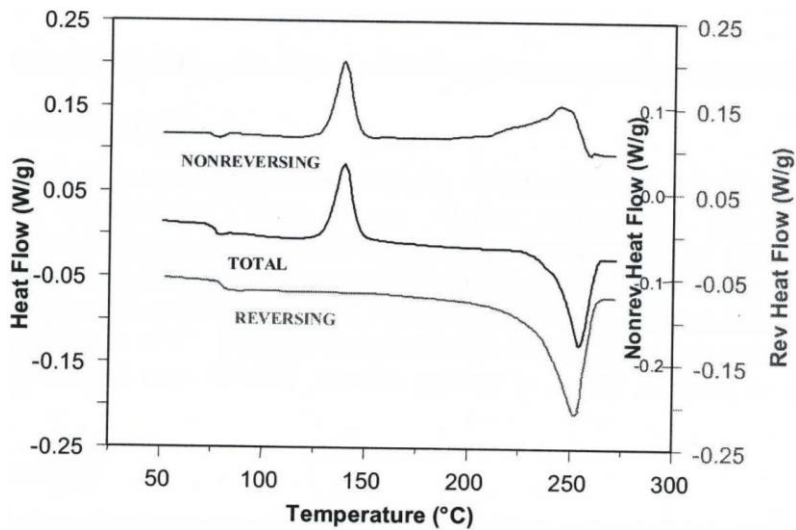


Figure 8.24. The middle curve represents a curve obtained by the classical DSC method. The other two curves are reversible and irreversible parts in TMDSC.

8.3.7.4 *Advantages of TMDSC*

- increased detection sensitivity for glass transition
- increased resolution capability – the process happens at two rates simultaneously
- ability to divide capacity change processes and kinetic processes
- the reversible component is suitable for glass transition and melting point measurements
- the irreversible component is suitable for measuring enthalpic relaxation, evaporation, crystallization, degradation, some types of melting
- ability to measure thermal capacity changes even during reactions (phase transitions)
- a better interpretation of crystallization processes and crystal structures of semicrystalline polymers
- possibility to identify recrystallization even during melting
- measuring of very low thermal conductivities
- elimination of the overlap of different thermal effects (separation of reversible and irreversible processes)
- mixture analysis
- high sensitivity

8.3.7.5 *Application of TMDSC in combination with DSC*

- measuring mixtures of various substances
- measuring mixtures of crystalline forms, including combinations with a content of one amorphous substance (Fig. 8.25)
- TMDSC does not replace classical DSC but complements the information obtained by DSC
- it is always advised to start with analyses using the classical DSC and use the TMDSC method in case of ambiguous results

- TMDSC complements the information from classical DSC for mixtures or compounds with low T_g

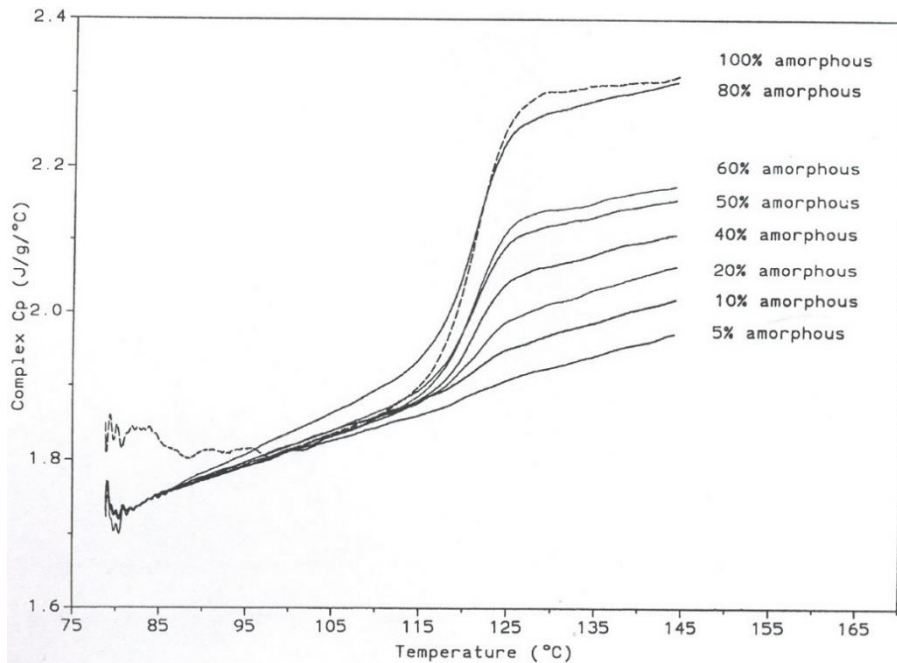


Figure 8.25. Dependence of thermal capacity on the content of an amorphous phase in a mixture with a crystalline substance.

8.3.8 Thermogravimetry (TGA)

Thermogravimetric analysis, or thermogravimetry in short (TG or TGA), is a thermal analysis that quantitatively monitors sample weight changes (increase, decrease) during temperature changes. The immediate weight w is evaluated in a static configuration depending on time t at a constant temperature T (isothermal technique). See the below-listed relation:

$$w = f(t) \quad T - \text{constant}$$

A problem that can affect the analysis in an undetermined manner is the initial sample heating to a working temperature. Another problem is the extent to which the heating to isothermal temperature changes the properties of the studied sample.

Thermogravimetry usually refers to a dynamic process when the sample weight w is recorded depending on a programmed temperature increase:

$$w = f(t)$$

Temperature T is a linear function of time in most commercially available devices:

$$\frac{dT}{dt} = \emptyset \quad \emptyset - \text{heat flux}$$

Hence:

$$T = T_0 + \emptyset t \quad T_0 - \text{initial sample, i.e., measurement, temperature}$$

Some devices currently enable periodic heating rate change, i.e., an analogy to TMDSC, which can be regarded as MDTA.

Apparatuses for TGA, i.e., thermobalances, are very accurate scales currently based on a compensation principle – sample weight change is compensated electromagnetically and thus quickly recorded. There are two configuration types of thermobalances: horizontal and vertical (more frequent). Each has its advantages and technical limitations. The construction of the instrument must allow operation under a defined atmosphere. An example of a TG built is shown in Fig. 8.26.

The measurement result is a thermogravimetric curve that states the actual sample weight dependent on temperature and time. The curve shape is affected by the heating rate. The higher the heating rate, the narrower the temperature interval for the weight change to occur. High heating rates may, however, cause that minor changes are not displayed in the curve. An evaluation may include the first derivation of the obtained curve, allowing better resolution of individual processes, see Fig. 8.27.

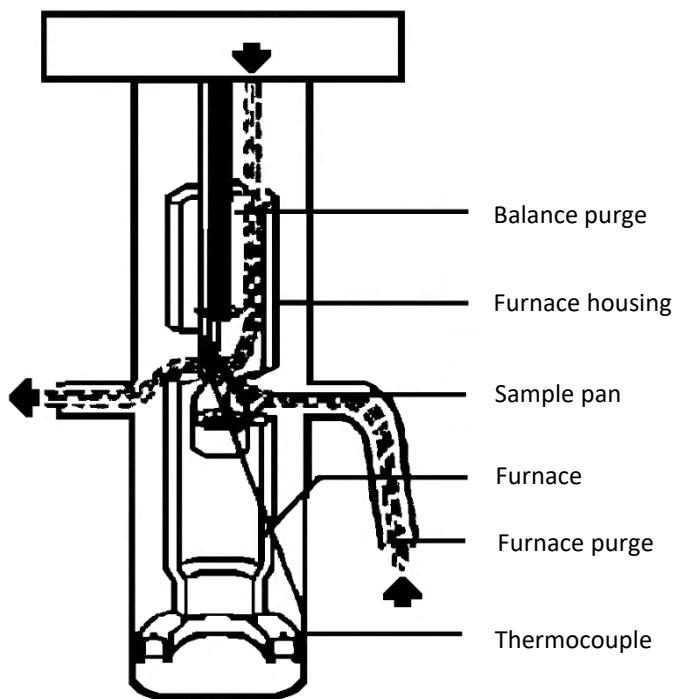


Figure 8.26. Design of TG.

(Source: *Aplikační listy. SETARAM Instrumentation.*)

Thermogravimetry measurement is affected by many factors based on:

- instrument construction and materials
- experimental design (heating rate, heat transfer, atmosphere in the reaction space, gas flow, a temperature measuring method, etc.)
- physical and chemical properties of the sample (weight, particle size, geometry, preparation method, and material history)

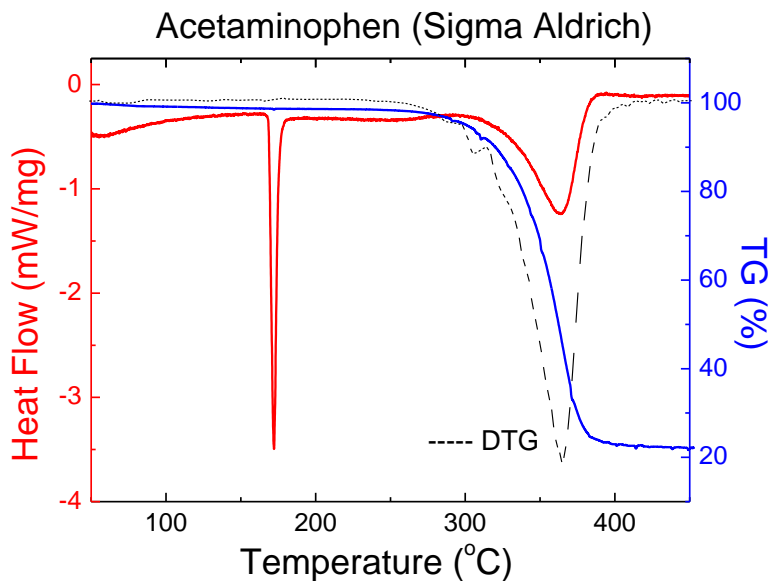


Figure 8.27. DSC and TGA curve with the first derivation DTG.
(Source: Jendrzejewska et al. *Molecules*, 2020.)

The following figures, Fig. 8.28–8.31, contain TGA and DSC curves dealing with the study of hydrates of a sample in development.

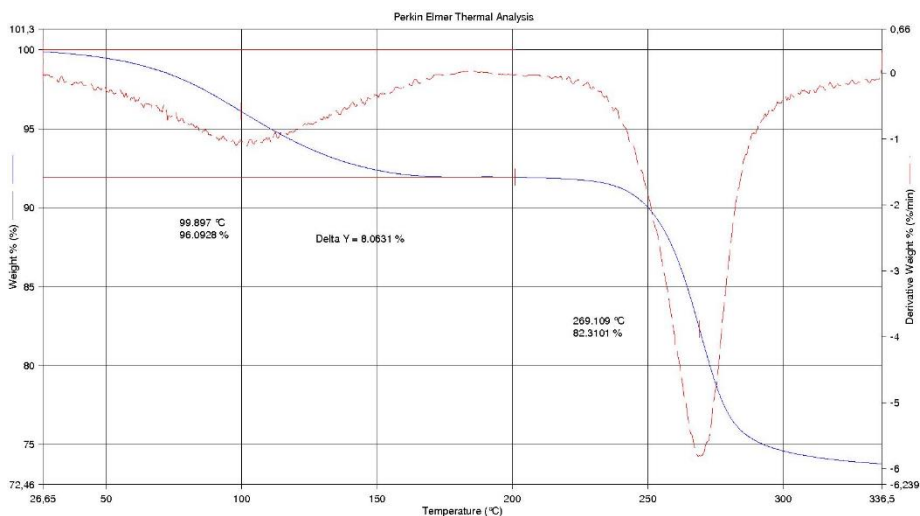


Figure 8.28. TG and DTG curves of a sample with water content around 8% (about 1–2 moles of H₂O after calculation). Sample decomposition occurs at around 270 °C.

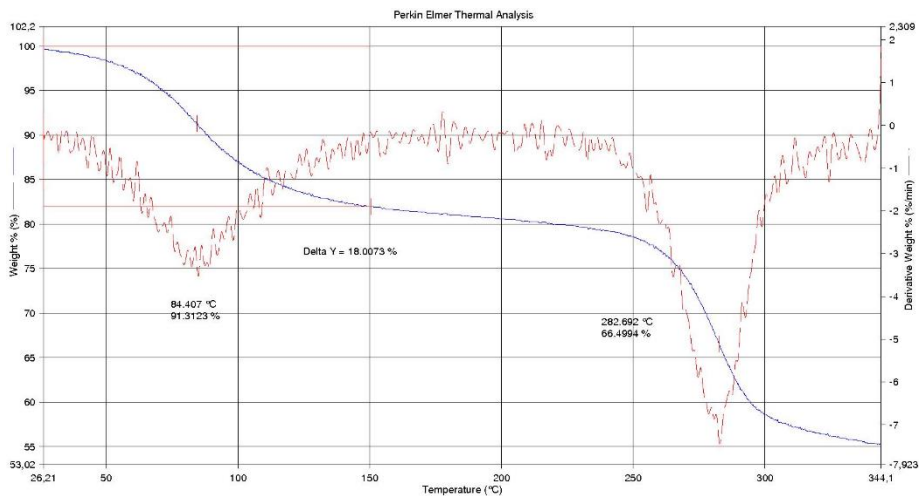


Figure 8.29. TG and DTG curves of a sample with a water content of around 18% (about 4–5 moles of H₂O after calculation). Sample decomposition occurs at approximately 282 °C.

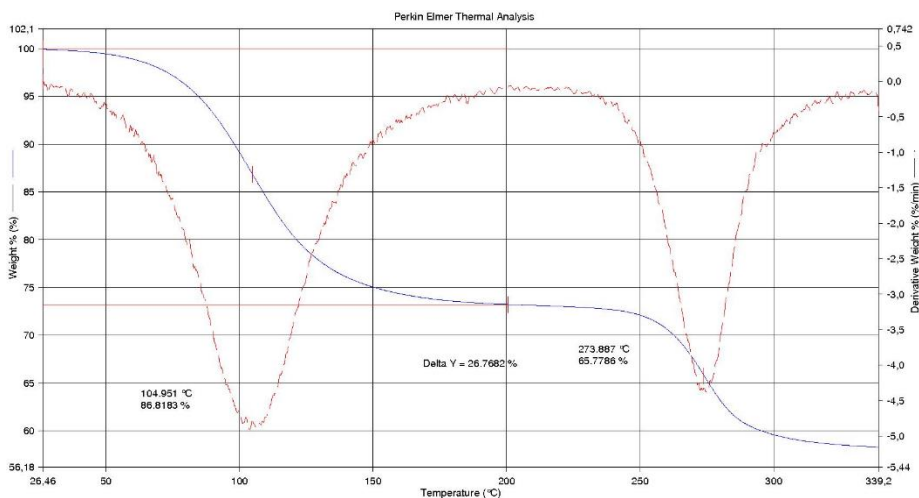


Figure 8.30. TG and DTG curves of a sample with a water content of around 26% (about 7–8 moles of H₂O after calculation). Sample decomposition occurs at about 273 °C.

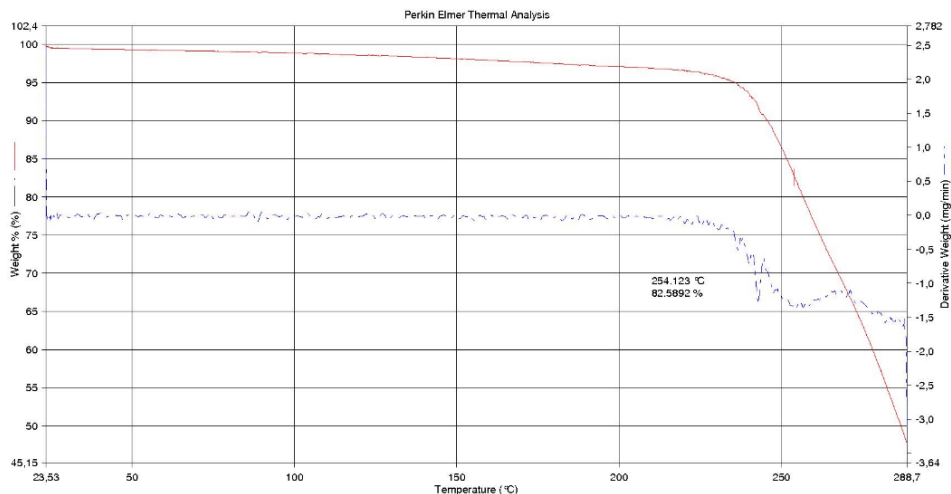


Figure 8.31. TG and DTG curves of a sample containing no water. Sample decomposition occurs at around 254 °C.

8.3.9 Thermally stimulated current (TSC)

This unique thermal method (thermally stimulated current, TSC) uses the so-called molecular mobility which provides information about the substance structure, dynamic parameters ΔH and ΔS , and relaxation (release) time τ .

In TSC, the substance is heated to a temperature T_P in an electric field with intensity E_P for a sufficiently long time t_P , allowing differently moving particles of the studied substance to reach identical orientation in the electric field. In this state, the sample is rapidly cooled to a temperature T_0 , ensuring zero particle motion. The effect of the electric field is then deactivated, and the substance is kept at temperature T_0 for time t_0 . The temperature then linearly increases, the substance returns to the previous state, and current depolarization I_D is recorded as a function of temperature. Temperature T_{max} characterizes each depolarization peak with intensity I_{max} (Fig. 8.32 and 8.33). This technique is particularly suitable for substances with polar character.

Application:

- interactions between the active substance and an excipient
- determination of the ratio of crystalline and amorphous phases in a sample
- detection of a low concentration of amorphous phase (< 1%; see Fig. 8.34)

- determination of crystallinity degree, polymorph resolution (Fig. 8.35).

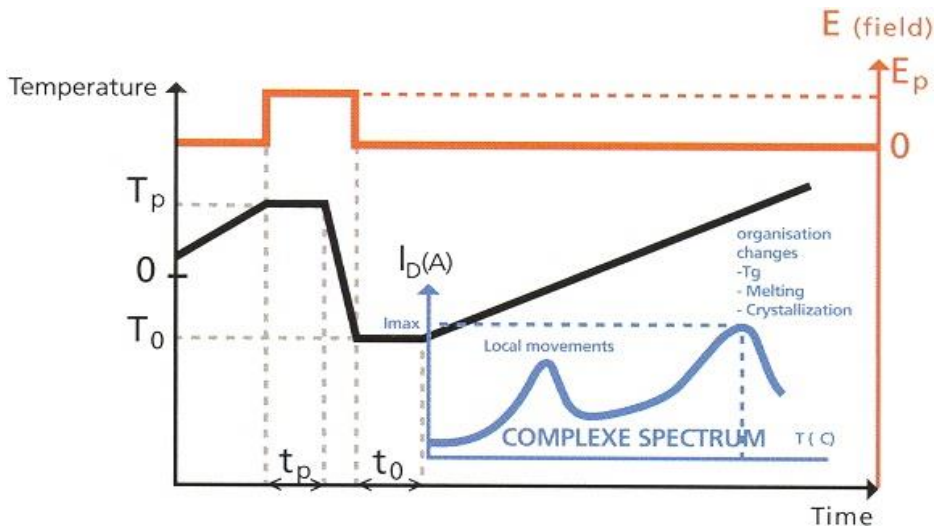


Figure 8.32. Schematic record of a TSC measurement.

(Source: Aplikační listy. SETARAM Instrumentation.)

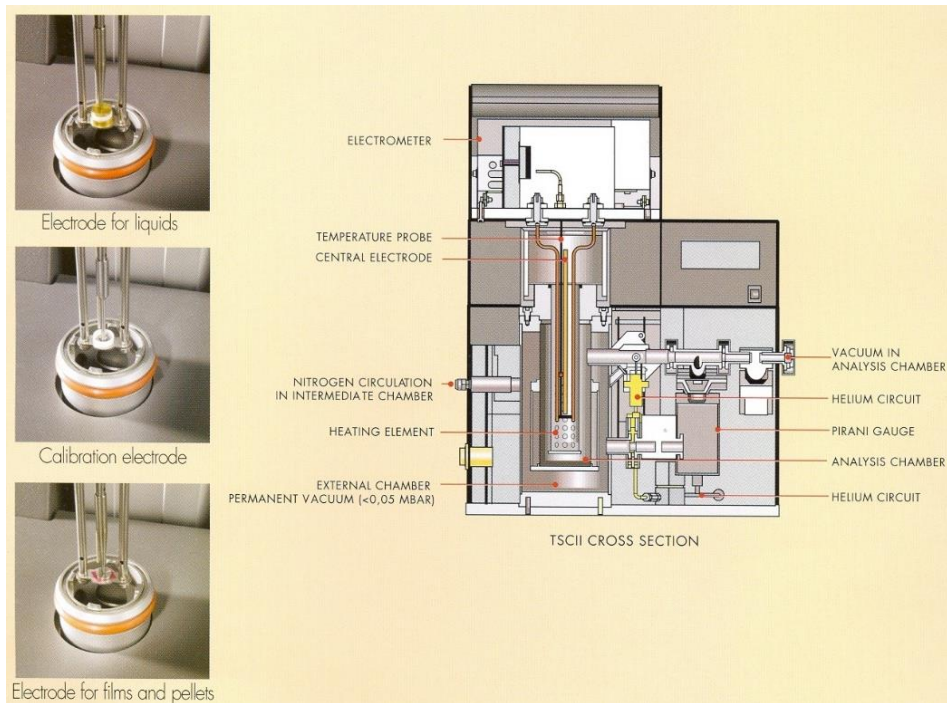


Figure 8.33. Scheme of a TSC instrument.

(Source: Aplikační listy. SETARAM Instrumentation.)

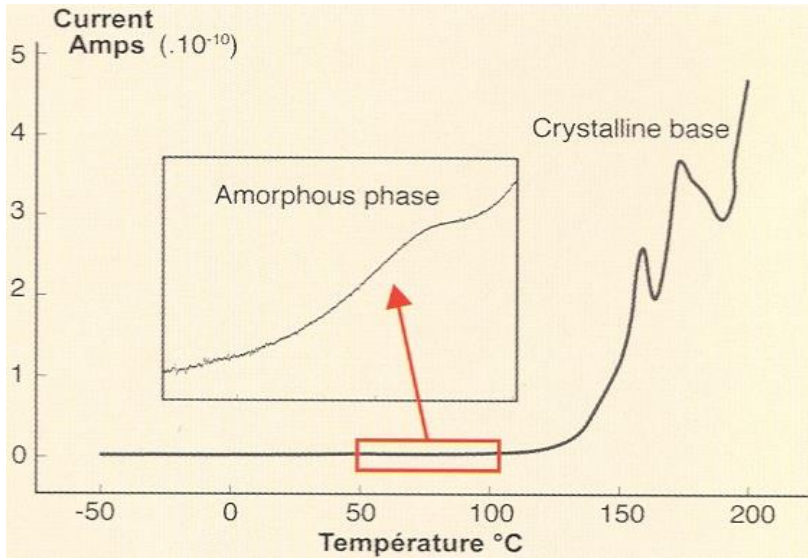


Figure 8.34. Purity of crystalline substances. Detection of amorphous phase content < 1%.

(Source: Aplikáční listy. SETARAM Instrumentation.)

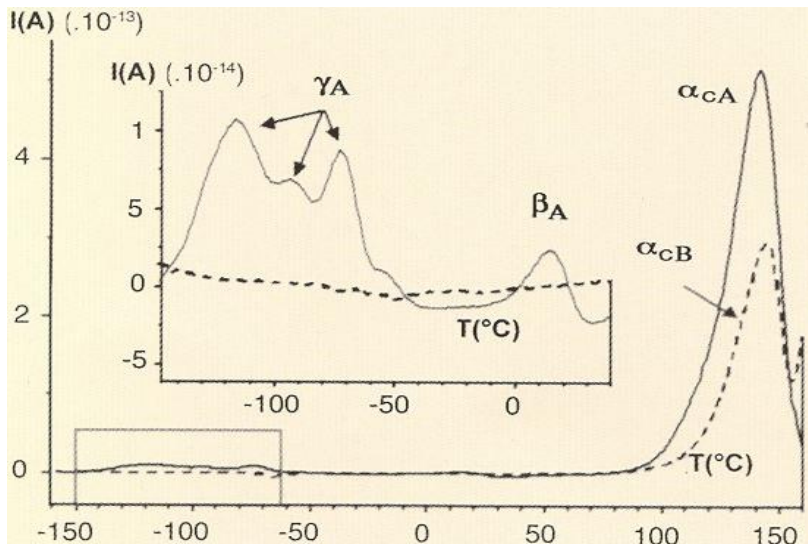


Figure 8.35. Resolution of polymorphic forms A (continuous line) and B (dashed line) of irbesartan using the TSC method. Classical DSC does not allow this differentiation. The peak between 100 and 150 °C is visible also in DSC. Peaks between -150 and -50 °C are only detectable by the TSC method and are characteristic of polymorph A. The α , β , γ denote molecular mobilities.

(Source: Sample measurement record from SETARAM Instrumentation application laboratory.)

8.4 Resources and recommended literature

1. Nicoara M., Locovei C., Opris C., Ursu D., VasIU R., Stoica M. Optimizing the Parameters for In-situ Fabrication of Hybrid Al-Al₂O₃ Composites. *J. Therm. Anal. Calorim.* 2016. <https://doi.org/10.1007/s10973-016-5595-3>
2. Araújo A. A. S., Bezerra M. S., Storpirtis S., Matos J. R. Determination of the melting temperature, heat of fusion, and purity analysis of different samples of zidovudine (AZT) using DSC. *Braz. J. Pharm. Sci.* 2010, 46 (1). <https://doi.org/10.1590/S1984-82502010000100005>
3. Joseph K., Asuvathraman R., Madhavan R. R., Jena H. Studies on Novel Matrices for High Level Waste from Fast Reactor Fuel Reprocessing. *Energy Procedia.* 2011, 7, 518-524. <https://doi.org/10.1016/j.egypro.2011.06.071>
4. Brittain H. G. *Polymorphism in Pharmaceutical Solids.* Marcel Dekker: New York, USA, 1999.
5. *Comprehensive Handbook of Calorimetry and Thermal Analysis.* Sorai M. (Ed.) John Wiley & Sons: New York, USA, 2004.
6. Vaniček J. *Metody termické analýzy. Studijní materiály. Katedra textilních materiálů, Fakulta textilní, Technická univerzita v Liberci: Liberec, Czech republic, 2007.*
7. Řehula, M. *Příručka termoanalytických charakteristik pomocných látek. Studijní materiály. Katedra farmaceutické technologie, Farmaceutická fakulta v Hradci Králové, Univerzita Karlova v Praze: Prague, Czech Republic, 2007.*
8. Gabbott P. *Principles and Applications of Thermal Analysis.* Blackwell Publishing: Singapore, 2008. <https://doi.org/10.1002/9780470697702>
9. Feng X., Ye X., Park J. B., Lu W. Evaluation of the recrystallization kinetics of hot-melt extruded polymeric solid dispersions using an improved Avrami equation. *Drug Dev. Ind. Pharm.* 2014, 41 (9), 1-9. <https://doi.org/10.3109/03639045.2014.958755>
10. Jendrzewska I., Goryczka T., Pietrasik E., Klimontko J., Jampilek J. X-Ray and Thermal Analysis of Selected Drugs Containing Acetaminophen. *Molecules*, 2020, 25 (2020), 5909. <https://doi.org/10.3390/molecules25245909>
11. Qi S. *Analytical Techniques in the Pharmaceutical Sciences.* Eds.; Müllertz A., Perrie Y., Rades T. Springer: New York, USA, 2016.
12. Chiu M. H., Prenner E. J. Differential scanning calorimetry: An invaluable tool for a detailed thermodynamic characterization of macromolecules and their interactions. *J. Pharm. Bioallied. Sci.* 2011, 3 (1), 39-59. <https://doi.org/10.4103/0975-7406.76463>

13. Craig D. Q. M. Reading M. *Thermal Analysis of Pharmaceuticals*. CRC Press: Boca Raton, USA, 2006. <https://doi.org/10.1201/9781420014891>
14. Ebeid E. Z. M., Zakaria M. B. *Thermal Analysis: From Introductory Fundamentals to Advanced Applications*. Elsevier: Amsterdam, Netherlands, 2021. <https://doi.org/10.1016/B978-0-323-90191-8.00004-X>
15. Zainal N. F. A., Saiter J. M., Halim S. I. A., Lucas R., Chan C. H. Thermal analysis: basic concept of differential scanning calorimetry and thermogravimetry for beginners. *Chemistry Teacher International*. 2021, 3 (2), 59-75. <https://doi.org/10.1515/cti-2020-0010>

9 Dissolution testing in pharmaceutical industry

Martin Čulen, Anna Řezáčová

9.1 Biopharmaceutical classification system

Biopharmaceutical classification system (BCS) proposed by Amidon *et al.* in 1995 divides drugs into four different classes depending on their solubility and permeability (Table 9.1). The aim of this system was to create a theoretical basis for correlation of *in vitro* dissolution profiles with *in vivo* drug bioavailability. A drug is considered highly soluble when its highest dose is soluble in 250 ml of dissolution medium (the usual volume of juices in stomach during bioavailability testing) at a physiological pH range (1.0–7.5). A drug is classified as highly permeable if its absorbed amount (from a solution) is greater than 90%.

Table 9.1. Biopharmaceutical classification system.

Class	Solubility	Permeability
Class I	high	high
Class II	low	high
Class III	high	low
Class IV	low	low

BCS is based on a simple absorption model in which the intestine is represented by a cylindrical pipe where the absorption takes place. In this model, there are round identically sized, inert (does not allow metabolism) particles. Solubility is independent on the size of these particles and on the intestinal pH gradient, and there is no possibility of aggregation. Amidon *et al.* demonstrated that key parameters that control the absorption of drugs are three variables: A_n – absorption number, D_n – dissolution number, D_o – dose number.

9 Dissolution testing in pharmaceutical industry

These parameters represent the basic processes, such as: permeability of membranes, dissolution rate and drug dose:

M_0 – administered drug dose

$$D_o = \frac{M_o/V_o}{C_s}$$

V_0 – standardized stomach volume (~ 250 ml)

C_s – saturation (balanced) solubility of a substance, in mg/ml

$$D_n = \frac{t_{res}}{t_{diss}}$$

t_{res} – average drug residence time drug in the gastrointestinal tract (GIT) (~ 180 min)

t_{diss} – time needed to dissolve the dosage form,

$$A_n = \frac{P_{eff}}{R} t_{res}$$

P_{eff} – effective permeability

R – radius of the intestinal segment

Pharmaceuticals of the BCS class I exhibit good solubility and permeability and have very good absorption in general. Immediate release (IR) tablets containing an API from this class are expected to have 100% intestinal absorption, provided that at least 85% of the total amount is dissolved in 30 minutes within the whole physiological pH range. For this reason, these products do not have to undergo bioequivalence studies.

Class II substances are poorly soluble and highly permeable compounds. They are characterized by high A_n and D_o . Here, dissolution significantly affects the absorption rate and extent, which may lead to incomplete absorption and bioavailability despite good membrane permeability (A_n). These drugs may be influenced by the length of their GIT transit time. The longer the transit time at the absorption site, the greater the expected absorption. Absorption can be limited by equilibrium or kinetics type. For drugs with high D_o , the API dose is too high, considering the solubility of the substance in the GIT fluids. For drugs with $D_n < 1$, the dissolution process is too slow to be completed before the drug leaves the intestinal absorption site. For these drugs, the in vitro – in vivo correlation is expected to be good when in vitro dissolution rate is similar to the in vivo dissolution rate. As a general rule, any factor that increases the speed and extent of in vivo dissolution of class II drugs also increases their bioavailability. It is therefore assumed that administration of high-fat meals increases solubility and thus also bioavailability of class II drugs.

Class III substances have high solubility but poor permeability. Intestinal absorption of these substances is limited by the speed of their permeation through the membrane, while their dissolution is fast.

Class IV substances are characterized by low solubility and low permeability and exhibit large inter- and intrapersonal variability.

9.2 Dissolution testing of substances

9.2.1 Intrinsic dissolution

These tests determine the rate of true (intrinsic) dissolution of pure solid substances (APIs) or their mixtures with excipients. The rate of true dissolution is a theoretical quantity related to a chemically pure solid substance with no porosity. In reality, the tests are conducted with samples of pure APIs or APIs in mixtures which do not have a non-zero but still a minimal porosity achieved by compaction (into tablets). The rate of true dissolution (dm/dt) is defined as a mass of tested substance dissolved per time from a unit of surface ($\text{mg}/\text{min}\cdot\text{cm}^2$):

S – API solubility

A – release surface for the API

$$\frac{dm}{dt} = \frac{VdC}{dt} = -kA(S - C) \quad m - \text{sample mass}$$

k – rate of true dissolution

C – concentration in time t

Physical properties of solid materials such as polymorphism, crystal shape, particle size, specific surface, etc., all affect dissolution rate. The rate is also influenced by environmental conditions, i.e., experiment parameters. Thus, the dissolution rate is affected by compacting pressure, temperature, pH, medium composition, medium ionic strength, and buffer capacity. A critical parameter of true dissolution is tablet preparation – compaction – which must meet the dissolution requirements. A basic requirement is that no phase changes occur (crystal form, solvate formation, etc.) during the whole sample preparation and dissolution process. This must be confirmed by X-ray diffraction or another suitable analysis at all stages of the dissolution test (sample at input, after compaction, remaining material after dissolution). The experiment ends after the comprimete is released or falls out of its matrix (see below), because the process no longer meets the condition of a constant contact surface.

9.2.1.1 Experimental design

Weighed amount of a powdered material is compressed into a special metallic matrix with a hole sized 0.5 cm^2 (Fig. 9.1). The matrix with the sample is fixed to the dissolution instrument axis and immersed into a selected dissolution medium (defined composition, pH, ionic strength, temperature, surfactants, etc.) which is stirred with a predefined speed. Samples of the medium are collected at predetermined time intervals during a selected part of the test. The total testing time varies depending on the nature of the tested material. As a rule, the sampling should be maintained until at least 10% of the sample is transferred into solution.

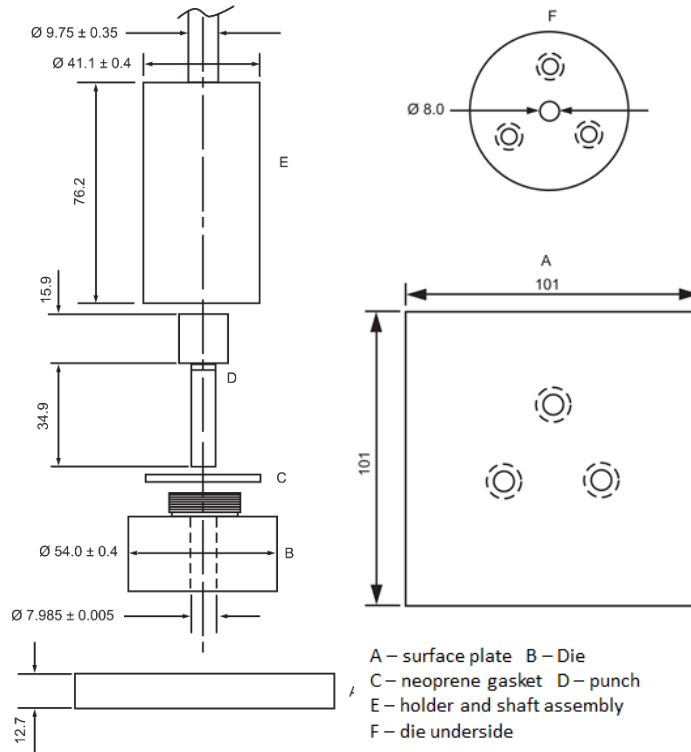


Figure 9.1. Continued.

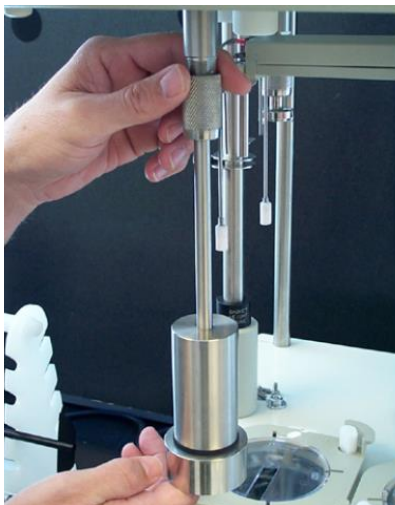


Figure 9.1. Apparatus for intrinsic dissolution, dimensions in millimetres.
(Edited according to: *European Pharmacopea 10.0* and commercial materials of *Varian* company.)

Calculations are based on integrated form of modified Noyes-Whitney equation. Providing that the immersion condition is met, the concentration gradient can be considered as constant. Data on the cumulative dissolved amount from each sampling must be corrected by the loss of the medium during sampling. To calculate the true dissolution rate, cumulative amount of the solved substance per area unit of the comprimate is plotted against time needed to dissolve 10% of the sample. The cumulative amount of the dissolved sample per area unit is given by the ratio of the cumulative amount of substance solved during the specified time and the area of the comprimate exposed to the solvent solution (usually a matrix of 0.5 cm^2). The dissolution rate in $\text{mg}/\text{min}\cdot\text{cm}^2$, at the given rotation speed, is then given by the direction of the calculated regression line (Fig. 9.2).

Results must always be interpreted according to the experimental conditions. The method is not absolute, but comparative, and therefore suitable for comparing quality of substances or intermediates from specific stages of pharmaceutical production. The experiment parameters are set to achieve discrimination between different sample types (Fig. 9.3–9.6).

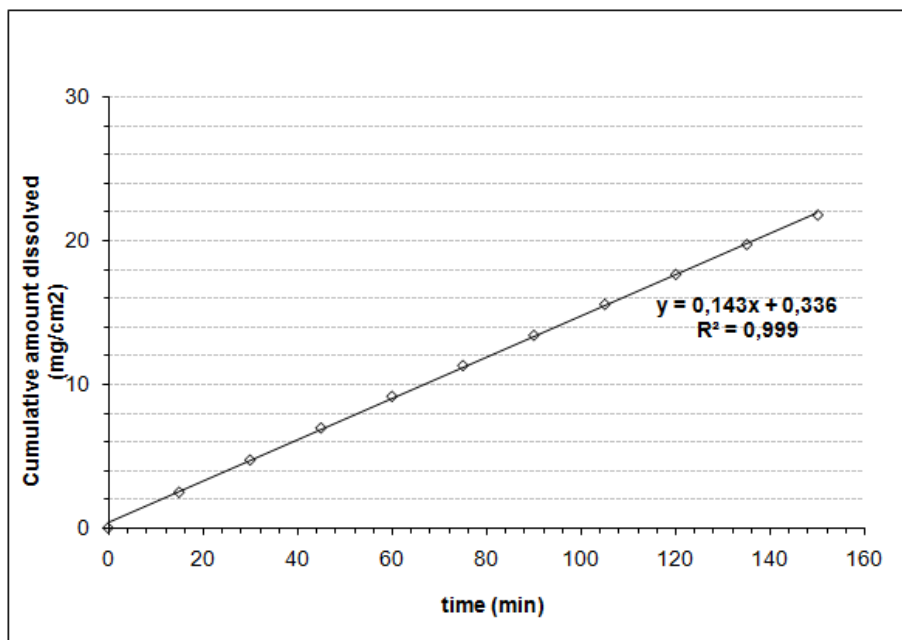


Figure 9.2. Evaluation of intrinsic dissolution – calculated regression line.

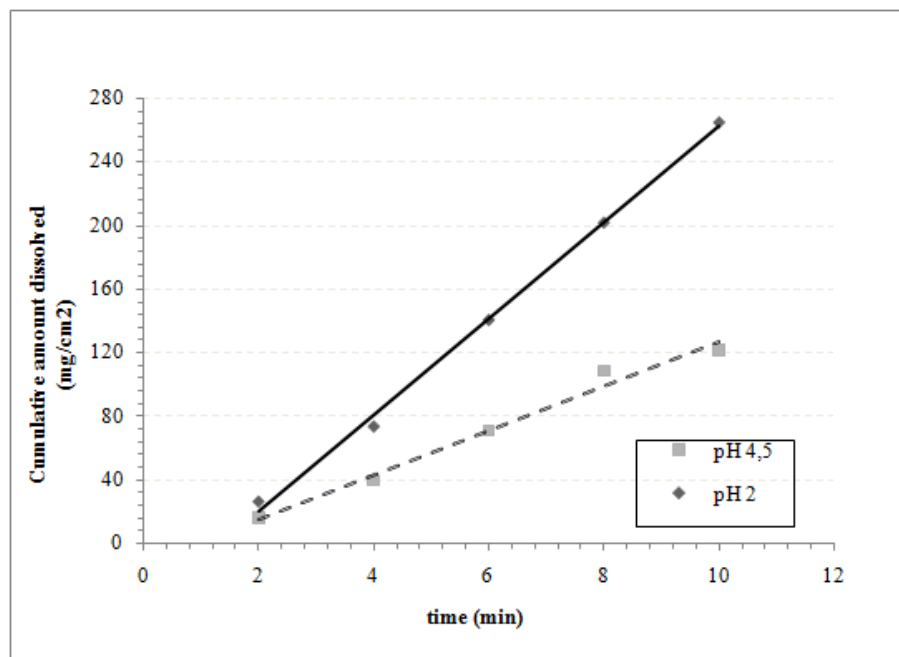


Figure 9.3. Comparison of dissolution profiles of one substance at different pH.

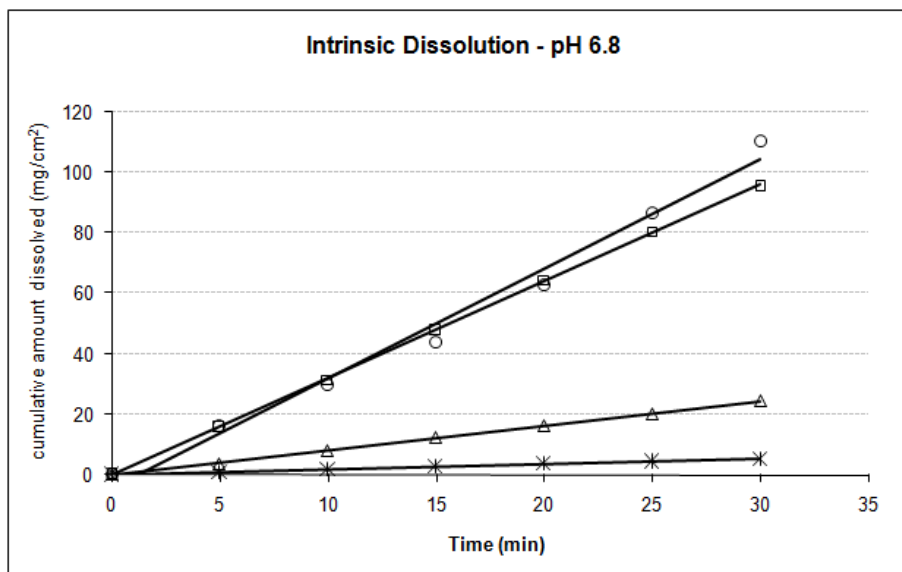


Figure 9.4. Comparison of dissolution profiles of different salts of one substance, in phosphate buffer of pH 6.8, at 37 °C.

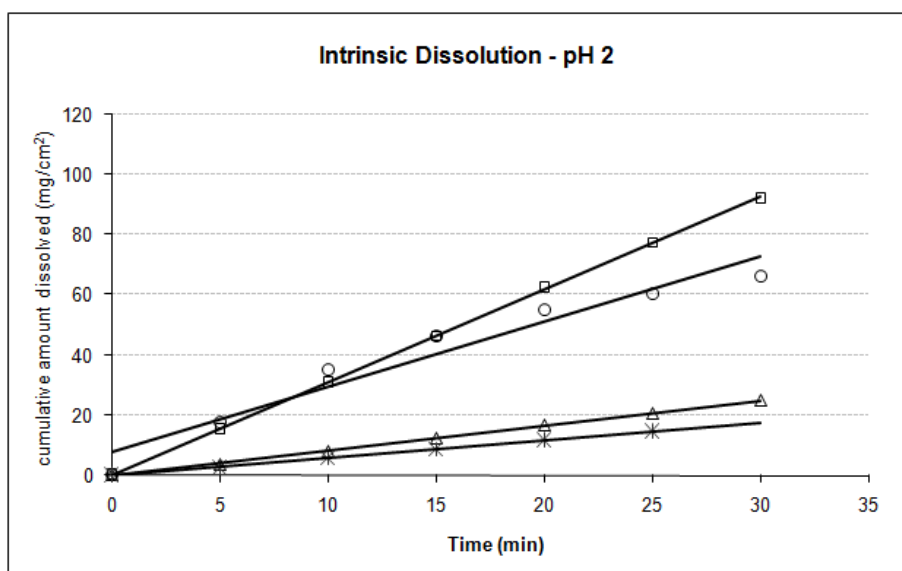


Figure 9.5. Comparison of dissolution profiles of different salts of one substance, in 0.01M HCl, at 37 °C.

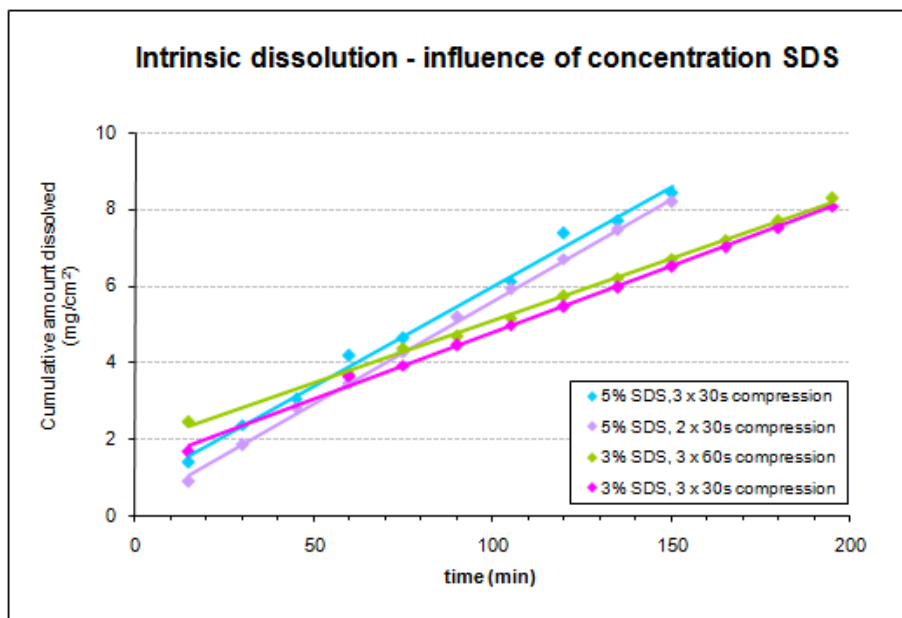


Figure 9.6. Effect of different SDS (surfactant) concentrations and different compaction parameters.

9.2.2 Apparent dissolution

This method is used for testing of substances, powder mixtures, or grained powders. It uses flow-through dissolution method (USP apparatus IV). The system with the flow-through cell is also used for sustained-release formulations, or formulations containing poorly soluble APIs. The flow-through cell system is used for dosage forms such as tablets and capsules. Dissolution rate of pure substances can be characterized using specific cells designed for powder samples.

Method advantages:

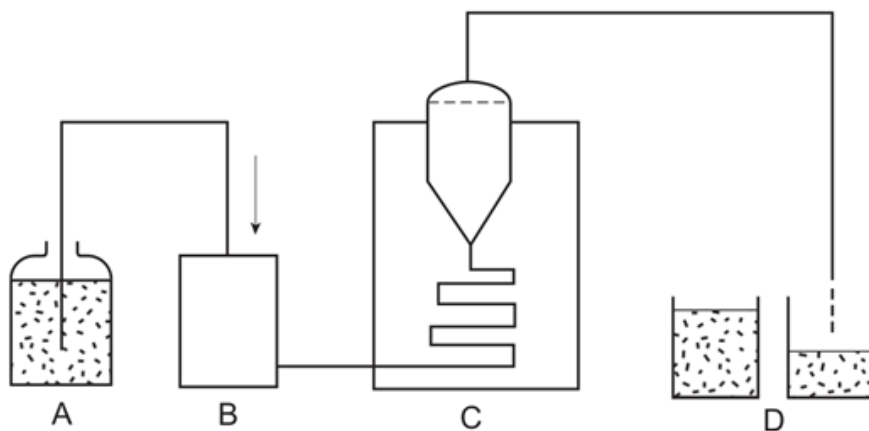
- elimination of problematic behavior of powder samples in USP I and USP II apparatuses, i.e., floatation in the vessel or sticking to the spindle
- immediate wetting of the studied powders
- simple changing of the medium pH
- prevention of settling of heavier granulates in USP II apparatuses

- improved alternative for true (intrinsic) API dissolution without possible unwanted modifications occurring during API compaction
- comparison of different dissolution rates as pure substance kinetics; these differences in dissolution rates can be caused by various crystal configurations, particle morphologies, etc.

9.2.2.1 Experimental procedure

All parts of the instrument that come into contact with the formulation or the dissolution medium must be chemically inert, i.e., not absorbing the tested substances, non-reactive, and not interfering with the tested sample. All metal parts that come into contact with the product or dissolution medium are made of stainless steel or coated in a suitable inert material that prevents reaction or interference with the product or the dissolution medium.

Eluate is filtered at cell exit and can be analyzed directly (on-line) or collected by a fraction collector (off-line). Dissolved gases can cause formation of bubbles in the medium, which may bias the results. In such case, the dissolved gases must be removed prior the test. The problem of API agglomeration can be prevented by using surfactants.



A – reservoir for dissolution medium B – pump C – thermostatically controlled flow-through cell and filter D – collection vessels for analysis

Figure 9.7. Scheme of a flow-through cell apparatus.

(Edited according to: *European Pharmacopea 10.0.*)

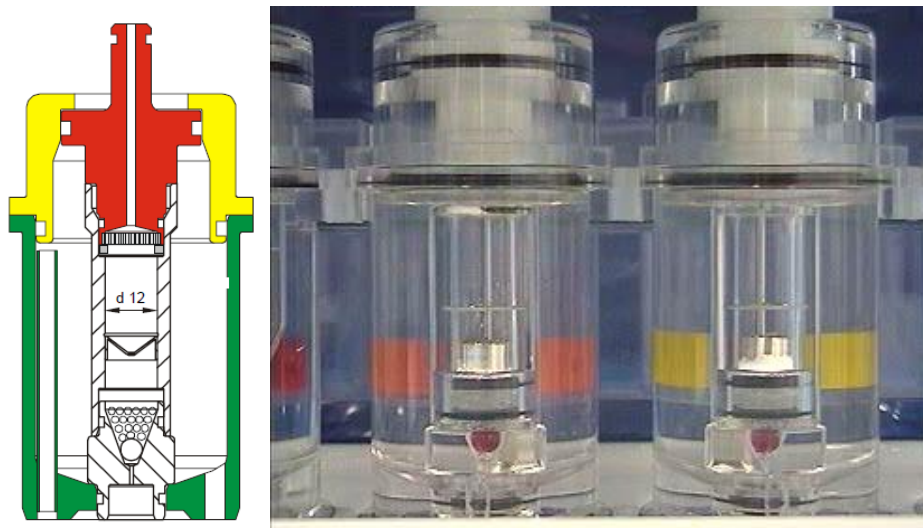


Figure 9.8. Flow-through cell for powders.

(Edited according to commercial materials by Sotax company.)

Open circuit: fresh dissolution medium is continuously pumped through the cells while a known amount of the eluate is analyzed and the rest is pumped out as a waste. Open circuit enables simple pH changes, analysis of low soluble substances, working with small API amounts, maintaining sink conditions (i.e., preventing drug saturation), *in vivo* – *in vitro* correlations even with multiple pH changes (as there is no method means for automatic medium change in the USP).

Closed circuit: the medium circulates in the system after flowing through the cells. In this case it is possible to work with small volumes – less than 400 ml (or even 5 ml), large volumes – higher than 1000 ml (depending on the cell type), to detect very low API concentrations, and to perform dissolution of special dosage forms (powders, pellets, suspensions, soft gelatin capsules, implants, gels and creams, etc.).

Samples are collected at the cell exit, regardless of whether the circuit is open or closed. The amount of the released active substance during a defined time is expressed as a percentage of the declared amount.

This is the only dissolution method to express dissolution rate as kinetics, not as an equilibrium state. In the case of a closed circuit, the data have a shape of a classic dissolution curve – cumulative (like for USP apparatus I and II). With an open system, the curve has a shape of a differential shape (see Fig. 9.9).

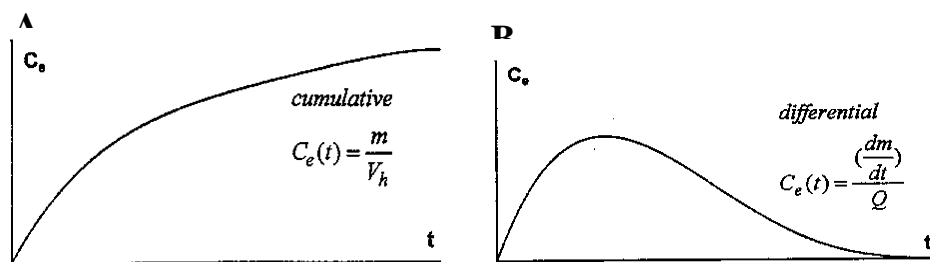


Figure 9.9. A. Dissolution profile from a closed circuit. B. Dissolution profile from an open circuit.

(Source: commercial presentation by Sotax company)

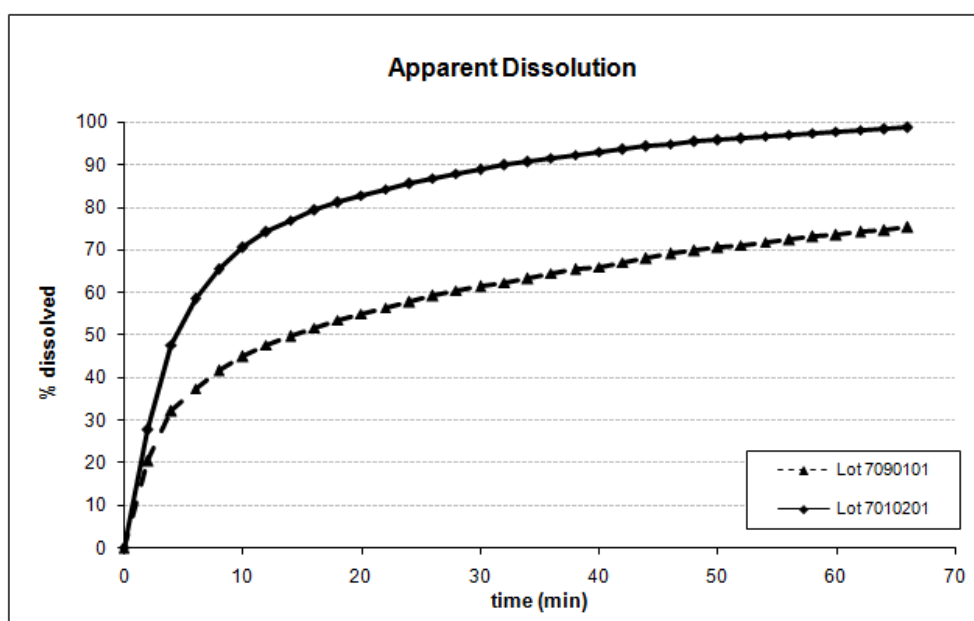


Figure 9.10. Comparison of dissolution profiles of one substance originating from different production sites, tested in a closed circuit in phosphate buffer with pH 6.8 at 37 °C.

9.3 Dissolution testing of solid dosage forms

9.3.1 Dissolution

Before an API is absorbed, it must be first released from the dosage form. Depending on the dosage form, the following processes occur:

- disintegration (disintegration of a solid dosage form to smaller particle clusters – aggregates)
- disaggregation (disintegration of aggregates into undissolved API particles)
- dissolution (dissolution of solid API particles in the digestion fluid)

Solid dosage forms consisting of coarse grains are subjected to all three steps whereas an API that is already dissolved in a dosage form is only mixed with the juice in the digestive tract.

Dissolution of a solid compound can be described as a two-step process. First, the API molecules are released from the solid dosage form surface into the surrounding environment of the dissolution medium. At this stage, a saturated layer is formed, i.e., a diffusion layer adjacent to the API surface. Second, the API diffuses into the whole solution volume according to the concentration gradient – from area with high API concentration to areas with low concentrations. Dissolution rate in time is described by Noyes-Whitney equation:

Dx/dt – dissolution rate

A – surface area of the dissolving dosage form

D – diffusion coefficient

$$\frac{Dx}{dt} = \frac{AD}{\delta} C_s - \left(\frac{X_d}{V} \right)$$

δ – thickness of the diffusion layer surrounding the dosage form

C_s – saturation (equilibrium) dissolution of active substance in mg/ml

X_d – amount of dissolved substance in time t and volume of the dissolution medium V

Dissolution rate is influenced by the physico-chemical properties of the tested API and the prevailing physiological conditions in the gastrointestinal tract (GIT) that are different for individual patients and depend on fed or fasted state. The aim of formulation strategies is to change these properties so that the dissolution rate of low soluble active substances is increased. These strategies include micronization, preparation of nanosuspensions, microemulsions, oil formulations, and use of complexing substances, such as cyclodextrins.

Table 2.2. List of physico-chemical and physiological characteristics which influence dissolution of an API in GIT.

Parameter	Physico-chemical characteristic	Physiological characteristic
Surface area (A)	Particle wettability	size, Surfactants contained in gastric fluid and bile
Diffusion coefficient (D)	Molecular shape	size and Viscosity of luminal content
Diffusion layer thickness (δ)		Motility type, flow rate
API solubility (C_s)	Hydrophilicity, crystal arrangement, solubilization, pKa	pH, buffer capacity, bile, food composition
Amount of dissolved API (X_d)		API removal by absorption – sink condition
Solvent volume (V)		Secretion, administered fluids

According to the equation above, any changes in the dissolution medium which effectively increase the solubility of the studied formulation should theoretically lead to higher dissolution rate. If the substance dissolution rate is < 1 , it is required

to use a dissolution medium similar to the GIT juices in order to achieve an adequate *in vitro* – *in vivo* correlation (correlation between test results and bioavailability *in vivo*). However, the use of surfactants in dissolution media, aimed to increase solubility and simulate environment similar to GIT, conversely leads to slowing of the dissolution rate. This effect indicates that dissolution of substances with poor water solubility is more complex in such media than described by the equation.

9.3.2 Experimental dissolution methods

Dissolution test determines the quantity of an API released from a solid dosage form (e.g., tablet, capsule, or suppository). The following dosage form types are discerned according to API release rates:

- immediate release (also conventional release)
- extended release (also prolonged release)
- delayed release (also sustained release, enteric coated, gastro-resistant)

Such test is used to determine compliance with the requirements for dissolution of orally administered solid dosage forms. The dissolution test is required for all solid dosage forms as an output quality control. Dissolution test must be discriminatory, precise, accurate, robust, and transferrable.

Selection of an instrument depends on the physico-chemical properties of the dosage form. The following four types of dissolution apparatuses are commonly used for dissolution testing:

- basket
- paddle
- reciprocating cylinder
- flow-through cell

The following parameters are specified when determining dissolution rate of an API from a solid dosage form:

- apparatus; in case of a flow-through cell, it is required to state the cell type
- composition, volume, and temperature of the dissolution medium

- rotation or dissolution medium flow rate
- duration, method, and amount of the testing solution used for sample collection, or conditions of continuous monitoring
- analysis method
- acceptance criteria

9.3.2.1 Experimental procedure

The procedure for a basket, paddle, and reciprocating cylinder apparatus is usually designed to maintain sink conditions. This represents an approach where the material that is already in solution does not significantly affect the release rate of the rest of the API. "Sink" condition normally occurs when the volume of the dissolution medium is 3–10 times higher than the volume of a saturated solution.

The dissolution medium is usually aqueous. The composition of the medium is selected according to physico-chemical properties of the API and the excipients, and falls in the range of biorelevant conditions that the dosage form would be subjected to after administration. This applies especially to pH and ionic strength of the dissolution medium. The pH of a dissolution medium is usually set in the range from 1 to 8. In certain cases, a higher pH value may be required. Hydrochloric acid with concentration of 0.1 mol/l is used to maintain lower pH in the acid region. Pure water is recommended as a dissolution medium, only if pH does not affect dissolution. In specific cases, upon approval by a legitimate authority, the dissolution medium may contain enzymes, surfactants, and other inorganic and organic substances. Testing of products with poorly water-soluble active substances may require a necessary adjustment of the medium. In these cases, it is recommended to use low concentrations of a surfactant and to avoid use of organic solvents. Gases dissolved in the dissolution medium may also affect dissolution results. This applies especially to the flow-through cell, where it is necessary to degas the dissolution medium to prevent bubble formation in the cell. In paddle and basket apparatuses, the volume of a dissolution medium is usually 500–1000 ml. Stirring speed is usually between 50 and 100 rev/min and must not exceed 150 rev/min. The flow rate of the medium in a flow-through cell is usually between 4 and 50 ml/min.

9.3.3 Dissolution apparatuses

The selection is based on the physico-chemical characteristics of the tested dosage form. All parts of the device that come into contact with the product or the dissolution medium must be chemically inert, i.e., non-absorbing, non-reactive, and not interfering with the tested sample. All metal parts that meet the product or the dissolution medium must be made of stainless steel or coated in a suitable inert material that prevents reactions or interference with the product or the dissolution medium. No part of the apparatus or its accessories may exhibit vibrations or fluctuations, and the rotation of the spindle and the flow through the cell must be continuous.

The dissolution apparatuses are typically termed according to US pharmacopeia (USP).

9.3.3.1 USP 1 apparatus – basket

The instrument consists of: a vessel made of glass or other inert, transparent material and may be covered with a lid; engine; drive shaft and a cylindrical basket (mixing unit). The vessel is partially immersed in a water bath of an adequate size or equipped with a suitable heating equipment, such as a heating jacket. Water bath or heating equipment enables to maintain temperature of 37 ± 0.5 °C inside the vessel. A see-through instrument that allows free observation of the processes is more appropriate. The engine allows speed adjustment and its maintenance within $\pm 4\%$. The dosage form is put into a dry basket at the beginning of each experiment. The distance between the inner bottom of the vessel and the bottom of the basket is kept at 25 ± 2 mm during the test.

9 Dissolution testing in pharmaceutical industry

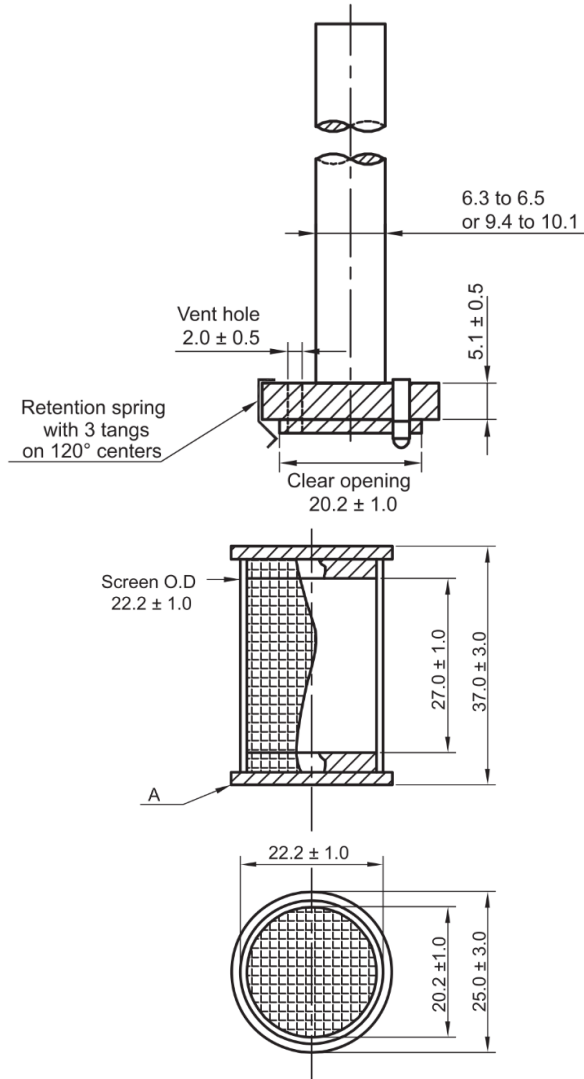


Figure 9.11. Continued.



Figure 9.11. A sectional view and a photo of a USP 1 dissolution apparatus (dimensions in millimeters).

(Edited according to: European Pharmacopea 10.0, commercial materials by Varian company, and www.cecilinstruments.com, 18.6.2010.)

9.3.3.2 USP 2 apparatus – paddle

The same apparatus is used as with USP 1, with the exception that the mixing unit consists of a paddle attached to the shaft. The shaft must be centered with the vertical axis of the vessel, and its rotation must be smooth and without noticeable vibrations that could affect the results. The vertical central axis of the paddle stirrer passes through the axis of the shaft so that the bottom of the paddle is in level with the bottom of the shaft. The paddle must meet the specifications given in Fig. 9.12. The distance between the bottom of the paddle and the inside bottom of the vessel is maintained at 25 ± 2 mm. The paddle is made of metal or a suitable inert, inflexible material, and forms a single unit with the shaft. To prevent the floating of the dosage form, a small, free piece of a non-reactive material such as a small wire spiral can be used. The dosage form is then kept in this spiral or a similar housing, as shown in Fig. 9.13. Other proven attachment tools can also be applied.

The limitations of USP methods 1 and 2 are that they represent traditional closed models where the dissolved API remains and accumulates in the system, opposed to

9 Dissolution testing in pharmaceutical industry

in vivo conditions where the API is rapidly absorbed, and the concentration gradient is renewed. Floating of the dosage form on the surface or its sticking to the bottom of the basket may also occur. Another disadvantage is the unequal hydrodynamics in different parts of the system.

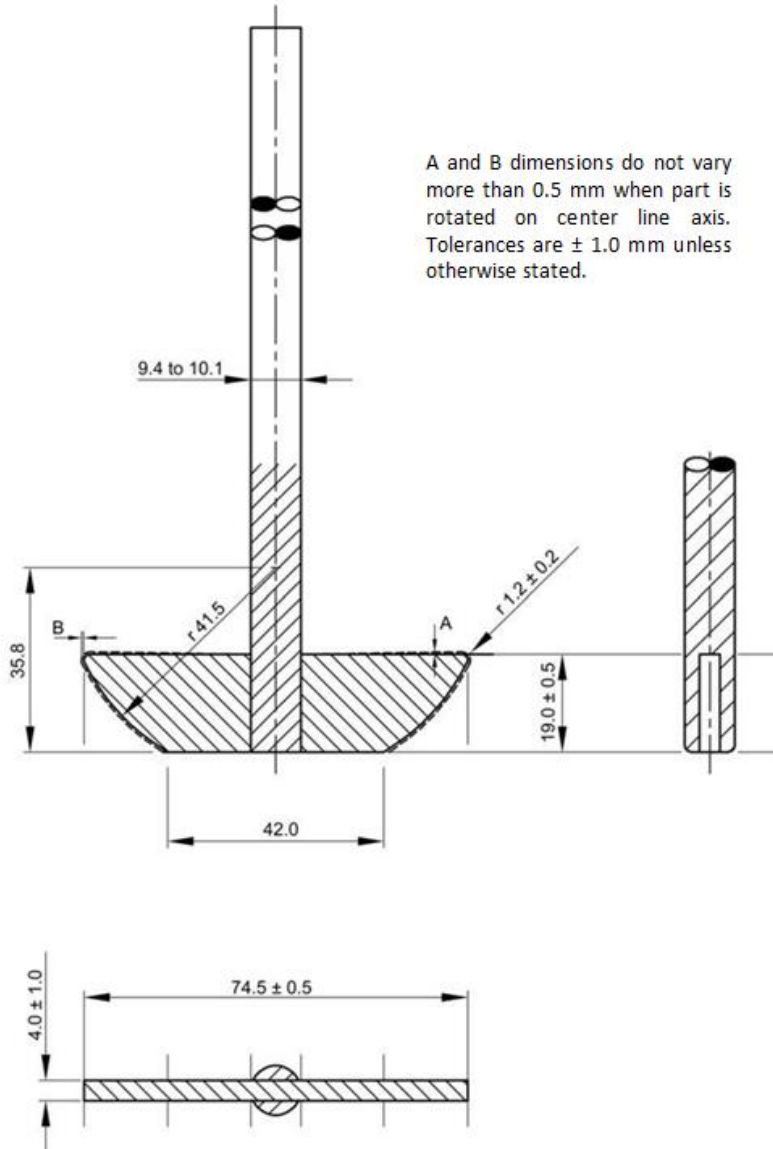
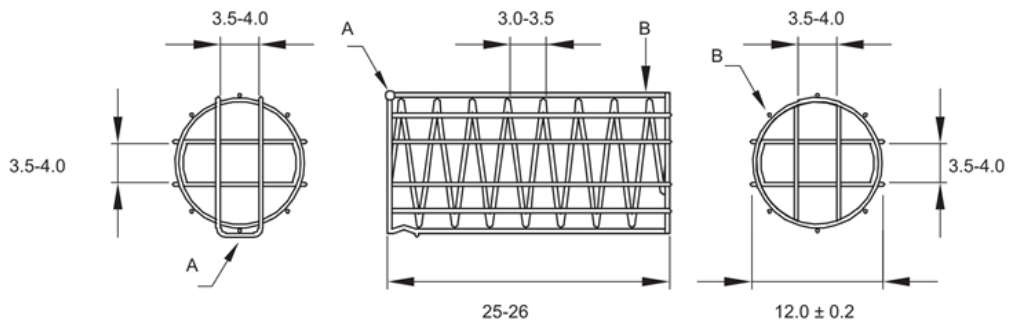


Figure 9.12. Continued.



Figure 9.12. A sectional view and a photo of a USP 2 dissolution apparatus (dimensions in millimeters).

(Edited according to: European Pharmacopea 10.0, and commercial materials by Varian company)



A – acid-resistant wire clasp B – acid-resistant wire support

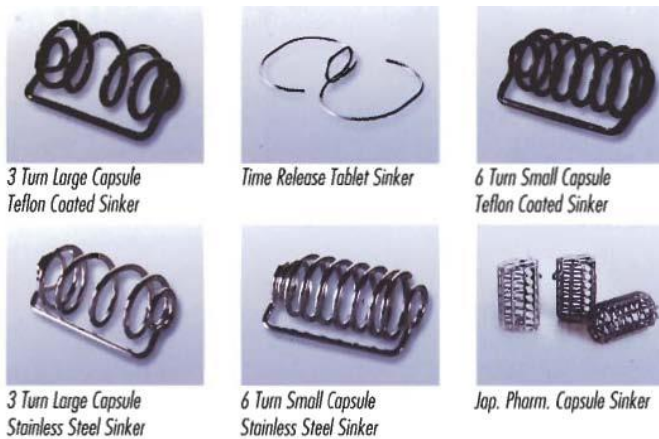


Figure 9.13. A sectional view and a photo of an alternative holding cage (dimensions in millimeters).

(Edited according to: European Pharmacopea 10.0, and commercial materials by LabHut company.)

9.3.3.3 Dissolution testing procedure for USP 1 and 2 apparatuses

Solid dosage forms with normal and sustained release

An apparatus is assembled, and the vessels are filled with a specified volume of a dissolution medium which is then heated to 37 ± 0.5 °C. Dosage form is placed into the vessel. It is necessary to carefully avoid formation of air bubbles on the surface of the tested product. The rotation is switched on at a specified rotation speed. Collection of samples is performed at each specified time or time interval. In the case of repeated samplings, the volume removed for analysis is replaced with the same volume of a fresh dissolution medium with temperature of 37 °C. In cases, where the medium replacement is proven unnecessary, the volume change is corrected in the calculations. During the test, the vessel is covered with a lid and the medium temperature of the medium is controlled at appropriate intervals. The analysis is carried out using appropriate analytical methods for quantitative determination of the given active substance. The test is repeated using other dosage forms.

Solid dosage forms with sustained release

The test consists of a phase in an acidic environment and then a phase with a buffered solution. It may differ in the dosage form transfer between the buffered solutions – addition to the acid environment (method A) or total replacement of the medium (method B).

9.3.3.4 USP 3 apparatus – reciprocating cylinder

The apparatus consists of a set of cylindrical glass vessels with a flat bottom, a set of reciprocating glass cylinders, inert clips and meshes designed to cover the upper and the lower parts of the reciprocating cylinders, engine and a drive component for the reciprocating vertical movement of the cylinders inside the vessels or also for their horizontal movement into another vessel series. The vessels are partially submerged in a water bath which allows to maintain a temperature of 37 ± 0.5 °C. An apparatus allowing observation of the product and the reciprocating cylinders is preferred. The vessels are equipped with evaporation lids, which remain in place during the test. Unless specified otherwise, the dimensions of components correspond to the values shown in Fig. 9.14.

The apparatus enables easier simulation of the GIT conditions (pH changes and the corresponding transit times). The release of an API from a product occurs in 6 media with different pH. The method is particularly suitable for sustained release (SR) products and verification of the resistance of a dosage form against a strong mechanical stress.

9 Dissolution testing in pharmaceutical industry

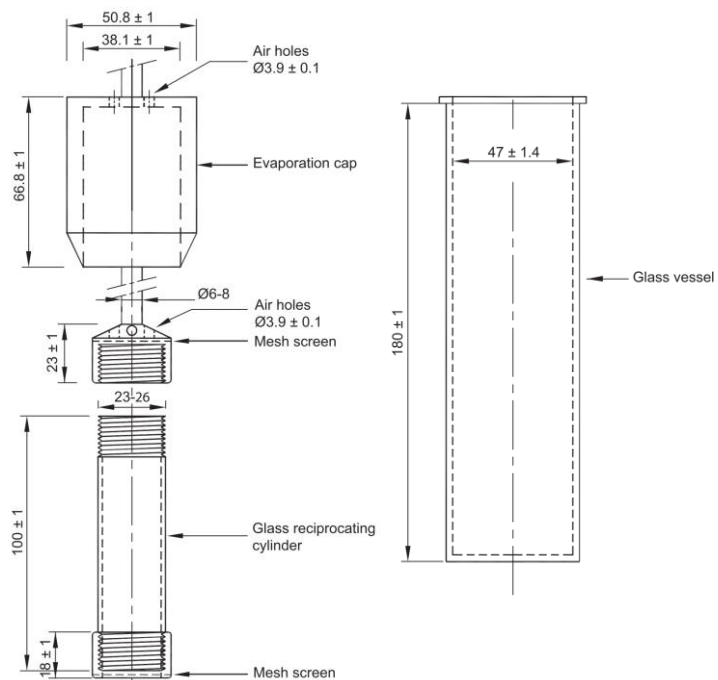


Figure 9.14. A sectional view and a photo of a USP 3 dissolution apparatus (dimensions in millimeters).

(Edited according to: European Pharmacopea 10.0, and commercial materials by Varian company)

9.3.3.5 USP 4 apparatus – flow-through cell

The apparatus consists of a storage tank, a pump driving the dissolution medium, a flow-through cell, and a water bath which keeps the dissolution medium at 37 ± 0.5 °C. The cells have specified dimensions. The pump which propels the dissolution medium through the cell must maintain a constant flow and a sinusoidal flow profile. The flow-through cell (Fig. 9.15–1.17) is made of a transparent and inert material and is vertically connected with a filter system that prevents leakage of undissolved particles from the top of the cell. Standard cell diameters are 12 mm and 22.6 mm. The bottom conical part of the cell is usually filled with small glass beads, and one bead that is placed into the tip of the cone to prevent entry of the small glass beads (if used) into the cell. There are special holders designed for some special types of dosage forms (Fig. 9.15 and 1.16).

If the dissolution medium is formed by a buffer solution, its pH is adjusted to ± 0.05 pH units of the specified value. Dissolved gases must be removed from the dissolution medium as they may result in formation of bubbles released during the test and may affect the progress and results.

9 Dissolution testing in pharmaceutical industry

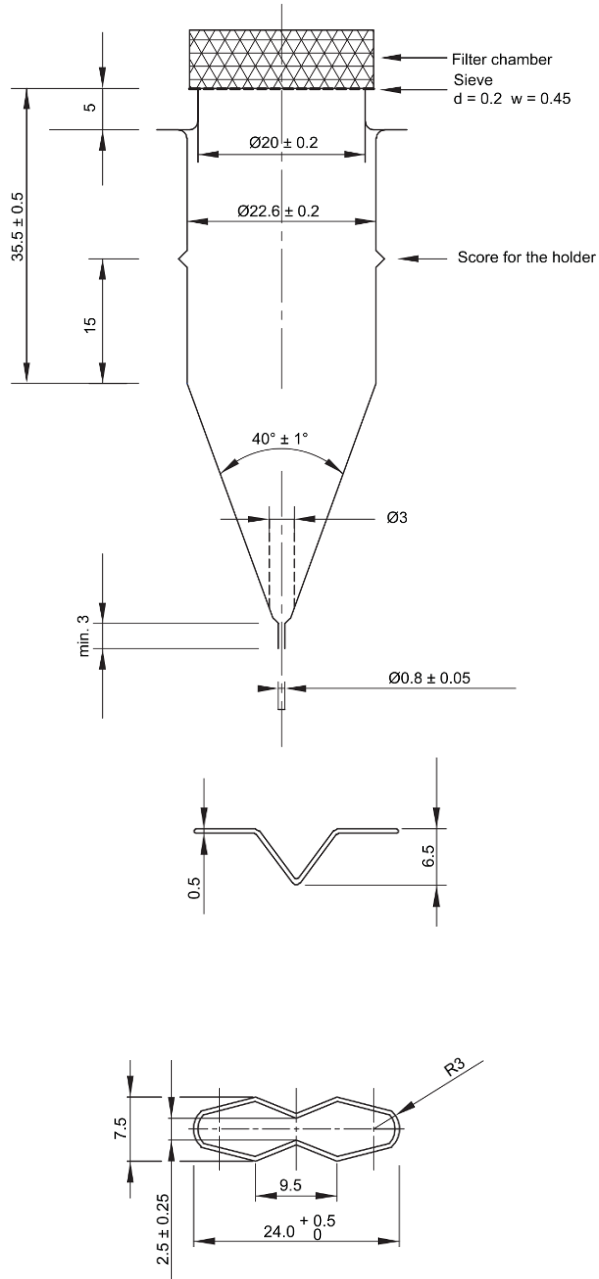


Figure 9.15. Continued.



Figure 9.15. A sectional view and a photo of a USP 4 dissolution apparatus: large cell for tablets and capsules (upper picture part), tablet holder (dimensions in millimetres).

(Edited according to: European Pharmacopea 10.0, and commercial materials by Sotax company)

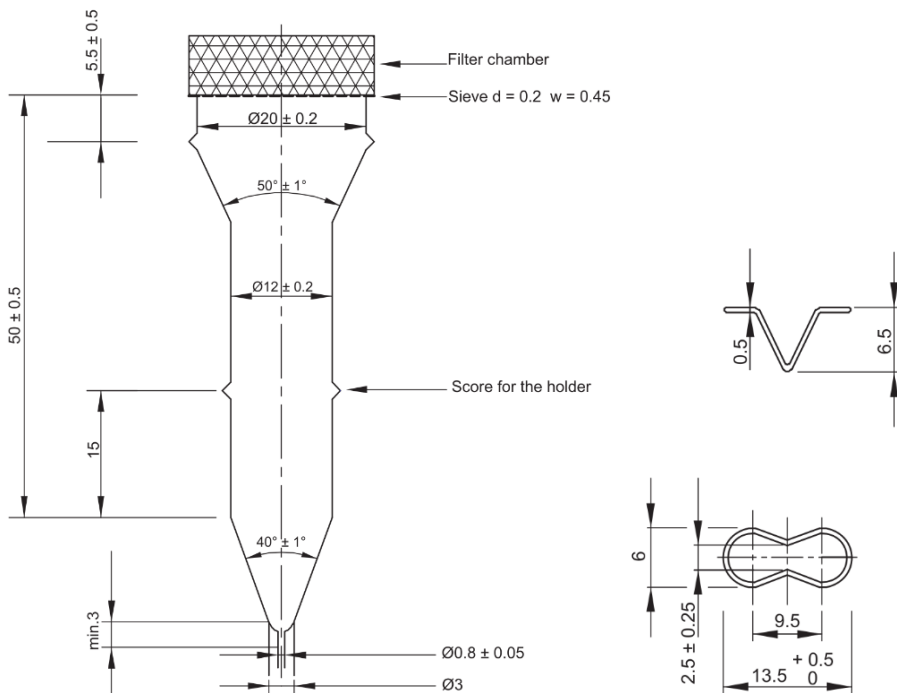


Figure 9.16. A sectional view of a USP 4 dissolution apparatus: small cell for tablets and capsules (upper picture part), tablet holder for small cell (lower picture part), dimensions in millimeters.

(Edited according to: European Pharmacopea 10.0)

Samples are collected at the cell outlet regardless of closed or open circuit type. If the collection is repeated, the removed volume is always replaced with an equal volume of the dissolution medium or its loss is considered in calculations, except for automatic evaluation where the dissolution fluid is returned to the vessel. The amount of API released during a prescribed time is expressed as a percentage of the declared amount.

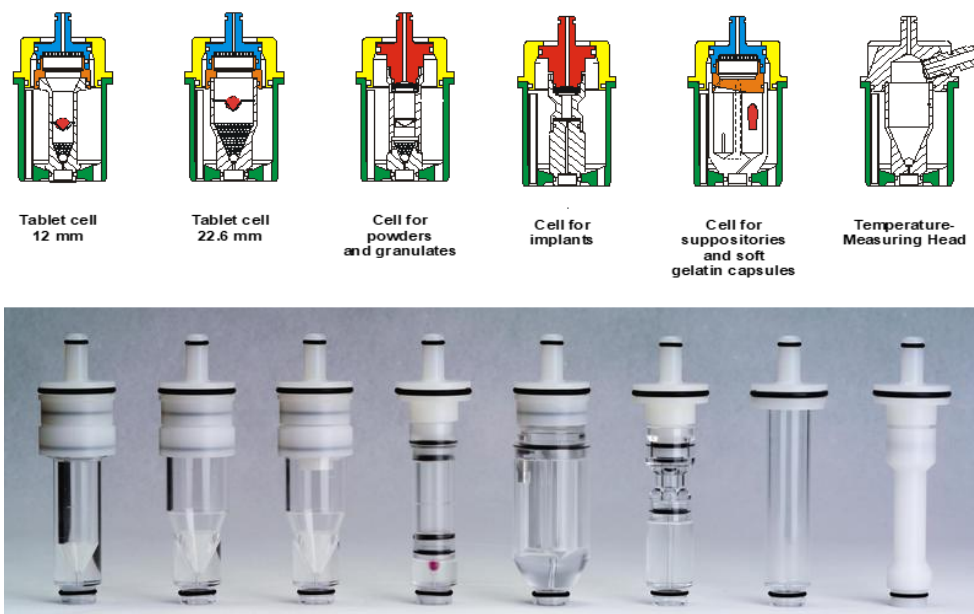


Figure 9.17. Different types of cells for flow-through systems.

(Source: commercial materials by Sotax company).

9.3.4 Advanced dissolution systems

Special dissolution instruments were developed for research and development purposes to answer the need for more accurate simulation of the *in vivo* dissolution. In body, the drug passes through the different parts of the GIT and faces various environments and conditions – from acidic pH in stomach to slightly basic distal parts of SI; gastric secretions with pepsin and later pancreatic enzymes and bile in duodenum; high liquid content in stomach followed by air-pockets in small intestine; intense mixing in stomach and progressively decreasing peristaltic strength in SI. Moreover, the GIT processes are not always regular. For example, the frequency and amplitude of peristaltics is not regular but consists of occasional short housekeeping waves to expel food from stomach, followed by longer periods of more regular low-intensity motility. There is also a large intra- and inter-subject variability, for example in the frequency of gastric emptying. Simulation of fed-

state is even more complex as food administration increases dynamics and variability of the GI processes. All of these examples underline the complexity of the GIT and show that a faithful in vitro simulation of GI conditions is tricky and requires in-depth knowledge and complex instrumentation.

One of the most renowned artificial GIT systems is the TIM-1, introduced by Dutch company TNO in the early '90s, which still remains one of the most advanced instruments to date. It includes one gastric and three small intestinal compartments, with simulation of pH, gastric, biliary, and pancreatic secretions, and a controlled emptying of all the individual compartments. It works with a more realistic motility provided by flexible tubes and more physiological medium volumes and composition than the commonly used dissolution apparatuses (USP 2–4). The TIM-1 measures drug absorption, which also maintains sink condition. The device can be used to study pure APIs, binary mixtures of APIs with various excipients, as well as finalized formulations. The acquired values give information about the solubility at various pH, about stability of coating layers, about release profile of the active substance, and consequently also about the availability of the drug for absorption. Moreover, there is the possibility to monitor all these parameters in interaction with food. Because of these characteristics, the device is also recognized by the FDA. Its complexity however requires laborious cleaning and maintenance, which led to development of a simplified version with only one SI compartment, named TinyTIM. Other similarly complex multicompartimental dissolution apparatuses include Engineered Stomach and small INtestine (ESIN) model and Golem apparatus.

A number of other advanced apparatuses have been developed to simulate only one part of the GIT. For precise simulation of the complex mechanical forces in the stomach, systems such as Gastric Digestion Simulator (GDS), Advanced Gastric Simulator (AGS), Gastric Simulation Model (GSM), and GastroDuo have been designed. Most originate from nutrition research and vary in build, stress-force simulation, and presence or absence of enzymatic secretion. Accurate gastric simulation finds application for formulations where liberation is dictated by mechanical forces (hydroxypropyl methylcellulose, HPMC, matrices) or in case of a gastro-resistant controlled release. Novel approach to simulation of small intestine has brought several apparatuses that mimic the tube geometry and peristaltics of SI, such as the Intestine Model for Simulating the Peristaltic Action (IMSPA). Another apparatus, the Human Duodenal Model (HDM) then focuses only on the simulation of sigmoidal duodenum but with addition of enzymatic secretion and absorption.

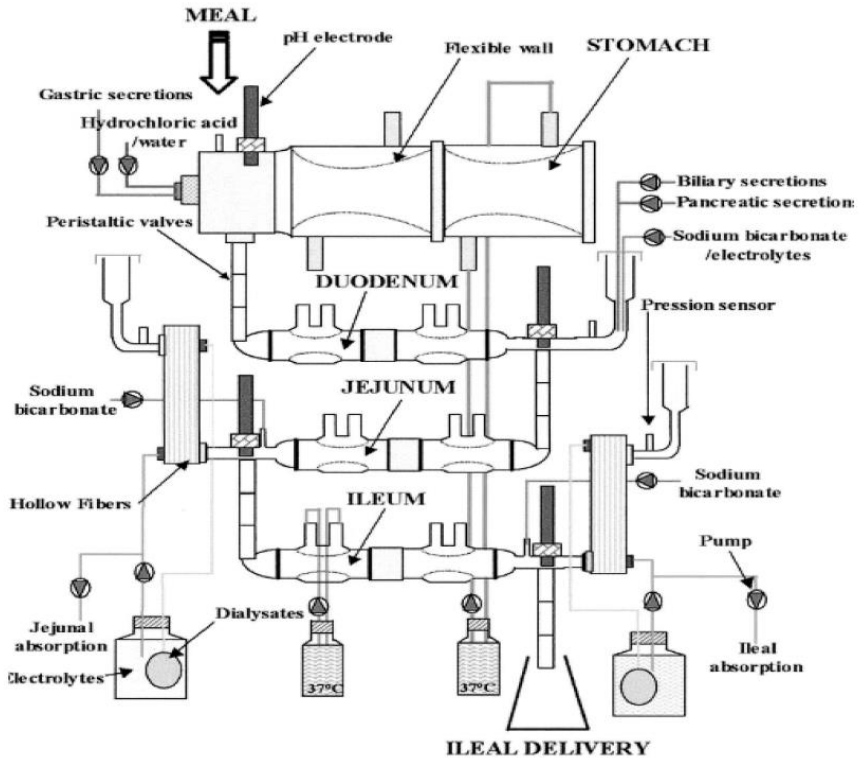


Figure 1.18. A scheme and a photo of TNO TIM-1 instrument.
(Source: commercial materials by TNO company.)

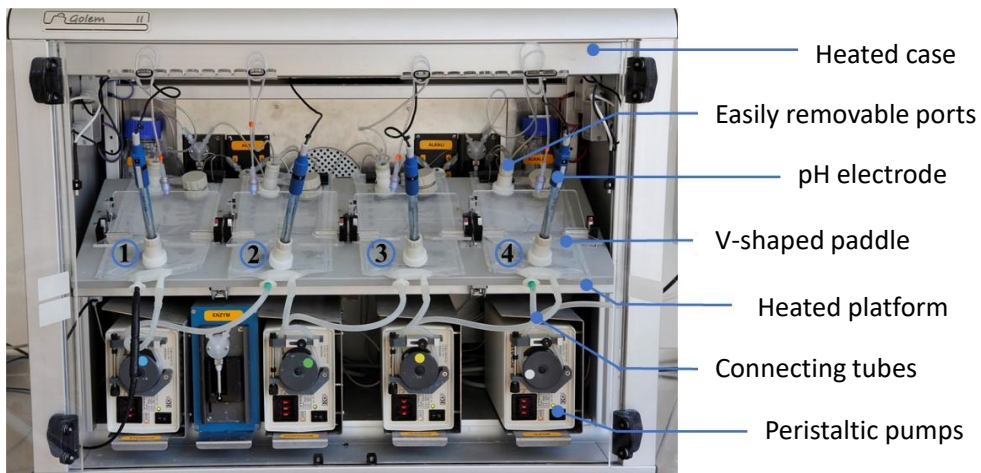


Figure 1.19. A photo of Golem v2 apparatus. Numbers 1-4 designate compartments – stomach, duodenum, jejunum, ileum, respectively.

(Source: Stupak I. Optimalizace disolučních kompartmentů k nové verzi přístroje pro biorelevantní disoluce – Golem v2. Masaryk University, 2021.)

9.4 Resources and recommended literature

1. Amidon G. L., Lennemas H., Shah V. P., Crison J. R. A theoretical basis for a biopharmaceutic drug classification: the correlation of in vitro drug product dissolution and in vivo bioavailability. *Pharm. Res.* 1995, 12.
2. Martinez M. N., Amidon G. L. A mechanistic approach to understand the factors affecting drug absorption: a review of fundamentals, *J. Pharmacokinet. Pharmacodyn.* 2002, 42. <https://doi.org/10.1177/00970002042006005>
3. Dressman J. B., Amidon G. L., Reppas C., Shah V. P. Dissolution testing as a prognostic tool for oral drug absorption: immediate release dosage forms. *Pharm. Res.* 1998, 15.
4. Český lékopis 2009. Grada Publishing a.s., Prague, Czech Republic, 2009.
5. *Pharmeuropa* Vol. 16, No. 1, 2004.
6. *European pharmacopeia 5.7, EDQM*, 2006.
7. Viegas T. X., Curatella R. U., Van Winkle L. L., Brinker G. Measurement of Intrinsic Drug Dissolution Rates Using Two Types of Apparatus, *Pharm. Tech.* 2001.
8. Bhattachar S. N., Wesley J. A., Fioritto A., Martin P. J., Babu S. R. Dissolution testing of a poorly soluble compound using the flow-through cell dissolution apparatus, *Int. J. Pharm.* 236, 2002. [https://doi.org/10.1016/S0378-5173\(02\)00027-3](https://doi.org/10.1016/S0378-5173(02)00027-3)
9. E. Beyssac. Examining recent developments in powder dissolution testing: prezentace na konferenci Dissolution testing symposium, Prague, Czech Republic, 2008.
10. Brown C. K., Chokshi H. P., Nickerson B., Reed R. A., Rohrs B. R., Shah P. A. Acceptable Analytical Practices for Dissolution Testing of Poorly Soluble Compounds, *Pharm. Tech.* 2004. <https://doi.org/10.14227/DT120405P6>
11. Cardot J. M., Beyssac E., Alric M. In Vitro–In Vivo Correlation: Importance of Dissolution in IVIVC, *Dissolution Technologies*, 2007. <https://doi.org/10.14227/DT140107P15>
12. E. Beyssac and J. Lavigne. Dissolution Study of Active Pharmaceutical Ingredients Using the Flow Through Apparatus *Usp 4, Dissolution Technol.* 2005. <https://doi.org/10.14227/DT120205P23>
13. Haddouchi S., SPS Pharma. Spotlight session – flow through dissolution testing for low dose products, prezentace na konferenci Dissolution testing symposium, Prague, Czech Republic, 2008.

9 Dissolution testing in pharmaceutical industry

14. Glantzmann J. M., Raton J. L. Dissolution tests with the flow through method. www.pharmaquality.com, 2005.
15. www.dissolutiontech.com. June 2010.
16. Culen M., Rezacova, A. Jampilek J., Dohnal J. Designing a Dynamic Dissolution Method: A Review of Instrumental Options and Corresponding Physiology of Stomach and Small Intestine. *J. Pharm. Sci.* 2013, 102 (9), 2995-3017. <https://doi.org/10.1002/jps.23494>
17. Minekus M.. Chapter 5 The TNO Gastro-Intestinal Model (TIM). In: *The Impact of Food Bioactives on Health: in vitro and ex vivo models*. Verhoeckx K., Cotter P., López-Expósito I., et al. (Ed.). Springer: 2015. https://doi.org/10.1007/978-3-319-16104-4_5
18. Guerra A., Denis S., le Goff O., Sicardi V., François O., Yao A.F., Garrait G., Manzi A.P., Beyssac E., Alric M., Blanquet-Diot S. Development and validation of a new dynamic computer-controlled model of the human stomach and small intestine. *Biotechnol. Bioeng.* 2016, 113 (6), 1325-35. <https://doi.org/10.1002/bit.25890>
19. Culen M., Dohnal J. Advances in dissolution instrumentation and their practical applications. *Drug. Dev. Ind. Pharm.* 2014, 40 (10), 1277-82. <https://doi.org/10.3109/03639045.2013.841184>
20. Stupak I., Bilik T., Vyslouzil J., Culen M., Dohnal J. Prehľad a vývoj biorelevantných dynamických disolučných prístrojov. *Chem. Listy.* 2021, 115 (11), 602-608.

10 Summary

Jiří Dohnal

Pharmacy is one of the most regulated fields and the choice of appropriate quality and safety assurance of pharmaceuticals depends, to a large extent, on the approval of the regulators. This is especially true if adhering to GMP, which may lead to a certain conservatism. The application of modern analytical methods ranges from routine quality control to highly specialized research and development analyses, and they also find place in works of a normative nature, such as pharmacopoeias. In the field of research and development a higher degree of freedom can be applied in the selection and use of methods for process monitoring and optimization. Regarding pharmaceutical control, it is important to emphasize that the focus is increasingly shifting from final control to in-process control and continual monitoring of production processes to obtain a quality, effective, and safe final product.

The following text provides a brief summary of the real-life use of the individual methods in pharmaceutical areas. Since the selection of an appropriate analytical technique depends mainly on the desired level of focus, the following text is structured accordingly, into three parts:

Molecular level

Here, probably the most important are infrared spectrometry techniques – attenuated total reflectance (ATR) technique, diffuse reflectance infrared Fourier transform (DRIFT) technique, Raman spectrometry, X-ray structural analysis of single crystal or powder material, solid state nuclear magnetic resonance (ssNMR).

Application of MIR lies mostly in the development and partially also in QC.

NIR spectroscopy is used in pharmacy in both qualitative and quantitative applications. Main advantage of the NIR spectroscopy is the ability to measure samples through glass and other transparent packaging materials. The measurement is fast, non-destructive, and requires no special sample preparation. This minimizes the consumption of chemicals and disposable analytical material. NIR techniques maintain a special position in PAT (process analytical technology). Whole NIR spectrometers can be attached to other devices so that an entire production process can be directly observed, and its course monitored on-line/in-line.

The expansion of Raman spectroscopy is closely related to the development of lasers and their higher availability. Raman spectroscopy is a non-destructive analytical method. Its complementarity with IR spectroscopy and characterization

of the molecular and crystal structures enables its utilization for identification of unknown samples. Raman spectroscopy is often used together with IR spectroscopy in the mid-infrared region to obtain as much spectral information as possible. Raman spectroscopy can be a supplementary technique for the structural analysis of organic molecules in combination with nuclear magnetic resonance (NMR) and/or mass spectrometry (MS). Within the pharmaceutical field, very important applications are those such as Raman mapping and imaging. These techniques are crucial where component distribution and surface homogeneity are to be observed and assessed.

For certain reasons, Raman spectroscopy is not suitable for determining crystal structures without standards. In such a case, X-Ray Diffraction (XRD) analysis will be the method of choice. Raman spectroscopy is however a fast and non-destructive technique and requires smaller amount of sample than thermal methods, e.g., Differential Scanning Calorimetry (DSC) which is used for polymorph differentiation as well. Raman spectroscopy is also cheaper compared to XRD.

Solid state NMR and terahertz spectroscopy are typically used in pharmaceutical development. They share some general characteristics, such as expensive instrumentation and requirement for highly specialized personnel. Solid state NMR offers broad application options, namely polymorph characterization, excipient analysis, and selective and highly attractive analysis of APIs containing heteroatoms directly in mixtures or finished dosage forms.

The terahertz spectroscopy originates from military setting and is gradually being adopted in pharma industry, where it may find a widespread application potential.

Intermolecular level, particles

At this level, the techniques of interest are, for example powder X-ray diffraction (PXRD), optical and electron microscopy – scanning electron microscopy (SEM) and its modification – electron tomography, transmission electron microscopy (TEM), terahertz spectroscopy (applies to intermolecular bond vibrations), and thermal methods – differential scanning calorimetry (DSC), micro DSC, hyper DSC, thermogravimetry analysis (TGA), thermally stimulated current (TSC).

Of the X-ray techniques, powder diffraction is well established and is used for determination of polymorphic purity of active substances in development laboratories and routinely in QCs, besides other applications.

Thermal analysis represents standard techniques that are typically used for detection of solvents in APIs, determination of API purity (DSC techniques). Its disadvantage is the limited possibility of analysis of mixtures.

Bulk, surface region

The suitable methods include inverse gas chromatography (IGC), techniques for finding high energy regions, thickness, porousness, flow characteristics (of powders), dynamic vapor sorption (DVS); also small angle X-ray scattering (SAXS) for determination of particle size and shape etc.

Mass spectrometry is amply used as detection in LC-MS setting. In QC, it is often used for QC impurity detection. In development, it is used for example for characterization of large biomolecules, such as monoclonal antibodies.

Dissolution testing is routinely used for quality testing of complete dosage forms, but at the same time it is irreplaceable in formulation development to assess the dissolution of APIs and dosage forms and to predict bioavailability of the product.

Based on the above mentioned, it is clear that without these modern analytical methods, it would not be possible to ensure control during the entire life cycle of the drug.

11 Abbreviations

ADSC Alternating Differential Scanning Calorimetry

APCI Atmospheric Pressure Chemical Ionization

API Active Pharmaceutical Ingredient

APPI Atmospheric Pressure Photoionization

APT Attached Proton Test

ATR Attenuated Total Reflectance

CCD Charge Coupled Device

CCDC Cambridge Crystallographic Data Centre

CDCI₃ Deuteriochloroform

CE-MS Capillary Electrophoresis – Mass Spectrometry

cGMP common Good Manufacturing Practice

CI Chemical Ionization

COSY Correlated Spectroscopy

CP/MAS Cross Polarization Magic Angle Spinning

CSA Chemical Shift Anisotropy

CSD Cambridge Structural Database

D₂O Deuterium Oxide (Heavy Water)

DART Direct Analysis in Real Time

DDSC Dynamic Differential Scanning Calorimetry

DESI Electrospray Desorption Ionization

DF Dosage Form

DMSO-d₆ Hexadeuterodimethyl Sulfoxide

DRIFT Diffuse Reflectance Infrared Fourier Transform

DRIFTS Diffuse Reflectance Infrared Fourier Transform Spectroscopy

DSC Differential Scanning Calorimetry

DTA Differential Thermal Analysis

DTGA Differential Thermogravimetric Analysis

EI Electron Ionization

EMA European Medicines Agency

ESI Electrospray Ionization

FAB Fast Atom Bombardment

FDA Food and Drug Administration

FIA Flow Injection Analysis

FIB Fast Ion Bombardment

FID Free Induction Decay

FIR Far-Infrared

FT Fourier Transform

FT-ICR Fourier Transform – Ion Cyclotron Resonance

FT-IR Fourier Transform – Infrared

FT-NMR Fourier Transform – Nuclear Magnetic Resonance

FWHM Full Width at Half Maximum

GC Gas Chromatography

GC-MS Gas Chromatography – Mass Spectrometry

GIT Gastrointestinal Tract

GMP Good Manufacturing Practice

HETCOR Heteronuclear Shift Correlated Spectroscopy

HMBC Heteronuclear Multiple Bond Correlation

HPLC High Performance Liquid Chromatography

HPLC-MS High Performance Liquid Chromatography – Mass Spectrometry

HPMC Hydroxypropyl Methylcellulose
HSQC Heteronuclear Single Quantum Coherence
ICH Q International Conference on Harmonization – Quality
IR Infrared
ISO International Organization for Standardization
IT Ion Trap
LC-MS Liquid Chromatography – Mass Spectrometry
LIT Linear Ion Trap
MALDI Matrix-Assisted Laser Desorption/Ionization
MAS Magic Angle Spinning
MDSC Modulated Differential Scanning Calorimetry
MDTA Modulated Differential Thermogravimetry Analysis
MIR Mid-Infrared
MS Mass Spectrometry
MS/MS (MS_n) Tandem Mass Spectrometry
NIR Near-Infrared
NMR Nuclear Magnetic Resonance
NQS Non-Quaternary Suppression
PAT Process Analytical Technology
PCR Principal Component Regression
PDG Pharmacopeial Discussion Group
PE Polyethylene
Ph. Eur. European Pharmacopoeia
PLS Partial Least Squares
PXRD Powder X-Ray Diffraction

Q Quadrupole

QqTOF Quadrupole/Quadrupole/Time of Flight

QqQ Triple Quadrupole

RP Reversed Phase

RP-HPLC Reversed Phase – High Performance Liquid Chromatography

r-TOF Reflection Time of Flight

SDS Sodium Dodecyl Sulphate

SIM Selected Ion Monitoring

SRM Selected Reaction Monitoring

SSI Sonic Spray Ionization

ssNMR Solid State Nuclear Magnetic Resonance

TEM Transmission Electron Microscopy

TG(A) Thermogravimetry Analysis

TIC Total Ion Current

TMA Thermomechanical Analysis

TMDSC Temperature-Modulated Differential Scanning Calorimetry

TMS Tetramethyl silane

TOF Time of Flight

TOSS Total Sidebands Suppression

TSC Thermally Stimulated Current

TSI Thermospray Ionization

USP United States Pharmacopeia

UV Ultraviolet

UV-VIS Ultraviolet – Visible

VIS Visible

XRD X-Ray Diffraction

YAG Yttrium Aluminum Garnet $Y_3Al_5O_{12}$

12 Authors

Editors

Martin Čulen

Department of Internal Medicine, Hematology and Oncology, Faculty of Medicine
Department of Chemical Drugs, Faculty of Pharmacy Masaryk University
Kamenice 5, 625 00 Brno, Czech Republic
233554@mail.muni.cz

Jiří Dohnal

Department of Applied Pharmacy
Masaryk University, Brno, Czech Republic

Josef Jampílek

Department of Analytical Chemistry, Faculty of Natural Sciences
Comenius University, Bratislava, Slovakia

Authors

Hana Brusová

Zentiva, Prague, Czech Republic

Martin Čulen

Department of Internal Medicine, Hematology and Oncology, Faculty of Medicine
Department of Chemical Drugs, Faculty of Pharmacy
Masaryk University, Brno, Czech Republic

Jiří Dohnal

Department of Applied Pharmacy, Faculty of Pharmacy
Masaryk University, Brno, Czech Republic

Jaroslav Havlíček

Zentiva, Prague, Czech Republic

Josef Jampílek

Department of Analytical Chemistry, Faculty of Natural Sciences
Comenius University, Bratislava, Slovakia

Izabela Jendrzejewska

Institute of Chemistry
University of Silesia in Katowice, Poland

Christelle Kadlec

Department of Dielectrics, Institute of Physics
Czech Academy of Sciences, Prague, Czech Republic

Filip Kadlec

Department of Dielectrics, Institute of Physics
Czech Academy of Sciences, Prague, Czech Republic

Bohumil Kratochvíl

Department of Solid State Chemistry
University of Chemistry and Technology Prague, Czech Republic

Lucie Krumbholcová

Zentiva, Prague, Czech Republic

Tomáš Pekárek

Zentiva, Prague, Czech Republic

Lukáš Plaček

Pragolab, Prague, Czech Republic

Anna Řezáčová

Icon Clinical Research, Prague, Czech Republic

Dita Spálovská

Zentiva, Prague, Czech Republic

Translation: Martin Čulen

Design and typesetting: Martin Čulen

Cover design: Kateřina Škrlová (www.deart.cz)

Published by Masaryk University Press, Žerotínovo nám. 617/9, 601 77 Brno,
Czech Republic

First electronic edition, 2023

ISBN: 978-80-280-0193-3

<https://doi.org/10.5817/CZ.MUNI.O280-0193-2022>

The textbook provides an overview of the main techniques applied in the pharmaceutical industry, with the focus on solid-state analysis. It discusses spectral methods, thermal analysis, and dissolution testing, explains the theoretical background for each method and shows practical examples from real-life drug-design and quality control applications. The textbook is intended for both pharmacy students and early career professionals.

MUNI
PRESS

MUNI
PHARM

MUNI
MED